ADVANCED BIOTECH APPLICATIONS FOR FOOD AND FEED SAFETY

Anna Pennacchio

Dottorato in Scienze Biotecnologiche – XXVII° ciclo
Indirizzo Biotecnologie industriali e Molecolari
Università di Napoli Federico II

Dottorato in Scienze Biotecnologiche – XXVII° ciclo
Indirizzo Biotecnologie Industriali e Molecolari
Università di Napoli Federico II

ADVANCED BIOTECH APPLICATIONS FOR FOOD AND FEED SAFETY

Anna Pennacchio

Dottoranda:	Anna Pennacchio
Relatore:	Prof. Gennaro Piccialli
Correlatore:	Dr. Sabato D'Auria
Coordinatore:	Prof. Giovanni Sannia

There will be a time
when you believe everything is finished.
That will be the beginning.
Louis L'Amour

A chi mi è stato sempre accanto

INDEX

SUMMARY

The growing concern for human and animal health and the existence of Community directives, which set maximum permitted levels of certain mycotoxins, antibiotics and hormones in many food products, require the need for methods of analysis for the strict monitoring of the levels of mycotoxins, antibiotics and hormones in raw materials and in processed products. A mycotoxin is a toxic secondary metabolite produced by fungi. Among the micotoxins, we are interested in patulin that is associated with fruits and vegetables, in particular apples and figs. Food is also contaminated by antibiotics because of their use in veterinary medicine. The antibiotics widely used are β-lactams, which include penicillin G, present in milk. Hormones, in particular estradiol, are often used to increase milk production in cows, stimulate the growth of livestock and reduce the amount of feed they need to grow.

The main aim of this work is the development of advanced diagnostic systems for a simple determination of mycotoxins, antibiotics and hormones in foods, to ensure the safety of use and the quality of raw materials, with particular reference to milk, apple juices, processed food and feed products. Optical biosensors, offer several advantages compared to conventional analysis such as HPLC and LC-MS. These include a low cost per sample, high selectivity, high sensitivity, and high throughput, no extensive extraction and sample clean-up, a fast response and the use of non-trained personnel for their utilization.

This objective is pursued through the study and the development of methodologies that utilize proteins, enzymes, antibodies and/or aptamers as specific probes for the design of advanced optical biosensors (assays such as Surface plasmon resonance (SPR) and fluorescence polarization assays). I immobilized patulin, penicillin G and estradiol conjugated with a carrier protein, Glutamine binding protein, on the SPR sensing surface and I produced the antibodies anti patulin, anti penicillin G and anti estradiol. This has been successfully implemented in a new, efficient SPR-based competitive immuno-assay for the detection of the analyte of interest. Then I have combined an immuno-chemical approach with SPR spectroscopy to develop an efficient biosensor to detect an analyte of interest in foods outside the laboratory.

Moreover, I present a novel and sensitive polarization-based method for the detection of patulin, penicillin G and estradiol directly in apple juice and in milk. The proposed method is based on the use of patulin, penicillin G and estradiol conjugate, labeled with a NIR probe and the use of properly produced anti-analyte antibodies. The fluorescence biosensor works in the near infrared-region of light. In fact, in this spectral region, there is almost no unspecific absorption of food matrices making possible both qualitative and quantitative assays.

The obtained results confirm that this methodology can be applied outside the laboratory and directly in apple-juice and in milk without interference. In addition, these techniques are more sensitive than commonly used techniques. The results of the SPR and fluorescence polarization assay show the possibility to detect an amount of patulin, penicillin G and estradiol less than the MRL of the EU regulation limit.

Riassunto

La crescente preoccupazione per la salute umana e l'esistenza di direttive comunitarie che fissano i livelli massimi di micotossine, alcuni antibiotici e ormoni in molti prodotti alimentari, richiedono la necessità di metodi di analisi per un controllo rigoroso dei livelli di queste sostanze in materie prime e in prodotti derivati. Le micotossine sono metaboliti tossici prodotti da diversi tipi di funghi, appartenenti principalmente ai generi *Aspergillus*, *Penicillium* e *Fusarium* [1]. In particolari condizioni ambientali, quando la temperatura e l'umidità sono favorevoli, questi funghi proliferano e possono produrre micotossine. Generalmente queste ultime entrano nella filiera alimentare attraverso colture contaminate destinate alla produzione di alimenti e mangimi, principalmente di cereali, frutta e verdure [1-3]. Tra le diverse micotossine, abbiamo focalizzato la nostra attenzione sulla patulina, micotossina prodotta da diversi tipi di muffe, in particolare, Aspergillus e Penicillium. Si ritrova comunemente nelle mele marce e danneggiate; la quantità di patulina presente nei prodotti a base di mele è generalmente indice della qualità del prodotto utilizzato durante il processo di produzione. Studi hanno dimostrato che è genotossica e crea disturbi a livello gastrointestinale e renale e secondo alcune teorie, sembra essere un agente cancerogeno [4-9].

Il cibo può essere contaminato anche da antibiotici a causa del loro uso in medicina veterinaria. Gli antibiotici più utilizzati sono i β-lattamici, che includono la penicillina G, riscontrabile nel latte [10-11]. I farmaci con attività antimicrobica hanno cominciato ad avere un largo impiego in medicina veterinaria immediatamente dopo la loro scoperta: la prima applicazione terapeutica nella cura degli animali era nel trattamento della mastite. Oltre cinquanta anni dopo, la scoperta della capacità di questi farmaci di aumentare il peso degli animali, ne ha causato un aumento dell'uso come additivi per mangimi. Infatti, gli allevatori e gli agricoltori nutrono il loro bestiame con una bassa dose giornaliera di antibiotici, non per evitare malattie ma per aumentarne il peso [12-14]. L'uso massiccio e indiscriminato provoca inevitabilmente la presenza di residui negli alimenti, con conseguente preoccupazione per la salute dei consumatori. Le principali preoccupazioni sono la possibile sensibilizzazione allergica d'individui esposti, la possibilità di selezionare batteri resistenti agli antibiotici e la pressione selettiva che i residui di farmaci antimicrobici possono esercitare sulla microflora intestinale umana: si teme anche che gli antibiotici negli alimenti possano favorire l'adesione di batteri patogeni.

Gli ormoni, in particolare l'estradiolo, sono spesso utilizzati per aumentare la produzione di latte nelle mucche, stimolare la crescita del bestiame e ridurre la quantità di mangime di cui hanno bisogno. Gli ormoni permangono come residui nelle carni e nel latte; tali residui provocano gravi conseguenze al consumatore e in particolare ai bambini: sono stati infatti osservati numerosi casi di alterazioni a carico dell'apparato riproduttore maschile e femminile, nonché la genesi di cancro al seno e all' utero nelle donne. Poiché le micotossine, gli antibiotici e gli ormoni causano gravi problemi alla salute umana, l'Organizzazione Mondiale della Sanità ha stabilito un limite tollerabile per patulina, penicillina G ed estradiolo nei prodotti alimentari. Il contenuto di patulina negli alimenti è stato fissato a 50 µg/L in molti paesi. I requisiti regolamentari per i residui di β-lattamici nel latte sono abbastanza rigorosi: le tolleranze sono state fissate a 12 nM per penicillina G e 10 nM per ampicillina.

I metodi di rilevazione analitici convenzionali utilizzati per la determinazione di micotossine e ormoni comprendono analisi cromatografiche, quali HPLC, GC e recentemente, tecniche quali LC/MS e GC/MS [15-19]. Invece, le tecniche per il rilevamento di residui di antibiotici consistono nel test microbiologico e nel metodo immunologico [14]. L'analisi microbiologica è utilizzata per lo screening di antibiotici negli alimenti sia per la sua praticità e per i bassi costi, che per le caratteristiche ad ampio spettro. Questo test, però, è necessario che sia effettuato in laboratorio, è quindi lento e poco sensibile. Tutti questi metodi presentano una serie di svantaggi: sono necessari lunghi protocolli di purificazione del campione prima dell'analisi, è richiesto personale qualificato, non è possibile fare indagini sul campo e inoltre la strumentazione è molto costosa. Per tali motivi, negli ultimi tempi è stata posta molta attenzione allo sviluppo dei biosensori, strumenti analitici che hanno trovato larga applicazione biotecnologica in molteplici campi, quali la diagnostica clinica, l'analisi d'inquinanti ambientali e l'industria alimentare. I biosensori possono essere considerati dei dispositivi molto innovativi, poiché coniugano alla specificità del riconoscimento molecolare un'efficiente trasduzione del segnale e avanzate tecniche di rivelazione; inoltre, l'ampio spettro di reazioni impiegate e l'elevata sensibilità e selettività rendono i biosensori idonei a molteplici settori di applicabilità. I biosensori sono strumenti che incorporano un elemento biologicamente attivo, una proteina, una cellula o un anticorpo, accoppiato a idonei trasduttori di segnale per la determinazione selettiva e reversibile della concentrazione o dell'attività di specie chimiche in un campione. Essi sono classificati sia in base alla natura del mediatore biologico che al tipo di trasduzione impiegata. In accordo con il primo criterio, i biosensori possono essere biosensori enzimatici, chemorecettoriali o immunosensori; in base al tipo di trasduttore di segnale, invece, si distinguono biosensori ottici, elettrochimici, calorimetrici e acustici. Negli ultimi tempi sta avendo larga diffusione l'utilizzo di biosensori proteici a fluorescenza; la tecnologia per proteine sensibili alla fluorescenza è ormai lo strumento analitico dominante per la rilevazione di contaminanti ambientali e alimentari o per lo sviluppo di test medici e biotecnologici, in quanto si introducono continuamente nuovi fluorofori e proteine ingegnerizzate per rilevare analiti specifici. In questo lavoro proponiamo come metodo alternativo alle comuni metodiche per la determinazione di micotossine, antibiotici e ormoni, i biosensori ottici.
I biosensori ottici offrono diversi vantaggi rispetto alle tecniche di analisi convenzionali. Questi includono basso costo per il campione, alta selettività, elevata sensibilità, elevata produttività, risposta veloce, tempo di dosaggio ridotto da giorni a minuti in alcuni casi, impiego di personale non qualificato per il loro utilizzo, analisi sul campo e soprattutto non richiedono pre-trattamento del campione.

Scopo del progetto di tesi

Lo scopo di questo progetto è sviluppare sistemi diagnostici avanzati per una semplice e rapida determinazione di tossine,antibiotici e ormoni in matrici alimentari per uso umano e animale al fine di garantire la sicurezza e la qualità delle materie prime, con particolare riferimento ai succhi di frutta, al latte e ai prodotti derivati. Tale obiettivo è stato perseguito attraverso lo sviluppo di metodologie che utilizzano proteine, anticorpi e

aptameri per la progettazione di biosensori ottici avanzati (saggi di Risonanza Plasmonica di Superficie e saggi di fluorescenza con luce polarizzata).

Risultati conseguiti

- **Saggi SPR**

È stato sviluppato un saggio immunoenzimatico basato sulla risonanza plasmonica di superficie (SPR) per la rilevazione di patulina, penicillina G ed estradiolo in matrici alimentari. Tale metodologia ottica permette di studiare l'interazione tra biomolecola e analita, come variazione dell'onda evanescente di superficie che si genera all'interfaccia tra il liquido e la superficie. In questa tecnica, infatti, una delle due molecole è immobilizzata su una superficie di chip d'oro funzionalizzato con i carbossi-metil-destrano e l'altra è in soluzione. La formazione del complesso biomolecola/analita modifica le proprietà dell'onda evanescente, variando
l'indice di rifrazione del mezzo. La variazione dell'angolo di risonanza è direttamente proporzionale alla quantità di ligando legato alla biomolecola [20]. Il test, eseguito con il SensiQ Discovery, strumento portatile, si basa sull'uso di un coniugato sintetizzato ad-hoc (GlnBP-patulina, GlnBP-penicillina G e GlnBP-estradiolo) immobilizzato sulla superficie d'oro del chip del SensiQ e di anticorpi specifici generati contro l'analita. Una volta immobilizzato il coniugato ad-hoc sulla superficie, sono state eseguite le misure di SPR per valutare il legame tra gli anticorpi anti-analita prodotti e l'analita immobilizzato sulla superficie. Con questo esperimento sono stati calcolati i parametri cinetici alla base del riconoscimento molecolare dell'anticorpo e dell'analita, in particolare le costanti di associazione e di dissociazione relative alla formazione del complesso.
Sono stati usati gli anticorpi anti-analita in un saggio SPR competitivo. Tale saggio è stato condotto pre-incubando concentrazioni fisse di anticorpo con quantità crescenti di analita. All'aumentare della concentrazione di analita presente in soluzione, si riscontra una diminuzione del segnale dovuta alla competizione degli anticorpi tra l'analita presente in soluzione e l'analita immobilizzato sul chip. La presenza dell'analita a concentrazioni crescenti nei campioni ha permesso di risalire al valore minimo di analita misurabile con questa metodologia. Questo valore è molto inferiore rispetto alla quantità attualmente misurabile con le tecniche classiche d'indagine.

- **Saggi di fluorescenza**

Inoltre, è stato sviluppato un saggio di fluorescenza con luce polarizzata per rilevare tracce di patulina, penicillina G ed estradiolo direttamente in matrici alimentari come succhi di frutta e latte.
La fluorescenza oggi riveste un ruolo di primo piano nei saggi di binding perché permette di effettuare i vari processi con un notevole risparmio di tempo ed è quindi adatta agli screening ad alta risoluzione; basti pensare che gli step di separazione e di lavaggio svolti con le classiche metodiche di analisi che sono dispendiosi, lenti e causa di probabili errori, vengono evitati [21-22].
Un composto fluorescente legato ad una macromolecola (una proteina ad esempio) risulta congelato in una specifica orientazione e permette quindi l'emissione di luce

fluorescente. Questo è il principio base su cui si fondano i saggi di binding con la tecnica della fluorescenza polarizzata. La teoria della fluorescenza polarizzata è fondata sulla constatazione che le molecole fluorescenti in soluzione, eccitate con una luce piano polarizzata, emetteranno luce in un piano fisso se le molecole rimangono ferme durante l'eccitazione del fluoroforo. In particolare, abbiamo utilizzato un fluoroforo che emette nella regione del vicino infrarosso della luce, per effettuare analisi direttamente nelle matrici alimentari. Infatti, in questa regione spettrale, non vi è quasi nessun assorbimento da parte delle matrici alimentari, rendendo possibili analisi sia qualitative che quantitative. La scelta di utilizzare questa classe di fluoroforo è correlata ai vantaggi fondamentali offerti da questo composto: una significativa riduzione del segnale di fondo, basso assorbimento nella regione visibile della luce, scarsa dispersione di luminosità ed utilizzo di una sorgente di luce poco costosa.
Il saggio consta nell'impiego di un coniugato sintetizzato ad-hoc (GlnBP-patulina, GlnBP-penicillina G e GlnBP-estradiolo) marcato con un probe fluorescente che emette nella regione del vicino infrarosso e di anticorpi generati contro l'analita di interesse [23]. Il saggio si basa su reazioni immunologiche rilevate mediante polarizzazione della fluorescenza. Essa combina i principi delle reazioni a competizione di legame con i principi della polarizzazione della fluorescenza, per fornire una misura diretta del legame con l'analita d'interesse. Il coniugato sintetizzato ad-hoc, marcato con una sonda fluorescente, agisce da tracciante. Quando il tracciante è eccitato con un fascio di luce polarizzata linearmente, esso emette fluorescenza con un grado di polarizzazione inversamente proporzionale alla sua velocità di rotazione. Appena il tracciante si lega al suo anticorpo specifico, l'intensità di fluorescenza aumenta. Aggiungendo l'analita non marcato al campione, questo compete con il tracciante per i siti limitati dell'anticorpo e l'intensità di fluorescenza diminuisce. Aggiunta di concentrazioni crescenti di analita non marcato ai campioni ha permesso di risalire al valore minimo di analita misurabile. La tecnica è molto sensibile rispetto alle comuni metodologie fino ad oggi impiegate e il limite minimo rilevabile è molto inferiore al limite imposto dalla Comunità Europea sia per la patulina che per la penicillina G che per l'estradiolo.

Conclusioni

In sintesi sono stati sviluppati due saggi innovativi per la determinazione di contaminanti quali patulina, penicillina G e estradiolo negli alimenti, per garantire qualità e sicurezza delle materie prime:

• un approccio immuno-enzimatico combinato con spettroscopia SPR per lo sviluppo di un biosensore ottico, che può essere utilizzato sul campo, anche da personale non esperto.
• un immunodosaggio basato sulla fluorescenza con luce polarizzata per la rilevazione di patulina, penicillina G e estradiolo direttamente negli alimenti come succhi di mela e latte. Questo metodo ha il vantaggio di essere più sensibile rispetto al metodo SPR ma non può essere utilizzato direttamente sul campo.

Entrambi i metodi consentono la determinazione di quantità di patulina, penicillina G e estradiolo molto inferiori rispetto a quelle imposte dalla Comunità Europea.

	Limite Comunità Europea	Limite Spettroscopia SPR	Limite Fluorescenza Polarizzata
Patulina	50 ug/L	0.1 ug/L	0.06 ug/L
Penicillina G	12 nM	8 pM	0.4 pM
Estradiolo	20 pmoli	_	0.5 pmoli

References

1. Turner N. W., Subrahmanyam S. and Piletsky S. A. (2009). Analytical methods for determination of mycotoxins: a review. Anal. Chim. Acta; 632 (2): 168–80.

2. Richard J. L. (2007). Some major mycotoxins and their mycotoxicoses-an overview. Int. J. Food Microbiol.; 119 (1–2): 3–10.

3. Robbins C. A., Swenson L.J., Nealley M. L., Gots R. E. and Kelman B. J. (2000). Health effects of mycotoxins in indoor air: a critical review. Appl Occup Environ Hyg; 15 (10): 773–84.

4. Moss M. O. (2008). Fungi, quality and safety issues in fresh fruits and vegetables. J. Appl. Microbiol.; 104 (5): 1239–43.

5. Trucksess M. W. and Scott P. M. (2008). Mycotoxins in botanicals and dried fruits: A review. Food Addit Contam.; 25 (2): 181–92.

6. Cornely O. A. (2008). *Aspergillus* to Zygomycetes: causes, risk factors, prevention, and treatment of invasive fungal infections. Infection; 36 (4): 296–313.

7. Desjardins A. E. and Proctor R. H. (2007). Molecular biology of *Fusarium* mycotoxins. Int. J. Food Microbiol.; 119 (1–2): 47–50.

8. Bennett J. W. and Klich M. (2003). Mycotoxins. Clin. Microbiol. Rev.; 16 (3): 497-516.

9. Pennacchio A., Ruggiero G., Staiano M., Piccialli G., Oliviero G., Lewkowicz A., Synak A., Bojarski P. , D'Auria S. (2014). A surface plasmon resonance based biochip for the detection of patulin toxin. Optical Materials; 36 (10): 1670–1675.

10. Achi O. K. and Ugbogu G. A. (2006). Characterization of Drug Resistant *Staphylococcus Aureus* of Animal Origin. Journal of Biological Sciences; 6 (6): 1088-1092.

11. Jukes T. H. and Williams W. L. (1953). Nutritional effects of antibiotics. Pharmacol. Rev.; 5: 381-420.

12. Phillips I., Casewell M., Cox T., De Groot B., Friis C., Jones R., Nightingale C., Preston R. and Waddell J. (2004). Does the use of antibiotics in food animals pose a risk to human health? A critical review of published data. Journal of Antimicrobial Chemotherapy; 53: 28–52.

13. Witte W. (1998). Medical consequences of antibiotic use in agriculture. Science; 279: 996–7.

14. Blasco C., Di Corcia A. and Picó Y. (2009). Determination of tetracyclines in multi-specie animal tissues by pressurized liquid extraction and liquid chromatography- tandem mass spectrometry. Food Chem.; 116: 1005-1012.

15. Kokkonen M. K. and Jestoi M. N. (2009). A Multi-compound LC-MS/MS Method for the Screening of Mycotoxins in Grains. Food Anal. Methods; 2 (2) : 128-140.

16. Vdovenko M.M., Gribas A.V., Vylegzhanina A.V. and Sakharov I.Y. (2012). Development of a chemiluminescent enzyme immunoassay for the determination of dexamethasone in milk. Analytical Methods: 4 (8): 2550-2554.

17. Ehling S. and Reddy T. M. (2013). Liquid Chromatography−Mass Spectrometry Method for the Quantitative Determination of Residues of Selected Veterinary Hormones in Powdered Ingredients Derived from Bovine Milk. Agric. Food Chem.; 61: 11782−11791.

18. Noppe H., Le Bizec B. and Verheyden K. (2008). Novel analytical methods for the determination of steroid hormones in edible matrices**.** Analytica chimica Acta; 1–16.

19. Blasco C, Van Poucke C. and Van Peteghem C. (2007). Analysis of meat samples for anabolic steroids residues by liquid chromatography/tandem mass spectrometry. Journal of Chromatography A; 1154 (1–2): 230–239.

20. Jorgenson R.C. and Yee S. S. (1993). A fiber-optic chemical sensor based on surface plasmon resonance. Sensors and Actuators B: Chemical; 12 (3): 213–220.

21. Seethala R. and Menzel R. (1997). A Homogeneous, Fluorescence Polarization Assay for Src-Family Tyrosine Kinases. Analytical Biochemistry; 253: 210-218.

22. Szmacinski H. and Lakowicz J. R. (1995). Fluorescence lifetime-based sensing and imaging. Sensors and Actuators B: Chemical; 29 (1-3): 16-24.

23. Frangioni J. V. (2003). *In vivo* near-infrared fluorescence imaging. Current Opinion in Chemical Biology; 7 (5): 626–634.

General Introduction

1. Food Safety

It is generally accepted that the assurance of food safety is primarily connected with the elimination of contamination in the full cycle of food production, starting from the growing of cereals, fruits and vegetables through the manufacturing, storage, and distribution, until the final preparation of the food in the kitchen [1]. Although the wide use of chemicals, such as pesticides or hormones, in agriculture, has provided numerous benefits, the residues of these substances represent an additional hazard for consumer's health. Food safety involves the safe handling of food from the time it is grown, packaged, distributed, and prepared to prevent food borne illnesses [2].
Food borne illness, or food poisoning, may be caused by bacteria or fungi that grow on food or by viruses that are spread because food is not cleaned, stored, or handled properly. These illnesses may cause minor or serious symptoms and even death in some people. Contaminated foods also can carry harmful parasites, toxins, hormones, antibiotics, chemicals, and physical contaminants [3]. Ensuring the safety of food is a shared responsibility among producers, industry, government, and consumers. Safe food is food that is free not only from microbiological pathogens such as bacteria, parasites, and viruses but also from toxins, pesticides, hormones and chemical and physical contaminants that can cause illness [2-3].
The main factors that contribute to food borne illness are improper holding temperatures, inadequate cooking, contaminated equipment, excessive and indiscriminate use of hormones and antibiotics to increase the food making and to reduce production costs and poor personal hygiene [4].
There is an on-going need to protect the health of humans and of susceptible animals by limiting their exposure to mycotoxins, antibiotics and hormones. In spite of many years of research, and the introduction of good practices in the food production, storage and distribution chain, these contaminants continue to be a problem [1]. Many countries regulate or suggest permitted levels of mycotoxins, antibiotics and hormones in food and feed because of their public health significance and commercial impact. Many countries regulate or suggest permitted levels of mycotoxins, antibiotics and hormones in food and feed because of their public health significance and commercial impact.

2. Mycotoxin

A mycotoxin is a toxic secondary metabolite produced by organisms belonging to the fungus kingdom [5-6]. Their contamination is greatly influenced by climatic and geographical conditions, cultivation practices, conservation and the type of substrate affected, since some products are more susceptible than others to fungal growth. Mycotoxins are developed both on the plants before harvesting (contamination from the field) and in food crops after the harvest itself, during the processes of conservation (in warehouses, silos, etc.) [7]. The most vulnerable foods to direct contamination are cereals (maize, wheat, rice, barley, rye, etc.), oilseeds (groundnut, sunflower, cottonseed, etc..), dried fruit and dried vegetables, spices, coffee and cocoa [8-11]. In addition, mycotoxins can be found as residues or toxic metabolites in food derived from animals fed with contaminated feed, creating a kind of important indirect contamination for humans because of the high levels of mycotoxins potentially present in cereals. The accumulation of mycotoxins in foods and feeds represents a major threat to human and animal health as they are responsible for many different toxicities including the induction of cancer, mutagenicity and

estrogenic, gastrointestinal, urogenital, vascular, kidney and nervous disorders [5]. Some mycotoxins are also immuno-compromising, and can thus reduce resistance to infectious disease. Significant economic losses are associated with their impact on human health, animal productivity, and both domestic and international trade. Mycotoxins have a great resistance to decomposition or being broken down in digestion, so they remain in the food chain: fruit, vegetables, meat and dairy products [12]. Even temperature treatments, such as cooking and freezing, do not destroy mycotoxins [13]. Because of their detrimental action on cellular function, they exert some actions: nephrotoxic (ochratoxins), hepatotoxic (aflatoxin), immunotoxic (aflatoxins, ochratoxins), mutagenic (aflatoxins, patulin), teratogenic (ochratoxins) and carcinogenic (aflatoxins, ochratoxins, fumonisins and patulin) [7].

Among micotoxins, patulin is particularly interesting because it is widespread. Patulin is a toxin produced by the P. expansum, Aspergillus, Penicillium, and Paecilomyces fungal species. P. expansum is especially associated with a range of mouldy fruits and vegetables, in particular rotting apples and figs [14-16]. It has been reported that patulin damages the immune system [17]. One important aspect of patulin toxicity in vivo is injury to the gastrointestinal tract including ulceration and inflammation of the stomach and intestine [18]. Recently, patulin has been shown to be genotoxic by causing oxidative damage to the DNA, and oxidative DNA base modifications have been considered to play a role in mutagenesis and cancer initiation [19,20]. Patulin is believed to exert its cytotoxic effects mainly by forming covalent adducts with essential cellular thiol groups in proteins and amino acids [21]. From a chemical point of view patulin is a water-soluble unsaturated lactone, readily reactive toward thiol groups and also amino groups. Glutathione represents one of the most abundant cellular nucleophiles, and it has been shown to form covalent adducts with patulin spontaneously [22]. The same reactivity is responsible for the ability of patulin to induce in-vitro intra and intermolecular protein cross-links involving the cysteine residues, the lysine and histidine of side chains and for its capability to inhibit the activity of several enzymes [23-24]. Patulin is also reported to be endowed with selective DNA damaging activity [25].

The widespread presence of fungi in the environment renders mycotoxins practically ubiquitous contaminants in food and feeds; therefore, one of the most effective measures to protect public health is to establish reasonable regulatory levels of these toxins on the basis of valid toxicological data [26]. To ensure the safety and quality of foods, a number of regulatory authorities have decreed maximum residue levels of several mycotoxins in foods. In 2004, the European Community set limits to the concentrations of patulin in food products. They currently stand at 50 µg/kg in all fruit juice concentrations, at 25 µg/kg in solid apple products used for direct consumption, and at 10 µg/kg for children's apple products, including apple juice [27-28]. In agreement with the results of a long-term investigation in rats, the World Health Organization (WHO) has set a tolerable weekly intake of 7 ppb for each kilogram of body weight.

Conventional analytical methods to detect the presence of micotoxins, involve chromatographic analyses, such as HPLC, GC, and, more recently, techniques such as LC/MS and GC/MS [29-31]. HPLC is currently the preferred method since it provides greater sensitivity and accuracy and also allows the automation of the analysis. Though both HPLC and GC-MS have a high sensitivity and reproducibility, they have some drawbacks, such as:

- the high quality of solvents (the mobile phase) and the fact that, most of these, need to be degassed and filtered before they can be used. In addition there is a problem linked to long time analysis;
- samples have to be subjected to a purification process because the analysis must reach the sensitivity shown by the limits of detection;
- only one sample at a time can be analyzed (you can automate the auto-sampler by multiple analysis, but the times become longer);
- investment costs are high and even those incurred routinely for the analysis are relevant (these include: depreciation and maintenance tools, charged columns and pre-columns, chromatography reagents, standard certificates, etc.);
- it is also essential that the analysis is carried out by skilled and properly trained staff to interpret the results.

Moreover, extensive protocols of sample clean-up are required prior to the analysis, and expensive analytical instrumentation is necessary to accomplish it [32-34]. Furthermore, the problem of the determination of mycotoxins by these methods is particularly important due to fact that the high variability of the real limitations makes difficult to extend this analysis outside the laboratory.

3. Antibiotics

Antibiotics are naturally occurring, semi-synthetic and synthetic compounds with antimicrobial activity that can be administered orally, parentally or topically. They are used in human and veterinary medicine to treat and prevent disease, and for other purposes including growth promotion of animals [35]. All antibiotics can select resistant bacterial mutants: they can acquire this capability by transfer from other bacteria. These resistant variants, as well as species that are inherently resistant, can become dominant and widespread in host-animal populations. If the use of an antibiotic is protracted, the resistant population among pathogens and commensal bacteria grows. However, there is great diversity in the development of resistance; some of this resistant population generates a real resistance but an other part remains just susceptible [36]. The campaign against the excessive use of antibiotics has been mostly directed to human and animal medicine, but there has been an increasing attention to the agricultural use, based on the assumption that their abuse might have an important role in the genesis of resistance in bacteria affecting humans [37]. Drugs with an antimicrobial activity began to be used in veterinary medicine immediately after their discovery: the first therapeutic application in the care of animals was in the treatment of mastitis [38]. Over fifty years later, the discovery of the ability of these drugs to increase the weight growth of animals, caused an increased use of antimicrobials as feed additives. This massive use inevitably causes residues in food. The presence of antimicrobial drug residues causes concerns for consumer health [39]. The main concerns are: the possible allergic sensibilization of exposed individuals, the possibility of selecting antibiotic resistant bacteria, and the selective pressure that antimicrobial drug residues may exert over human gut micro-flora: it is feared that antimicrobials in food can deplete the human intestinal exposed micro-flora, thus promoting adhesion of pathogenic bacteria [37]. The extent of such use in animal feed has even led some to claim that livestock production would not be possible, or at least would be uneconomic without the deployment of such additives

[40]. It is obvious that the use of antimicrobial drugs on such a large scale has given and determined the presence of drug residues in food [39]. There are various normally used methods to search for antimicrobial drug residues in food: tests based on the inhibition of microbial growth, the microbial test, enzyme-colorimetric tests and chromatographic methods [41-44]. These methods usually require very sophisticated and expensive tools to measure with precision and accuracy the response to the test. Generally, the microbiological test is used for the screening of antibiotics in food for its convenience, low cost and the characteristics of a broad spectrum. This test, however, is carried out in the laboratory, is slow, and not very sensitive.

4. Hormones

Anabolic steroids have been widely used as growth promoting agents in cattle to increase the weight of animals and reduce the feed conversion efficiency [45]. The administration of naturally and synthetic anabolic growth promoters in food-producing animals is now prohibited by the EU [46] because of their potential risk to humans. A lot of evidence has documented that exposure to both natural and synthetic chemicals at low levels may lead to toxic effects in humans, and this is associated with many diseases such as breast and uterine cancer [45]. Some hormonal anabolic compounds, such as 17β- estradiol, are still being used illegally in livestock production to promote growth rate. This compound is a natural estrogen which can be carcinogenic even at low levels, and it is listed within Group A in Annex I of the Council Directive 96/22/EC (Group A, substances having an anabolic effect and unauthorized substances) [46]. The monitoring of estradiol in milk samples is a challenging task due to the low level concentrations that should be detected and because of the complexity of the matrix. In general, the determination of estradiol in milk has been dominated by immunological [47] and microbiological techniques, which are easy to perform, but are not specific enough to ensure accurate identification. Chromatographic techniques (LC or GC), using mass spectrometry detection [48-50] have been used and can overcome these problems. However, previous sample preparation processes are necessary to achieve the optimal sensitivity, selectivity and specificity. In recent years, several sample preparation procedures for the isolation of the analyte and purification of the sample have been developed for the concentration and clean-up of estradiol in milk samples. These include liquid-liquid extraction (LLE) [49], solid-liquid extraction (SPE) [50], molecularly imprinted solid phase extraction (MISPE) [51],and multi step solid phase extraction (MSPEE) [51], which can be time-consuming and tedious to perform.

5. State of art

The growing concern for human and animal health and the existence of Community directives, which set maximum permitted levels of certain mycotoxins, antibiotics and hormones in many food products, require the need for methods of analysis for the strict monitoring of the levels of these substances in raw materials and processed products. As an alternative method, for instance, optical biosensors, offer several advantages compared to conventional analysis [52]. A biosensor is an analytical device, used for the detection of an analyte, that consists:

- the *sensitive biological element* (e.g. tissue, microorganisms, organelles, cell receptors, enzymes, antibodies, nucleic acids, etc.), a biologically derived

material or biomimetic component that interacts (binds or recognizes) the analyte under study.

- the *transducer* or the *detector element* (works in a physicochemical way; optical, piezoelectric, electrochemical, etc.) that transforms the signal resulting from the interaction of the analyte with the biological element into another signal (i.e., transduces) that can be more easily measured and quantified.

Biosensors can be grouped according to their biological element or their transduction element. Biological elements include enzymes, antibodies, micro-organisms, biological tissue, and organelles. Antibody-based biosensors are also called immunosensors. When the binding between the sensing element and the analyte is a detected event, the instrument is described as an affinity sensor. When the interaction between the biological element and the analyte is accompanied or followed by a chemical change in which the concentration of one of the substrates or products is measured, the instrument is described as a metabolism sensor. Finally, when the signal is produced after binding the analyte, without chemically changing, but by converting an auxiliary substrate, the biosensor is called a catalytic sensor. The method of transduction depends on the type of physicochemical change resulting from the sensing event. Optical biosensors that exploit light absorption, fluorescence, luminescence, reflectance, Raman scattering and refractive index are powerful alternatives to conventional analytical techniques [53]. A schematic representation of an optical biosensor is shown in figure 1.

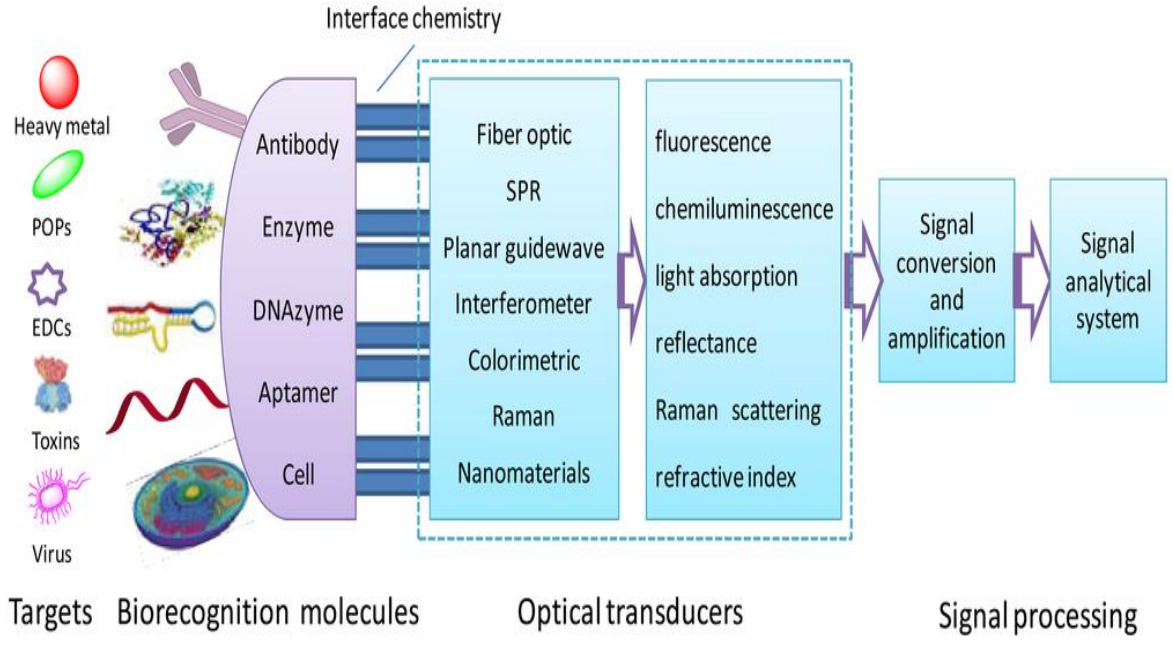

Figure 1. A schematic representation of an optical biosensor.

The advantages of using advanced optical biosensors for sensing analytes are the fast response, the efficiency and the use of non-trained personnel for their utilization, low cost for sample, high selectivity, high sensitivity, and high throughput**.** Extensive

extraction and sample clean-up are not needed. Such methods have been shown to have a potential for the routine analysis of many mycotoxins.

6. Aim of the thesis

The aim of this project is the development of an advanced diagnostic optical platform for simple determinations of micotoxins, antibiotics and hormones in food. This will help to ensure a high quality of raw materials, with particular reference to milk, apple juice and processed products; more in general it will contribute to food safety. This objective is pursued through the study and development of methodologies that utilize proteins, enzymes, antibodies and/or aptamers as specific probes for the design of advanced optical biosensors (assays such as Surface plasmon resonance (SPR), fluorescence polarization assays).

7. Surface Plasmon Resonance

Surface plasmon resonance (SPR) has become an important optical biosensing technology in the areas of biochemistry, biology, and medical sciences because of its real-time, label-free, and non invasive nature [54-55]. The surface plasmon resonance (SPR) technique is a well-established method for the quantification of binding constants between surface-immobilized molecules and molecules in solution. Surface plasmon resonance (SPR) spectroscopy is a powerful, label-free technique to monitor non covalent molecular interactions in real time and in a non invasive fashion. As a label-free assay, SPR does not require tags, dyes, or specialized reagents (e.g., enzymes–substrate complexes) to elicit a visible or a fluorescence signal.
Surface Plasmon resonance is an evanescent-wave phenomenon, in simplest terms, it is a technique used to detect changes in refractive index at the surface of a sensor. The sensor is comprised of a glass substrate and thin gold coating. Light passes through the substrate and is reflected off of the gold coating (Figure 2). At certain angles of incidence, a portion of the light energy couples through the gold coating and creates a surface plasmon wave at the sample and gold surface interface. The angle of incident light required to sustain the surface plasmon wave is very sensitive to changes in refractive index at the surface (due to mass change), and it is these changes that are used to monitor the association and dissociation of biomolecules. This change in the resonance angle can be followed in real time, thus providing kinetic information on film formation.

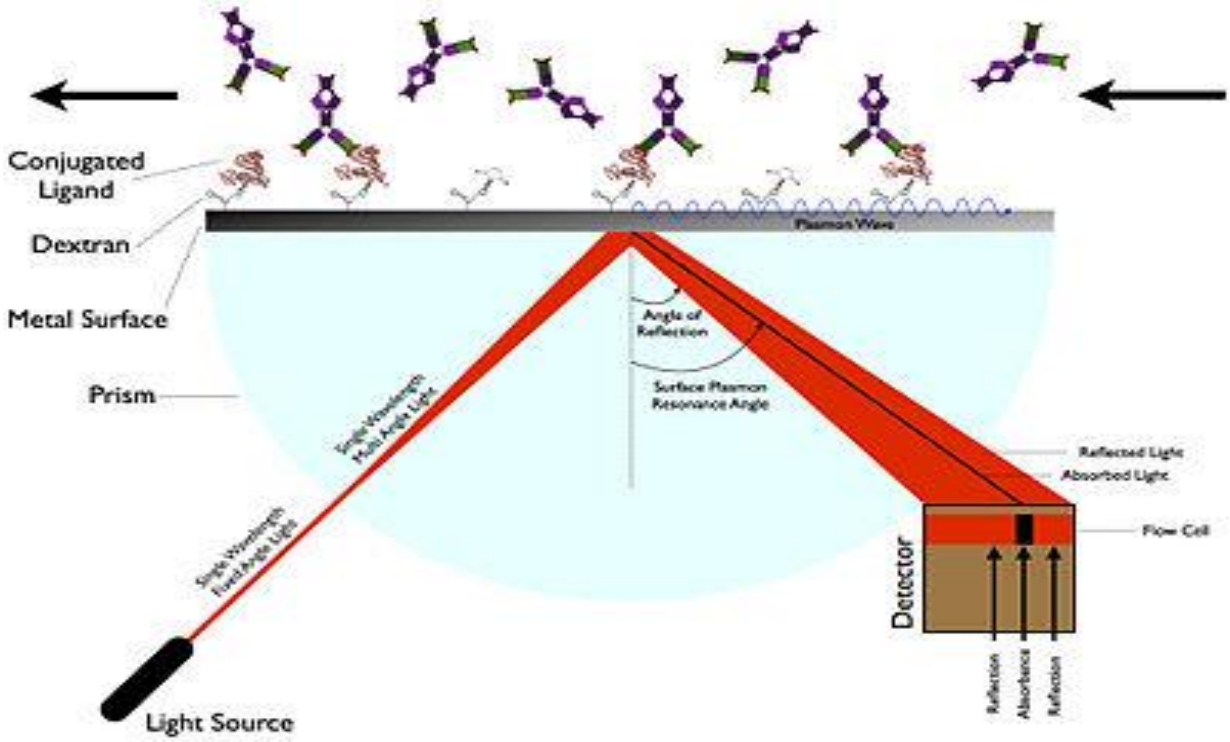

Figure 2. Surface Plasmon Resonance.

The fully integrated SPR sensor used by SensiQ Technologies is a highly sensitive, static, and stable optical design. Light emitted by an LED passes through a polarizer and reflects off of the gold sensing surface. A detector array then measures the reflected light and calculates the angle at which light has coupled through the gold surface as an attenuation or dip in the signal.
As mass accumulates at the sensor surface during a binding interaction, the refractive index increases and an increase in signal is observed. After the sample is replaced by buffer, mass will decrease at the surface during the dissociation phase and with a subsequent decrease in the resonance unit response (Figure 3).

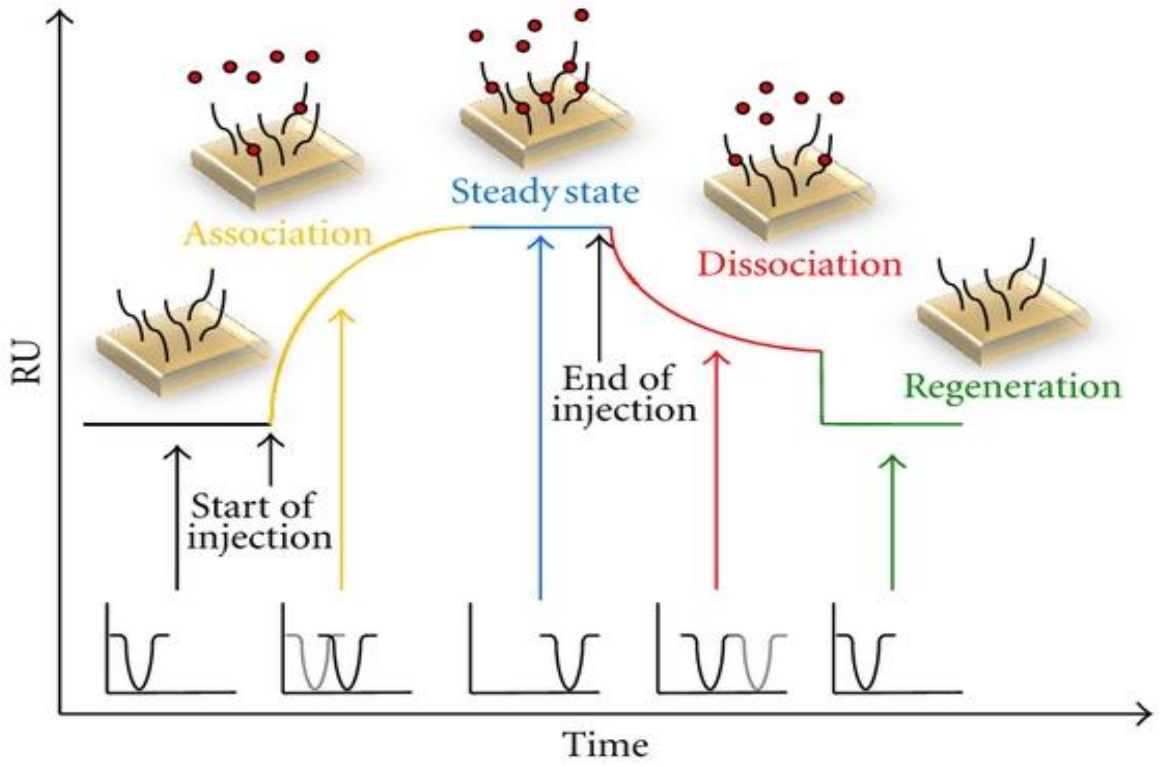

Figure 3. Typical shape of an SPR-sensorgram. It can be divided into four phases: association phase, steady state or equilibrium phase, dissociation phase, and regeneration phase.

8. Fluorescence Polarization Assay

The theory of Fluorescence Polarization, first described in 1926 by Perrin, is based on the observation that fluorescent molecules in solution, excited with plane-polarized light, will emit light back into a fixed plane if the molecules remain stationary during the excitation of the fluorophore [56]. Molecules, however, rotate and tumble, and the planes into which light is emitted can be very different from the plane used for initial excitation. Fluorescence Polarization assays are homogeneous, single-step assays ideally suited for high-throughput screening of large numbers of samples. All Fluorescence Polarization assays employ a large molecular species, or binding partner, in conjunction with a low molecular weight analyte or molecule labeled with a fluorophore. When the large binding partner molecule is an antibody, the assay is referred to as a fluorescence polarization immunoassay. Fluorescence is by definition the ability of a molecule to absorb the energy of an incoming (excitation) photon and then re-emit most of this energy as a new, slightly less energetic (emission) photon. A small fluorescent molecule will rotate appreciably during the very small interval of time between absorption of a photon and emission of the fluorescence photon. If the excitation light is polarized, this rotation will result in complete randomization of the plane of the emitted light. Thus, small fluorescent molecules depolarize an excitation pulse of polarized light. Large fluorescent

molecules (MW > 100,000) do not rotate appreciably in the same small interval of time. They will therefore emit light that retains some of the polarization of the polarized excitation light. When a small fluorescent molecule becomes tightly bound to a large one, as in the binding of labeled molecule to an antibody, the rotational speed of the small molecule is abruptly reduced to that of the entire complex as a whole. Therefore, labeled molecule bound to its antibody represents a large fluorescent molecule, which exhibits a high degree of fluorescence polarization. Fluorescence polarization immunoassays are based on the competition of labeled analyte with free (i.e. unlabeled) analyte in the samples or standards for the high affinity binding site an antibody. The labeled analyte-antibody complex gives a high fluorescence polarization before the addition of a increasing amounts of unlabeled analyte, after the addition there will be a competition between the unlabeled and labeled analyte for the antibody. As the competition happens, some of the labeled analyte will be released from the antibody, and will resume its intrinsic, rapid rate of rotation. This will cause a detectable loss of fluorescence polarization (Figure 4).

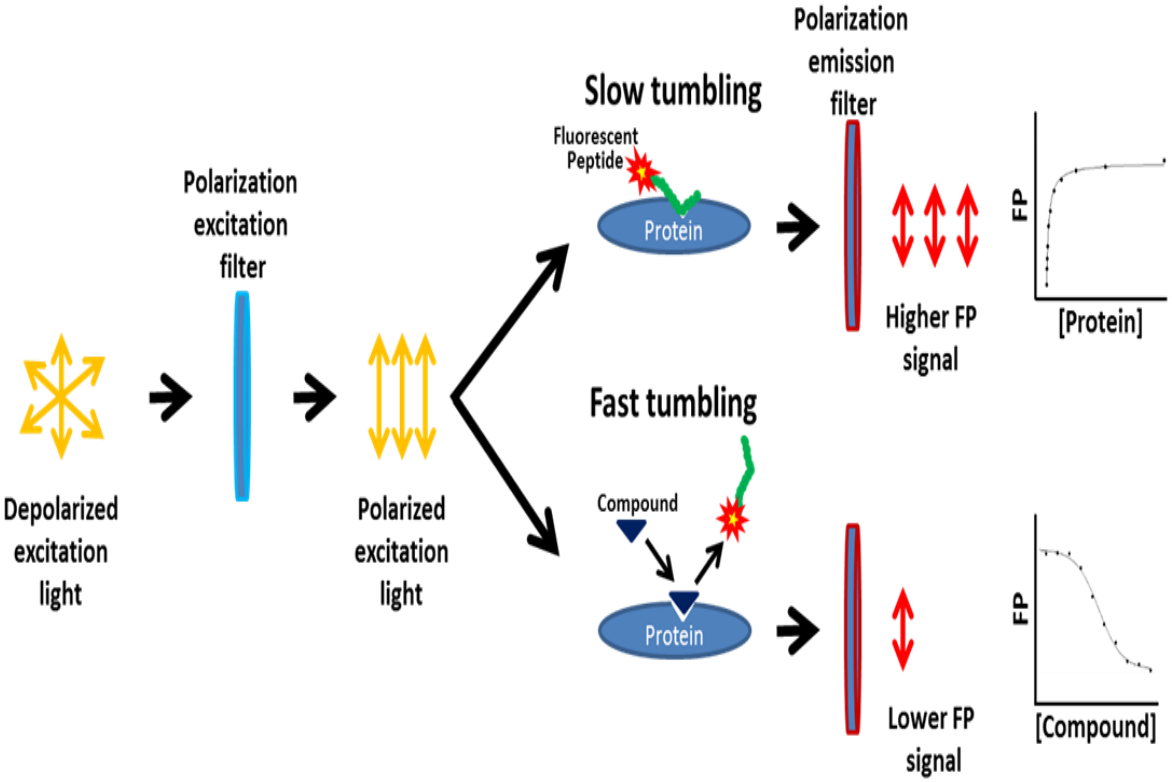

Figure 4. Schematic representation of fluorescence polarization immune-assay.

FP experiments are done in solution without solid supports, allowing true equilibrium analysis down to the low picomolar range. FP measurements do not adulterate samples, so they can be treated and reanalyzed in order to ascertain the effect on binding by changes such as pH, temperature, and salt concentration. Additionally, FP experiments are taken in "real-time" and experiments are not limited to equilibrium binding studies. Fluorescence Polarization offers numerous advantages over more conventional methods to study the binding between analytes (particularly in that no hazardous radioactive waste is generated) and has a lower limit of detection in the

pico-nanomolar range [57]. Fluorescence polarization technology provides very rapid answers with minimal effort. The homogeneous assay technology does not require any washing steps, which not only speeds up the assay process, but also eliminates the need for additional instrumentation. The assays are easy to run, require few reagent additions, and yet provide accurate quantitative results with a sensitivity and specificity equivalent to or greater than other existing methods.
In particular, we used a fluorophore that emits in the near infrared-region of light to make analyses directly in food matrices (Figure 4). In fact, in this spectral region, there is almost no unspecific absorption of food matrices making possible both qualitative and quantitative assays [58].

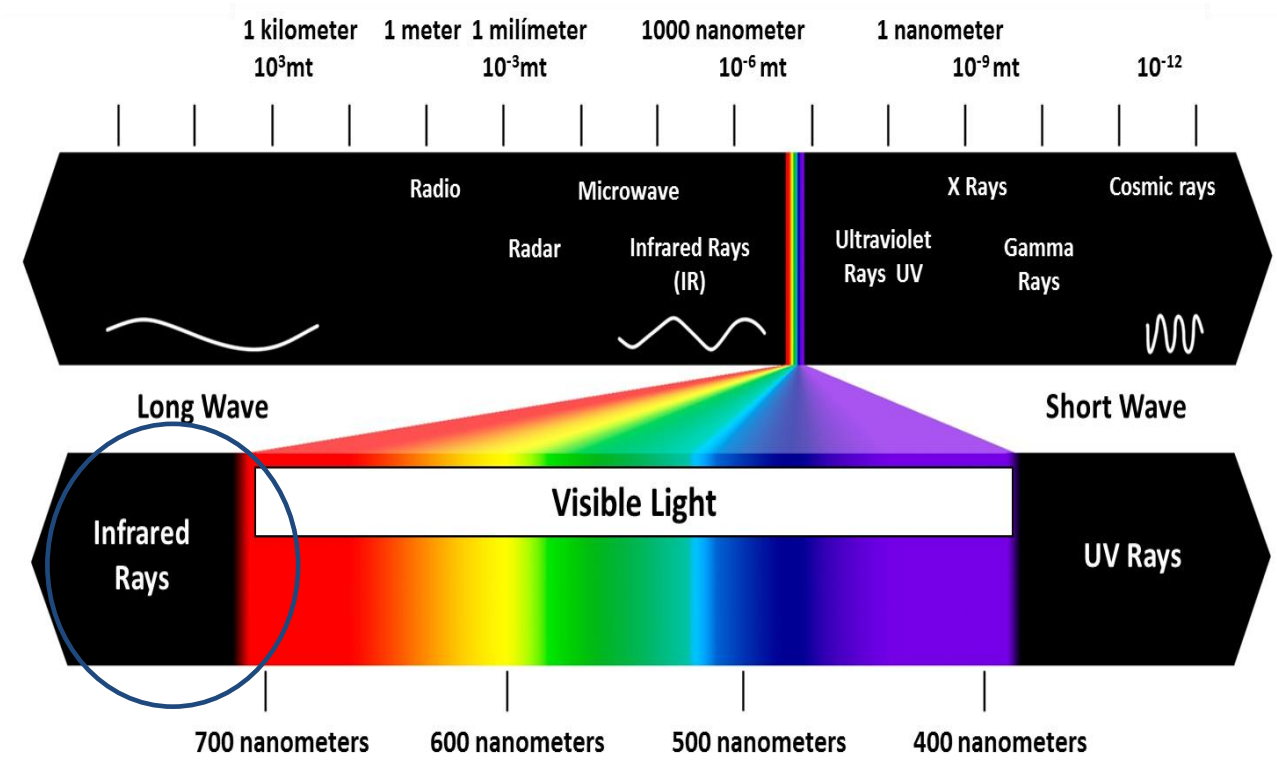

Figure 4. Light spectrum.

The choice to use this class of dye is related to the fundamental advantages offered from this compound such a significant reduction of the background signal, low absorption in the visible region of the light, low light scattering and the requirement of an inexpensive illumination light source. In particular, in some instances, auto-fluorescence may limit the detection of weak signals with fluorophores that emit in the visible region. Since most biomolecules have very low absorption in the NIR region, the fluorescence probes (e.g. the infrared emitting DayLight IF800) provide a level of performance not achievable with the use of visible emitting fluorescence dyes. Bright, clear images with extremely clean backgrounds and excellent sensitivity are provided with this approach. In addition, the use of NIR dyes is currently part of the emerging technologies related to numerous different relevant biological uses. In fact, in the recent years, NIR fluorescence dyes have found several applications in biomedical and material applications [58]. The minimal interference in absorption and

fluorescence emission from biological samples due to their low absorption coefficient in the NIR region, allow for the use this class of fluorescence dyes for monitoring *in vitro* and *in vivo* the levels of many biologically relevant molecules [58]. We used the NIR dyes properties to detect traces of patulin in apple juice samples and traces of penicillin G and estradiol in milk.

Traditionally spectroscopic instruments such as a fluorometer (see Fig.5) are used for fluorescence polarization studies. In these instruments the sample is placed in a cuvette. As shown in this figure, the excitation and emission wavelengths of light are selected using monochromators. The signal intensity from the fluorophores is recorded on a non pixelated detector such as a PMT. This allows for the measurement of bulk properties of a population of fluorophores. Fluorescence polarization (FP) measurements are made through two different polarizing filters that are parallel and perpendicular to the plane of the polarized excitation source. Polarization values for any fluorophore complex are inversely related to the speed of molecular rotation of that complex. Because the speed of rotation is also inversely related to the size of the molecule, polarization values will be high with large molecule complexes, and low with small molecules. The fluorescence intensity of the emitted light is monitored through both parallel and perpendicular filters. The degree of transfer of emission intensity from parallel to perpendicular is proportional to the rotational speed of the fluorescent molecule. If a molecule is very large, there is very little movement during excitation and thus little transfer from the parallel signal to the perpendicular signal. However, if the fluorescent molecule is small, rotational speed is faster, resulting in a greater degree of transfer from the parallel to perpendicular signal

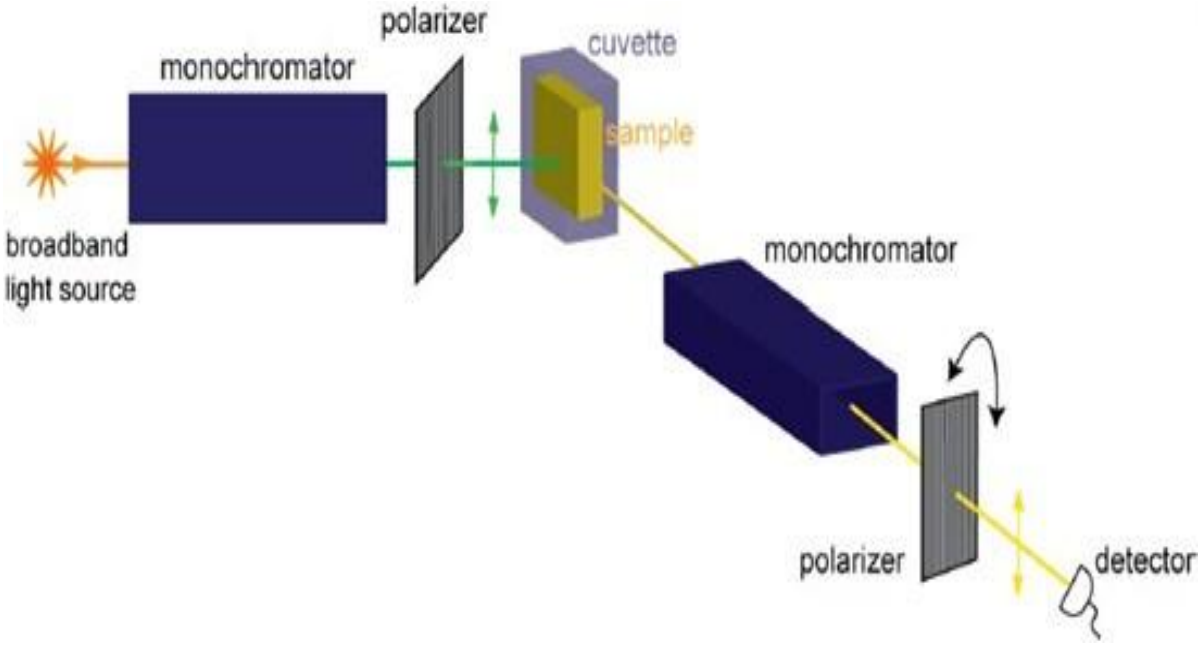

Figure 5. Spectrofluorometer for polarization measurement. One of the polarizers (typically the polarizer in the emission light path) is rotated along parallel or orthogonal directions to obtain I|| and I⊥measurements.

Fluorescence polarization measurements have long been a valuable biophysical research tool for investigating processes such as membrane lipid mobility, myosin reorientation and protein–protein interactions at the molecular level. Immunoassays that have been developed and used extensively for clinical diagnostics represent the largest group of bioanalytical applications. Other biological applications include the study of association of proteins with larger molecules.

9. Work Description

Work description has been organized in the following sections:

SECTION I-PATULIN

- Synthesis of Patulin Derivatives
- Conjugating of patulin to protein carrier BSA to immunize the rabbits to obtain antibodies against patulin
- Antibody production and polyclonal monospecific antipatulin antibodies purification
- Development of an innovative method of immunoassay outside the laboratory based on surface plasmon resonance (SPR) for the detection of patulin in foods using SensIQ Discovery of ICX.
- Synthesis of labeled GlnBP-Pat with probe Dylight IF 800 (GlnBP-Pat-IF800) to develop the fluorescence polarization immunoassay in PBS buffer
- The fluorescence polarization assay was performed directly in fruit juice.

SECTION II- PENICILLIN G

- Conjugating of penicillin G to protein carrier BSA to immunize the rabbits to obtain antibodies against penicillin G
- Antibody production and polyclonal monospecific antipenicillin G antibodies purification
- Development of an innovative method of immunoassay outside the laboratory based on surface plasmon resonance (SPR) for the detection of penicillin G
- Synthesis of labeled GlnBP-PenG with probe CF 647 (GlnBP-PenG-CF647) to develop the fluorescence polarization immunoassay in PBS buffer
- The fluorescence polarization assay was performed directly in milk.

SECTION III – ESTRADIOL

- Synthesis of Estradiol Succinate
- Conjugating estradiol to protein carrier BSA to immunize the rabbits to obtain the antibodies against estradiol
- Antibody production and polyclonal monospecific antiestradiol antibodies purification
- Development of an innovative method of immunoassay outside the laboratory based on surface plasmon resonance (SPR) for the detection of estradiol
- Synthesis of labeled GlnBP-ES with probe CF 647 (GlnBP-ES-CF647) to develop the fluorescence polarization immunoassay in PBS buffer
- The fluorescence polarization assay was performed directly in milk.

10. References

1. Wills W. J., Meah A., Dickinson A. M. and Short F. (2013). 'I don't think I ever had food poisoning'. A practice-based approach to understanding foodborne disease that originates in the home. Appetite; 85: 118-125.

2. Todd E. C. (1997). Epidemiology of foodborne diseases: a worldwide review. World Health Stat Q; 50 (1-2): 30-50.

3. Girma K., Tilahun Z. and Haimanot D. (2014). Review on Milk Safety with Emphasis on Its Public Health. World Journal of Dairy & Food Sciences; 9 (2): 166-183.

4. Redmond E. C. and Griffith C. J. (2003). Consumer food handling in the home: a review of food safety studies. J Food Prot.;66 (1):130-61.

5. Turner N. W., Subrahmanyam S. and Piletsky S. A. (2009). Analytical methods for determination of mycotoxins: a review. Anal. Chim. Acta; 632 (2): 168–80.

6. Richard J. L. (2007). Some major mycotoxins and their mycotoxicoses-an overview. Int. J. Food Microbiol.; 119 (1–2): 3–10.

7. Robbins C. A., Swenson L.J., Nealley M. L., Gots R. E. and Kelman B. J. (2000). Health effects of mycotoxins in indoor air: a critical review. Appl Occup Environ Hyg; 15 (10): 773–84.

8. Moss M. O. (2008). Fungi, quality and safety issues in fresh fruits and vegetables. J. Appl. Microbiol.; 104 (5): 1239–43.

9. Trucksess M. W. and Scott P. M. (2008). Mycotoxins in botanicals and dried fruits: A review. Food Addit Contam.; 25 (2): 181–92.

10. Cornely O. A. (2008). *Aspergillus* to Zygomycetes: causes, risk factors, prevention, and treatment of invasive fungal infections. Infection; 36 (4): 296–313.

11. Desjardins A. E. and Proctor R. H. (2007). Molecular biology of *Fusarium* mycotoxins. Int. J. Food Microbiol.; 119 (1–2): 47–50.

12. Bennett J. W. and Klich M. (2003). Mycotoxins. Clin. Microbiol. Rev.; 16 (3): 497-516.

13. Junaid S. A., Olarubofin F. and Olabode A.O. (2010). Mycotic contamination of stockfish sold in Jos, Nigeria. Journal of Yeast and Fungal Research; 1(7): 136-141.

14. De Champdoré M., Bazzicalupo P., De Napoli L., Montesarchio D., Di Fabio G., Cocozza I., Parracino A., Rossi M. and D'Auria S. (2007). A New Competitive Fluorescence Assay for the Detection of Patulin Toxin. Anal. Chem.; 79 (2): 751–757.

15. Wilson D. M. (1976). Mycotoxins and other fungal related problems. In *Advances in chemistry*; Rodriks, J. V., Ed.; American Chemical Society: Washington, DC; 149: 90.

16. Bullerman L. B. (1976). Examination of Swiss cheese for incidence of mycotoxin producing molds. J. Food Sci.; 41: 26.

17. CAST, (2003). Mycotoxins: Risks in plant, animal, and human systems. Council of Agricultural Science and Technology, CAST, Ames, IA. Task Force Report No. 139. 199 pp.

18. Rychlik M., Kircher F., Schusdziarra V. and Lippl F. (2004). Absorption of the mycotoxin patulin from the rat stomach. Food Chem. Toxicol.; 42: 729−735.

19. Liu B. H., Yu F. Y., Wu T. S., Li S. Y., Su M. C., Wang M. C. and Shi S.M. (2003). Evaluation of genotoxic risk and oxidative DNA damage in mammalian cells exposed to mycotoxins, patulin and citrinin. Toxicol Appl Pharmacol.; 191: 255–263.

20. Olinski R., Jaruga P. and Zastawny T. H. (1998). Oxidative DNA base modifications as factors in carcinogenesis. Acta Biochim. Pol.; 45: 561−572.

21. Riley R. T. and Showker J. L. (1991). The mechanism of patulin's cytotoxicity and the antioxidant activity of indole tetramic acids. Toxicol. Appl. Pharmacol.; 109: 108−126.

22. Fliege R. and Metzler M. (2000). Electrophilic properties of patulin. Adduct structures and reaction pathways with 4-bromothiophenol and other model nucleophiles. Chem. Res. Toxicol.; 13: 373−381.

23. Pfeiffer E., Diwald T. T. and Metzler M. (2005). Patulin reduces glutathione level and enzyme activities in rat liver slices. Mol. Nutr. Food Res.; 49 (4): 329−336.

24. Arafat W., Kern D. and Dirheimer G. (1985). Inhibition of aminoacyl-tRNA synthetases by the mycotoxin patulin. Biochem. Int.; 56 (2−3): 333−349.

25. Lee K. S. and Roschenthaler R.(1986). DNA damaging activity of patulin in E.coli. Appl. Environ. Microbiol.; 152 (5): 1046−1054.

26. Pennacchio A., Ruggiero G., Staiano M., Piccialli G., Oliviero G., Lewkowicz A., Synak A., Bojarski P., D'Auria S. (2014). A surface plasmon resonance based biochip for the detection of patulin toxin. Optical Materials; 36 (10): 1670–1675.

27. WHO, Joint FAO/WHO Expert Committee on Food Additives (JEFCA) 1998. Position paper on patulin, 30th session, The Hague, The Netherlands, 9−13.

28. European Commission (2003). EC No. 1425/2003; Brussels, Belgium.

29. Lai C. L., Fuh Y. M. and Shih D. Y. C. (2000). Detection of mycotoxin patulin in apple juice. J. Food Drug Anal.; 8 (2): 85−96.

30. Watanabe M. and Shimitzu H. (2005). Detection of Patulin in Apple Juices Marketed in the Tohoku District, Japan. J. Food Protection; 68 (3): 610−612.

31. Sforza S., Dall'Asta C. and Marchelli R. (2006). Recent advances in mycotoxin determination in food and feed by hyphenated chromatographic techniques/mass spectrometry. Mass Spectrom. Rev.; 25 (1): 54-76.

32. Azcona-Olivera J. I., Abouzied M. M., Plattner R. D. and Pestka J. J. (1992). Production of monoclonal antibodies to the mycotoxins fumonisins B1,B2 and B3. J. Agric. Food Chem.; 40: 531−534.

33. Fun S. Chu. (2009). Recent Studies on Immunoassays for Mycotoxins.; ACS Symposium Series-Chapter (Book); 621 (22): 294–313.

34. Chu F. S. and Ueno I. (1977). Production of antibody against aflatoxin B1. Appl. Environ. Microbiol.; 33: 1125−1128.

35. Achi O. K. and Ugbogu G. A. (2006). Characterization of Drug Resistant *Staphylococcus Aureus* of Animal Origin. Journal of Biological Sciences; 6 (6): 1088-1092.

36. Jukes T. H. and Williams W. L. (1953). Nutritional effects of antibiotics. Pharmacol. Rev.; 5: 381-420.

37. Phillips I., Casewell M., Cox T., De Groot B., Friis C., Jones R., Nightingale C., Preston R. and Waddell J. (2004). Does the use of antibiotics in food animals pose a risk to human health? A critical review of published data. Journal of Antimicrobial Chemotherapy; 53: 28–52.

38. Committee on Animal Health and the Committee on Animal Nutrition (1980). The Effects on Human Health of Subtherapeutic Use of Antimicrobials in Animal Feeds. Appendix K Antibiotics In Animal Feeds.

39. Lee M. H., Lee H. J. and Ryu P. D. (2001). Public Health Risks: Chemical and Antibiotic Residues–Review. Asian-Australasian Journal of Animal Sciences;14(3): 402-413.

40. Witte W. (1998). Medical consequences of antibiotic use in agriculture. Science; 279: 996–7.

41. Kyung M. S., Minseon C., Hunho J., Kyoungin M., Sung H. J., Taisun K., Min S. H., Ja K. K. and Changill B. (2001). Gold nanoparticle-based colorimetric detection of kanamycin using a DNA aptamer. Analytical Biochemistry; 415 (2-15), 175–181.

42. Blasco C., Di Corcia A. and Picó Y. (2009). Determination of tetracyclines in multi-specie animal tissues by pressurized liquid extraction and liquid chromatography- tandem mass spectrometry. Food Chem.; 116: 1005-1012.

43. Kokkonen M. K. and Jestoi M. N. (2009). A Multi-compound LC-MS/MS Method for the Screening of Mycotoxins in Grains. Food Anal. Methods; 2 (2) : 128-140.

44. Benito-Peña E., Urraca J. L. and Moreno-Bondi M. C. (2009). Quantitative determination of penicillin V and amoxicillin in feed samples by pressurised liquid extraction and liquid chromatography with ultraviolet detection. Journal of Pharmaceutical and Biomedical Analysis; 49 (2): 289-294.

45. Johnson B. J., Ribeiro F. R. B. and Beckett J. L. (2013). Application of growth technologies in enhancing food security and sustainability. Animal Frontiers. The review magazine of animal agriculture: 3 (3): 8-13.

46. Council Directive 96/22 EC, Off. J. Eur. Comm., L125 (1996) 3.

47. Vdovenko M.M., Gribas A.V., Vylegzhanina A.V. and Sakharov I.Y. (2012). Development of a chemiluminescent enzyme immunoassay for the determination of dexamethasone in milk. Analytical Methods: 4 (8): 2550-2554.

48. Ehling S. and Reddy T. M. (2013). Liquid Chromatography−Mass Spectrometry Method for the Quantitative Determination of Residues of Selected Veterinary Hormones in Powdered Ingredients Derived from Bovine Milk. Agric. Food Chem.; 61: 11782−11791.

49. Noppe H., Le Bizec B. and Verheyden K. (2008). Novel analytical methods for the determination of steroid hormones in edible matrices**.** Analytica chimica Acta; 1–16.

50. Blasco CC.,, Van Poucke C. and Van Peteghem C. (2007). Analysis of meat samples for anabolic steroids residues by liquid chromatography/tandem mass spectrometry. Journal of Chromatography A; 1154 (1–2): 230–239.

51. Zander A., Findlay P., Renner T., Sellergren B. and Swietlow A. (1998). Analysis of Nicotine and Its Oxidation Products in Nicotine Chewing Gum by a Molecularly Imprinted Solid-Phase Extraction. Anal. Chem.; 70 (15): 3304–3314.

52. Long F., Zhu A. and Shi H. (2013). Recent Advances in Optical Biosensors for Environmental Monitoring and Early Warning. Sensors; 13: 13928-13948; doi:10.3390/s131013928.

53. Dey D. and Goswami T. (2011). Optical Biosensors: A Revolution Towards Quantum Nanoscale Electronics Device Fabrication. Journal of Biomedicine and Biotechnology; 2011 Article ID 348218, http://dx.doi.org/10.1155/2011/348218.

54. Haes A. J. and Van Duyne R. P. (2002). A Nanoscale Optical Biosensor: Sensitivity and Selectivity of an Approach Based on the Localized Surface Plasmon Resonance Spectroscopy of Triangular Silver Nanoparticles. J. Am. Chem. Soc., 124 (35):10596–10604.

55. Jorgenson R.C. and Yee S. S. (1993). A fiber-optic chemical sensor based on surface plasmon resonance. Sensors and Actuators B: Chemical; 12 (3): 213–220.

56. Seethala R. and Menzel R. (1997). A Homogeneous, Fluorescence Polarization Assay for Src-Family Tyrosine Kinases. Analytical Biochemistry; 253: 210-218.

57. Szmacinski H. and Lakowicz J. R. (1995). Fluorescence lifetime-based sensing and imaging. Sensors and Actuators B: Chemical; 29 (1-3): 16-24.

58. Frangioni J. V. (2003). *In vivo* near-infrared fluorescence imaging. Current Opinion in Chemical Biology; 7 (5): 626–634.

CHAPTER 1
A surface plasmon resonance based biochip for the detection of patulin toxin

Optical Materials 36 (2014) 1670–1675

Contents lists available at ScienceDirect

Optical Materials

journal homepage: www.elsevier.com/locate/optmat

A surface plasmon resonance based biochip for the detection of patulin toxin

Anna Pennacchio [a], Giuseppe Ruggiero [a], Maria Staiano [a], Gennaro Piccialli [b], Giorgia Oliviero [b], Aneta Lewkowicz [c], Anna Synak [c], Piotr Bojarski [c,*], Sabato D'Auria [a,*]

[a] Laboratory for Molecular Sensing, IBP-CNR, Naples, Italy
[b] Dipartimento di Farmacia, University of Naples Federico II, Naples, Italy
[c] Institute of Experimental Physics, University of Gdansk, Gdansk, Poland

ARTICLE INFO

Article history:
Available online 29 January 2014

Keywords:
Surface plasmon resonance
Biosensors
Patulin
Food
Health

ABSTRACT

Patulin is a toxic secondary metabolite of a number of fungal species belonging to the genera *Penicillium* and *Aspergillus*.

One important aspect of the patulin toxicity *in vivo* is an injury of the gastrointestinal tract including ulceration and inflammation of the stomach and intestine. Recently, patulin has been shown to be genotoxic by causing oxidative damage to the DNA, and oxidative DNA base modifications have been considered to play a role in mutagenesis and cancer initiation.

Conventional analytical methods for patulin detection involve chromatographic analyses, such as HPLC, GC, and, more recently, techniques such as LC/MS and GC/MS. All of these methods require the use of extensive protocols and the use of expensive analytical instrumentation.

In this work, the conjugation of a new derivative of patulin to the bovine serum albumin for the production of polyclonal antibodies is described, and an innovative competitive immune-assay for detection of patulin is presented. Experimentally, an important part of the detection method is based on the optical technique called surface plasmon resonance (SPR). Laser beam induced interactions between probe and target molecules in the vicinity of gold surface of the biochip lead to the shift in resonance conditions and consequently to slight but easily detectable change of reflectivity.

1. Introduction

The enhanced intensity of fluorescence by gold and silver in the form of nanoparticles and thin films in the optical detection process called surface plasmon resonance (SPR) are the most extensively investigated due to their applications in sensing, detecting, and imaging [1–6].

A surface plasmon is an electro-magnetic wave propagating along the surface of a thin metal layer or nanoparticles. Optical excitation of the surface plasmon can be achieved in the Kretschmann geometry, where p-polarised, collimated light beam undergoes total internal reflection at a glass-metal film-dielectric interface [6]. The specific angle at which the resonance occurs is sensitive to any change in the refractive index of the medium contiguous to the metal surface.

The growing concern for human and animal health is expressed by EU Community directives, which set maximum permitted levels of certain mycotoxins in many food products. Therefore, there is a need to elaborate methods of analysis for the strict monitoring of the levels of mycotoxins in raw materials and processed products. A mycotoxin is a toxic secondary metabolite produced by organisms of the fungus kingdom [7,8]. Mycotoxins are developed both on the plants before harvesting (contamination from the field) and in food crops after the harvest itself, during the processes of conservation. The foods most vulnerable to direct contamination are mainly cereals, oilseeds, dried fruit and dried vegetables, spices, coffee and cocoa [9–13]. Mycotoxins greatly resist decomposition or being broken down in digestion, so they remain in the food chain in meat and dairy products. Because of their detrimental action on the cellular function, they exert some actions: nephrotoxic (ochratoxin), hepatotoxic (aflatoxin), immune-toxic (aflatoxins, ochratoxin), mutagenic (aflatoxins), teratogen (OA) and carcinogenic (aflatoxins, ochratoxin, fumonisin) [9]. Patulin is a toxin produced by the *P. expansum, Aspergillus, Penicillium,* and

Abbreviations: SPR, surface plasmon resonance; GlnBP, glutamine-binding protein.

* Corresponding authors. Address: University of Gdansk, Institute of Experimental Physics, Wita Stwosza 57, 80-952 Gdansk, Poland. Tel.: +48 725 991 221; fax: +48 58 5232026 (P. Bojarski). Address: Laboratory for Molecular Sensing, IBP-CNR, Via Pietro Castellino, 111, 80131 Naples, Italy. Tel.: +39 0816132250; fax: +39 0816132277 (S. D'Auria).

E-mail addresses: fizpb@univ.gda.pl (P. Bojarski), s.dauria@ibp.cnr.it (S. D'Auria).

0925-3467/$ - see front matter © 2014 Elsevier B.V. All rights reserved.
http://dx.doi.org/10.1016/j.optmat.2013.12.045

Paecilomyces fungal species [14,15]. Although patulin has not been shown to be carcinogenic, it has been reported to damage the immune system [15]. In 2004, the European Community set limits to the concentrations of patulin in food products. They currently stand at 50 μg/kg in all fruit juice concentrations, at 25 μg/kg in solid apple products used for direct consumption, and at 10 μg/kg for children's apple products, including apple juice [14,15]. One important aspect of patulin toxicity *in vivo* is an injury of the gastrointestinal tract including ulceration and inflammation of the stomach and intestine. Recently, patulin has been shown to be genotoxic by causing oxidative damage to the DNA, and oxidative DNA base modifications have been considered to play a role in mutagenesis and cancer initiation. Patulin is believed to exert its cytotoxic effects mainly by forming covalent adducts with essential cellular thiol groups in proteins and amino acids. From a chemical point of view patulin is a water-soluble unsaturated lactone, readily reactive toward thiol groups and also amino groups. Glutathione represents one of the most abundant cellular nucleophiles, and it has been shown to spontaneously form covalent adducts with patulin. The same reactivity is responsible for the ability of patulin to induce in vitro intra- and intermolecular protein cross-links involving cysteine residues and lysine and histidine side chains and for the capability to inhibit the activity of several enzymes.

The widespread presence of fungi in the environment renders mycotoxins practically ubiquitous contaminants in food and feeds; therefore, one of the most effective measures to protect public health is to establish reasonable regulatory levels of these toxins on the basis of valid toxicological data. Conventional analytical methods of patulin detection involve chromatographic analyses, such as HPLC, GC [16,17] and, more recently, techniques such as LC/MS and GC/MS [18]. However, extensive protocols of sample cleanup are required prior to the analysis, and expensive analytical instrumentation is necessary to accomplish it. Furthermore, the problem of precise quantitative determination of patulin and other mycotoxins by these methods is particularly important due to the high variability of the real matrixes and can be solved only by exploiting isotopically labeled internal standards. All these limitations make it difficult to extend the methods to detect patulin outside the laboratory.

As an alternative, optical biosensors offer several advantages compared to conventional analysis matrices. Some of the advantages of using advanced optical biosensors for sensing analytes are the fast response, the efficiency, high sensitivity and the use of non-trained personnel for their utilization. In fact, these methods have been shown to have a potential for the routine analysis of many mycotoxins [19–21].

However, to develop an immunoassay for patulin detection it is necessary to produce specific antibodies. Patulin is, like other non-proteinaceous toxins, anon-immunogenic low molecular weight compound (MW 154). This implies that to develop antibodies it is necessary to conjugate patulin to a protein carrier. Recently, some of us have reported the conjugation of new patulin derivative to the bovine serum albumin carrier protein for the production of polyclonal antibodies in rabbits [22].

In this work, we present a novel optical surface plasmon resonance (SPR) based assay for patulin detection. The obtained results are discussed.

2. Experimental section

All reagents were of the highest commercially available quality and were used as received. 1-[3-(Dimethylamino)propyl]-3-ethylcarbodiimide (EDC), bovine serum albumin (BSA; fraction V), and ovalbumin (OVA; grade V) were purchased from Sigma. PURE1A Protein A Antibody Purification Kit was purchased from Sigma. Goat polyclonal to rabbit IgG-HRP conjugate (secondary antibody) was from Abcam. Affinity resin EAH Sepharose 4B was purchased from Amersham Biosciences. Nitrocellulose transfer membrane Protran from Schleicher & Schuell and ECL detection reagents from Amersham Biosciences were used in dot blot and Western blot experiments. Microplates (96-well), LockWell MaxiSorp from Nunc, 3,5,-tetramethylbenzidine (TMB) enzyme substrate from Sigma, and a microplate reader, Multiskan EX from Thermo, were used for ELISA experiments. UV measurements (detection at 278 nm) were carried out with Varian Cary 50 Bio spectrophotometer. The amino coupling group kit with HSA, NHS/EDC, HBS-EP buffer and CO_2H5 chips were purchased from ICX.

2.1. Synthesis of P-Sat–BSA conjugate

The patulin derivate (P-Sat) was synthesized from L-arabinose as described in [16]. To a solution of P-Sat (1.5 mg, 0.0054 mmol) in Tris (pH 8)/dioxane, 1:1 (v/v, 0.4 mL), were added 20 μL (1.0 mg, 0.0054 mmol) of an EDC solution in H_2O (50 mg/mL) and 0.5 mL of a BSA solution (8 mg/mL) in PBS (0.1 M) at pH 7.4. After 2 h at room temperature, the reaction mixture was dialyzed against PBS (0.01 M), NaCl (0.01 M), pH 7.4 (0.5 L, for 3 days with daily buffer changes). The conjugate concentration determined spectrophotometrically at 278 nm was 4.2 mg/mL.

2.2. Antibody production and IgG purification

Two rabbits were immunized following a standard protocol by intradermal inoculation of an antigen (0.5 mg per rabbit). After the immunization period, the rabbits were sacrificed and their blood recovered and centrifuged to separate blood cells from serum. A 2.0 mL sample of rabbit serum was applied to a protein A column of the PURE1A Protein A Antibody Purification Kit, Sigma, and the IgG fraction was purified according to the manufacturer's instructions. Elution of proteins was monitored by absorbance at λ = 278 nm. The IgG fraction was eluted with glycine (0.1 M) at pH 2.8 and immediately buffered in Tris 1.0 M at pH 9.0. SDS PAGE was carried out to evaluate the purity of the sample.

2.3. Affinity column preparation

The affinity column was obtained by conjugating derivative P-Sat to EAH Sepharose 4B as follows. A 1.0 mL sample of resin was washed with H_2O at pH 4.5 (20 mL), with NaCl (0.5 M) (20 mL), and again with H_2O at pH 4.5 (20 mL) and finally suspended in 2.0 mL of H_2O. The Sepharose resin was added to a solution of P-Sat (5 mg in 0.5 mL of H_2O at pH 4.5), and the resulting suspension was gently shaken. The slurry was cooled to 0 °C, and EDC was added in two steps to a final concentration of 0.1 M (52 mg). After 12 h at 4 °C, the reaction mixture was taken to room temperature, and after an additional 4 h the resin was extensively washed with H_2O at pH 4.5 and then treated with 1.0 mL of AcOH (0.1 M) and 38 mg of EDC for 1 h at room temperature. The suspension was washed with H_2O at pH 4.5 (20 mL), acetate buffer (0.1 M) containing NaCl (0.5 M) (20 mL), pH 4.0, and PBS (0.1 M) containing NaCl (0.3 M), pH 7.4 (20 mL), and finally packed into a polystyrene column (2 mL, BIORAD).

2.4. Antibody purification by affinity chromatography

For the affinity chromatography purification, a 2.0 mL aliquot of IgG (obtained from serum) was applied dropwise to the affinity column prepared as described above. To eliminate unspecific antibodies, the column, before elution, was washed with three high-salt buffers: (1) PBS (0.01 M), NaCl (0.1 M), pH 7.0 (20 mL);

(2) PBS (0.01 M), NaCl (0.5 M), pH 7.0 (20 mL); (3) PBS (0.01 M), NaCl (1.0 M), pH 7.0 (20 mL). At that point absorbance at 278 nm had fallen to 0.0. For the elution step glycine (0.1 M), pH 2.7 (2.5 mL), was applied to the column, and the eluate was collected in 0.5 mL fractions and monitored by absorbance measurements at 278 nm. The fractions containing the antibodies were collected, concentrated by means of a Centricon YM-3 membrane to a volume of 1.0 mL, and dialyzed against PBS (0.1 M), NaCl (0.1 M), pH 7.4. The concentration of the antibodies was spectrophotometrically determined by absorbance measurements at 278 nm.

2.5. Synthesis of GlnBP conjugates (P-Sat–GlnBP)

To avoid interference by the carrier protein in the polyclonal antibody detection process, P-Sat was conjugated to the glutamine-binding protein from Escherichia coli (GlnBP), a bacterial protein different from the protein used to carry out the immunization. The following procedure was used: 2.5 mg (0.0092 mmol) of P-Sat was dissolved in 0.25 mL of MES buffer (0.1 M), pH 5. The solution was incubated at room temperature with 0.25 mL of a GlnBP solution (5 mg/mL) in the same buffer and 0.1 mL of an aqueous solution of EDC (10 mg/mL). After 5 h, the reaction mixture was dialyzed against PBS (0.01 M) containing NaCl (0.1 M) at pH 7.4 (0.5 L, 3 days with daily buffer changes).

2.6. Antibody titration

The antibody titer was determined by an indirect ELISA assay by the following general procedure. The antigen (P-Sat–GlnBP), in PBS (0.1 M), pH 7.4, was used to coat 96-well microplates, varying the concentration by a factor 3 from 11 to $1.7 \cdot 10^{-3}$ μg/mL (one column for every antigen concentration, 100 μL per well), overnight at 4 °C. Control wells were incubated for the same period with BSA in the same buffer. The wells were rinsed three times with PBS (0.1 M) containing 0.05% Tween (PBS-T), pH 7.4, and blocked by incubation for 2 h at room temperature with PBS-T containing BSA (1%) (100 μL each well). After three washings with PBS-T, serially diluted antibody, aPsHS1 or aPsHS2, was added to the wells, incubated at room temperature for 1 h, and then rinsed three times with PBS-T. Horseradish peroxidase-conjugated anti-rabbit IgG antibodies, diluted 1:4000 in PBS-T containing BSA (1%), were added to the wells (100 μL) and incubated for 1 h at room temperature. After three washings with PBS-T, the enzyme substrate TMB was added (100 μL per well), and the color reaction was quenched after 5 min by addition of 1 M H_2SO_4 (100 μL per well). The absorbance was measured at 450 nm. The antibody titer was graphically determined by plotting the reciprocal of the antibody dilution *vs* absorbance for each dilution of antibodies. The titer was taken as the maximum antibody dilution able to give a reading of 0.1 absorbance unit. The following values were found: 1/25,000 for aPsHS1 and aPsHS2.

2.7. Surface plasmon resonance experiments (SPR)

The SPR measurements were carried out with the SensiQ Discovery instrument by SensiQ Technologies OK, USA) using the CO_2H5 sensor chip as a gold substrate (a glass slide coated with a thin layer of gold, to which a matrix of carboxy-methylated dextran is covalently attached). 10 mM HEPES (2-[4-(2-hydroxyethyl)-1-piperazinyl]-ethanesulfonic acid) buffer at pH 7.5, containing 150 mM NaCl, 0.005% polyoxyethylenes orbitan (P20) and 3.0 mM EDTA (ethylene-diammine-tetracetic acid) (HBS-EP) and sodium acetate 10 mM were used for all the experiments. The data collected during the experiments were deconvoluted using Qdat software. All experiments were carried out at a flow rate of 25 μL/min.

The fully integrated SPR sensor used by SensíQ Technologies is a highly sensitive, static, and stable optical design. Light emitted by an laser diode passes through a polarizer and reflects off of the gold sensing surface. A detector array then measures the intensity of reflected light and calculates the angle at which light has coupled through the gold surface as an attenuation or dip in the signal. As mass accumulates at the sensor surface during a binding interaction, the refractive index increases and an increase in signal is observed. After the sample is replaced by buffer, mass will decrease at the surface during the dissociation phase and with a subsequent decrease in the resonance unit response. By repeating this cycle at different concentrations, calculations can be made for k_a (on-rate) and k_d (off-rate) of the biomolecular interactions.

2.8. pH Scouting

Before immobilizing Pat-sat–GlnBP on the CO_2H5 chip the appropriate immobilization pH was found. In particular, in the case of a protein, the optimal pH of immobilization, should be in general higher than 3.5 and lower than the isoelectric point of the ligand. The procedure to look for the appropriate immobilization pH is called "pH scouting" and the analysis was performed with a SensiQ instrument. In our case the GlnBP-patulin was diluted in 10 mM sodium acetate pH 5.5, to a final concentration of 100 ng/mL in each sample. The flow rate was 25 μL/min and the contact time was 5 min. After the last injection, a washing solution (1 M ethanolamine pH 8.5) was injected to remove any remaining ligand molecule. From the sensor-gram analysis we found high immobilization level at pH 5.5. Therefore, this pH was chosen for the immobilization.

2.9. Surface preparation

The carboxy-methylated dextran layer in flow cell 2 was activated by injecting a 1:1 mixture of 0.05 M N-hydroxysuccinimide (NHS) and 0.2 M N-ethyl-N′-(dimethylaminopropyl) carbodiimide hydrochloride (EDC). The GlnBP-patulin was immobilized on the flow cell 2 of the chip CO_2H5. The remaining NHS esters were blocked by the injection of a 1.0 M ethanolamine hydrochloride solution (35 μL pH 8.5). The unreacted carboxymethylated dextran layer in flow cell 1 was used as reference surface.

2.10. Binding measurement

The surface plasmon resonance measurements were carried out over the concentration range of 0.0–80.0 nM of antibodies against derivative P-Sat. The concentration of polyclonal antibodies at 59 days of 20 immunization was determined by molar absorptivity at 278 nm. The concentrated stock solution was diluted in HBS-EP pH 7.4 buffer at the specific concentrations. The binding flow was fixed to 25 μL/min and the time of injection was 3 min. For the regeneration process the solution used was phosphoric acid 50 mM pH 3.0. The results obtained were analyzed by Qdat software.

2.11. Competition assay

The competition SPR assay was carried out at fixed concentration of antibody (80.0 nM) in the presence of an increased concentration of patulin (0.0–80.0 nM). The patulin was dissolved in water. The flow was fixed at 25 μL/min and the time of injection was 3 min. For the regeneration process the solution used was phosphoric acid 10 mM pH 3.0. The results obtained were analyzed by Qdat software.

3. Results and discussion

Nelow, we present an innovative immune-assay based on the use of surface plasmon resonance for an easy detection of patulin toxin.

3.1. Conjugation of patulin derivatives to the bovine serum albumin

BSA was chosen as the carrier protein, and hapten Pat-sat was conjugated to it by the water-soluble carbodiimide method, leading to antigens A (Fig. 1). The efficiency of the conjugation reaction could not be determined because of the lack of a UV chromophore in the case of derivative and because the maximum absorption at 278 nm of 4 and BSA overlapped.

3.2. Production of antibodies against the patulin

The antigen A was used to immunize rabbits for the production of polyclonal antibodies against patulin, following a standard protocol. At the end of the immunization period the IgG fraction of rabbits were isolated by the protein A column kit by standard procedures. The IgG fractions collected were pooled, concentrated, dialyzed against PBS 20 mM pH 7.4. To exclude false reactions due to anti-BSA antibodies present in the rabbit serums, a protein different from BSA was conjugated to the patulin derivatives P-Sat. For this purpose, the glutamine-binding protein (GlnBP) from *E. coli* was chosen. The GlnBP conjugate was prepared by the same procedures already used for BSA conjugate. Pat-sat–GlnBP, BSA as the positive control, and GlnBP as the negative one were spotted on four nitrocellulose membranes, and each membrane was incubated with immune antiserums (SI1 and SI2, 1:250 dilution) and pre-immune serums from both rabbits (SPI1 and SPI2, respectively, from rabbit 1 and rabbit 2, dilution 1:250). After incubation of the HRP conjugate secondary antibody and development with ECL-specific reagent, pre-immune serums showed no response, while SI1 and SI2 gave signals with antigen P-Sat–GlnBP and with BSA but not with GlnBP (not shown).

3.3. Immunoglobulin purification from serums

The IgG fraction of each serum (IgG1 from rabbit 1 and IgG2 from rabbit 2) was isolated by the protein A column kit by standard procedures. After elution, the IgG fraction was concentrated and dialyzed against PBS (20 mM), NaCl (50 mM), pH 7.0.

3.4. Preparation of affinity column and purification of specific antibodies

Antibodies specific for either compound Pat-sat was purified from the IgG fraction by affinity chromatography conjugated with compound Pat-sat. After loading, the column was washed with high-salt buffers to eliminate unspecific antibodies and eluted using a buffer at pH 2.7. The fractions containing the antibodies, as judged by monitoring the absorbance at 278 nm, were pooled and tested against the patulin derivative by Western blot. These antibodies were used in the experiments of antibody titration (aPsHS1 from rabbit1 and aPsHS2 and from rabbit 2).

To the best of our knowledge, this is the first time that polyclonal antibodies produced against patulin have been purified by affinity chromatography, due to the chemical stability of derivative Pat-sat, which allowed them to be conjugated to an NH-functionalized resin.

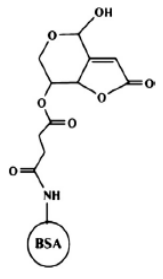

Antigen A

Fig. 1. Schematic representation of the BSA conjugate used for the production of the rabbit anti-patulin antibodies.

3.5. Specific antibody titration

The titer of purified antibodies was determined by indirect ELISA, by coating on the micro-plate wells several different concentrations of antigens Pat-sat–GlnBP and by testing serially diluted aPsHS1 and aPsHS2 against Pat-sat–GlnBP. Each experiment was performed in triplicate, and the results showed that the titer of antibodies, expressed as the reciprocal dilution giving 0.1 optical density (OD) unit at 450 nm, was 25,000 for all the tested antibodies (data not shown).

3.6. Surface plasmon resonance (SPR) binding studies

Since the chip has exposed carboxyl groups and a link is not possible between the Pat-sat and carboxyl group of the chip, the Pat-sat–GlnBP is covalently immobilized on the CO_2H5 surface chip by the amino reactive group, making use of an amino coupling kit.

The optimal buffer and pH value for the immobilization of the Pat-sat–GlnBP on CO_2H5 surface were found to be 10 mM sodium acetate pH 5.5. To test the sensing system, the binding of polyclonal mono-specific antibodies to the P-Sat–GlnBP functionalized CO_2H5 chip was monitored as a function of time. The sensorgram is shown in Fig. 2.

The RU were measured in the presence of a wide range of concentration of anti patulin antibodies (0.0–80.0 nM). As clearly visible from the traces in Fig. 2, the RUmax signal increases with increasing concentrations of anti patulin antibodies.

3.7. Surface plasmon resonance (SPR) competitive immune-assay

An immunoassay is a specific type of biochemical test that measures the presence or concentration of a substance (referred to as

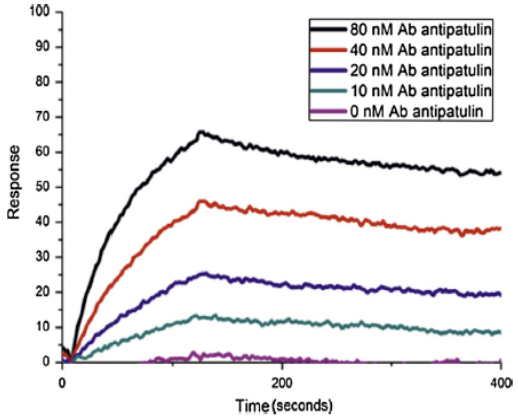

Fig. 2. Sensor-gram showing the binding of the antibodies anti-patulin to patulin immobilized on the gold chip.

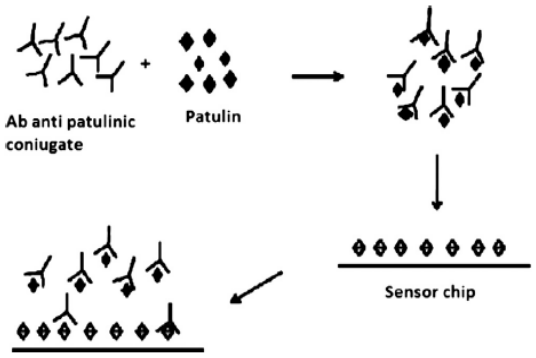

Fig. 3. Schematic representation of SPR-based immune-assay for detection of patulin.

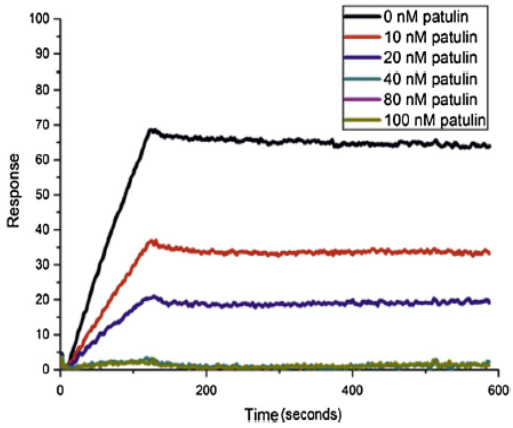

Fig. 4. Sensor-gram of the competitive immune-assay.

the "analyte") in solutions that frequently contain a complex mixture of substances. Analytes in biological liquids such as serum or urine are frequently assayed (i.e., measured) using immunoassay methods. In essence, the method depends upon the fact that the analyte in question is known to undergo a unique immune reaction with a second substance, which is used to determine the presence and amount of the analyte. This type of reaction involves the binding of one type of molecule, the antigen, with a second type, the antibody. Immunoassays can be carried out using either the antigen or the antibody in order to test for the other member of the antigen/antibody pair. In other words, the analyte may be either the antigen or the antibody. In either case the specificity of the assay depends on the degree to which the analytical reagent is able to bind to its specific binding partner to the exclusion of all other substances that might be present in the sample to be analyzed. In addition to the need for specificity, a binding protein must be selected that has a sufficiently high affinity for the analyte to permit an accurate measurement. Various formats for the detection of chemical and biological analytes have been applied in SPR sensors. The format of detection is usually chosen on the basis of the size of target analyte molecules, binding characteristics of available bio/molecular recognition element, range of concentrations of analyte to be measured, and sample matrix. The competitive immunoassay we devised belongs to the competitive detection format. Its working principle is shown in Fig. 3. To assess the potential of our system as a competitive assay for patulin detection, different samples with a fixed concentration of antibodies (80.0 nM) were incubated

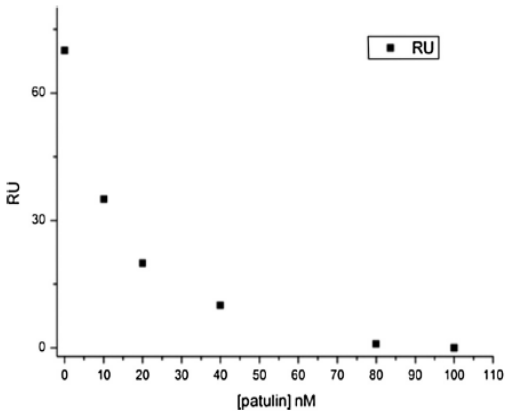

Fig. 5. Titration of the SPR-based sensing system with different amount of patulin. Optical signal intensity in RU is plotted versus the total patulin concentration.

with increasing concentrations of patulin in the range of 0.0–80.0 nM. Each sample was mixed off line and allowed to incubate for 10 min before the measurements. The bound anti-patulin was measured after injection and the sensor surface was regenerated with phosphoric acid 50 mM pH 3.0 at a 25 μL/min flow rate. The obtained sensor-gram is shown in Fig. 4. There is a decrease in the intensity of optical signal with increasing concentrations of patulin present in solution. Then the antibodies anti patulin compete between patulin present in solution and patulin immobilized on the chip. When plotting RUmax values from each SPR binding experiment against the patulin concentration, the dose response curve displayed in Fig. 5 was obtained.

By analysing the data reported in Fig. 5, it is possible to detect an amount of patulin as little as 0.1 nM.

In conclusion, the produced polyclonal mono-specific antibodies together with the patulin coated on the SPR sensing surface were successfully implemented in a new, cost effective and efficient SPR-based competitive immune-assay for patulin detection. That is to say that we combined an immune-chemical approach with SPR spectroscopy to develop an efficient patulin biosensor. The detection limit of this assay was found to be 0.1 nM.

Acknowledgments

This project is in the frame of CNR Commessa "Progettazione e sviluppo di biochip per la sicurezza e la salute umana" AG.P05.001. The project was also partially funded by the CNR project "Conoscenze integrate per sostenibilità e innovazione del Made in Italy agroalimentare (CISIA)" to A.P. and S.D. A.L. thanks the Foundation for Polish Science for the support within the International Ph.D. Studies Programme. P.B. and. A.S. acknowledge the support of NCN through the grant NCN2011/03/B/ST5/03094.

References

[1] S. Zeng, K.-T. Yong, I. Roy, X.-Q. Dinh, X. Yu, F. Luan, Plasmonics 6 (2011) 491–506.
[2] S.A. Maier, H.A. Atwater, J. Appl. Phys. 98 (2005) 011101.
[3] H. Raether, Surface Plasmons, Springer-Verlag, Berlin, 1988.
[4] J.N. Gollub, D.R. Smith, D.C. Vier, T. Perram, J.J. Mock, Phys. Rev. B 71 (2005). 195402-1.
[5] R. Reisfeld, V. Levchenko, T. Saraidarov, M. Behrendt, B. Kuklinski, M. Grinberg, Opt. Mater. 34 (2012) 2021–2024.
[6] S. Rangełowa-Jankowska, D. Jankowski, R. Bogdanowicz, B. Grobelna, P. Bojarski, J. Phys. Chem. Lett. 3 (2012) 3626–3631.
[7] N.W. Turner, S. Subrahmanyam, S.A. Piletsky, Anal. Chim. Acta 632 (2009) 168–180.
[8] J.L. Richard, Int. J. Food Microbiol. 119 (2007) 3–10.

[9] C.A. Robbins, L.J. Swenson, M.L. Nealley, R.E. Gots, B.J. Kelman, Appl. Occup. Environ. Hyg. 15 (2000) 773–784.
[10] M.O. Moss, J. Appl. Microbiol. 104 (2008) 1239–1243.
[11] M.W. Trucksess, P.M. Scott, Food Addit. Contam. 25 (2008) 181–192.
[12] O.A. Cornely, Infection 36 (2008) 296–313.
[13] A.E. Desjardins, R.H. Proctor, Int. J. Food Microbiol. 119 (2007) 47–50.
[14] B. Kabak, A.D. Dobson, I. Var, Crit. Rev. Food Sci. Nutr. 46 (2006) 593–619.
[15] F. Nielsen, Fungal. Genet. Biol. 39 (2003) 103–117.
[16] C.L. Lai, Y.M. Fuh, D.Y.C. Shih, J. Food Drug Anal. 8 (2000) 85–96.
[17] M. Watanabe, H.J. Shimitzu, Food Prot. 68 (2005) 610–612.
[18] S. Sforza, C. Dall'Asta, R. Marchelli, Mass Spectrom. Rev. 25 (2005) 54–76.
[19] J.I. Azcona-Olivera, M.M. Abouzied, R.D. Plattner, J.J.J. Pestka, Agric. Food Chem. 40 (1992) 531–534.
[20] X. Huang, F.S.J. Chu, Agric. Food Chem. 41 (1993) 329–333.
[21] F.S. Chu, I. Ueno, Appl. Environ. Microbiol. 33 (1977) 1125–1128.
[22] M. De Champdore, P. Bazzicalupo, L. De Napoli, D. Montesarchio, G. Di Fabio, I. Cocozza, A. Parracino, M. Rossi, S. D'Auria, Anal. Chem. 79 (2007) 751–757.

Chapter 2
An Advanced Near-Infrared Fluorescence Bio/sensing Methodology to Detect the Presence of Traces of Patulin Toxin in Real Food Matrices

Submitted to Bioanalytical Chemistry

An Advanced Near-Infrared Fluorescence Bio/sensing Methodology to Detect the Presence of Traces of Patulin Toxin in Real Food Matrices

Anna Pennacchio[§], Antonio Varriale[§], Maria Grazia Esposito, Maria Staiano, and Sabato D'Auria*

Laboratory for Molecular Sensing, IBP-CNR, Via Pietro Castellino, 111 80131, Naples, Italy
§ These authors equally contributed to the work.

*Correspondence to:
Dr. Sabato D'Auria
IBP, CNR Via Pietro Castellino, 111
80131 Naples, ITALY
Tel. +39-0816132250 Fax: +39-0816132277
Email: s.dauria@ibp.cnr.it

Abstract

Patulin is a toxic secondary metabolite (mycotoxin) of a number of fungal species belonging to the genera Penicillum, Aspergillus and Byssochlamys that may grow on a variety of foods including fruit (apples), grains and cheese. The amount of patulin in apple derivative products is viewed as a measure of the quality product related to the apples used in its production. Actually different analytical methods used to quantify the patulin are based on HPLC, mass spectrometry and electrophoresis techniques. These methodologies are time-consuming and require trained personnel. In addition, it is not easy to envisage the development of a portable device based on these methods for in-situ analyses. We present a novel and sensitive polarization-based method for the detection of patulin directly in apple juice. The proposed method is based on the use of a NIR probe labeled patulin conjugate with properly produced antibodies anti-patulin. The obtained results point out that our methodology can be applied directly apple-juice solution without interferences. The results show the possibility to detect an amount of patulin less than 0,06 µg/L. This value is much below to the MRL of EU regulation limit, that it has been fixed at 50 µg/L.

KeyWords: Fluorescence; Biosensors; Antibody; Patulin; Apple Juice

Introduction

Patulin (PAT) is a toxic fungal secondary metabolite (mycotoxin) produced by different genera of fungi such as Aspergillus, Penicillium and Byssochlamys that may grow on a variety of foods including fruit (apples), grains and cheese. The amount of PAT in apple derivative products is viewed as a measure of the quality product related to the apples used in its production. In fact several studies have demonstrated that PAT has been found to occur in a number of foods including apple juice, apples and pears with brown rot [1], flour [2] and malt feed.
A number of studies have shown that the PAT has several effects on human health, in fact it is a potent genotoxic com-pound and different countries have instituted PAT restrictions in products intended for human consumption. The World Health

Organization recommends a maximum concentration of 50 µg/L in apple juice. In the other hand European Union, has set the limit to 50 µg/kg in both apple juice and cider, and to half of that concentration, 25 µg/kg in solid apple A special restriction is set in products for infants and young children, 10 µg/kg [3].

Even though a lot of research and development work have been done on food safety and quality, more needs to be done to find economic and accurate ways of monitoring food safety. The traditional methods in this field are sensory evaluation, chemical analysis, and microbiological analysis. In particular, different analytical chemical methods are used to detect patulin in apple-juice concentrate, including thin layer chromatography (TLC) [1,4] mass spectrometry [5], colorimetry [6], micellar electro-kinetic chromatography (MEKC) [7], gas chromatography mass spectrometry (GC–MS) [8, 9], liquid chromatography mass spectrometry (LC–MS) [10-13] and high-performance liquid chromatography with ultraviolet detection (HPLC-UV) [14-17].

Generally, the chemical analysis is an objective technique, which often provides reliable results if the monitored batch is represented well by the samples measured. Despite these features, it has some limitations: the processes may not work correctly due to some substances, the need of accurate and correct calibrations, and the need of complex multi phased processing. It might not be suitable if the distribution of the substance con-tent is non-uniform.

To overcome the disadvantages and limitations of the previous methods, new economic, fast, and environment friendly techniques are sought after. As a result, optical spectral measurements and imaging have recently become more and more popular in food measurements because they lend themselves to easily monitor all samples components. The optical methods can be used for non-destructive, fast, real-time monitoring of food matrices [18]. Just in this field, our research group has contributed to increase the scientific relevance of these approaches, developing both a competitive fluorescence immune-assay and a surface plasmon resonance (SPR) assay for the detection of patulin. These two assays were based on the use of specific antibody anti-patulin as well as a novel chemically synthetized patulin derivative compound [19, 20].

Here, we describe a new method for the detection of PAT by using a fluorescence polarization approach. The fluorescence assay is based on the use of an ad hoc synthesized fluorescence Patulin-GlnBP (Pat-GlnBP) conjugate, labeled with a NIR–infrared fluorescent probe and specific antibodies generated against the analyte. A competitive immune-assay based on the use of mono-specific antibodies anti-PAT has been performed in order to directly detect PAT in raw sample of apple juice. In particular, we labeled the PAT-GlnBP conjugate with a fluorophore molecule (DayLigth IF800) that has absorption and emission spectra in the NIR region (from 650 nm to 900 nm) of the spectrum light. The choice to use this class of dye is related to the fundamental advantages offered from this compound such a significant reduction of the background signal, low absorption in the visible region of the light, low light scattering and the requirement of an inexpensive illumination light source. In particular, in some instances, auto-fluorescence may limit the detection of weak signals with fluorophores that emit in the visible region. Since most biomolecules have very low absorption in the NIR region, the fluorescence probes (e.g. the infrared emitting DayLight IF800) provide a level of performance not achievable with the use of visible emitting fluorescence dyes. Bright, clear images with extremely clean backgrounds and excellent sensitivity are provided with this approach. In addition, the use of NIR dyes is currently part of the emerging technologies related to

numerous different relevant biological uses. In fact, in the recent years, NIR fluorescence dyes have found several applications in biomedical and material applications [21]. The minimal interference in absorption and fluorescence emission from biological samples due to their low absorption coefficient in the NIR region, allow for the use this class of fluorescence dyes for monitoring in vitro and in vivo the levels of many biologically relevant molecules [21-23]. We used the NIR dyes properties to detect traces of PAT in apple juice samples. The obtained results are presented and discussed.

Materials and Methods

2.1. Reagents

All reagents were of the highest commercially available quali-ty and used as received. 1-[3-(Dimethylamino)-propyl]-3-ethyl-carbodiimide (EDC), bovine serum albumin (BSA),carboxymethoxylaminehemihydrochloride. The fluo-rescent probe Dylight IF 800 was purchased from Dylight Inc. Goat polyclonal to rabbit IgG-HRP conjugate (secondary anti-body) was from Abcam. Affinities resin EAH Sepharose 4B was purchased from Amersham Biosciences. Nitrocellulose transfer membrane Protran from Schleicher &Schuell and ECL detection reagents from Amersham Biosciences were used in dot blot and Western blot experiments. Microplates (96-well), LockWellMaxiSorp from Nunc, 3,5,-tetramethylbenzidine (TMB) enzyme substrate from Sigma, and a microplate reader, Multiskan EX from Thermo, were used for ELISA experiments. UV measurements (detection at 278 nm) were carried out on a Varian Cary 50 Bio spectrophotometer. Antibodies were produced and purchased from COVALAB S.A.S. Villeurbanne, France.

2.2. Synthesis of Pat-Sat-BSA Conjugate

The patulin derivate (Pat-sat) was synthesized from L-arabinose as described in De Champdorè et al [21]. In brief a solution of Pat-Sat (1.5 mg, 0.0054 mmol) in Tris (pH 8)/dioxane, 1:1 (v/v, 0.4 mL), were added 20 µL (1.0 mg, 0.0054 mmol) of an EDC solution in H2O (50 mg/mL) and 0.5 mL of a BSA solution (8 mg/mL) in PBS (0.1 M) at pH 7.4. After 2 h at room temperature, the reaction mixture was dialyzed against PBS (0.01 M), NaCl (0.01 M), pH 7.4 (0.5 L, for 3 days with daily buffer changes). The conjugate concentration determined spectrophotometrically at 278 nm was 4.2 mg/mL.

2.3.Antibody Production and IgG Purification

The antibodies used in the work were produced and purchased from COVALAB SAS France. (COVALAB Villeurbanne, France). The company used as antigen the conjugate reported in Figure 1. From the serum provided from COVALB, 2.0 mL sample of rabbit serum was applied to a protein-A column of the PURE1A Protein A Anti-body Purification Kit, by Sigma, and the IgG fraction was purified according to the manufacturer's instructions. Elution of proteins was monitored by absorbance at λ= 278 nm. The IgG fraction was eluted with glycine (0.1M) at pH 2.8 and immediately buffered in Tris 1.0 M at pH 9.0. SDS PAGE was carried out to evaluate the purity of the sample.

2.4.Affinity Column Preparation

The affinity column was obtained by conjugating derivative Pat-Sat to EAH Sepharose 4B as follows. A 1.0 mL sample of resin was washed with H2O at pH 4.5 (20 mL), with NaCl (0.5 M) (20 mL), and again with H2O at pH 4.5 (20 mL) and finally

suspended in 2.0 mL of H2O. The Sepharose resin was added to a solution of Pat-Sat (5 mg in 0.5 mL of H2O at pH 4.5), and the resulting suspension was gently shaken. The slurry was cooled to 0°C, and EDC was added in two steps to a final concentration of 0.1 M (52 mg). After 12 h at 4°C, the reaction mixture was taken to room temperature, and after an additional 4 h the resin was extensively washed with H2O at pH 4.5 and then treated with 1.0 mL of AcOH (0.1 M) and 38 mg of EDC for 1 h at room temperature. The suspension was washed with H2O at pH 4.5 (20 mL), acetate buffer (0.1 M) containing NaCl (0.5 M) (20 mL), pH 4.0, and PBS (0.1 M) containing NaCl (0.3 M), pH 7.4 (20 mL), and finally packed into a polystyrene column (2 mL, BIORAD).

2.5.Antibody Purification by Affinity Chromatography

For the affinity chromatography purification, a 2.0 mL aliquot of IgG (obtained from serum) was applied drop-wise to the affinity column prepared as described above. To eliminate un-specific antibodies, the column, before elution, was washed with three high-salt buffers: (1) PBS (0.01 M), NaCl (0.1 M), pH 7.0 (20 mL); (2) PBS (0.01 M), NaCl (0.5 M), pH 7.0 (20 mL); (3) PBS (0.01 M), NaCl (1.0 M), pH 7.0 (20 mL). At that point absorbance at 278 nm had fallen to 0.0. For the elution step glycine (0.1 M), pH 2.7 (2.5 mL), was applied to the column, and the eluate was collected in 0.5 mL fractions and monitored by absorbance measurements at 278 nm. The fractions containing the antibodies were collected, concentrated by means of a Centricon YM-3 membrane to a volume of 1.0 mL, and dialyzed against PBS (0.1 M), NaCl (0.1 M), pH 7.4. The concentration of the antibodies was spectrophotometrically determined by absorbance measurements at 278 nm.

2.6. Synthesis of GlnBP Conjugate (Pat-sat-GlnBP)

To avoid interference by the carrier protein in the polyclonal antibody detection process, Pat-Sat was conjugated to the glutamine-binding protein (GlnBP) from *E. coli*, a bacterial protein different from the protein used to carry out the immunization. The following procedure was used: 2.5 mg (0.0092 mmol) of Pat-Sat was dissolved in 0.25 mL of MES buffer (0.1 M), pH 5. The solution was incubated at room temperature with 0.25 mL of a GlnBP solution (5 mg/mL) in the same buffer and 0.1 mL of an aqueous solution of EDC (10 mg/mL). After 5 h, the reaction mixture was dialyzed against PBS (0.01 M) containing NaCl (0.1 M) at pH 7.4 (0.5 L, 3 days with daily buffer changes).

2.7. Western Blot Experiments

Proteins (BSA, Pat-Sat-GlnBP, and GlnBP, 10 ug each) were loaded, separated by sodium dodecyl sulphate-polyacrylamide gel electrophoresis (12% SDS-PAGE), and then transferred overnight at 4°C onto a nitrocellulose membrane. Membranes were blocked for 1 h at room temperature by rocking in 50 mL of the blocking buffer (PBS containing 5% skim milk, 0.2% Tween 20, and 0.05% Tryton). After two washings with PBS-TT and one with PBS (10 min per washing), the filters were incubated with antibodies anti Pat-Sat (1:500 in the blocking buffer), for 1 h at room temperature. After two washings with PBS-TT and one with PBS (10 min per washing), the filters were incubated with secondary antibody (goat anti-rabbit HRP conjugate, 1:3000 in the blocking buffer) for 1 h at room temperature. The filters were washed three times as described above and then developed with the detection reagent ECL.

2.8. Antibody Titration

The antibody titer was determined by an indirect ELISA assay by the following general procedure. The antigen (Pat-Sat-GlnBP), in PBS (0.1 M), pH 7.4, was used to coat 96-well micro-plates, varying the concentration from 1.1 to 1.7·10-3 µg/mL (one column for every antigen concentration, 100 µL per well), overnight at 4°C. Control wells were incubated for the same period with BSA in the same buffer. The wells were rinsed three times with PBS (0.1 M) containing 0.05% Tween (PBS-T), pH 7.4, and blocked by incubation for 2 h at room temperature with PBS-T containing BSA (1%) (100 µL each well). After three washings with PBS-T, serially diluted antibody was added to the wells, incubated at room temperature for 1 h, and then rinsed three times with PBS-T. Horseradish peroxidase-conjugated anti-rabbit IgG antibodies, diluted 1:4000 in PBS-T containing BSA (1%), were added to the wells (100 µL) and incubated for 1 h at room temperature. After three washings with PBS-T, the enzyme substrate TMB was added (100 µL per well), and the colour reaction was quenched after 5 min by addition of 1 M H2SO4 (100 µL per well). The absorbance was measured at 450 nm. The antibody titer was graphically determined by plotting the reciprocal of the antibody dilution vs absorbance for each dilution of anti-bodies. The titer was taken as the maximum antibody dilution able to give a reading of 0.1 absorbance unit. The following values were found: 1/25000 for Pat-Ser.

2.9. Labeling of Pat-Sat-GlnBP

A solution of Pat-Sat-GlnBP at concentration of 1.0 mg/mL in 1.0 mL was dissolved in 0.1 M sodium bicarbonate buffer, pH 7.0 and mixed with IF800. The molar ratio of the dye and the protein was kept 10:1. The reaction mixture was incubated for 1 hours at room temperature and the labelled molecules were separated from un-reacted probe by gel filtration and extensive dialysis procedure against 50 mM phosphate buffer pH 7.4 at 4°C.

2.10 Steady-state fluorescence measurements

Steady state fluorescence experiments were carried out on an FP-8600 Fluorescence Spectrometer (Jasco-Japan) equipped with a one-cell temperature controlled sample holder. For Pat-Sat-GlnBP-IF 800 (Abs IF 800 = 0.10 OD), the excitation wavelength was fixed at 760 nm and emission spectra were recorded between 765 nm and 850 nm with an emission slit-width of 2.5 nm. Measurements were per-formed in 10 mM phosphate buffer at pH 7.4, at room temperature. Pat-Sat-GlnBP-IF 800 was incubated with a range of concentration of antibodies against PAT from 0.0 to 2,4 nmoli for10 minutes, and fluorescence spectra were carried out. The polarization fluorescence measurements were carried out, by inserting a Glan polarizer between the excitation source and the sample, with a vertical (0) excitation polarized filter and with a vertical (0) emission polarized filter.

2.11 Pat competition assay

A competition polarization assay was carried out at a fixed concentration of antibody against Pat (2.4 nmoli) in the presence of an increasing concentration of un-labeled PAT (from 0.0 to 2.4 pmoli). The incubation was done at room temperature for 30 minutes. After this pre-incubation in the presence of un-labeled PAT, the polarization fluorescence measurements were carried out with an excitation polarized filter set at vertical (0) and an emission polarized filter set at vertical (0).

Results and discussion

Pat is a toxic secondary metabolite of a number of fungal species belonging to the genera *Penicillum* and *Aspergillus*. It has been mainly isolated from apples and apple products contaminated with the common storage-rot fungus of apples, *Penicillum expansum*, but it has also been extracted from rotten fruits, moldy feeds, and stored cheese. A rapid and simple method of concentration detection of PAT in apple juice is needed. In this work we describe a sensitive polarization-based method for the detection of PAT directly in apple juice.
For this purpose we used a new PAT derivative, whose synthesis is described in literature [21] because it is more stable than patulin compound. Since PAT is too small molecule to elicit any immunological response and we have covalently attached the Pat-Sat derivate to a protein carrier (BSA). In Figure 1 is shown the Pat-Sat structure covalently bound to BSA. This conjugate has been used to produce polyclonal antibodies anti-PAT in rabbit.

3.1. Production of antibodies against the PAT

Polyclonal antibodies against PAT were produced using Pat-Sat-BSA conjugate as an antigen and from serum provided from Covalab (COVALB-France), the IgG fractions were isolated from serums by the protein A column kit. The homogeneity of IgG fractions was evaluated by SDS-PAGE and the pure fractions were sequentially pooled, concentrated and dialyzed extensively against PBS 20 mM pH 7.4. To exclude false reactions due to anti-BSA antibodies present in the rabbit se-rums, the Pat-Sat was conjugate with a protein different from BSA. For this purpose, the glutamine-binding protein (GlnBP) purified from *E. coli* was chosen. The Pat-Sat-GlnBP conjugate was prepared by the same procedures already used for BSA conjugate and reported in material and methods section.

3.2. Preparation of affinity columns and purification of specific antibodies and western blotting

The obtained IgG fraction was loaded on affinity column in which the Pat-Sat was conjugated to EAH Sepharose-4B resin. After loading with the IgG fraction, the column was washed with buffer at neutral pH with high concentration of NaCl, in order to remove unspecific antibodies and the mono-specific antibodies were eluted using glycine buffer at pH 3.0. The different fractions were collected and an SDS-PAGE was carried out in order to evaluate the purity of the sample (data are not shown). In order to verify the specificity of the produced anti-bodies against the PAT, a western blotting experiment was performed. The results show a response to antibody binding was observed only for the conjugate Pat-Sat-GlnBP, and a negative response was registered for BSA and GlnBP. This confirms the specificity of antibodies versus PAT.

3.3. ELISA test

The titer of purified antibodies was determined by indirect ELISA, by coating on the micro-plate wells several different concentrations of antigens Pat-sat-GlnBP and by testing serially diluted mono-specific antibodies against Pat-sat-GlnBP. Each experiment was performed in triplicate, and the results showed that the titer of antibodies, expressed as the reciprocal dilution giving 0.1 optical density (OD) unit at 450 nm, was 25000 for all the tested antibodies (data not shown).

3.4. Fluorescence steady-state measurements of GlnBP-Pat-IF800 conjugate

In order to perform polarization immunoassay for PAT, we generate a labelled GlnBP-Pat-Sat with IF 800 (Pat-Sat-GlnBP-IF800). To ensure that the sample does not have any free dye in the solution, which could interfere in the measurements, gel filtration and dialysis were performed to remove the unreacted probe before the polarization measurements were made. The fluorescence polarization measurements were performed directly in apple juice. In particular, a solution of apple juice ten-times diluted (1:10) was used for the experiments. The excitation was fixed at 760 nm and the spectra were acquired from 765 nm to 850 nm. The figure 2 shows the polarization emission spectra of the IF800 dye in buffer solution and in a diluted apple-juice sample.

The results show that the spectra were completely superimposed and the fluorescence maximum in both cases was centered at 785 nm. This data indicate the possibility to perform in real matrices without any interference the developed assay using this NIR dye. The Figure 3 shows the polarized emission spectra of GlnBP-Pat-Sat-IF800 in the presence of increasing concentrations of PAT-mono-specific antibodies. The measurements were performed at RT and the solution of antibodies was added in a range of concentration from 0.0 to 2,4 nmoli. The obtained results revealed an increase of GlnBP-Pat-Sat-IF800 polarized fluorescence intensity at 785 nm as consequence of binding (Figure 3 inset).

3.5. Polarization competitive immunoassay

The FP immunoassay was used to measure the competition between the tracer of un-labeled Pat in solution and Pat-Sat-GlnBP-IF800 for binding with mono-specific antibodies anti-PAT. Different samples with a fixed concentration of antibody (2,4 nmoli) were incubated with increasing concentration of Pat in the range of 0.0 to 2,4 pmoli. Each sample was mixed off-line and allowed to incubate for 30 minutes before the fluorescence polarization measurements. The Figure 4 shows the decrease of polarized fluorescence emission as a consequence of increase of un-labelled PAT in solution. In Figure 5 is shown the dose response for PAT detection in a diluted apple juice solution reporting the polarization fluorescence intensity at 785 nm as function of PAT concentration. The results show the possibility to detect an amount of PAT less than 0,06 ug/L. This value is below to the MRL of EU regulation limit, that it has been fixed at 50 ug/L.

Conclusions

In conclusion, the obtained results point out that this method is a promising alternative approach compared to the analytical methods actually in use.

ACKNOWLEDGMENT

This project was realized in the frame of the CNR Commessa “Progettazione e Sviluppo di Biochip per la Sicurezza Alimentare e Salute Umana (SD; MS; AV)”. This Project was partially funded by the project CTN01_00230_240864 "SAFE &SMART-Nuove tecnologie abilitanti per la food safety e l'integrità delle fi-liere agro-alimentari in uno scenario globale" and it was also partially funded by the CNR project "Conoscenze integrate per sostenibilità e innovazione del Made in Italy agroalimentare (CISIA)”.

References

1) Harwig J, Chen YK, Kennedy BPC, Scott PM. (1973) Occurrence of patulin-producing strains of Penicillium expansum in natural rots of apple in Canada. Food Sci Technol 6: 22-25.
2) Graves RR, Hesseltine CW. (1996) Fungi in flour and refrigerated dough products. Mycopathol Mycol Appl 30, 29(3): 277-290.
3) Beretta B, Gaiaschi A, Galli CL, Restani P. (2000) Patulin in apple-based food: occurence and safety evaluation. Food Additives & Contaminants 17(5): 399-406.
4) Cheraghali AM, Mohammadi HR, Amirahmadi M, Yazdanpanah H, Abouhossain G, Zamanian F, Ghazi Khansari M, Afshar M. (2005) Incidence of patulin contamination in apple juice produced in Iran. Food Control 16(2): 165-167.
5) Abramson D, Thorsteinson T, Forrest D. (1989) Chromatography of mycotoxins on precoated reverse-phase thin-layer plates. Arch Environ Contam Toxicol 18(3): 327–330.
6) Sheu F, Shyu YT. (1999) Analysis of patulin in apple juice by diphasic dialysis extraction with in situ acylation and mass spectrometric determination. Agric Food Chem 47:2711–2714.
7) Subramanian T. (1982) Colorimetric determination of patulin produced by Penicillium patulum. J Assoc Off Anal Chem 65(1):5–7.
8) Murillo M, González-Penas E, Amézqueta S. (2008) Determination of patulin in commercial apple juice by micellar electrokinetic chromatography. Food Chem Toxicol 46: 57–64.
9) Roach JAG, White KD, Trucksess MW, Thomas FS. (2000) Capillary gas chromatography/mass spectrometry with chemical ionization and negative ion detection for confirmation of identity of patulin in apple juice. J AOAC Int 83: 104–112.
10) Rodríguez-Carrasco Y, Berrada H, Font G, Manes J. (2012) Multi mycotoxin analysis in wheat semolina using an acetonitrile-based extraction procedure and agas chromatography-tandem mass spectrometry. Journal of Chromatogr A 1270: 28–40.
11) Sewram V, Nair JJ, Nieuwoudt TW, Leggott NL, Shephard GS. (2000) Determination of patulin in apple juice by high-performance liquid chromatography-atmospheric pressure chemical ionization mass spectrometry. Journal of Chromatogr A 897: 365-374.
12) Zöllner P, Mayer-Helm B. (2006) Trace mycotoxin analysis in complex biological and food matrices by liquid chromatography–atmospheric pressure ionization mass spectrometry. Journal of Chromatogr A 1136: 123–169.
13) Ito R, Yamazaki H, Inoue K, Yoshimura Y, Kawaguchi M, Nakazawa H. (2004) Development of liquid chromatography-electrospray mass spectrometry for the determination of patulin in apple juice: investigation of its contamination levels in Japan. Journal of Agric Food Chem 52: 7464–7468.
14) Baert K, Meulenaer BD, Kasase C, Huyghebaert A, Ooghe W, Devlieghere F. (2007) Free and bound patulin in cloudy apple juice. Food Chem. 100 (3): 1278–128.
15) Turner NW, Subrahmanyam S, Piletsky SA. (2009) Analytical methods for determination of mycotoxins: a review. Anal ChimActa 632: 168–180.

16) Moukas A, Panagiotopoulou V, Markaki P. (2008) Occurrence of patulin in fruit juices in the Greek market determined with HPLC-DAD and GC-MSD. Comparison of the two methods. Food Chemistry 109(4): 860-867.
17) Katerere DR, Stockenstrom S, Shephard GS. (2008) HPLC-DAD method for the determination of patulin in dried apple rings. Food Control 19: 389-392.
18) Huang H, Yu H, Xu H, Ying Y. (2008) Near infrared spectroscopy for on/in-lie monitoring of quality in foods and beverages: a review. Journal of Food Engineering 87(3): 303–313.
19) De Champdorè M, Bazzicalupo P, De Napoli L, Montesarchio D, Di Fabio G, Cocozza I, Parracino A, Rossi M, D'Auria S. (2007) A new competitive fluorescence assay for the detection of patulin toxin. Analytical Chemistry 79:751-757.
20) Pennacchio A, Ruggiero G, Staiano M, Piccialli G, Oliviero G, Lewkowicz A, Synak A, D'Auria S. (2014) A surface plasmon resonance based biochip for the detection of patulin toxin. Optical Materials 36: 1670-1675.
21) Guo Z, Park S, Yoon J, Shin I. (2014) Recent progress in the development of near-infrared fluorescent probes for bioimaging applications. ChemSoc Rev 7, 43(1):16-29.
22) Pham W, Choi Y, Weissleder R, Tung CH. (2004) Developing a peptide-based near-infrared molecular probe for protease sensing. Bioconjug Chem 15(6): 1403-1407.
23) Khan F, Pickup JC. (2013) Near-infrared fluorescence glucose sensing based on glucose/galactose-binding protein coupled to 651-blue oxazine. BiochemBiophys Res Commun 438(3): 488-92.

Legend of figures

Figure 1 Anti-patulin antibodies production. Schematic representation of the BSA conjugate used for the production of the rabbit anti-patulin antibodies.
Figure 2. Polarization emission spectra of IF 800. The spectra of the IF 800 in in PBS and in apple juice were recorded at room temperature and the fluorescence emission spectra were recorded with an excitation set at 760 nm.
Figure 3. Fluorescence polarization antibody binding experiment. Polarization emission spectra of GlnBP-Pat-Sat-IF 800 in the presence of increasing concentration of patulin mono-specific antibodies.
Figure 4. Competitive immune-assay. Polarization emission spectra of GlnBP-Pat-Sat-IF 800 competitive immunoassay. The experiment was performed at room temperature and the fluorescence emission spectra were recorded with an excitation set at 760 nm.
Figure 5. Dose response curve of patulin detection. Titration of fluorescence polarization immune-assay with increasing concentration of un-labeled patulin.

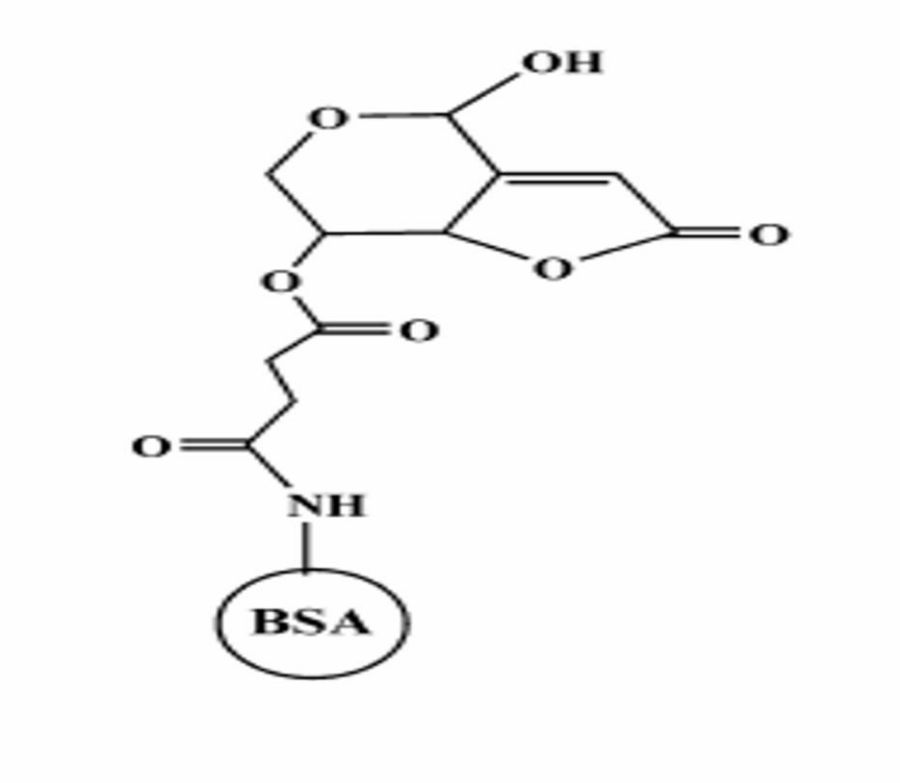

Figure 1

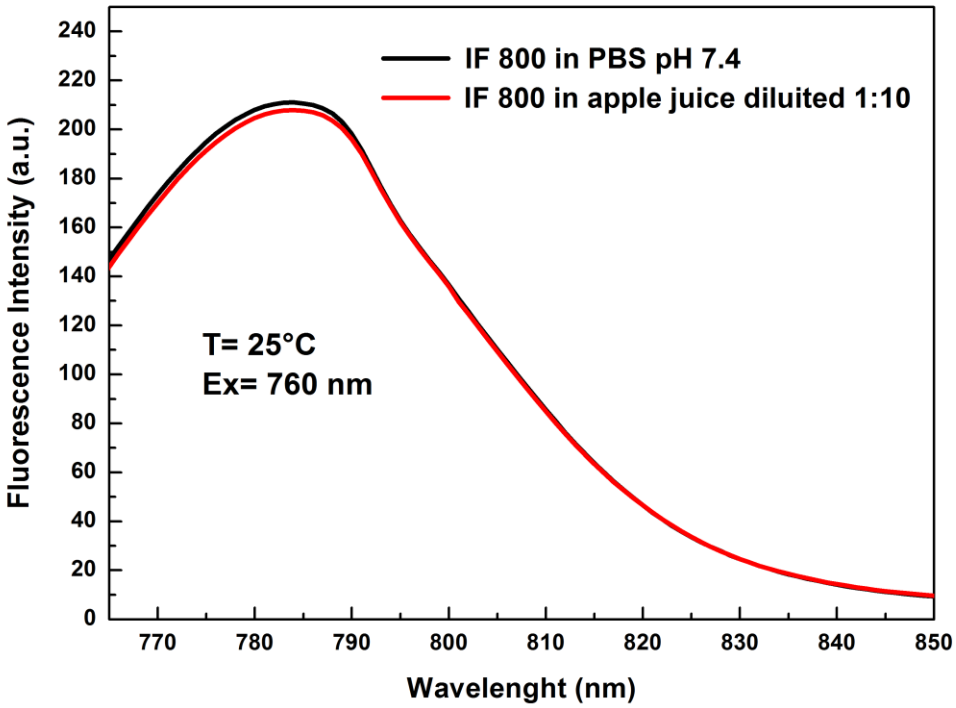

Figure 2

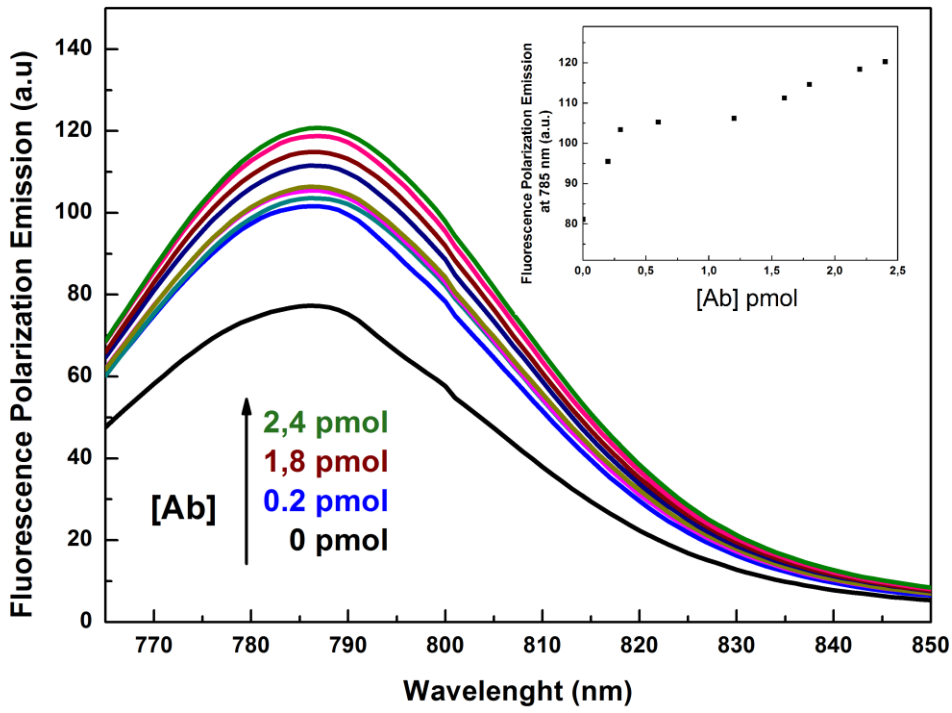

Figure 3

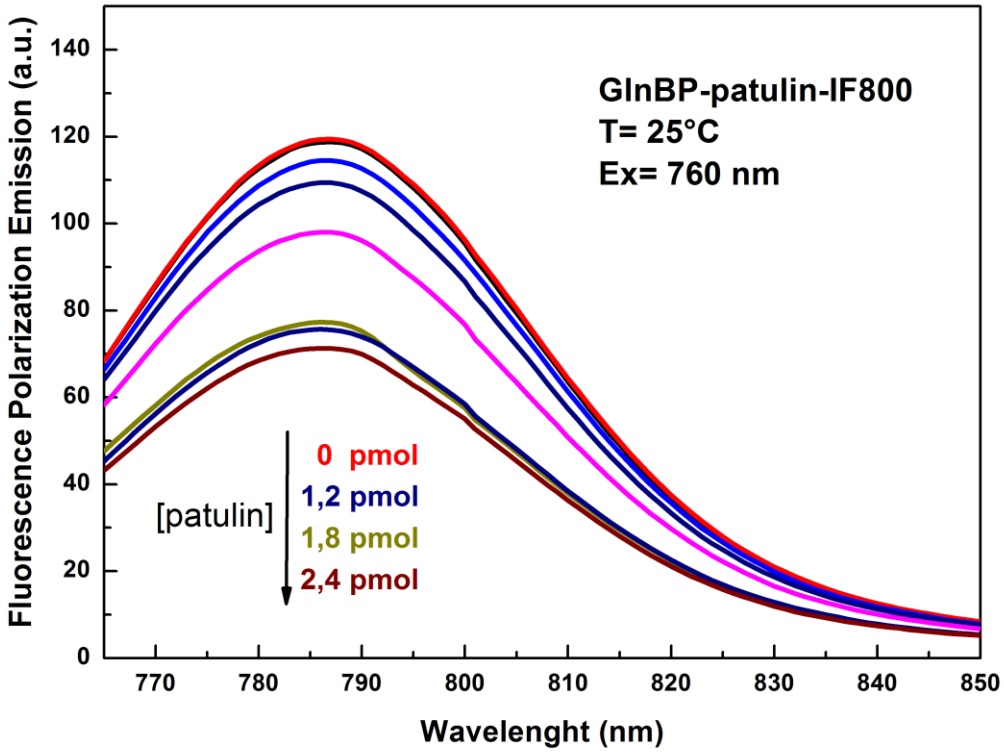

Figure 4

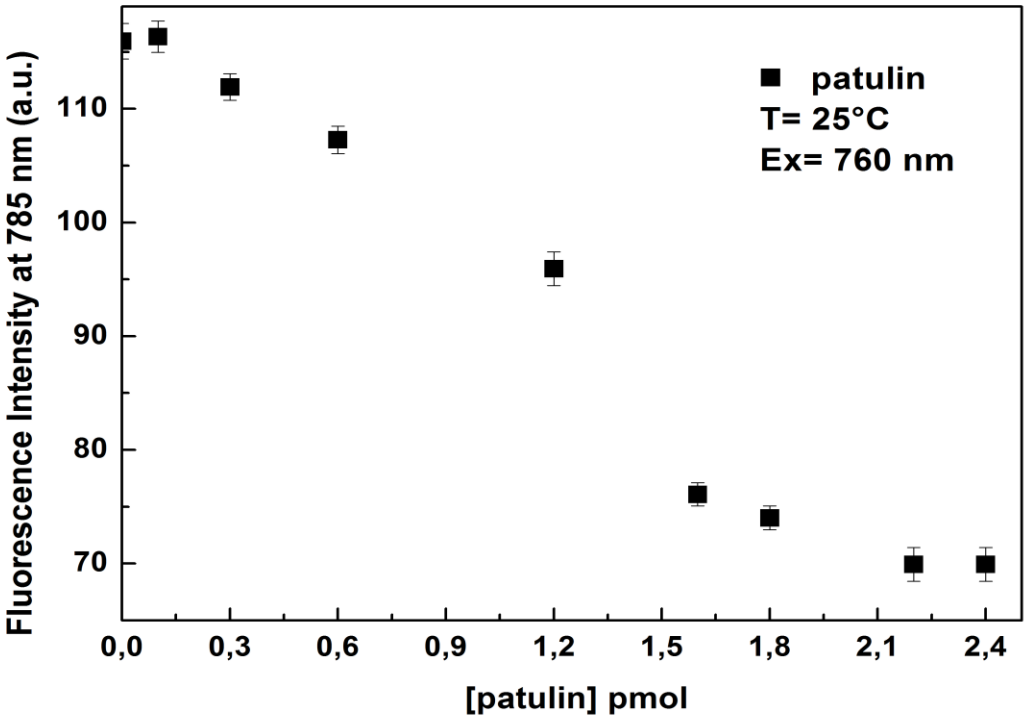

Figure 5

Chapter 3
A Rapid and Sensitive Assay for the Detection of Benzylpenicillin (Pen G) in Food

Submitted to Food Chemistry

A Rapid and Sensitive Assay for the Detection of Benzylpenicillin (Pen G) in Food

Anna Pennacchio[§], Antonio Varriale[§], Maria Grazia Esposito, Andrea Scala, Vincenzo Manuel Marzullo, Maria Staiano, and Sabato D'Auria*
Laboratory for Molecular Sensing, IBP-CNR, Naples, Italy
§ These authors equally contributed to the work

*Correspondence to:
Dr. SabatoD'Auria
IBP-CNR, Via Pietro Castellino, 111
80131 Naples, ITALY
Tel. +39-0816132250, Fax: +39-0816132277
Email: s.dauria@ibp.cnr.it

Abstract
Since antibiotics are provided to animals for therapy and prophylaxis, it has become increasingly important to monitor antibiotics traces in foodstuffs of animal origin. In fact it is well known that these traces give rise to antibiotic-resistant germs that can threaten humans. Food safety controls are especially addressed to the daily consumption of milk supplies and, in particular, the attention is focused on the antibiotic benzylpenicillin (Pen G). In order to cope with this problem here we propose an effective alternative, compared to the analytical methods actually employed, to quantify the presence of penicillin G using a SPR technique with SensiQ discovery portable instrument. The detection limit of these assays was found to be 20 pM, a value much lower than the MRL of EU regulation limit. Thus, our results clearly show that this system could be successfully suitable for accurate and easy-way analysis for PenG outside the laboratory.

Keywords: Surface Plasmon Resonance (SPR); Biosensors; Antibody; Penicillin G; Milk

1. Introduction

Nowadays the mainly compounds used in the treatment of animal diseases, such as mastitis are β-lactams, and in particular penicillin G and cephalosporin. Especially penicillin is the antimicrobial for which consultation is most frequently sought through Food Animal Residues Avoidance Databank (FARAD) and is one of the most commonly detected drug residues in tissue and milk. The presence of residues of these antibiotics in some milk products is probably due to injudicious use of antibiotics in the treatment of infections in animals and lack of adherence to withdrawal period before milking (Adetunji & Olaoye, 2012). These compounds are also used as food additives and its massive use inevitably causes presence of traces in food of animal origin (milk and meat) with several problems for human health. The frequent use of antimicrobials over the years has led to a widespread bacterial resistance to β-lactams, in particular to benzyl-penicillin (Pen G). Moreover, the presence of drug residues causes allergic sensibilization of exposed individuals and the selective pressure that antimicrobial drug residues may exert over human gut micro-flora: it is fearedthat antimicrobialsin foodcandepletethe human intestinal

exposed micro-flora, thus promotingadhesion ofpathogenic bacteria with subsequent ineffectiveness of medical treatment where antibiotics are prescribed. In fact public health officials are concerned that even small amounts of antibiotics, particularly penicillin, ingested by the human through the food chain is potentially dangerous. The presence of drug residues in milk and other daily supplies and products is of public health implications and are perceived by consumers as undesirable (Mcewen, Meek &Black 1991; Bencini & Pulina, 1997). Today, it is the general consensus that even slight traces of antibiotics in milk and food for human consumption should not be tolerated (Jepsen, 1990). Allergic reactions in highly sensitive consumers and potential carcinogenicity, mutagencity, teratogencity and long-term toxic effects of the residues of all classes of antibiotics which were presented in a report by Epstein, Chong & Le (2000) are of public health concern.

With the aim to prevent the negative impact of β-lactam, in particular of PenG residues present in the milk on customer's health, many countries have been established maximum residue limits (MRLs). The European Union (EU) Regulation 508/1999 has established the MRLs in milk and in meat for some antibiotics: for benzyl-penicillin in milk (penicillin G) is 12 nM.

At present, three methods for antibiotic residue detection are primarily applied: microbiological assay, instrument method, and immunoassay method. Microbiological assay is used for screening antibiotics in food because of its convenience, low costs, and broad-spectrum characteristics (Haasnoot, Stouten, Cazemier, Lommen, Nouws & Keukens, 1999; Haasnoot et al. 2002). But, this assay is currently done in a laboratory and is slow, with a low sensitivity (Verheijen, Osswald, Dietrich & Haasnoot, 2000). The current instrument methods used to analyze streptomycin are gas chromatography, high performance liquid chromatography (HPLC), and liquid chromatography with mass spectrometric detection (LC-MS) (Abbasi & Hellenas, 1998; Preu & Petz, 1999). These methods are sensitive and highly specific, but require expensive instrumentation and highly skilled analysts. They are time-consuming and expensive, and are not suitable for routine analysis of large-scale samples. Immunoassay has been an alternative to the instrument and microbiological methods for accurate measurements of antibiotic residues in complex matrices, because it is highly sensitive and specific, can be conducted on a large scale, is of low cost, and is rapid and simple to conduct. Unlike the instrument methods, immunoassays do not require sample pre-concentration and extraction (Abuknesha & Luk, 2005), so they can be used extensively in detecting trace amounts of chemicals such as antibiotics (Aga, Goldfish & Kulshrestha, 2003; Abuknesha & Luk, 2005; Jin, Gui, Guo, Wang, Wu & Zhu, 2008; Qian et al., 2009). But all the cited technologies present limitations that make difficult to extend the approach to detect PenG outside the laboratory. A rapid, specific and sensitive assay that can be used on field and in all steps of the milk production, such as in the cattle shed, during the milk collection and at consumer's home is needed and will allow controlling all phases of the milk production with the consequent reduction of human exposition to antibiotics contamination.

In order to cope with the necessity to enable a fast, easy and specific approach for food matrices analysis, biosensors application, on the other hand, offer a valuable alternative detection method. In the last year different biosensors including hybrid biosensor (Ferrini, Mannoni, Carpico & Pellegrini, 2008;) electrochemical biosensor (Zacco, Adrian, Galve, Marco, Alegret & Pividori, 2007), and surface Plasmon resonance imaging/surface Plasmon resonance (SPR) immune-sensor (Raz, Bremer, Haasnoot & Norde, 2009; Caldow, Stead, Day, Sharman, Chen & Elliot,

2005; Baxter, Ferguson, Connor & Elliot, 2001) have been developed for detection PenG. In particular, SPR biosensors have become a central tool for characterizing and quantifying biomolecular interactions and the number of publications reporting applications of SPR biosensors for detection of analytes related to medical diagnostics, environmental monitoring, and food safety and security has been rapidly growing. In food safety field, the targeted analytes include pathogens, toxins, drug residues, vitamins, hormones, antibodies, chemical contaminants, allergens, and proteins. The main advantages of SPR-based detection over alternative analytical techniques include ease of use, simpler and faster sample preparation and reduced assay time from days to minutes in some cases (Homola, 2008).
Recently our research group contributes to increase the knowledge about this topic developing a SPR assay for the detection of two different analytes, the patulin (food toxin produced from different spices of fungi) and the ephedrine (drug precursor of amphetamine). Both this assays were based on the use of specific antibody produced against the selected analytes (Pennacchio et al, 2014; Varriale et al 2012) enabling their rapid, sensitive, and specific detection in matrices of interest.
In this work, we present a novel sensing approach to quantify the presence of penicillin G using a SPR technique with SensiQ discovery portable instrument. The assay is based on the use of *ad hoc* synthesized penicillin G-GlnBP (PenG-GlnBP) conjugate immobilized on gold surface of SensiQ discovery chip and specific antibodies generated against the PenG. A competitive immune-assay based on the use of produced polyclonal mono-specific antibodies have been performed in order to directly detects penicillin G (in solution). The detection limit of this assay is 20 pM, much lower than the related European Union legislation value.

2. Materials and Method

2.1 Reagents

All reagents were purchased at highest commercially available. 1-[3-(Dimethylamino)-propyl]-3-ethylcarbodiimide (EDC), bovine serum albumin (BSA; fraction V), and ovalbumin (OVA; grade V) were purchased from Sigma.PURE1A Protein A Antibody Purification Kit was purchased from Sigma. Goat polyclonal to rabbit IgG-HRP conjugate (secondary antibody) was from Abcam. Affinities resin EAH Sepharose 4B was purchased from Amersham Biosciences. Nitrocellulose transfer membrane Protran from Schleicher &Schuell and ECL detection reagents from Amersham Biosciences were used in dot blot and Western blot experiments. Microplates (96-well), LockWell MaxiSorp from Nunc, 3,5, -tetramethylbenzidine (TMB) enzyme substrate from Sigma, and a microplate reader, Multiskan EX from Thermo, were used for ELISA experiments. UV measurements were carried out on a Varian Cary 50 Bio spectrophotometer.

2.3 Synthesis of the BSA Penicillin G conjugate

The penicillin G-BSA conjugate (PenG-BSA) was prepared according to Levine (1962) [Levine, B.B. 1962 J. Med. Pharm. Chem.], with slight modifications. Briefly: BSA (10 mg) was dissolved in 2 ml of (100 mM) sodium carbonate buffer, pH 10.5. Penicillin G (5.5 mg; 100-fold molar excess) was added and the reaction mixture incubated for 16 h at 4°C. Finally an extensive dialysis against potassium phosphate (20 mM) buffer pH 7.2 (0.5 L, for 3 days with daily buffer changes) and conjugate concentration was determined spectrophotometrically at 278 nm.

2.4 Antibody production and purification

Two rabbits were immunized following a standard protocol by intradermal inoculation of an antigen (0.5 mg per rabbit). After the immunization period, the rabbits were sacrificed and their blood recovered and centrifuged to separate blood cells from serum. A 2.0 mL sample of rabbit serum was applied to a Protein A column of the PURE 1A Protein A Antibody Purification Kit, Sigma, and the IgG fraction was purified according to the manufacturer's instructions. Elution of proteins was monitored by absorbance at λ= 278 nm. The IgG fraction was eluted with glycine (0.1M) at pH 2.8 and immediately buffered in Tris/HCl (1.0 M) at pH 9.0. Finally sodium dodecyl sulphate-polyacrylamide gel electrophoresis (SDS-PAGE) was carried out to evaluate the purity of the sample.

2.5 Affinity column preparation of Penicillin G–EAH Sepharose 4B

The affinity column was obtained by conjugating PenG to EAH Sepharose 4B as follows. A 1.0 mL sample of resin was washed with H_2O at pH 4.5 (20 mL), with NaCl (0.5 M) (20 mL), and again with H2O at pH 4.5 (20 mL) and finally suspended in 2.0 mL of H2O. The Sepharose resin was added to a solution of PenG (5 mg in 0.5 mL of H2O at pH 4.5), and the resulting suspension was gently shaken. The slurry was cooled to 0°C, and EDC were added in two steps to a final concentration of 0.1 M (52 mg). After 12 h at 4°C, the reaction mixture was taken to room temperature, and after an additional 4 h the resin was extensively washed with H2O at pH 4.5 and then treated with 1.0 mL of acetic acid (0.1 M) and 38 mg of EDC for 1 h at room temperature. The suspension was washed with H_2O at pH 4.5 (20 mL), acetate buffer (0.1 M) containing NaCl (0.5 M) (20 mL), pH 4.0, and PBS (0.1 M) containing NaCl (0.3 M), pH 7.4 (20 mL), and finally packed into a polystyrene column (2 mL, BIORAD). For the affinity chromatography purification, a 2.0 mL aliquot of IgG (obtained from serum) was applied drop-wise to the affinity column prepared as described above. To eliminate unspecific antibodies, the column, before elution, was washed with three high-salt buffers: (1) PBS (0.01 M), NaCl (0.1 M), pH 7.0 (20 mL); (2) PBS (0.01 M), NaCl (0.5 M), pH 7.0 (20 mL); (3) PBS (0.01 M), NaCl (1.0 M), pH 7.0 (20 mL). At that point absorbance at 278 nm had fallen to 0.0. For the elution step glycine (0.1 M) pH 2.8 (2.5 mL), was applied to the column, and the eluate was collected in 0.5 mL fractions and monitored by absorbance measurements at 278 nm. The fractions containing the antibodies were collected, concentrated and finally dialyzed against PBS (0.1 M), NaCl (0.1 M), pH 7.4. The concentration of the antibodies was spectrophotometrically determined by absorbance measurements at 278 nm.

2.6 Synthesis of GlnBP Conjugates (PenG-GlnBP)

To avoid interference by the carrier protein in the polyclonal antibody detection process, PenG was conjugated to the glutamine-binding protein from Escherichia coli (GlnBP), a bacterial protein different from the protein used to carry out the immunization (Staiano et al, 2005). The PenG conjugate to GlnBP (PenG-GlnBP) was prepared according to Levine (Levine, 1962).

2.7 Antibody Titration

The antibody titer was determined by an indirect ELISA assay by the following general procedure. The antigen (PenG-GlnBP), dissolved in PBS (0.1 M), pH 7.4, was used to coat 96-well micro-plates, varying the concentration from 1.1 to 1.7 ng/mL (one column for every antigen concentration, 100 µL per well), overnight at

4°C. Control wells were incubated for the same period with BSA in the same buffer. The wells were rinsed three times with PBS (0.1 M) containing 0.05% Tween (PBS-T), pH 7.4, and blocked by incubation for 2 h at room temperature with PBS-T containing BSA (1%) (100 µL each well). After three washings with PBS-T, serially diluted antibody, PenG-Ser1 and PenG-Ser2, was added to the wells, incubated at room temperature for 1 h, and then rinsed three times with PBS-T. Horseradish peroxidase-conjugated anti-rabbit IgG antibodies, diluted 1:4000 in PBS-T containing BSA (1%), were added to the wells (100 µL) and incubated for 1 h at room temperature. After three washings with PBS-T, the enzyme substrate TMB was added (100 µL per well), and the color reaction was quenched after 5 min by addition of 1 M H_2SO_4 (100 µL for well). The absorbance was measured at 450 nm. The antibody titer was graphically determined by plotting the reciprocal of the antibody dilution against absorbance for each dilution of antibodies. The titer was taken as the maximum antibody dilution able to give a reading of 0.1 absorbance unit. The following values were found: 1/75000 for PenG-Ser1 and PenG-Ser2.

2.8 Surface Plasmon Resonance (SPR) experiments

The SPR measurements were carried out on SensiQ discovery instrument using CO_2H_5 sensor chip composed by glass slide coated with a thin layer of gold, on which a matrix of carboxy-methylated dextran is covalently attached. HBS-EP buffer containing 10 mM HEPES (2-[4-(2-hydroxyethyl)-1-piperazinyl]-ethanesulfonic acid) buffer at pH 7.5, 150 mM NaCl, 0,005 % polyoxyethylenesorbitan (P20) and 3.0 mM EDTA (ethylene-diammine-tetracetic acid) was used for all SPR measurements. All experiments were carried out at a flow rate of 25 µl/min. The obtained data were de-convoluted using Qdat software (SensiQ discovery).

2.9 pH Scouting

Before immobilizing PenG-GlnBP on the CO_2H_5 chip, the suitable immobilization pH was found. In particular, in the case of a protein, the optimal pH of immobilization should be in general higher than 3.5 and lower than the isoelectric point has the ligand. The procedure used for determines the appropriate immobilization pH is defined *pH scouting* and was performed with SensiQ instrument. In the case of PenG-GlnBP, the sample was diluted in 10 mM sodium acetate at pH 3.5, 4.0, 4.5, 5.0 and 5.5 to a final concentration of 100 ng/ml in each sample. The flow rate was 25 µl/min and the contact time was 5 minutes. After the last injection, a washing solution (1 M ethanolamine pH 8.5) was injected to remove any un-bound molecules. From the sensor-gram analysis we found high immobilization level at pH 5.0. Therefore, this pH was chosen for the immobilization.

2.10 Surface preparation

The carboxy-methylated dextran layer in flow cell 2 was activated by injecting a 1:1 mixture of 0.05 M N-hydroxysuccinamide (NHS) and 0.2 M N-ethyl-N'-(dimethylaminopropyl) carbodiimide hydrochloride (EDC). The PenG-GlnBP diluted in 10 mM sodium acetate buffer at pH 5.0 and was immobilized on the flow cell 2 of the chip CO_2H_5. The remaining NHS esters were blocked by the injection of a 1.0 M ethanolamine hydrochloride solution (35 µl pH 8.5). The un-reacted carboxy-methylated dextran layer in flow cell 1 was used as the reference surface.

2.11 Binding measurement

The SPR measurements were carried out in the concentration range of 0.0-100 nM of antibodies against PenG. The antibody solution was diluted in HBS-EP pH 7.4 buffer at the definite concentrations. The binding flow was fixed to 25 µL/minute and the time of injection was 3 minutes. For the regeneration process was performed using phosphoric acid 50 mM pH 3.0. The results obtained were analyzed by Qdat software**.**

2.12 Competition assay

The competition SPR assay was carried out at fixed concentration of antibody (100 nM) in the presence of increased concentrations of PenG (0.0 pM to 100 pM). The flow was fixed at 25 µL/min and the time of injection was 3 minutes. For the regeneration process a solution of phosphoric acid 10 mM at pH 3.0 was used. The results obtained were analyzed by Qdat software.

3. Results and Discussion

In this work we describe the implementation of an easy and sensitive SPR-based method for the detection of PenG in milk. PenG is the most common compound used in the pharmacological treatment of mastitis infection and added to animal food. The illegal use and/or abuse of this compound, and in general of β-lactams antibiotics, in animal feed imply a contamination of produced milk with direct consequences presence in the human food chain.PenG is a low molecular weight compound (Figure 1A), too small to elicit any immunological response. Then, we covalently attached it to an immunological carrier as reported in Levine for producing the antibodies against PenG after its injected in rabbits. In Figure 1B is shown the Penicillin G structure covalently bound to BSA (PenG-BSA) in its open ring form obtained defined penicilloyl.

3.1 Production of antibodies anti penicillin G and dot blot

Polyclonal antibodies against penicillin G were produced using PenG-BSA conjugate as an antigen. Two different rabbits were immunized using a standard protocol of immunization and at the end of the immunization period the IgG fraction were isolated from serums by the protein A column kit. The homogeneity of IgG fractions was evaluated by SDS-PAGE and the pure fractions were sequentially pooled, concentrated and dialyzed against PBS 20 mM pH 7.4. To exclude false reactions due to anti-BSA antibodies present in the rabbit serums, the penicillin G was conjugate to the glutamine-binding protein (GlnBP) purified from *E. coli*. The GlnBP conjugate was prepared by the same procedures already used for BSA conjugate and reported in material and methods section. The obtained results show that pre-immune serum did not show response, while PenG serum of both rabbit gave signals with antigen penicillin G-GlnBP and with BSA but not with GlnBP (data not shown).

3.2 Preparation of affinity columns and purification of specific antibodies

The obtained IgG fraction was loaded on affinity column in which the PenG was conjugated to EAH Sepharose-4B resin. After loading with the IgG fraction, the column was washed with buffer at neutral pH with high concentration of NaCl, in order to remove unspecific antibodies and the mono-specific antibodies were eluted using glycine buffer at pH 3.0. The different fractions were collected and a SDS-PAGE was carried out in order to evaluate the purity of the sample (data does not

show). In order to verify the specificity of the produced antibodies against the PenG a western blotting experiment was performed (data not shown). Response to antibody binding was observed only for the conjugate PenG-GlnBP, and a negative response was registered for BSA and GlnBP. This confirms the specificity of antibodies versus PenG.

3.3 ELISA Test

In order to obtain the titer of purified antibodies an indirect ELISA test was performed. For this purpose we coated the micro-plate wells with different concentrations of antigens PenG-GlnBP and we tested serially diluted mono-specific antibodies against PenG produced in rabbits. For no-coating wells, no signal was registered as consequence of incubation with different diluted samples of IgG (data does not show). The obtained results displayed that the titer of anti-penicillin G antibodies seems excellent. In fact, it was possible to perform the ELISA test with IgG dilutions up 1 to 100000. Also a consistent response was detected on coated PenG-GlnBP at a concentration of 1.1 ng/ml (data not shown).

3.4 SPR binding studies

The PenG-GlnBP was covalently immobilized on the CO_2H_5 surface chip by its amino reactive groups, using amino coupling kit. From the analysis of the pH scouting results (data do not show) we decided to immobilize the PenG-GlnBP on CO_2H_5 surface using a buffer 10 mM sodium acetate pH 5.0. To test the sensing system, the binding of polyclonal mono-specific antibodies to the PenG-GlnBP functionalized CO_2H_5 chip was monitored as a function of time. The Figure 4 shows the obtained sensorgram in which is reported the variation of the Response Unit (RU) in absence and in the presence of a wide range of concentration of anti PenG antibodies (0.0-100 nM). As clearly visible in Figure 4 that the RU_{max} signal increases with increasing concentrations of anti PenG antibodies, as consequence of binding on the surface.

3.5 SPR competitive immunoassay

Accordingly to binding experiments a competitive immunoassay was performed. In figure 3 is shown the principle of competition between penicillin G immobilized on chip and PenG free in solution. In order to evaluate the potential of our system as a competitive assay for PenG detection, different samples with a fixed concentration of antibodies (100 nM) were incubated with increasing concentrations of PenG in the range of 0.0-100 pM. Each sample was mixed off line and allowed to incubate for 10 minutes before the measurements. The bound anti-penicillin G was measured after injection and the sensor surface was regenerated with a solution of phosphoric acid 50 mM pH 3.0 at a 25 µL/min flow rate. The obtained sensor-gram is shown in Figure 4. The obtained results show a decrease in the signal with increasing concentrationsof freePenGpresent in solution. Then theantibodies anti-PenGcompete for a binding between PenG presentin solutionand PenG immobilizedon the chip.
In figure 5 is shown the dose response curve, plotting RUmax values from each SPR binding experiment against the PenG concentration. By analyzing the data reported in Figure 5, it is possible to conclude that this described method allows for the detection of an amount of PenG less then 20 pM.

Conclusions

The obtained results point out that this method is a promising alternative approach compared to the analytical methods actually in use. Extensive extraction, non-trained personnel and sample clean-up are not needed.That is to say that we combined an immune-chemical approach with SPR spectroscopy to develop an efficient PenG biosensor for the detection of penicillin G outside the laboratory. The detection limit of these assays was found to be 20 pM, a value much lower than the MRL of EU regulation limit, that is the 12 nM.
In a feasible and not so far perspective this would certainly be an innovative approach providing the dairy industries with an easy-to-use, economical, rapid antibiotic test that enable them to meet regulatory requirements and provide consumers with safe, quality milk and dairy products.

Acknowledgments

This project was realized in the frame of the CNR Commessa “Progettazione e Sviluppo di Biochip per la Sicurezza Alimentare e Salute Umana (SD; MS; AV)”. This Project was partially funded by the project CTN01_00230_240864 "SAFE &SMART-Nuove tecnologie abilitanti per la food safety e l'integrità delle filiere agro-alimentari in uno scenario globale", and it was also partially funded by the CNR project "Conoscenze integrate per sostenibilità ed innovazione del Made in Italy agro-alimentare (CISIA)”.

References

1. Abbasi, H., Hellenas, K.E. (1998). Modified determination of dihydrostreptomycin in kidney, muscle and milk by HPLC. *Analyst*, 123(12):2725-2727.

2. Abuknesha, R.A., Luk, C. (2005). Enzyme immunoassays for the analysis of streptomycin in milk, serum and water: development and assessment of a polyclonal antiserum and assay procedures using novel streptomycin derivatives. *Analyst*, 130(6):964-970.

3. Adetunji, VO and Olaoye, OO*.* (2002). Detection of β- Lactam antibiotics (Penicillin and Amoxicillin) residues in Goat milk. *Nat. Sci.,* 10(10):60-64.

4. Aga, D.S., Goldfish, R., Kulshrestha, P. (2003). Application of ELISA in determining the fate of tetracyclines in land-applied livestock wastes. *Analyst*, 128(6):658-662.

5. Baxter, G. A., Ferguson, J. P., Connor, M.C.O., Elliott, C.T. (2001). Detection of streptomycin residues in whole milk using an optical immunobiosensor. *J. Agric. Food Chem.*, *49*, 3204-320.

6. Bencini, R. and Pulina G. (1997). The quality of sheep milk: a review. Australian Journal of Experimental Agricolture, 37(4):485-504.

7. Caldow, M., Stead, S. L., Day, J., Sharman, M., Chen, S.T., Elliott C. (2005). Development and validation of an optical SPR biosensor assay for tylosin residues in honey. *J. Agric. Food Chem*., *53*, 7367-7370.

8. Epstein, J.B., S. Chong and Le ND. (2000). A survey of antibiotic use in dentistry. J. Am. Dent. Assoc., 131:1600-1609.

9. Ferrini, A. M., Mannoni, V., Carpico, G., Pellegrini, G.E. (2008). Detection and identification of beta-lactam residues in milk using a hybrid biosensor. *J. Agric. Food Chem.*, *56*, 784-788.

10. Haasnoot, W., Loomans, E., Cazemier, G., Dietrich, R., Verheijen, R., Bergwerff, A.A., Stephany, R.W. (2002). Direct versus competitive biosensor immunoassays for the detection of (dihydro)streptomycin residues in milk. *Food Agric. Immunol*.,14(1):15-27.

11. Haasnoot, W., Stouten, P., Cazemier, G., Lommen, A., Nouws, J.F.M., Keukens, H.J. (1999). Immunochemical detection of aminoglycosides in milk and kidney. *Analyst*, 124(3): 301-305.

12. Homola, J. (2008). Surface Plasmon Resonance Sensors for Detection of Chemical and Biological Species. *Chem. Rev.,*108, 462-493.

13. Jepsen, A. (1990). Residues of disinfectants and antibiotics in milk: Milk hygiene. *Nord. Vet. Med.,* 2:447.

14. Jin, R.Y., Gui, W.J., Guo, Y.R., Wang, C.M., Wu, J.X., Zhu, G.N. (2008). Comparison of monoclonal antibody-based ELISA for triazophos between the indirect and direct formats. *Food Agric. Immunol*.,19(1):49-60.

15. Levine, B.B. (1962). N(□-D-penicilloyl) amines as univalent hapten inhibitors of antibody-dependent allergic reactions to penicillin. *J. Med. Pharm. Chem*., *5*, 1025-1034.

16. Mcewen, S.A., A.H. Meek, and Black, W.D. (1991). A dairy farm survey of antibiotic-treatment practices, residue control methods and associations with inhibitors in milk. *Journal of Food Protection*. 54(6): 454-459.

17. Pennacchio, A., Ruggiero, G., Staiano, M., Piccialli, G., Oliviero, G., Lewkowicz, A., Synak, A., D'Auria, S., (2014). A Surface Plasmon Resonance based biochip for the detection of Patulin Toxin. *Optical Materials*, 36, 1670-1675.

18. Preu, M., Petz, M. (1999). Development and optimisation of a new derivatisation procedure for gas chromatographic-mass spectrometric analysis of dihydrostreptomcycin: comparison of multivariate and step-by-step optimisation procedures. *J. Chromatogr. A*, 840(1):81-91.

19. Qian, G., Wang, L., Wu, Y., Zhang, Q., Sun, Q., Liu, Y., Liu, F. (2009). A monoclonal antibody-based sensitive enzyme-linked immunosorbent assay (ELISA) for the analysis of the organophosphorous pesticides chlorpyrifos-methyl in real samples. *Food Chem.*, 117(2):364-370.

20. Raz, S.R., Bremer, M.G.E.G., Haasnoot, W., Norde, W. (2009). Label-free and multiplex detection of antibiotic residues in milk using imaging surface plasmon resonance-based immunosensor. *Anal. Chem.*, *81*, 7743-7749.

21. Staiano, M., Scognamiglio, V., Rossi, M., D'Auria, S., Stepanenko, O.V., Kuznetsova, I.M., Turoverov, K.K. (2005). Unfolding and refolding of the glutamine-binding protein from Escherichia coli and its complex with glutamine-induced by guanidine hydrochloride. *Biochemistry*.,*44*, 5625-5633.

22. Varriale, M. Staiano, V. M. Marzullo, M. Strianese, S. Di Giovannni, G. Ruggiero, A. Secchi, M. Dispenza, A.M. Fiorello and S. D'Auria A surface plasmon resonance-based biochip to reveal traces of ephedrine. *Anal. Methods,* 2012, 4, 1940–1944.

23. Verheijen, R., Osswald, I.K., Dietrich, R., Haasnoot, W. (2000). Development of a one step strip test for the detection of (dihydro)streptomycin residues in raw milk. *Food Agric.Immunol.*,12(1):31-40.

24. Zacco, E., Adrian, J., Galve, R., Marco, M.P., Alegret, S., Pividori, M.I. (2007). Electrochemical magneto immunosensing of antibiotic residues in milk. *Biosens. Bioelectron.*,*22*, 2184-2191.

Legend of figures

Figure 1. PenG structure (1A) and schematic representation of the BSA conjugate (1B).

Figure 2. Sensorgram showing the binding of mono-specific antibodies anti-penicillin G. All measurements were performed in HBS-EP buffer at 25 °C

Figure 3. Schematic representation of competitive SPR-based immunoassay for detection of penicillin G using functionalized chip.

Figure 4. Sensorgram of the competitive immunoassay. All measurements were performed in HBS-EP buffer at 25 °C.

Figure 5. Titration of the SPR-based sensing system with penicillin G. RUmax are plotted versus the total penicillin G concentration.

Figures

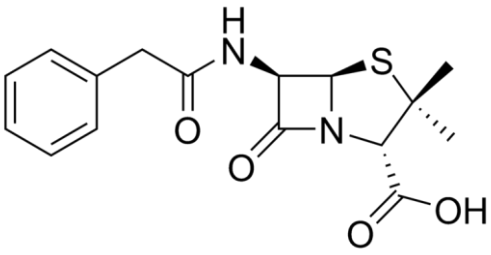

1A

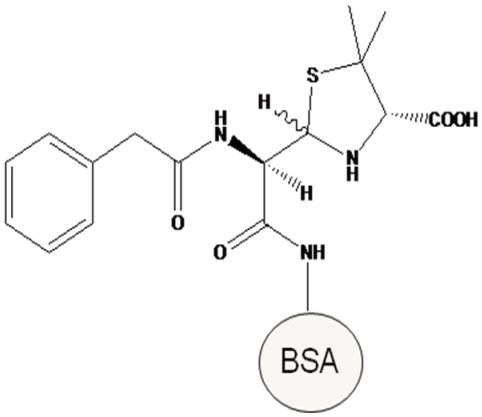

1B

Fig.1

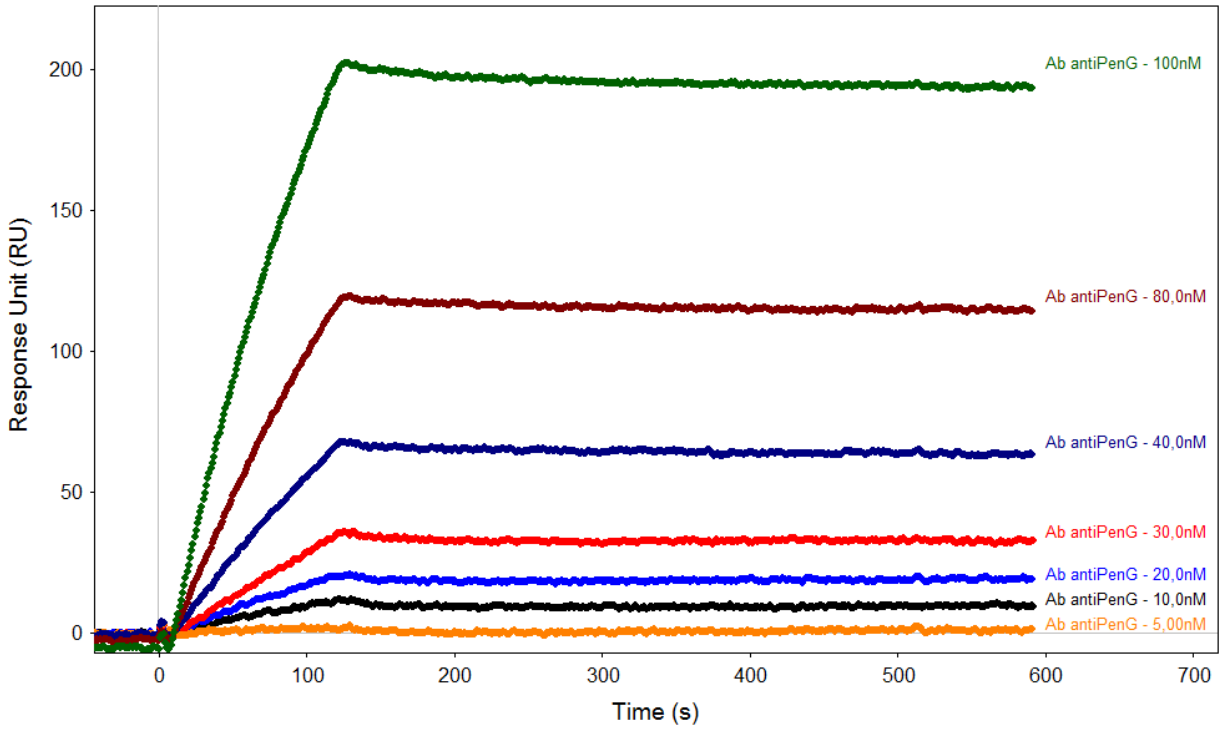
Response Unit (RU)
200
150
100
50
0
0
100
200
300
400
500
600
700
Time (s)
Ab antiPenG - 100nM
Ab antiPenG - 80,0nM
Ab antiPenG - 40,0nM
Ab antiPenG - 30,0nM
Ab antiPenG - 20,0nM
Ab antiPenG - 10,0nM
Ab antiPenG - 5,00nM

Fig. 2

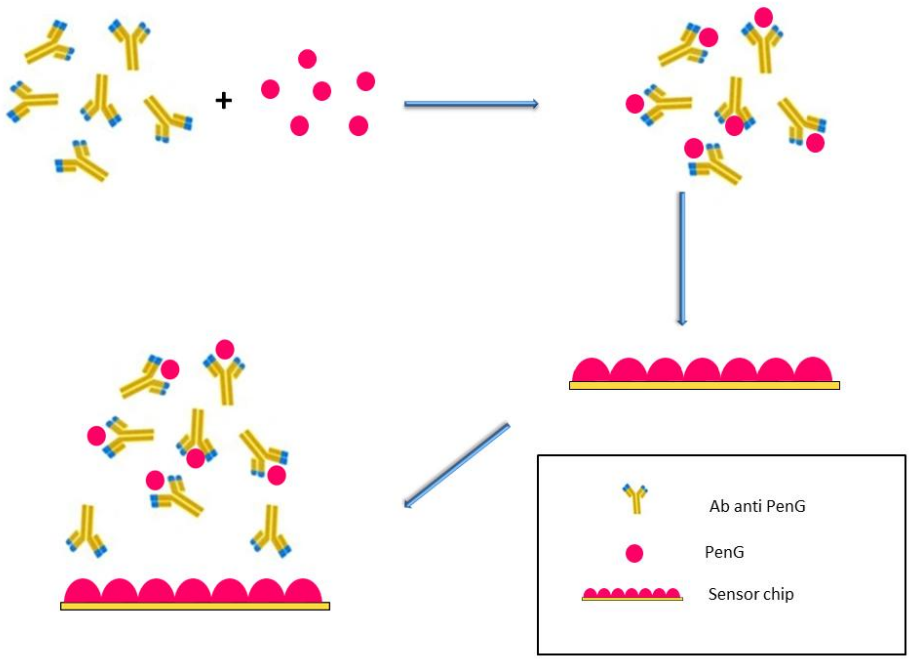
+
Ab anti PenG
PenG
Sensor chip

Fig.3

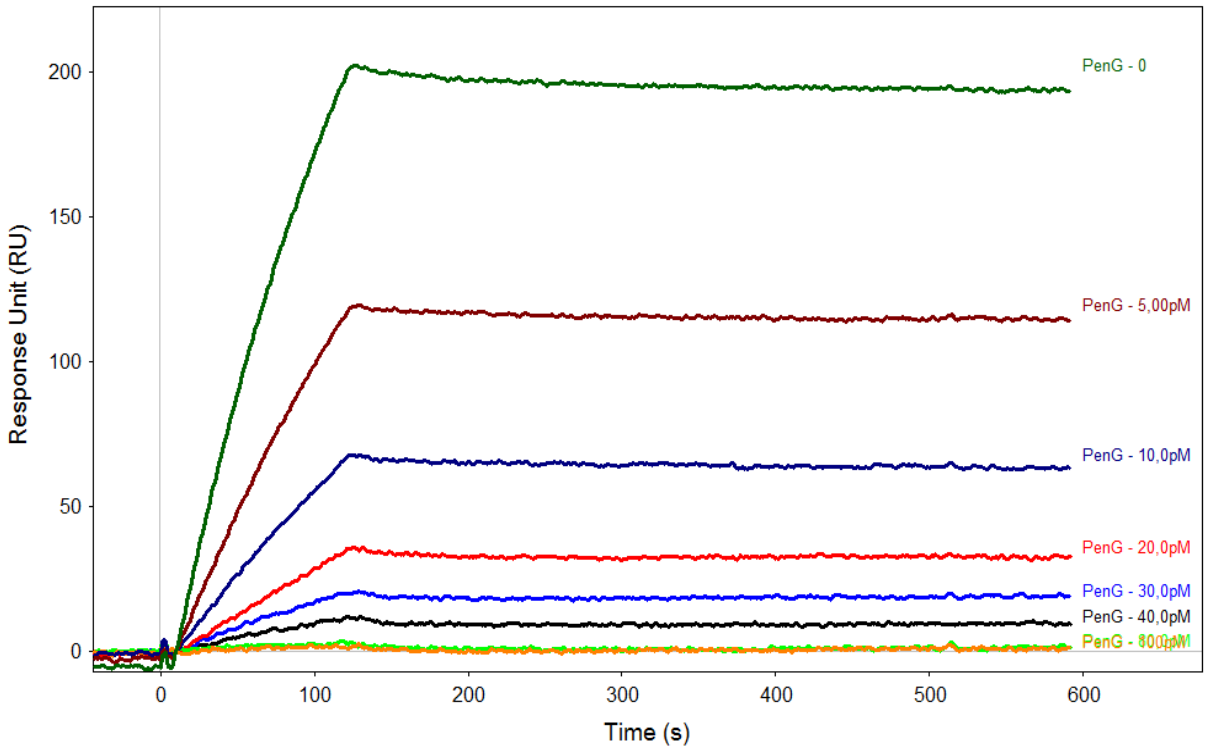
Response Unit (RU)
Time (s)
PenG - 0
PenG - 5,00pM
PenG - 10,0pM
PenG - 20,0pM
PenG - 30,0pM
PenG - 40,0pM
PenG - 800pM

Fig. 4

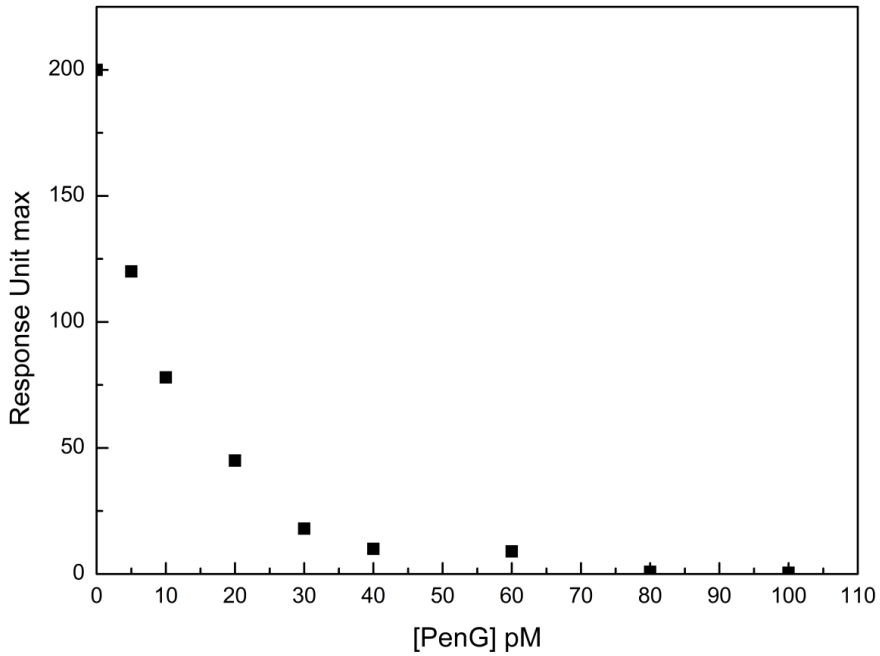
Response Unit max
[PenG] pM

Fig. 5

Chapter 4
A Novel Fluorescence Polarization Assay For Determination of Penicillin G in milk

Submitted to Food Chemistry (Article in press)

A Novel Fluorescence Polarization Assay for Determination of Penicillin G in Milk

Anna Pennacchio, Antonio Varriale, Andrea Scala, Vincenzo Manuel Marzullo, Maria Staiano and Sabato D'Auria*
Laboratory for Molecular Sensing, Institute of Protein Biochemistry CNR, Via P. Castellino N°111
80131, Naples, Italy

*Correspondence to:
Dr. Sabato D'Auria
Laboratory for Molecular Sensing, IBP-CNR, Via Pietro Castellino, 111
80131 Naples, ITALY
Tel. +39-0816132250Fax: +39-0816132277
Email: s.dauria@ibp.cnr.it

Abstract

Detection of Penicillin G in milk is of high interest due to the great extent of the use of antibiotics in livestock. The current analytical methods used to quantify the penicillin G in milk are based on HPLC, mass spectrometry and electrophoresis techniques. These methodologies are time-consuming and require trained personnel. In addition, it is not easy to envisage the development of a portable device based on these methods for in-situ analyses. We present a novel sensing approach to detect the presence of penicillin G in milk. The proposed method is based on the use of a red emitting penicillin G conjugate with properly produced antibodies anti-penicillin G. The obtained results point out that our methodology can be applied directly on milk solution without interferences. The limit of detection of the method is about 1.0 nM, a value much lower the MRL of EU regulation value, that is 12.0 nM.

Key Words: Fluorescence; Biosensors; Antibody; Penicillin G; Milk

Introduction

All over the world antibiotics have been widely used in animal husbandry for over 50 years with the principal aim to prevent and/or treat diseases affecting animals. Nowadays the compounds mainly used belong to β-lactams family that includes penicillin G and cephalosporins, both extensively employed in the treatment of food producing animals as food additives. Due to their use in animals for human consumption, the high risks of presence of unwanted residues in comestible products exist.
In particular, in the animal destined to milk production, these antibiotics are generally used in mastitis therapy, leading to the presence of residues in raw milk and therefore in dairy products.
The illegal use and/or abuse of β-lactams in animal feed lead to their presence in the food chain and to health risks for human, such as allergenic and/or toxicological responses and moreover it induces a selective pressure for antibiotic-resistant for particular strains. Furthermore the presence of antibiotic residues in milk causes a technological problem because it can inhibit the growth of starter cultures in

fermentative process, for example in cheese and in yogurt production (Grunwald, and Petz, 2003).
In order to prevent the negative impact of β-lactam and in particular of penicillin G residues present in the milk on customer's health many countries have been established maximum residue limits (MRLs). The European Union (EU) Regulation 508/1999 has established the MRLs in milk and in animal tissues fore some antibiotics, for benzyl-penicillin in milk (penicillin G) is 4 μg kg^{-1} or 1.2 10^{-8} M (European Communities, 1990).
Actually the most commonly used methodologies for the determination of β-lactams in milk are Liquid chromatography (LC) (Bailon-Perez, Garcia-Campana, Del Olmo and Iruela Cruces-Blanco, 2009), gas chromatography (GC) (Le, Wan and Lam, 2002; Galbusera and Chen, 2003), High Performance Liquid Chromatography (HPLC) (Dasenbrock and La Course, 1998) and Mass Spectrometry (MS) (Xu et al, 2010). These methods are time-consuming, required complex sample preparation and the use of expensive equipment. Furthermore many microbiological assays based on inhibition grow of test microorganisms are widely used (Kavanagh, 1989). These tests are specific for the commonly used antibiotics, but require long time of incubation. In addition to the immunochemical analytical methods, enzyme-linked immune-sorbent assay (ELISA) (Jin, Jang and Lee, 2006; Adrian, Font, Diserens and Baeza, 2009; Font, Adrian, Galve, Esterves and Castellari, 2008) for detection of penicillin G in milk has been developed. These assays offer several advantages compared to conventional analysis, i.e., low cost per sample, high selectivity and high sensitivity even if it is time-consuming.
In this contest a rapid, specific and sensitive assay that can be used in all steps of the milk production, such as in the cattle shed, during the milk collection and at consumer's home is needed. This will allow controlling all phases of the milk production with the consequent reduction of human exposition to antibiotics contamination.
Recently biosensors including hybrid biosensor (Ferrini, Mannoni, Carpico and Pellegrini, 2008), electrochemical biosensor (Zacco et al, 2007) , and surface Plasmon resonance imaging/surface Plasmon resonance (SPR) immune-sensor (Raz, Bremer, Haasnoot and Norde, 2009; Caldow et al, 2005; Baxter, Ferguson, Connor and Elliott, 2001) have been developed. Biosensors represent very alternative methods of analysis and they are a potential approach able to solve several problems related to food safety.
In this work we describe a new method for the detection of penicillin G in raw milk using a fluorescence polarization technique. The assay is based on the use of an *ad hoc* synthesized fluorescence penicillin G-GlnBP (PenG-GlnBP) conjugate labeled with fluorescent probe (Biotium CF647) and of a specific antibodies generated against the analyte. A competitive immunoassay based on the use of polyclonal mono-specific antibodies have been performed in order to directly detect penicillin G in raw sample of milk.
Recently we have developed, using the same approach a fluorescence polarization assay for detection of benzyl methyl ketone, a precursor in amphetamine synthesis (Di Giovanni et al, 2012). Importantly the whole apparatus used for our experiments could be replaced by a small and cheap optical device which is capable of revealing polarization fluorescence changes upon interaction between the penicillin G derivative and anti-Penicillin G antibodies. Finally this method could be apply for other contaminates of milk by changing fluorescent conjugate molecules and specific antibodies.

Material and Methods

2.1. Reagents

All reagents were purchased at highest commercially available. 1-[3-(Dimethylamino)-propyl]-3-ethylcarbodiimide (EDC), bovine serum albumin (BSA; fraction V), and ovalbumin (OVA; grade V) were purchased from Sigma. PURE1A Protein A Antibody Purification Kit was purchased from Sigma. Goat polyclonal to rabbit IgG-HRP conjugate (secondary antibody) was from Abcam. Affinities resin EAH Sepharose 4B was purchased from Amersham Biosciences. Nitrocellulose transfer membrane Protran from Schleicher & Schuell and ECL detection reagents from Amersham Biosciences were used in dot blot and Western blot experiments. Microplates (96-well), LockWell MaxiSorp from Nunc, 3,5,-tetramethylbenzidine (TMB) enzyme substrate from Sigma, and a micro-plate reader, Multiskan EX from Thermo, were used for ELISA experiments. UV measurements (detection at 278 nm) were carried out on a Varian Cary 50 Bio spectrophotometer. The fluorescent probe CF647 was purchased from Biotium.

2.2. Synthesis of the BSA Penicillin G conjugate

The penicillin G BSA conjugate was (PenG-BSA) prepared according to Levine (1962) (Levine, 1962) with slight modifications. Briefly: BSA (10 mg) was dissolved in 2 ml of (100 mM) sodium carbonate buffer, pH 10.5. Penicillin G (5.5 mg; 100-fold molar excess) was added and the reaction mixture incubated for 16 h at 4°C. After dialysis against (20 mM) potassium phosphate buffer, pH 7.2 (0.5 L, for 3 days with daily buffer changes). The conjugate concentration was 4.0 mg/mL.

2.3. Antibody production and purification

Two rabbits were immunized following a standard protocol by intradermal inoculation of an antigen (0.5 mg per rabbit). After the immunization period, the rabbits were sacrificed and their blood recovered and centrifuged to separate blood cells from serum. A 2.0 mL sample of rabbit serum was applied to a Protein A column of the PURE 1A Protein A Antibody Purification Kit, Sigma, and the IgG fraction was purified according to the manufacturer's instructions. Elution of proteins was monitored by absorbance at λ= 278 nm. The IgG fraction was eluted with glycine (0.1M) at pH 2.8 and immediately buffered in Tris/HCl (1.0 M) at pH 9.0. Finally sodium dodecyl sulfate-polyacrylamide gel electrophoresis (SDS-PAGE) was carried out to evaluate the purity of the sample.

2.4. Affinity column preparation of Penicillin G–EAH Sepharose 4B

The affinity column was obtained by conjugating Penicillin G to EAH Sepharose 4B as follows. A 1.0 mL sample of resin was washed with H_2O at pH 4.5 (20 mL), with NaCl (0.5 M) (20 mL), and again with H_2O at pH 4.5 (20 mL) and finally suspended in 2.0 mL of H_2O. The Sepharose resin was added to a solution of Penicillin G (5 mg in 0.5 mL of H_2O at pH 4.5), and the resulting suspension was gently shaken. The slurry was cooled to 0°C, and EDC was added in two steps to a final concentration of 0.1 M (52 mg). After 12 h at 4°C, the reaction mixture was taken to room temperature, and after an additional 4 h the resin was extensively washed with H_2O at pH 4.5 and then treated with 1.0 mL of acetic acid (0.1 M) and 38 mg of EDC for 1 h at room temperature. The suspension was washed with H_2O at pH 4.5 (20 mL), acetate buffer (0.1 M) containing NaCl (0.5 M) (20 mL), pH 4.0, and PBS (0.1 M) containing NaCl (0.3 M), pH 7.4 (20 mL), and finally packed into a polystyrene column (2 mL,

BIORAD). For the affinity chromatography purification, a 2.0 mL aliquot of IgG (obtained from serum) was applied drop-wise to the affinity column prepared as described above. To eliminate unspecific antibodies, the column, before elution, was washed with three high-salt buffers: (1) PBS (0.01 M), NaCl (0.1 M), pH 7.0 (20 mL); (2PBS (0.01 M), NaCl (0.5 M), pH 7.0 (20 mL); (3) PBS (0.01 M), NaCl (1.0 M), pH 7.0 (20 mL). At that point absorbance at 278 nm had fallen to 0.0. For the elution step glycine (0.1 M), pH 2.8 (2.5 mL), was applied to the column and the eluate was collected in 0.5 mL fractions and monitored by absorbance measurements at 278 nm. The fractions containing the antibodies were collected, concentrated by means of a Centricon YM-3 membrane to a volume of 1.0 mL, and dialyzed against PBS (0.1 M), NaCl (0.1 M), pH 7.4. The concentration of the antibodies was determined by absorbance measurements at 278 nm.

2.5. Synthesis of GlnBP Conjugates (PenG-GlnBP)

To avoid interference by the carrier protein in the polyclonal antibody detection process, PenG was conjugated to the glutamine-binding protein from *Escherichia coli* (GlnBP), a bacterial protein different from the protein used to carry out the immunization. The following procedure was used: GlnBP (10 mg) was dissolved in 2 ml of sodium carbonate buffer, (100 mM) pH 10.5. Penicillin G (5.5 mg; 100-fold molar excess) was added and the reaction mixture incubated for 16 hours at 4°C. After dialysis against potassium phosphate buffer (20 mM), pH 7.2 (0.5 L, for 3 days with daily buffer changes). The conjugate concentration, determined at 278 nm, was 4.0 mg/mL.

2.6. *Western Blot Experiments*

Proteins (BSA, PenG-GlnBP, and GlnBP, 10 µg each) were loaded, separated by sodium dodecyl sulfate-polyacrylamide gel electrophoresis (12% SDS-PAGE), and then transferred overnight at 4°C onto a nitrocellulose membrane. Membranes were blocked for 1 h at room temperature in 50 mL of the blocking buffer (PBS containing 5% of milk and 0.05% Triton X100). After two washings with PBS-TT and one with PBS (10 min per washing), the filters were incubated with purified IgG, at respectively (1:500 in the blocking buffer), for 1 h at room temperature. After two washings with PBS-TT and one with PBS (10 min per washing), the filters were incubated with secondary antibody (goat anti-rabbit HRP conjugate, 1:6000 in the blocking buffer) for 1 hours at room temperature. The filters were washed three times as described above and then developed with the detection reagent ECL.

2.7. Antibody Titration Experiments

The antibody titer was determined by an indirect ELISA assay by the following general procedure. The antigen (PenG-GlnBP), dissolved in PBS (0.1 M), pH 7.4, was used to coat 96-well micro-plates, varying the concentration by a factor 3 from 1.1 to 1.7 ng/mL (one column for every antigen concentration, 100 µL per well), overnight at 4°C. Control wells were incubated for the same period with BSA in the same buffer. The wells were rinsed three times with PBS (0.1 M) containing 0.05% Tween (PBS-T), pH 7.4, and blocked by incubation for 2 h at room temperature with PBS-T containing BSA (1%) (100 µL each well). After three washings with PBS-T, serially diluted antibody, PenG-Ser1 and PenG-Ser2, was added to the wells, incubated at room temperature for 1 h, and then rinsed three times with PBS-T. Horseradish peroxidase-conjugated anti-rabbit IgG antibodies, diluted 1:4000 in PBS-T containing BSA (1%), were added to the wells (100 µL) and incubated for 1 h at

room temperature. After three washings with PBS-T, the enzyme substrate TMB was added (100 µL per well), and the color reaction was quenched after 5 min by addition of 1 M H_2SO_4 (100 µL per well). The absorbance was measured at 450 nm. The antibody titer was graphically determined by plotting the reciprocal of the antibody dilution against absorbance for each dilution of antibodies. The titer was taken as the maximum antibody dilution able to give a reading of 0.1 absorbance unit. The following values were found: 1/75000 for PenG-Ser1 and PenG-Ser2.

2.8. Fluorescence Labeling of PenG-GlnBP

A solution of PenG-GlnBP at concentration of 1.0 mg/mL in 1.0 mL was dissolved in 0.1 M sodium bicarbonate buffer, pH 7.0 and mixed with CF647. The molar ratio of the dye and the protein was kept 10:1. The reaction mixture was incubated for 1 hours at room temperature and the labeled molecules were separated from un-reacted probe by gel filtration and extensive dialysis procedure against 50 mM phosphate buffer pH 7.4 at 4°C.

2.9. *Steady-state fluorescence measurements*

Steady state fluorescence experiments were carried out with FP-8600 Fluorescence Spectrometer (Jasco-Japan) equipped with a one-cell temperature controlled sample holder. The excitation wavelength was fixed at 630 nm and emission spectra were recorded between 650 nm and 800 nm with an emission slit-width of 2.5 nm. The measurements were performed in milk solution diluted 1.10, at room temperature. PenG-GlnBP-CF647 was incubated with a range of concentration of antibodies against penicillin G from 0.0 to 2,2 pmol for 10 minutes, and fluorescence spectra were carried out. The polarization fluorescence measurements were acquired by inserting a Glan polarizer between the excitation source and the sample, with a vertical (0°) excitation polarized filter and with a horizontal (90°) emission polarized filter.

2.10. Penicillin G competition assay

A competition polarization assay was carried out at a fixed concentration of antibody against PenG (2,2 pmol) in the presence of increased concentrations of un-labeled PenG in the range of concentration from 0.0 to 2.4 pM. The incubation was done at room temperature for 30 minutes. After this pre-incubation in the presence of unlabeled PenG, the polarization fluorescence measurements were carried out with FP-8600 Fluorescence Spectrometer with an excitation polarized filter set at 0° and an emission polarized filter set at 90°.

3. Results and Discussion

Penicillin G is the most common compound used in the pharmacological treatment of mastitis infectionin food producing animals. Illegal use and/or abuse of Penicillin G, and in general of β-lactams in animal feed, imply a contamination of produced milk with several consequences for human health. A rapid and simple method of detection able to control in all phases of milk production, form the cattle shed to the table of the consumers, the concentration of penicillin G in milk is needed. For this purpose we have covalently attached the penicillin G to a protein carrier. In Figure 1 is shown the PenG structure covalently bound to BSA in its open ring form (penicilloyl). This conjugate was been used to produce polyclonal antibodies anti-PenG in rabbit.

3.1. Production of against the penicillin G and dot blot

Polyclonal antibodies against penicillin G were produced using PenG-BSA conjugate as an antigen. Two different rabbits were immunized using a standard protocol of immunization and at the end of the immunization period the IgG fraction were isolated from serums by the protein A column kit. The homogeneity of IgG fractions was evaluated by SDS-PAGE and the pure fractions were sequentially pooled, concentrated and dialyzed against PBS 20 mM pH 7.4. These antibodies were used in dot blot experiment (PenG-Ser1 and PenG-Ser2 from rabbit 1 and rabbit 2 respectively). To exclude false reactions due to anti-BSA antibodies present in the rabbit serums, the penicillin G was conjugate with a protein different from BSA. For this purpose, the glutamine-binding protein (GlnBP) purified from *E. coli* was chosen (Staiano et al, 2005).

The GlnBP conjugate was prepared by the same procedures already used for BSA conjugate and reported in material and methods section. PenG-GlnBP, BSA as the positive control, and GlnBP as the negative one were spotted on four nitrocellulose membranes, and each membrane was incubated with immune antiserums (PenG-Ser1 and PenG-Ser2, respectively, from rabbit 1 and rabbit 2 at 1:250 dilution) and pre-immune serums from both rabbits (PenG-Ser1 and PenG-Ser2, dilution 1:250). The obtained results show that pre-immune serums did not show response, while PenG-Ser1 and PenG-Ser2 gave signals with antigen penicillin G-GlnBP and with BSA but not with GlnBP (not shown).

3.2. Preparation of affinity columns and purification of specific antibodies and western blotting

The obtained IgG fraction was loaded on affinity column in which the PenG was conjugated to EAH Sepharose-4B resin. After loading with the IgG fraction, the column was washed with buffer at neutral pH with high concentration of NaCl, in order to remove unspecific antibodies and the mono-specific antibodies were eluted using glycine buffer at pH 3.0. The different fractions were collected and a SDS-PAGE was carried out in order to evaluate the purity of the sample (data does not show). In order to verify the specificity of the produced antibodies against the penicillin G a western blotting experiment was performed. In Figure 2A and 2B are showed the SDS-PAGE and western blotting experiment results. Response to antibody binding was observed only for the conjugate PenG-GlnBP, and a negative response was registered for BSA and GlnBP. This confirms the specificity of antibodies versus PenG.

3.3. ELISA Test

In order to obtain the titer of purified antibodies an indirect ELISA test was performed. For this purpose we coated the micro-plate wells with different concentrations of antigens PenG-GlnBP and we tested serially diluted mono-specific antibodies against PenG produced in rabbits. In Figure 3 are showed the results of the ELISA tests reported as bar histogram in witch the absorbance value at 450 nm was plotted versus different concentrations of coated PenG-GlnBP. For no-coating wells, no signal was registered as consequence of incubation with different diluted samples of IgG. The obtained value shows an increase of the absorbance in function of decrease of the dilution factor of mono-specific antibodies anti-PenG. The results showed that the titer of antibodies anti-penicillin G seems excellent. In fact, it was possible to perform the ELISA test with IgG dilutions up 1 to 100000. Also a

consistent response was detected on coated PenG-GlnBP at a concentration of 1.1 ng/ml.

3.4. Fluorescence steady-state measurements of PenG-GlnBP-CF647 conjugate

In Figure 4 is shown the polarized emission spectra of penG-GlnBP-CF647 in the absence and in the presence of increasing concentrations of antibodies anti-PenG. Before the polarization measurements were performed, in order to be sure that the fluorescence conjugate PenG-GlnBP-CF647 was not contaminated with the presence of free dye, gel filtration experiments followed by an extensive dialysis process were performed. The fluorescence polarization measurements were performed directly in milk. In particular, a solution of milk ten-times diluted was used for the experiments. The excitation value was fixed at 630 nm, and the emission spectra were acquired from 650 nm to 800 nm. The maximum of fluorescence emission was centered at 668 nm. The measurements were performed at room temperature, and an antibody solution from 0.0 to 2,2 pmol was added. The acquired results revealed an increase of PenG-GlnBP-CF647polarized fluorescence intensity as consequence of binding.

3.5. Fluorescence polarization competitive immunoassay

The fluorescence polarization (FP) competitive immune-assay was used to measure the competition between the tracer of un-labeled PenG in solution and PenG-GlnBP-CF647 for binding with mono-specific antibodies anti-penicillin G. For this purpose different samples at a fixed concentration of antibody (2,2 pmol) were incubated in the presence of increasing concentrations of un-labeled penicillin G in the range of 0.0 to 2.4 pM. Each sample was mixed off-line and incubated for 30 minutes at room temperature before fluorescence polarization measurements were performed. In Figure 5 are shown the polarized fluorescence emission spectra in the presence of increasing concentrations of un-labeled PenG. As consequence of addition of un-labeled PenG, a reduction (almost 47%) of the maximum of fluorescence emission was registered.

In Figure 6 is shown the dose response for PenG detection in a diluted milk solution reporting the polarization fluorescence intensity at 668 nm as function of PenG concentration. The results show it is possible to detect an amount of penG less than 1.0 nM. This value is below to the MRL of EU regulation value, that is 12.0 nM.

In conclusion, the obtained results point out that this method is a promising alternative approach compared to the analytical methods actually in use. Also, we can image to implement our methodology in portable and user-friendly device to detect PenG during all steps of milk production and collection.

Acknowledgement

This project was realized in the frame of the CNR Commessa “Progettazione e Sviluppo di Biochip per la Sicurezza Alimentare e Salute Umana (SD; MS; AV)”. This Project was partially funded by the project CTN01_00230_240864 "SAFE &SMART-Nuove tecnologie abilitanti per la food safety e l'integrità delle filiere agro-alimentari in uno scenario globale" and it was also partially funded by the CNR project "Conoscenze integrate per sostenibilità e innovazione del Made in Italy agroalimentare (CISIA)”.

References

Adrian, J., Font, H., Diserens, J.M., Baeza, F.S. (2009). Generation of broad specificity antibodies for sulfonamide antibiotics and development of an enzyme-linked immunosorbent assay (ELISA) for the analysis of milk samples.*J. Agric. Food Chem.*, *57*, 385 -394.

Bailon-Perez, A.M., Garcia-Campana, M.I., del Olmo, M., Iruela Cruces-Blanco, C. (2009). Trace determination of 10 β-lactam antibiotics in environmental and food samples by capillary liquid chromatography. *J.Chromatogr. A*, *1216*, 8355–8361.

Baxter, G. A., Ferguson, J. P., Connor, M.C.O., Elliott, C.T. (2001). Detection of streptomycin residues in whole milk using an optical immunobiosensor.*J. Agric. Food Chem.*, *49*, 3204-3207

Caldow, M., Stead, S. L., Day, J., Sharman, M., Chen, S.T., Elliott C. (2005). Development and validation of an optical SPR biosensor assay for tylosin residues in honey. *J. Agric. Food Chem*., *53*, 7367-7370.

Dasenbrock, C.O., La Course W.R. (1998). Assay for cephapirin and ampicillin in raw milk by high-performance liquid chromatography--integrated pulsed amperometric detection. *Anal. Chem., 70*, 2415-20.

Di Giovanni, S., Varriale, A., Marzullo, V. M., Ruggiero, G., Staiano, M., Secchi, A.,Pierno, L., Fiorello, A. M., and D'Auria, S. (2012). Determination of benzyl methyl ketone- a commonly used precursor in amphetamine manufacture.*Anal. Methods*.,*4*, 3558-3564.

European Communities (1990).*Official Journal of the European Communities*, Commission Regulation (EEC) NO 2377/90, L 224, 1–8.

Ferrini, A. M., Mannoni, V., Carpico, G., Pellegrini, G.E. (2008). Detection and identification of beta-lactam residues in milk using a hybrid biosensor.*J. Agric. Food Chem.*, *56*, 784-788.

Font, H., Adrian, J., Galve, R., Esterves, M.C., Castellari, M. (2008). Immunochemical assays for direct sulfonamide antibiotic detection in milk and hair samples using antibody derivatized magnetic nanoparticles. *J. Agric. Food Chem.*, *56*, 736-743.

Galbusera, C., Chen, D. D. Y. (2003). Molecular interaction in capillary electrophoresis.*Curr. Opin. Biotech*.,*14*, 126.

Grunwald, L., Petz, M. (2003).Food processing effects on residues: penicillins in milk and yoghurt. *Anal. Chim. Acta*.,*483*, 73–79.

Jin, Y., Jang, W., Lee, M. H. (2006). Development of ELISA and immune chromatographic assay for the detection of neomycin.*Clin. Chim. Acta*.,*364*, 260-266.

Kavanagh, F. (1989). Theory and practice of microbiological assaying for antibiotics.*J. Assoc. Off. Anal. Chem*., *72*, 6-10.

Le, X. C., Wan, Q. H., Lam, M. T. (2002). Fluorescence polarization detection for affinity capillary electrophoresis.*Electrophoresis*, *23*, 903-908.

Levine, B.B. (1962). N(□-D-penicilloyl) amines as univalent hapten inhibitors of antibody-dependent allergic reactions to penicillin. *J. Med. Pharm. Chem*., *5*, 1025-1034.

Raz, S.R., Bremer, M.G.E.G., Haasnoot, W., Norde, W. (2009).Label-free and multiplex detection of antibiotic residues in milk using imaging surface plasmon resonance-based immunosensor.*Anal. Chem.*, *81*, 7743-7749.

Staiano, M., Scognamiglio, V., Rossi, M., D'Auria, S., Stepanenko, O.V., Kuznetsova, I.M., Turoverov, K.K. (2005). Unfolding and refolding of the glutamine-binding protein from Escherichia coli and its complex with glutamine-induced by guanidine hydrochloride. *Biochemistry*.,*44*, 5625-5633.

Xu, Z., Wang, H. Y., Huang, S. X., Wei, Y. L., Yao, S. J., Guo, Y. L. (2010). Determination of beta-lactamase residues in milk using matrix-assisted laser desorption/ionization Fourier transform mass spectrometry. *Anal. Chem*.,*82*, 2113- 2118.

Zacco, E., Adrian, J., Galve, R., Marco, M.P., Alegret, S., Pividori, M.I. (2007). Electrochemical magneto immunosensing of antibiotic residues in milk.*Biosens. Bioelectron.*,*22*, 2184-2191.

Legends to Figures

Figure 1. Schematic representation of the BSA conjugate used for the production of the rabbit anti- PenG antibodies.

Figure 2. SDS-PAGE (A) and nitrocellulose filter (B) after incubation with Penicillin G antibodies; lane 1, molecular weight standards; lane 2, GlnBP; lane 3, PenG-GlnBP; lane 4, bovine serum albumin.

Figure 3. ELISA test of mono-specific anti-Penicillin G IgG purified from the serum of two different rabbit. The assay was performed in the Tris–borate buffer in the presence of 0.005% Tween and 1% milk. Temperature was set at 25 °C.

Figure 4. Polarization emission spectra of penG-GlnBP-CF647 in the absence and in the presence of increasing concentration anti-PenG antibodies. The measurements were performed in PBS buffer at 7.4. The temperature was set at 25 °C.

Figure 5. Polarization fluorescence emission spectra of penG-GlnBP-CF647. The measurements were performed in PBS buffer at 7.4. The temperature was set at 25 °C.

Figure 6. Titration of FP immune-assay with increasing concentration of un-labeled PenG

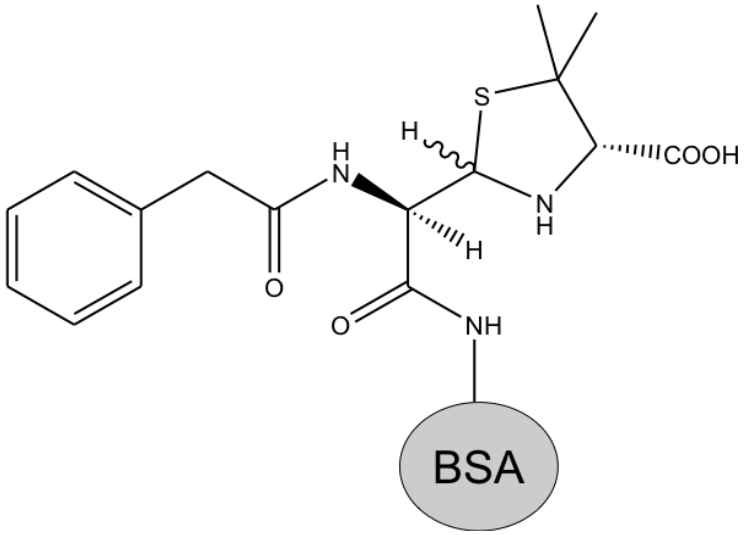
S
H
COOH
H
N
N
H
H
O
O
NH
BSA

Fig. 1

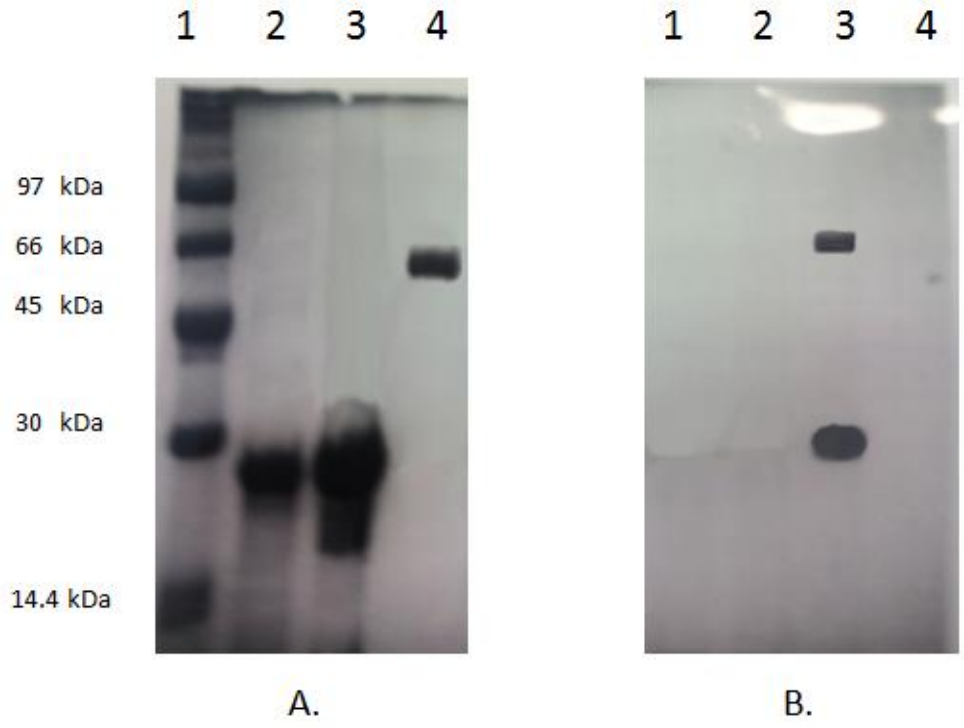
1 2 3 4
97 kDa
66 kDa
45 kDa
30 kDa
14.4 kDa
A.
1 2 3 4
B.

Fig.2

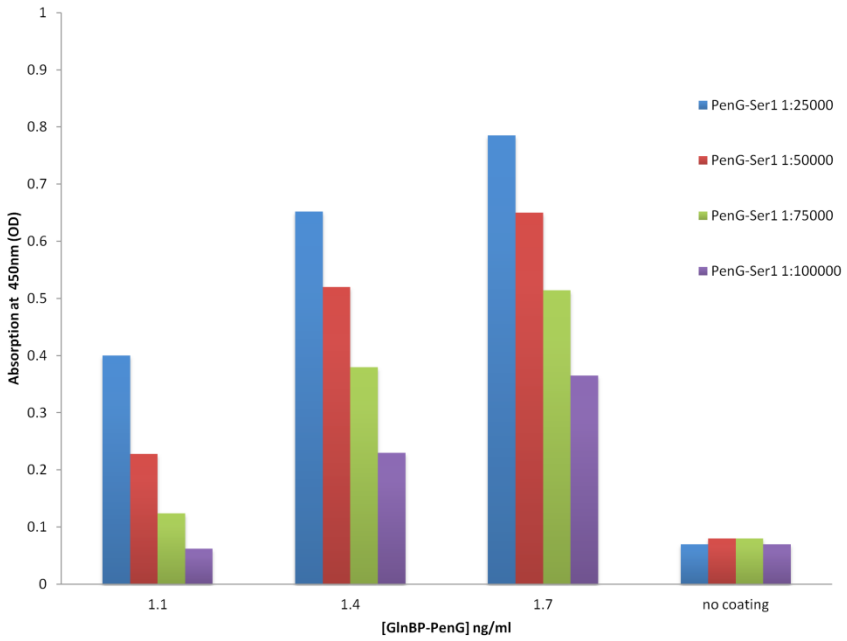
Absorption at 450nm (OD)
1
0.9
0.8
0.7
0.6
0.5
0.4
0.3
0.2
0.1
0
1.1
1.4
1.7
no coating
[GlnBP-PenG] ng/ml
PenG-Ser1 1:25000
PenG-Ser1 1:50000
PenG-Ser1 1:75000
PenG-Ser1 1:100000

Fig. 3

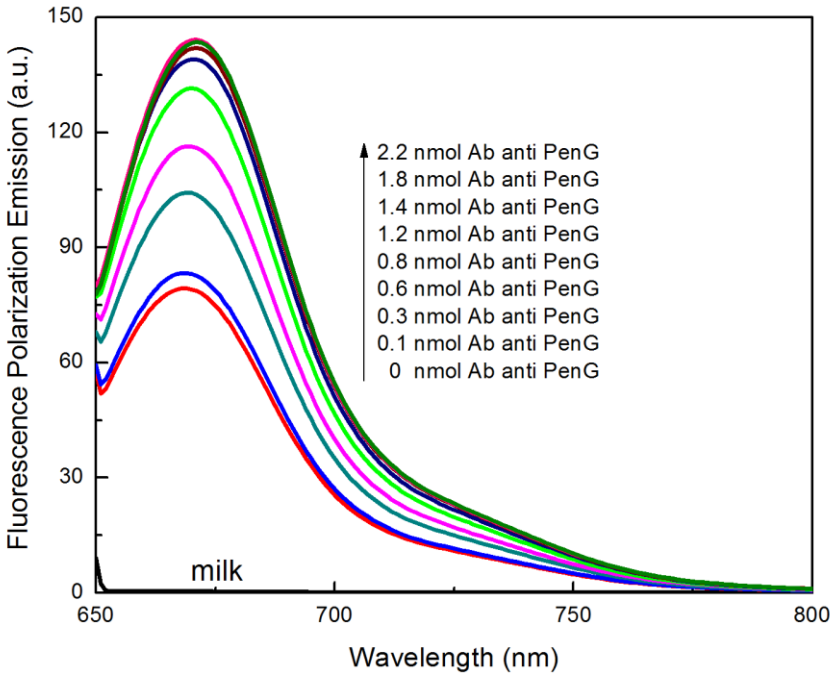
Fluorescence Polarization Emission (a.u.)
150
120
90
60
30
0
650
700
750
800
Wavelength (nm)
2.2 nmol Ab anti PenG
1.8 nmol Ab anti PenG
1.4 nmol Ab anti PenG
1.2 nmol Ab anti PenG
0.8 nmol Ab anti PenG
0.6 nmol Ab anti PenG
0.3 nmol Ab anti PenG
0.1 nmol Ab anti PenG
0 nmol Ab anti PenG
milk

Fig. 4

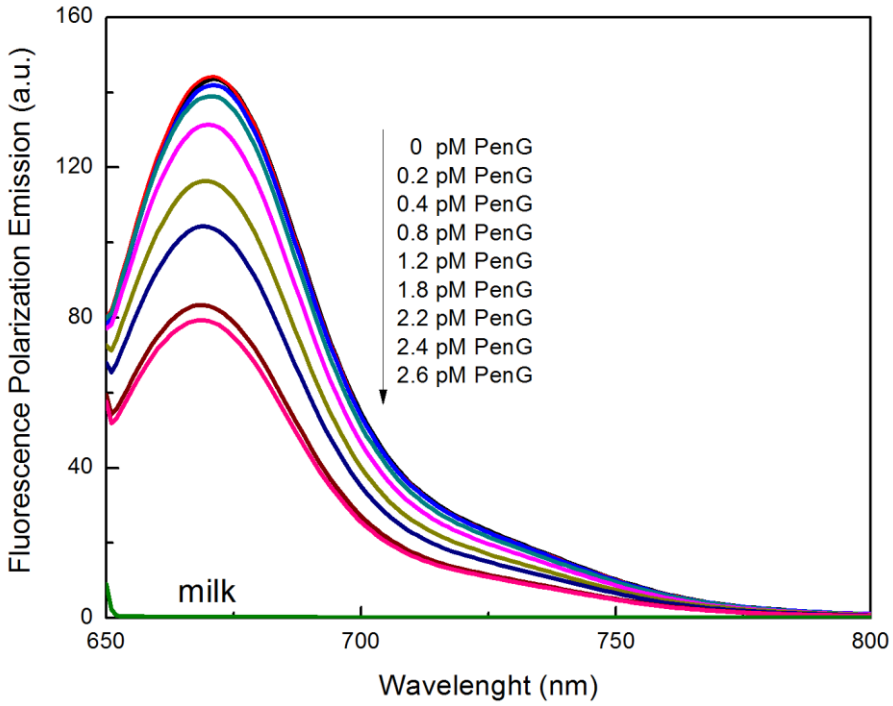
Fluorescence Polarization Emission (a.u.)
Wavelenght (nm)
0 pM PenG
0.2 pM PenG
0.4 pM PenG
0.8 pM PenG
1.2 pM PenG
1.8 pM PenG
2.2 pM PenG
2.4 pM PenG
2.6 pM PenG
milk
160
120
80
40
0
650
700
750
800

Fig. 5

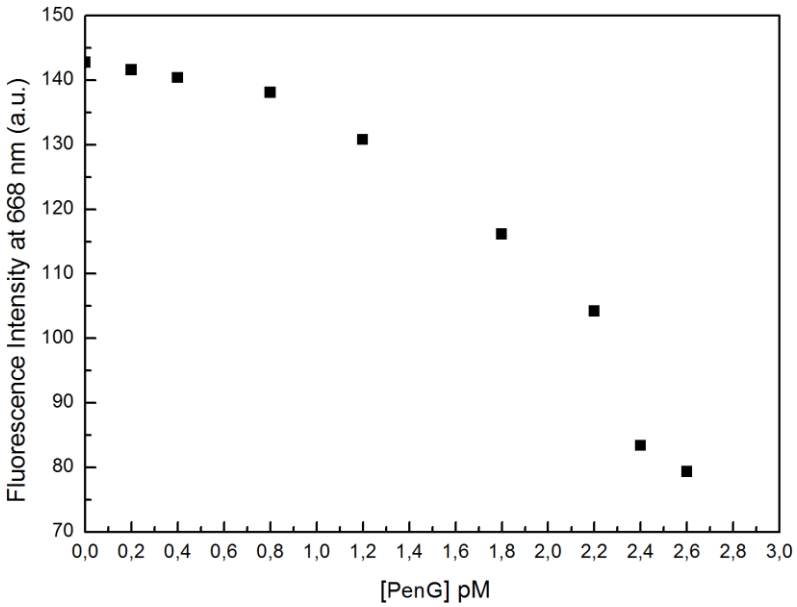
Fluorescence Intensity at 668 nm (a.u.)
[PenG] pM
150
140
130
120
110
100
90
80
70
0,0
0,2
0,4
0,6
0,8
1,0
1,2
1,4
1,6
1,8
2,0
2,2
2,4
2,6
2,8
3,0

Fig. 6

Chapter 5
A Novel Sensing Approach to Detect the Presence of Estradiol in Milk

Submitted to Bioanalycal Chemistry

A Novel Sensing Approach to Detect the Presence of 17 β-Estradiol in Milk

Anna Pennacchio, Antonio Varriale, Andrea Scala, Vincenzo Manuel Marzullo, Maria Staiano and Sabato D'Auria*

Laboratory for Molecular Sensing, Institute of Protein Biochemistry CNR, Via P. Castellino N°111 80131, Naples, Italy
*Correspondence to:
Dr. Sabato D'Auria
Laboratory for Molecular Sensing, IBP-CNR
Via Pietro Castellino, 111 80131 Naples, ITALY
Tel. +39-0816132250
Fax: +39-0816132277
Email: s.dauria@ibp.cnr.it

Abstract
Detection of 17 β-estradiol in milk is very important because farmers use this compound to increase the weight growths of animals. The increase of weight in animals means more profit for farmers. The massive use inevitably causes residues in food destined for the consumers table. Most studies have shown that the presence of 17 β-estradiol residues in foods causes allergies and cancer, in particular intestine and uterine cancer.
Therefore the growing concern for human and animal health and the existence of Community directives, which set maximum permitted levels of certain hormones in many food products, require the need for methods of analysis for the strict monitoring of the levels of these contaminates in raw materials. We proposed a novel and fast method to detect 17 β-estradiol residues directly in milk without interferences. This method is based on the use of a fluorescence 17 β-estradiol conjugate with antibodies anti-17 β-estradiol. The detection limit of this method is 0.5 pmol, a value much lower the MRL of EU regulation value, that is 20 pmol.

Keywords: Fluorescence; Biosensors; Antibody; 17 β-Estradiol; Milk

Introduction

Steroid hormones have been largely used to promote livestock growth, increase the weight of animals, reducing in this way production costs. EU has forbidden administration of naturally and synthetic anabolic growth promoters in food-producing animals because of their risk to human health. Most of documented evidence demonstrate that exposure to both natural and synthetic hormones at low levels may be harmful to humans, leading to many diseases as breast and uterine cancer [1]. Moreover, use of hormones in breeding, produces in consumers many symptoms such as nausea, inappetence, even hepatic jaundice, if food contains abundant or excessive quantity of them. What is more, their indiscriminate use may leads to irreversible abnormalities in early development [2], such as sexual precosity to young females and feminization of male reproductive system [3]. 17β-estradiol is widely illegally used in the chain of production; although this compound is a natural estrogen, can be carcinogenic even at low levels, and it is listed within Group A in Annex I of the Council Directive 96/22/EC (Group A, substances having anabolic effect and unauthorized substances) [4].

A lot of techniques have been used to detect hormones, such as gas or liquid chromatography with mass spectrometry technology (GS–MS or LC–MS)[5-9] and enzyme-linked immuno-sorbent assay (ELISA) etc [10]. Chromatographic techniques (LC or GC), using mass spectrometry detection [11-13], present different disadvantages: high cost, complicated operations, fussy sample preparation and time-consuming. In the recent years, several sample preparation procedures for isolation of the analyte and purification of the sample have been developed for concentration and clean-up of estradiol in milk samples. These include liquid-liquid extraction (LLE) [11], solid-liquid extraction (SPE) [12], molecularly imprinted solid phase extraction (MISPE) [13],and multi step solid phase extraction (MSPEE) [1], which can be time-consumig and tedious.

On the other hand, traditional ELISA involves numerous steps of incubation and washing and it is, thus, not readily compatible to screen a large number of samples.

The determination of 17β-estradiol levels in milk samples is an arduous target because of its low concentration in real and complex matrix. The determination of 17β-estradiol in milk has been also dominated by immunological [14] and microbiological techniques, which are easy to perform, but are not specific enough to ensure accurate identification.

An alternative method of analysis to detect 17β-estradiol levels in milk is the biosensor; its potential approach is the capacity to solve several problems related to food safety.

In this work we describe a novel methodology to measure traces of 17β-estradiol in raw milk using a fluorescence polarization approach. This technique is founded on the use of an *ad hoc* synthesized fluorescence 17β-estradiol hemisuccinate-GlnBP (ES-GlnBP) conjugate labeled with fluorescent probe (Biotium CF647) and of polyclonal mono-specific anti 17β-estradiol antibodies. In order to detect 17β-estradiol in raw sample of milk without pretreatment steps, a competitive immunoassay, based on the use of specific antibodies generated against the analyte, has been performed.

Recently we have developed, using the same approach, a fluorescence polarization assay for the detection of penicillin G in milk and of patulin in fruit juices (Pennacchio et al, in preparation).

This method is innovative and rapid because sample pretreatment is not requested: the analysis can be conducted directly in the real matrix with no interferences due to different milk compounds, using an infra-red emitting probe.
Finally, this technique represents a novel approach, related to traditional techniques, and allows to detect any contaminates in milk by changing fluorescent conjugate molecules and specific antibodies, therefore it ensures quality and safety food.

2.Material and Methods

2.1. Reagents
All reagents were acquired at highest commercially available. 1-[3-(Dimethylamino)-propyl]-3-ethylcarbodiimide (EDC), bovine serum albumin (BSA; fraction V) and ovalbumin (OVA) were purchased from Sigma. PURE1A Protein A Antibody Purification Kit was purchased from Sigma. Goat polyclonal to rabbit IgG-HRP conjugate (secondary antibody) was from Abcam. Affinities resin EAH Sepharose 4B was purchased from Amersham Biosciences. Nitrocellulose transfer membrane Protran from Schleicher & Schuell and ECL detection reagents from Amersham Biosciences were used in Western blot experiments. Microplates (96-well), LockWell MaxiSorp from Nunc, 3,5,-tetramethylbenzidine (TMB) enzyme substrate from Sigma, and a micro-plate reader, Multiskan EX from Thermo, were used for ELISA experiments. UV measurements (detection at 278 nm) were carried out on a Varian Cary 50 Bio spectrophotometer. The fluorescent probe CF647 was purchased from Biotium. Fluorescence experiments were performed with FP-8600 Fluorescence Spectrometer (Jasco-Japan).

2.2 *Synthesis of 17β-Estradiol-hemisuccinate*
The 17β-estradiol-hemisuccinate (Figure 1 B) was synthesized essentially following the previously reported procedure [15]. In particular, 17β-estradiol (270 mg, 1.0 mmol) was dissolved in 12 mL of a mixture of benzene/pyridine (8:2, v/v) and succinic anhydride was added to the solution (600 mg, 6 mmol). The mixture was refluxed for 24 h. TLC analysis showed the disappearance of 17β-estradiol and the formation of two bands having lower Rf compared to 17β-estradiol. The reaction mixture was dried under reduced pressure and the residue, dissolved in acetone/ethanol (3 mL, 1:1, v/v), was purified by silica gel chromatography. For this purpose the solution was adsorbed on a small amount of silica gel (5.0 g) and after evaporation of the solvent the silica was applied on the top of a silica gel column, which was eluted with an increasing amount of methanol in DCM (from 0 to 5% of MeOH). The purification furnished the estradiol-3,17β-bis-succinate (70% yield, lower Rf) and a product (at higher Rf) which was identified as a mixture of estradiol-3-hemisuccinate (15% yield) and 17β-hemisuccinate (15% yield). The estradiol-3,17β-bis-succinate, (300 mg) suspended in 10 mL of MeOH, was then treated with 10 mL of a 1,2 M solution of $NaHCO_3$ and the mixture was kept at room temperature, under stirring for 15 h. The selective hydrolysis of phenolic ester furnished, as expected, a mixture of estradiol and estradiol-17β-hemisuccinate. The latter (95% yield from bis-succinate) was purified on a silica gel column (as previously described) eluted with an increasing amount of MeOH in dichlorometane (from 0 to 20%, v/v). ^{1}H NMR analyses were in agreement with those reported [15]. *m/z* (HRESIMS) 395.1840 ([M + Na]$^+$, $C_{22}H_{28}O_5Na$, requires 395.1834).

2.3 *Synthesis of the 17β-Estradiol-hemisuccinate-GlnBP conjugate.*
The 17β-Estradiol-hemisuccinate-GlnBP conjugate was prepared adding a solution of 17β-Estradiol-hemisuccinate (2 mg) in 1 mL of MES buffer (0.1M), pH 6.0 to a solution of glutamine-binding protein from *Escherichia coli* (GlnBP) (2 mg/mL) in 0,5 mL of the same buffer and 0,1 mL of an EDC solution in H_2O (10 mg/mL). The reaction mixture was incubated for 16 h at 4°C and then dialyzed against potassium phosphate buffer (20 mM), pH 7.4 (1 L, for 3 days with daily buffer changes). The concentration of the conjugate, spectrophotometrically determined at λ = 278 nm, was 2 mg/mL.

2.4 Antibody production and purification
Two rabbits were immunized following a standard protocol by intradermal inoculation of an antigen (0.5 mg per rabbit). After the immunization period, the rabbits were sacrificed and their blood recovered and centrifuged to separate blood cells from serum. A 1.5 mL sample of rabbit serum diluited with 1.5 mL of binding buffer Tris 50 mM pH 7.0, was applied to a Protein A column of the PURE 1A Protein A Antibody Purification Kit, Sigma, and the IgG fraction was purified according to the manufacturer's instructions. Elution of proteins was monitored by absorbance at λ= 278 nm. The IgG fraction was eluted with glycine (0.1M) at pH 3.0 and immediately buffered in Tris/HCl (1.0 M) at pH 9.0. Finally, to evaluate the purity of the sample, sodium dodecyl sulfate-polyacrylamide gel electrophoresis (SDS-PAGE) was carried out.

2.5 *Affinity column preparation of 17β-Estradiol-hemisuccinate –EAH Sepharose 4B*
The affinity column was obtained by conjugating 17β-Estradiol-hemisuccinate to EAH Sepharose 4B as follows. A 0.6 mL of resin was washed with H_2O at pH 4.5 (20 mL), with NaCl (0.5 M) (20 mL), and with H_2O at pH 4.5 (20 mL) again. The solution of 17β-Estradiol-hemisuccinate (2 mg in 0.5 mL of H_2O at pH 4.5) was added to Sepharose resin, and the resulting suspension was gently shaken. The slurry was cooled to 0°C, and EDC was added in to a final concentration of 0.1 M (52 mg). The reaction mixture was incubated for overnight at 4°C and then it was taken to room temperature. The suspension was washed with H_2O at pH 4.5 (20 mL), acetate buffer (0.1 M) containing NaCl (0.5 M) (20 mL), pH 4.0, and PBS (0.1 M) containing NaCl (0.3 M), pH 7.4 (20 mL), and finally packed into a polystyrene column (2 mL, BIORAD). For the affinity chromatography purification, a 1.0 mL of IgG (obtained from purification) was applied drop-wise to the affinity column prepared as described above. To eliminate unspecific antibodies, the column, before elution, was washed with three high-salt buffers: (1) PBS (0.01 M), NaCl (0.1 M), pH 7.0 (20 mL); (2) PBS (0.01 M), NaCl (0.5 M), pH 7.0 (20 mL); (3) PBS (0.01 M), NaCl (1.0 M), pH 7.0 (20 mL). At that point, absorbance at 278 nm was 0.0. For the elution step, glycine (0.1 M), pH 3.0 was used, and the eluate was collected in fractions of 0.5 mL and monitored by absorbance measurements at 278 nm. The fractions containing the antibodies were collected and dialyzed against PBS (0.1 M), NaCl (0.1 M), pH 7.4. The concentration of the monospecific antibodies, spectrophotometrically determined at λ = 278 nm, was 1.3 mg/mL.

2.6. Synthesis of 17β-Estradiol-hemisuccinate-*BSA Conjugate.*
17β-Estradiol-hemisuccinate was conjugated to BSA, a protein different from the protein used to carry out the immunization to avoid interference by the carrier protein in the polyclonal antibody detection process. The following procedure was used: BSA

(2 mg/mL) in 0,5 mL of MES buffer (0.1 M), pH 6.0, was added to a solution of 17β-Estradiol-hemisuccinate (2 mg) in 1 mL of the same buffer and 0,1 mL of an EDC solution in H2O (10 mg/mL). The reaction mixture was incubated for 16 h at 4°C and then dialyzed against potassium phosphate buffer (20 mM), pH 7.4 (1 L, for 3 days with daily buffer changes). The concentration of the conjugate, spectrophotometrically determined at λ = 278 nm, was 2.2 mg/mL.

2.7. Antibody Titration Experiments

The antibody titer was determined by an indirect ELISA assay by the following general procedure. The antigen (17β-Estradiol-hemisuccinate-BSA), dissolved in PBS (0.1 M), pH 7.4, was used to coat 96-well micro-plates, varying the concentration from 125 to 5000 ng/mL (one column for every antigen concentration, 100 µL per well), overnight at 4°C. Control wells were incubated for the same period with BSA in the same buffer. The wells were flushed three times with TBS 1X containing 0.05% Tween (TBS-T), pH 7.4, and blocked by incubation for 1 h at room temperature with TBS-T containing OVA (1%) (100 µL each well). After two washings with TBS-T, polyclonal and polyclonal monospecific anti estradiol antibodies in blocking buffer, serially diluted, was added to the wells, incubated at room temperature for 1 h, and then washed two times with TBS-T. Horseradish peroxidase-conjugated anti-rabbit IgG antibodies, diluted 1:12000 in TBS-T containing OVA (1%), were added to the wells (100 µL) and incubated for 1 h at room temperature. After two washings with TBS-T, the enzyme substrate TMB was added (100 µL per well), and the color reaction was quenched after 5 min by addition of 2 M HCl (100 µL per well). The absorbance was measured at 450 nm.

2.8. *Western Blot Experiments*

Proteins (BSA, GlnBP and 17β-Estradiol-hemisuccinate-GlnBP, 20 □g each) were loaded, separated by sodium dodecyl sulfate-polyacrylamide gel electrophoresis (12% SDS-PAGE), and then transferred overnight at 4°C onto a nitrocellulose membrane. Membranes were blocked for 30 minutes at room temperature in 50 mL of the blocking buffer (TBS containing 5% of milk). After one washing with TBS 1 X-Tween 0.05% (10 min for washing), the filters were incubated with purified monospecific IgG (1:100000 in the blocking buffer), for 1 h at room temperature. After three washings with TBS 1X-Tween 0.05% (10 min for washing), the filters were incubated with secondary antibody (goat anti-rabbit HRP conjugate, 1:6000 in the blocking buffer) for 1 hours at room temperature. The filters were washed three times as described above and then developed with the detection reagent ECL.

2.9. Fluorescence Labeling of 17β-Estradiol-hemisuccinate-GlnBP

A solution of 2.0 mg/mL 17β-Estradiol-hemisuccinate-GlnBP was concentrated at 4.0 mg/mL in 1.0 mL, dissolved in 0.1 M sodium bicarbonate buffer, pH 7.0 and mixed with CF647. The molar ratio of the protein and the dye was kept 1:10. The reaction mixture was incubated for 1 hours at 37°C and the labeled molecules were separated from un-reacted probe by gel filtration.

2.10. *Steady-state fluorescence measurements*

Steady state fluorescence experiments were performed with FP-8600 Fluorescence Spectrometer (Jasco-Japan) equipped with a one-cell temperature controlled sample holder. The excitation wavelength was fixed at 630 nm and emission spectra were recorded between 650 nm and 800 nm with an emission slit-width of 2.5 nm and an

excitation slit-width of 5 nm. The measurements were performed in milk solution diluted 1.5, at room temperature. 17β-Estradiol-hemisuccinate-GlnBP-CF647 was incubated with a range of concentration of antibodies against 17β-estradiol from 0.0 to 2.2 pmol for 10 minutes, and fluorescence spectra were carried out. The polarization fluorescence measurements were acquired by inserting a Glan polarizer between the excitation source and the sample, with a vertical (0°) excitation polarized filter and with a vertical (0°) emission polarized filter.

2.10. 17β-Estradiol competitive assay

A competitive polarization assay was performed at a fixed concentration of antibody against 17β-Estradiol (2.2 pmol) in presence of increasing concentrations of un-labeled 17β-Estradiol in a range of concentration from 0.0 to 47 pmol. The incubation was done at room temperature for 10 minutes. After this pre-incubation in presence of unlabeled 17β-Estradiol, polarization fluorescence measurements were carried out with FP-8600 Fluorescence Spectrometer with an excitation polarized filter set at 0° and an emission polarized filter set at 0°.

3.Results and Discussion

Anabolic steroids have been widely used as growth promoting agents in cattle to increase the weight gain of animals and reduce the feed conversion efficiency. The administration of naturally and synthetic anabolic growth promoters in food-producing animals is now prohibited by the EU because of their potential risk to humans.

Illegal use and/or abuse of 17β-estradiol in animal feed, imply a contamination of produced milk with several consequences for human health. A rapid and simple method to detect the concentration of 17β-estradiol in milk, able to control all phases of milk production, from the cattle shed to the table of the consumers, is needed. Therefore we have covalently attached the 17β-Estradiol-hemisuccinate to a bacterial protein carrier, glutamine binding protein (GlnBP). The structure of 17β-Estradiol-hemisuccinate covalently bound to GlnBP is shown in Figure 2. This conjugate was used to produce polyclonal antibodies anti-17β-Estradiol in rabbit.

3.1 Synthesis of 17β-Estradiol-hemisuccinate

The presence of a carrier protein conjugated to the hormone is required for the production of antibodies against 17β-Estradiol, which is, too small to elicit any immunological response. In order to conjugate 17β-Estradiol to the carrier protein, an hemisuccinic arm is needed. 17β-Estradiol-hemisuccinate was obtained from commercial 17β-Estradiol prepared as described in Materials and methods.

3.2. Production of antibodies against the estradiol

GlnBP was chosen as carrier protein. Antigen 17β-Estradiol-hemisuccinate-GlnBP was used to produce polyclonal antibodies against 17β-estradiol. Two different rabbits were immunized using a standard protocol of immunization and at the end of the immunization period the IgG fraction were isolated from serums by the protein A column kit. The purity of IgG fractions was evaluated by SDS-PAGE and the pure fractions were pooled and dialyzed against PBS 20 mM pH 7.4.

The BSA conjugate was prepared by the same procedures already used for GlnBP conjugate and reported in material and methods section.

3.3. ELISA test

An indirect ELISA test was performed to evaluate the titer of polyclonal and polyclonal monospecific purified antibodies. The micro-plate wells was coated with 17β-Estradiol-hemisuccinate-BSA and we tested serially diluted polyclonal and polyclonal monospecific antibodies against 17β-estradiol. The result of the ELISA test is shown in Figure 3. It is reported as bar histogram in which the absorbance value at 450 nm was plotted versus different concentrations of coated 17β-Estradiol-hemisuccinate-BSA. No signal was registered as consequence of incubation with different diluted samples of IgG for wells no-coated. The result shows an increase of the absorbance in function to the decrease of the dilution factor of anti 17β-estradiol polyclonal monospecific antibodies; polyclonal monospecific antibodies are more sensible than polyclonal antibodies. The titer was taken as the maximum antibody dilution able to give a reading of 0.1 absorbance unit. The following value was found: 1/100000 for polyclonal monospecific anti 17β-estradiol antibodies. Therefore the titer of antibodies anti 17β-estradiol seems excellent.

3.4. Preparation of affinity columns and purification of specific antibodies and western blotting

The 17β-Estradiol-hemisuccinate was conjugated to EAH Sepharose-4B resin and the obtained purified IgG fraction was loaded. After the loading with the IgG fraction, the column was washed with buffer at neutral pH with high concentration of NaCl, in order to remove unspecific antibodies and monospecific antibodies were eluted using glycine buffer at pH 3.0. The different fractions were collected and a SDS-PAGE was carried out in order to evaluate the purity of the sample (data not shown). In order to verify the specificity of the produced antibodies against the 17β-estradiol, a western blotting experiment was performed. In Figure 4A and 4B are shown the SDS-PAGE and western blotting experiment results. Response to antibody binding was observed only for the conjugate 17β-Estradiol-hemisuccinate-GlnBP, and a negative response was registered for BSA and GlnBP. This confirms the specificity of antibodies versus the only estradiol.

3.5. Fluorescence steady-state measurements of 17β-Estradiol-hemisuccinate-GlnBP-CF 647 conjugate

The polarized emission spectra of 17β-Estradiol-hemisuccinate-GlnBP-CF647 in absence and in presence of increasing concentrations of anti-estradiol antibodies is shown in Figure 5. Before the polarization measurements were performed, to avoid interference of un-reacted probe, the labeled molecules were separated by gel filtration. The fluorescence polarization measurements were performed directly in milk. In particular, a solution of milk five-times diluted was used for the experiments. The excitation value was fixed at 630 nm, and the emission spectra were acquired from 650 nm to 800 nm. The maximum of fluorescence emission was centered at 668 nm. The measurements were performed at room temperature, and an antibody solution from 0.0 to 2.2 pmol was added. The acquired results revealed an increase of 17β-Estradiol-hemisuccinate-GlnBP-CF647 polarized fluorescence intensity as consequence of binding with anti 17β-Estradiol antibodies.

3.6. Fluorescence polarization competitive immunoassay

Fluorescence polarization competitive immunoassay was used to measure the tracer of 17β-estradiol in solution. To evaluate the competition between 17β-Estradiol-

hemisuccinate-GlnBP-CF647 and un-labeled 17β-estradiol for binding with monospecific antibodies against 17β-estradiol, different samples at a fixed concentration of antibody (2.2 pmol) were incubated in presence of increasing concentrations of un-labeled 17β-estradiol in a range between 0.0 and 47 pmol.
Each sample was incubated for 10 minutes at room temperature before that fluorescence polarization measurements were performed. The polarized fluorescence emission spectra in presence of increasing concentrations of un-labeled 17β-estradiol is shown in Figure 6. There is a reduction of fluorescence emission in conjunction to increasing concentrations of un-labeled 17β-estradiol.
The presence of increasing concentrations of the analyte in the samples allowed to go back to the minimum measurable value of the analyte.
In Figure 7 is shown the dose response curve for 17β-estradiol detection in diluted milk; it reports the polarization fluorescence intensity at 668 nm as function of pmol of 17β-estradiol. The results show that it is possible to detect an amount of 17β-estradiol less than 10 pmol.
In conclusion, this methodology is more sensitive than the analytical techniques actually in use. It allows rapid analysis, directly in real matrices without samples pre-treatment steps. This method is a promising alternative approach to detect 17β-estradiol during all steps of milk production and collection.

Acknowledgement

This project was realized in the frame of the CNR Commessa “Progettazione e Sviluppo di Biochip per la Sicurezza Alimentare e Salute Umana (SD; MS; AV)”. This Project was partially funded by the project CTN01_00230_240864 "SAFE &SMART-Nuove tecnologie abilitanti per la food safety e l'integrità delle filiere agro-alimentari in uno scenario globale" and it was also partially funded by the CNR project "Conoscenze integrate per sostenibilità e innovazione del Made in Italy agroalimentare (CISIA)”.

References

1. Shao B, Zhao R, Meng J, Xu Y, Wu G, Hu J, Tu X, (2005). Simultaneous determination of residual hormonal chemicals in meat, kidney, liver tissues and milk by liquid chromatography-tandem mass spectrometry. Anal Chim. Acta 548:41-50 .
2. Spearow, Jimmy L., and Barkley, Marylynn. 1999. Genetic Control of Hormone-Induced Ovulation Rate in mice. Biology of Reproduction 61: 851-856.
3. P.C. MacDonald, J.D. Madden, P.F. Brenner, J.D. Wilson, P.K. Siiteri. Origin of estrogen in normal men and women with testicular feminization. J.Clin.Endocr.Metab.49 (1979) 905.
4. Council Directive 96/22 EC, Off. J. Eur. Comm., L125 (1996) 3.
5. Nan Liu, Pu Su, Zhixian Gao, Maoxiang Zhu, Zhihua Yang, Xiujie Pan, Yanjun Fang, Fuhuan Chao. Simultaneous detection fot three kinds of veterinary drugs: chloromphenicol, clenbuterol and 17–beta-estradiol by high-throughput suspension array technology. Analytica Chimica Acta. 632 (2009) 128-134.
6. N. Perez, R. Gutierrez, M. Noa, G. Diaz, H. Luna, J. Escobar, Z. Munire. Liquid chromatographic determination of multiple sulfonamides, nitrofurans, and chloramphenicol residues in pasteurized milk. J. AOAC. Int. 85 (2002) 20.
7. P. Andrzej, Z. Jan, N. Jolanta. Evaluation of sample preparation for control of chloramphenicol residues in porcine tissues by enzyme-linked immunosorbent assay and liquid chromatography Anal. Chim. Acta 483 (2003) 307.
8. P. González, C.A. Fente, C. Franco, B. Vázquez, E. Quinto, A. Cepeda. Determination of residues of the beta-agonist clenbuterol in liver of medicated farm animals by gas chromatography-mass spectrometry using diphasic dialysis as an extraction procedure. J Chromatogr.B:Biomed. Sci. Appl. 693 (1997) 321.
9. T.L. Li, W.Y.J. Chung, Y.C. Shih. Determination and Confirmation of Chloramphenicol Residues in Swine Muscle and Liver. J. Food Sci. 67 (2002) 21.
10. G.Scortichini, L.Annunziata, M.N.Haouet, F.Benedetti, I.Krustevaa, R.Galarini. ELISA qualitative screening of chloramphenicol in muscle, eggs, honey and milk: method validation according to the Commission Decision 2002/657/EC criteria. Anal. Chim. Acta 535 (2005) 43.
11. Courant F, Antignac JP, Maume D, Monteau F, Andre F, Le Bizec B (2007). Determination of naturally occurring oestrogens and androgens in retail samples of milk and eggs. Food Additives and Contaminants 24:1358-1366.
12. Yan W, Li Y, Zhao L, Lin JM (2009). Determination of estrogens and bisphenol A in bovine milk by automated on-line C30 solid-phase extraction coupled with high-performance liquid chromatography–mass spectrometry. J Chromatog A 1216:7539-7545.
13. Qiujin Z, Liping W, Shengfang W, Wasswa J, Xiaohong G, Jian T (2009). Selectivity of molecularly imprinted solid phase extraction for sterol compounds. Food Chem 113:608–615.
14. Scippo ML, Van De Weerdt C, Willemsen P, François JM, Rentier-Delrue F, Muller M, Martial JA, Maghuin-Rogister G (2002). Detection of illegal growth promoters in biological samples using receptor binding assays. Anal Chim Acta 473:135-141.

15. Manasmita Das , Raman Preet Singh , Satyajit R. Datir , and Sanyog Jain. Intranuclear Drug Delivery and Effective in Vivo Cancer Therapy via Estradiol–PEG-Appended Multiwalled Carbon Nanotubes. Mol. Pharmaceutics (2013) 10, 3404-3416.

Legends to Figures

Figure 1. Schematic representation of the 17β-Estradiol (A) and 17β-Estradiol-hemisuccinate (B).

Figure 2. Schematic representation of the GlnBP conjugate used for the production of the rabbit anti 17β-Estradiol antibodies.

Figure 3. ELISA test of polyclonal and polyclonal monospecific anti 17β-Estradiol IgG purified from the serum of rabbit. The assay was performed in the Tris–borate buffer in the presence of 0.005% Tween and 1% milk. Temperature was set at 25 °C.

Figure 4. SDS-PAGE (A) and nitrocellulose filter (B) after incubation with 17β-Estradiol antibodies; lane 1, molecular weight standards; lane 2, BSA; lane 3, GlnBP; lane 4, 17β-Estradiol-hemisuccinate-GlnBP.

Figure 5. Polarization emission spectra of 17β-Estradiol-hemisuccinate-GlnBP-CF647 in the absence and in the presence of increasing concentration antibodies against 17β-Estradiol. The measurements were performed in PBS buffer at 7.4. The temperature was set at 25 °C.

Figure 6. Polarization fluorescence emission spectra of 17β-Estradiol-hemisuccinate-GlnBP-CF647. The measurements were performed in PBS buffer at 7.4. The temperature was set at 25 °C.

Figure 7. Titration of Fluorescence Polarization immune-assay with increasing concentration of un-labeled 17β-Estradiol.

Figures

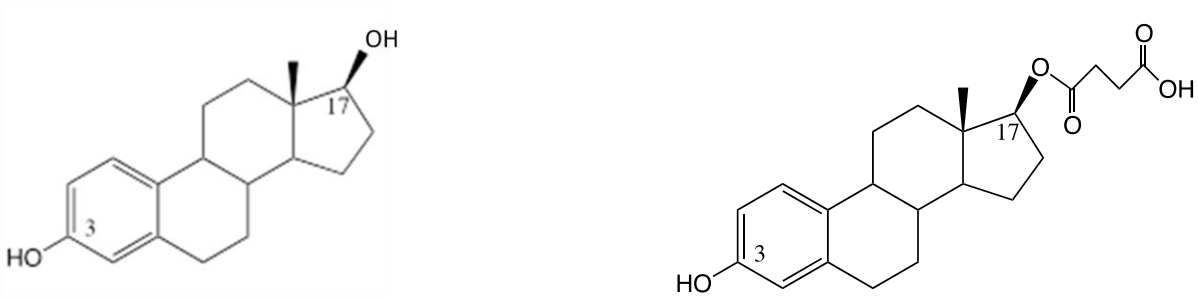

(A) **(B)**

Fig.1

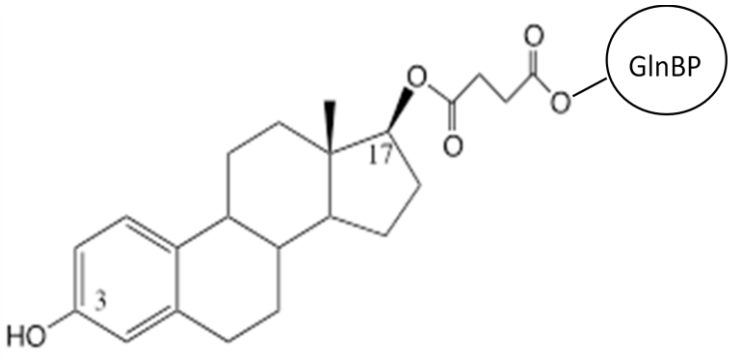

Fig. 2

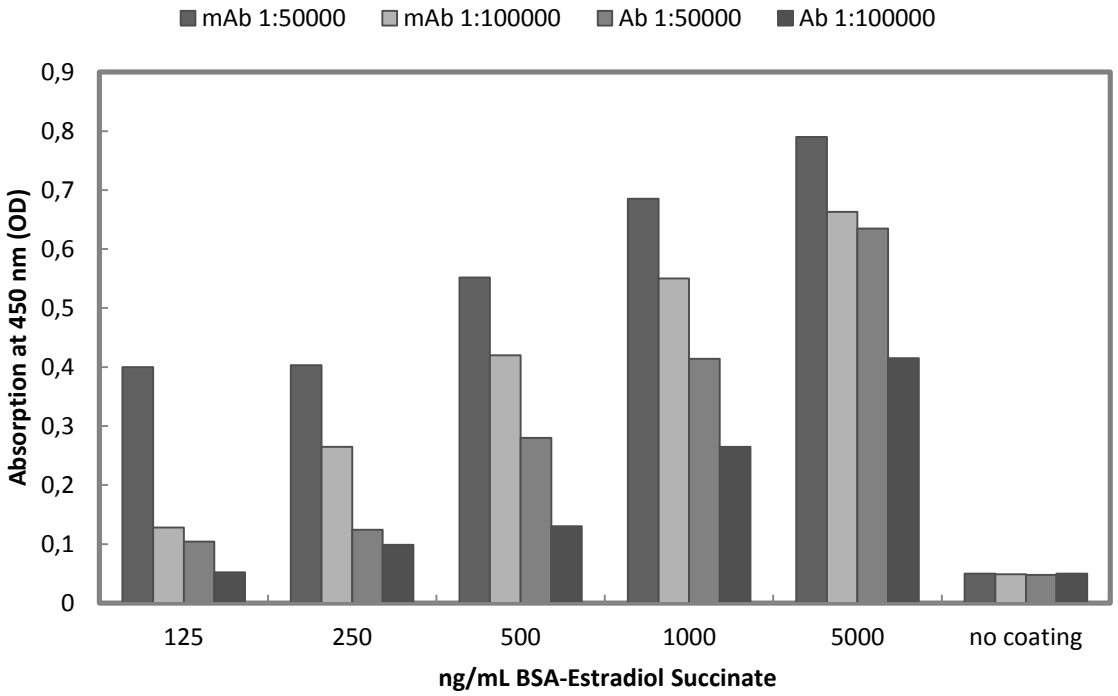
mAb 1:50000
mAb 1:100000
Ab 1:50000
Ab 1:100000
Absorption at 450 nm (OD)
0,9
0,8
0,7
0,6
0,5
0,4
0,3
0,2
0,1
0
125
250
500
1000
5000
no coating
ng/mL BSA-Estradiol Succinate

Fig. 3

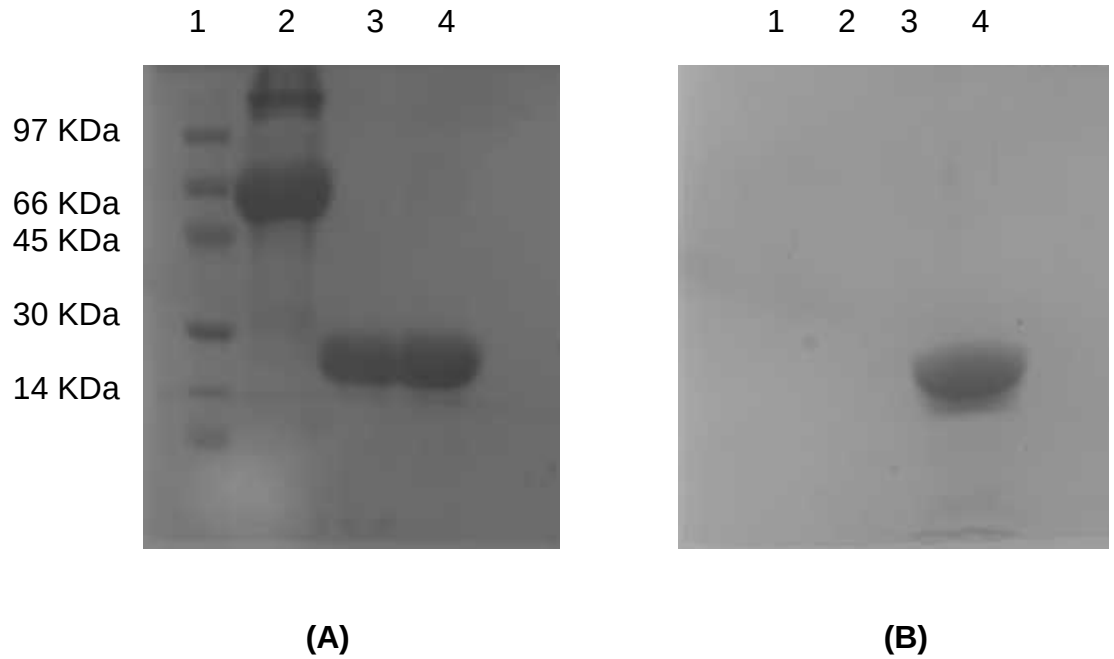
1 2 3 4
1 2 3 4
97 KDa
66 KDa
45 KDa
30 KDa
14 KDa
(A)
(B)

Fig.4

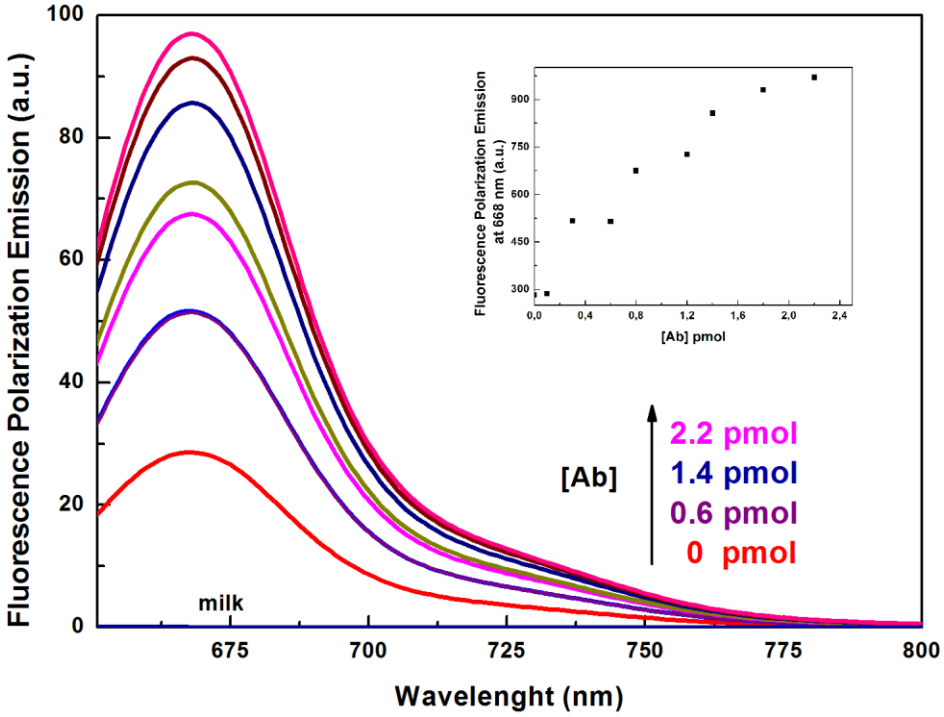
Fluorescence Polarization Emission (a.u.)
Wavelenght (nm)
milk
[Ab]
2.2 pmol
1.4 pmol
0.6 pmol
0 pmol
Fluorescence Polarization Emission at 668 nm (a.u.)
[Ab] pmol

Fig.5

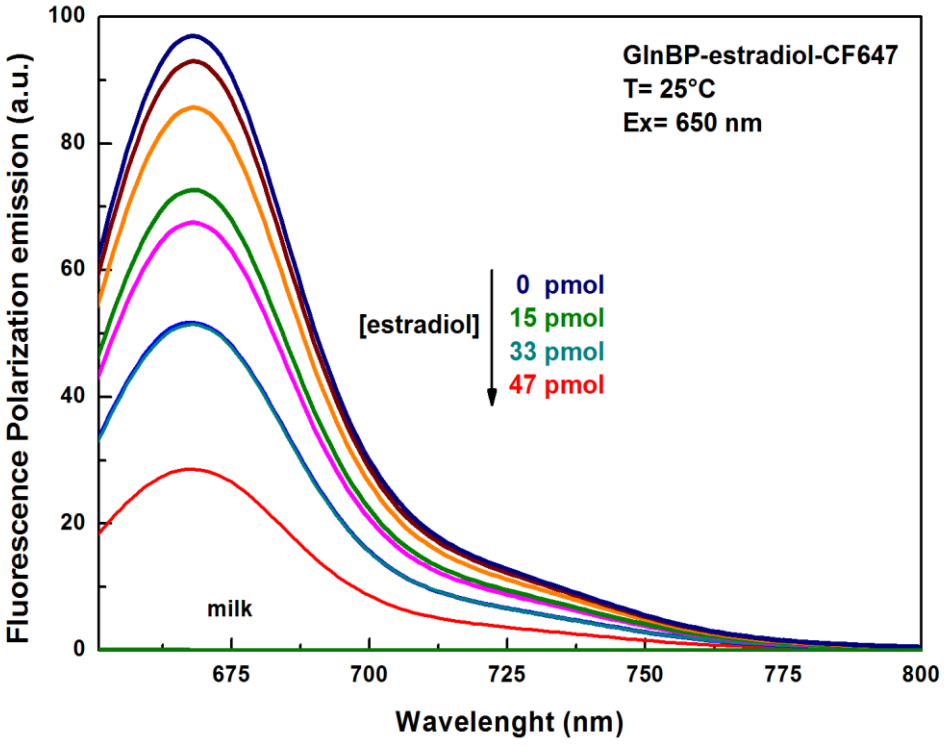
Fluorescence Polarization emission (a.u.)
Wavelenght (nm)
milk
GlnBP-estradiol-CF647
T= 25°C
Ex= 650 nm
[estradiol]
0 pmol
15 pmol
33 pmol
47 pmol

Fig.6

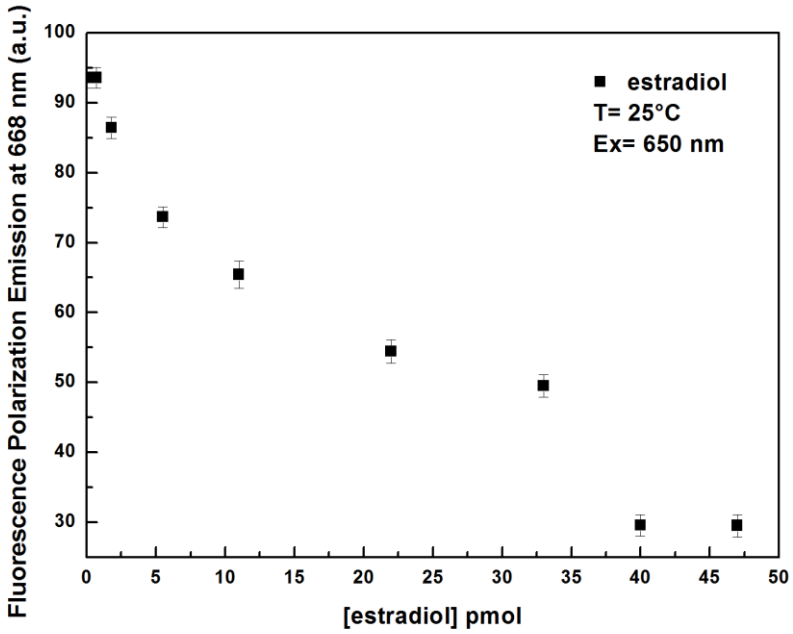
Fluorescence Polarization Emission at 668 nm (a.u.)
[estradiol] pmol
estradiol
T= 25°C
Ex= 650 nm
100
90
80
70
60
50
40
30
0
5
10
15
20
25
30
35
40
45
50

Fig. 7

CONCLUSIONS

The present PhD work was aimed to develop two methods to detect contaminants such as toxins, antibiotics and hormones in foods to ensure the quality and the safety of raw materials:

- An immune-chemical approach was combined with SPR spectroscopy to develop an efficient patulin, penicillin G and estradiol biosensor, which can also be used outside in the field.

- A novel fluorescence polarization immunoassay was developed to detect traces of patulin, penicillin G and estradiol directly in apple juices and in milk. It is more sensitive than SPR method.

These methods allow you to determine an amount of patulin, penicillin G and estradiol much lower than conventional techniques and much lower than the European limit.

	European Limit	SPR spectroscopy Limit	Fluorescence Polarization Limit
Patulin	50 ug/L	0.1 ug/L	0.06 ug/L
Penicillin G	12 nM	8 pM	0.4 pM
Estradiol	20 pmol	_	0.5 pmol

APPENDIX

Publications and Communications

A Surface Plasmon Resonance based biochip for the detection of Patulin Toxin **A. Pennacchio**, G. Ruggiero, M. Staiano, G. Piccialli, G, Oliviero, A. Lewkowicz, A. Synak, Sabato D'Auria. Optical Materials (2014) 36:1609-1768.

An Innovative Plastic Optical Fiber-based Biosensor for new Bio/applications. The Case of Celiac Disease. N. Cennamo, A. Varriale, **A. Pennacchio**, M. Staiano, D. Massarotti, L. Zeni, and Sabato D'Auria. Sensors Actuators B Chemical (2013) 176:1008–1014.

Amino acid transport in thermophiles: characterization of an arginine-binding protein from Thermotoga maritima. 3. Conformational dynamics and stability.
A. Ausili, **A. Pennacchio**, M. Staiano, J. D. Dattelbaum, D. Fessas, A. Schiraldi, and Sabato D'Auria. J Photochem Photobiol B. (2013) 118:66-73

Tryptophan-scanning mutagenesis of the ligand binding pocket in *Thermotoga maritima* arginine-binding protein.
LJ. Deacon, H. Billones, AA. Galyean, T. Donaldson, **A. Pennacchio**, L. Iozzino, Sabato D'Auria, JD. Dattelbaum. Biochemie (2014) In Press doi: 10.1016/j.biochi.2013.12.011.

Crystallization and preliminary X-ray crystallographic analysis of the ligand-free and the arginine-bound form of Thermotoga maritima arginine-binding protein" Ruggiero A, Dattelbaum J, **Pennacchio A**, Iozzino L, Staiano M, Luchansky M, Der B, Berisio R, D'Auria S, Vitagliano L. Acta Crystallographica. (2011) 67: 1462-1465.

A new competitive fluorescence immunoassay for detection of Listeria monocytogenes
Stephane Beauchamp, Sabato D'Auria, **Anna Pennacchio,** and MoniqueLacroix Analytical Methods (2012) 4 (12): 4187.

A new optical method to sense coumpounds of high social interst
Strianese M., Staiano M., Di Giovanni S, **Pennacchio A**, Dell'Angelo V, Ruggiero G, Labella T, Pellecchia C, D'Auria S
Proceedings of 1° International Conference on Microbial Diversity: 2011 - Environmental Stress and Adaptation 26-28 October, Milan, Italy

Biosensor: advanced methodology for detection of ochratoxin A in food of animal origin.
Russo R,Varriale A, **Pennacchio A**, Iozzino L, Anastasio A, D'Auria S, and Severino L. 1st International workshop on veterinary biosignals and biodevices 1-4 february 2012 Vilamoura, Portugal

D-serine detection via a shear horizontal surface acoustic wave (SAW) biosensor for space applications.
Di Pietrantonio F, Staiano M, Cannatà D, Di Giovanni S, Beretti M, **Pennacchio A**, Verona E, D'Auria S
V Congresso Nazionale ISSBb 17-19 November 2011, Padova, Italy

An Emergent Sensing Fluorescence Platform For Food Safety & Health. **Anna Pennacchio**, Andrea Scala, Gennaro Piccialli and Sabato D'Auria. 16-17 June 2014: IBP Retreat, Salerno.

A novel fluorescent method to detect traces of penicillin G in milk.
Anna Pennacchio, Andrea Scala, Antonio Varriale and Sabato D'Auria. 8-10 September 2013: Methods and Analysis in Fluorescence (MAF 2013) in Genova, Italy.

SPR-based sensing for patulin detection.
Anna Pennacchio, Gennaro Piccialli, Piotr Bojarski and Sabato D'Auria.
10-14 June 2013: XXV Riunione Nazionale Dottorandi-Brallo di Pregola, Pavia.

Poster: Biosensor: advanced methodology for detection of ochratoxin A in food of animal origin.
Antonio Varriale, **Anna Pennacchio**, Luisa Iozzino and Sabato D'Auria.
1-4 February 2012: 1st International workshop on veterinary biosignals and biodevices, Vilamoura, Portugal.

Sensors and Actuators B 176 (2013) 1008–1014

Contents lists available at SciVerse ScienceDirect

Sensors and Actuators B: Chemical

journal homepage: www.elsevier.com/locate/snb

An innovative plastic optical fiber-based biosensor for new bio/applications. The case of celiac disease

Nunzio Cennamo[a], Antonio Varriale[b], Anna Pennacchio[b], Maria Staiano[b], Davide Massarotti[c], Luigi Zeni[a,*], Sabato D'Auria[b,**]

[a] Second University of Naples, Department of Information Engineering, Via Roma 29, 81031 Aversa, Italy
[b] Laboratory for Molecular Sensing, IBP-CNR, Via Pietro Castellino 111, 80131 Napoli, Italy
[c] University of Naples "Federico II", Department of Physical Sciences, Via Cinthia, Naples, Italy

ARTICLE INFO

Article history:
Received 13 September 2012
Received in revised form 8 October 2012
Accepted 10 October 2012
Available online 22 October 2012

Keywords:
Plastic optical fiber
Surface plasmon resonance
Biosensors
Celiac disease

ABSTRACT

In this work an innovative and low cost surface plasmon resonance (SPR) biosensor, based on the utilization of plastic optical fibers (POF), is presented and experimentally tested for the diagnosis and/or follow-up of celiac disease. In particular, the POF-based sensor was used to monitor the formation of the transglutaminase/anti-transglutaminase antibodies formation, a new hallmark for the diagnosis of celiac disease. In particular, on the gold layer surface of the POF sensor, the guinea pig transglutaminase was immobilized. The ability of the POF-sensor to detect the binding of anti-transglutaminase antibodies to the immobilized transglutaminase was studied.

The obtained results showed that the POF-sensor is able to sense the transglutaminase/anti-transglutaminase complex in the range of concentrations between 30 nM and 3000 nM. Importantly, the proposed sensing method could be easily expanded to different target compounds.

1. Introduction

Over the past years, surface plasmon resonance (SPR) biosensor technology has made great strides, and a large number of SPR sensors, biomolecular recognition elements, and measurement configurations have been developed. SPR is a very sensitive technique for determining small refractive index changes at the interface between a metallic layer and a dielectric medium (analyte) [1]. This technique is widely used as a detection principle for many sensors that operate in the areas of biological and chemical sensing. Biological targets are generally transported through a microfluidic system by a buffer fluid or a carrier fluid. With SPR sensors, when the transducing media (ligands) react with the target molecules present in the analyte, the refractive index at the surface changes, and this change is detected by optical interrogation. In many works, the SPR sensor system is based on a high refractive index prism coated with a thin metallic layer. The incidence angle of the light can change in a wide range and as a consequence the surface plasma waves (plasmons) may exist whatever the surrounding medium, i.e. a gas or a liquid. Nevertheless, the sensors are usually bulky and require expensive optical equipment, it is not easy to miniaturize them and, in addition, their remote sensing may be difficult to develop. Very recently, Jorgenson et al. replaced the prism by a multimode optical fiber [2]. The metal was deposited on the bare core of the fiber. The use of an optical fiber allows for a remote sensing and may reduce the cost and dimensions of the device. Due to the propagation of the light in the fiber, the angle of incidence on the metallic layer exceeds the critical angle which depends on the refractive indices of both core and cladding components. Therefore SPR only exists for surrounding dielectrics whose refractive index lies in a narrow range. To overcome this drawback, Jorgenson et al. used a polychromatic light source and a spectrograph. This device is low cost, easy to implement and can offer some attractive advantages such as the possibility of the use in the presence of flammable substances and human hazardous environments because of its electricity-free and remote sensing capabilities. Furthermore, because of the small size and non-invasive features, it can be used for medical (self-) diagnosis with the possibility of integration of SPR sensor platforms with optoelectronic devices, eventually leading to "lab on a chip" [3].

In particular, sensors based on bent or straight plastic optical fibers (POF) represent a simple approach to low cost bio-sensing [4–6]. Very recently, SPR biosensors have been shown to be likely able to play an important role in numerous important fields including pharmaceutical research, medical diagnostics, environmental monitoring, food safety and security, where fast, portable, low cost and rugged units are needed for early detection and identification

Abbreviations: SPR, surface plasmon resonance; POF, plastic optical fiber; tTG, transglutaminase; anti-tTG, anti-transglutaminase antibodies.

* Corresponding author. Tel.: +39 081 5010 269.
** Corresponding author. Tel.: +39 081 6132 250.
E-mail addresses: luigi.zeni@unina2.it (L. Zeni), s.dauria@ibp.cnr.it (S. D'Auria).

0925-4005/$ – see front matter © 2012 Elsevier B.V. All rights reserved.
http://dx.doi.org/10.1016/j.snb.2012.10.055

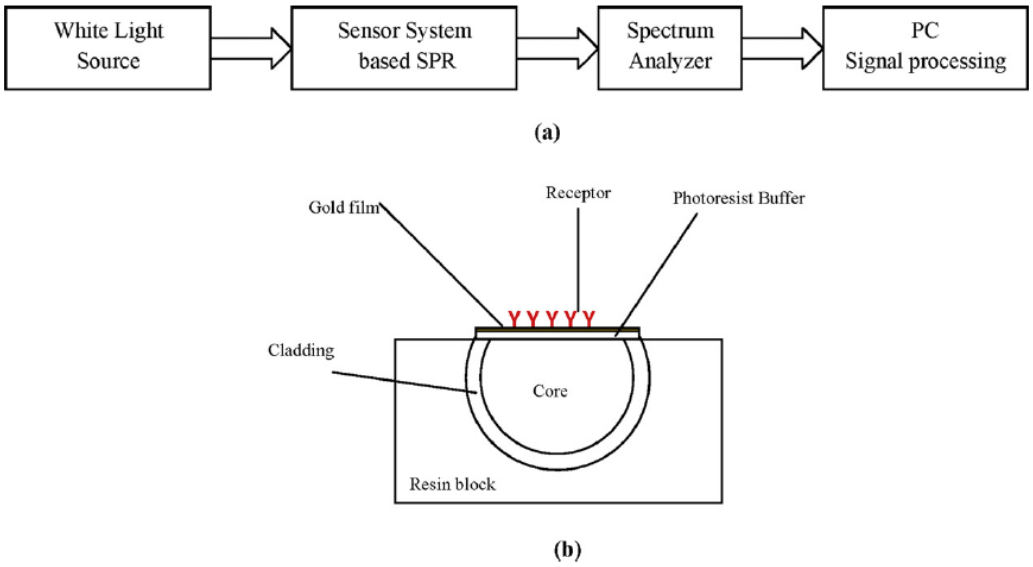

Fig. 1. (a) Experimental setup and (b) detail of POF sensor system based SPR.

of molecules and biological agents in the field. Anyway, detection limits for large sized analytes, such as bacteria and viruses, still need to be improved to meet today's needs [4–6].

Recently, we have developed a new geometry for low cost sensor system based on the use of SPR in POF [5] with two attractive features enabling it to be a candidate for successful biosensors implementation. It works with a planar gold layer and an external medium refractive index ranging from 1.332 to 1.418 (RIU). The planar gold layer can be employed for immobilization of the typical molecular recognition elements (MRE) used as probes for biosensor design and the refractive index range is just the right one for measurements in aqueous medium. The future development of this system for a quick multi-target detection will require significant advances toward the miniaturization of POF SPR bio-sensing platform, the development of robust bio/molecular recognition elements and the full integration of SPR sensor platform with microfluidic and optoelectronics devices.

In the present work, we show the possibility to develop a POF-based biosensor to detect the presence of the antigen–antibody complex. In particular, as a proof of principle we have developed a POF-biosensor for the detection of antibodies related to celiac disease (CD). CD is an immune-mediated disorder that is caused by the ingestion of wheat gluten and related prolamins present in barley and rye. Around 1% of the general population in developed and developing countries, with an increasing prevalence over time reported in Europe and the United States is affected by this disease. At the moment, only a life-long gluten-free diet (GFD) is mandatory to alleviate the symptoms and to normalize antibodies and intestinal mucosa. Two different types of antibodies have been associated with CD: serum antibodies against gliadin, and auto-antibodies against connective matrix proteins, in particular anti-endomysium and anti-transglutaminase (anti-tTG). The tTG is an enzyme that plays an important role in the pathogenesis of the disease and antibodies against tTG are used as serological markers for the diagnosis of CD. In scientific literature, different works show different analytical methods for the diagnosis and follow up of CD [7,8]. We will show in the following the potentialities offered by our low cost biosensor, based on SPR in a plastic optical fiber (POF), in the detection of anti-tTG antibodies presence in the serum of patients affected by CD.

2. Materials and methods

The commercial preparation of guinea pig liver transglutaminase (tTG), used to perform all the experiments, was purchased from Zedira GmbH (Darmstadt, Germany). Rabbit anti-tTG polyclonal sera were provided by IgTech, Paestum, SA, Italy. The rabbits were immunized by an intra-peritoneal injection using the commercial pure preparation of guinea pig liver transglutaminase and Freund's complete adjuvant.

2.1. Bio-sensor system fabrication

The optical sensor system was realized by removing the cladding of a plastic optical fiber along half the circumference, spin coating on the exposed core a buffer of Microposit S1813 photoresist, and finally sputtering a thin gold film using a sputtering machine [9]. The plastic optical fiber has a PMMA core of 980 μm and a fluorinated polymer cladding of 20 μm. The refractive index, in the wavelength range of interest (visible spectrum), is about 1.49 for PMMA, 1.41 for fluorinated polymer and 1.61 for Microposit S1813 photoresist, respectively. The sample consisted in a plastic optical fiber without jacket embedded in a resin block, with the purpose of easing the polishing process. The polishing process was carried out with a 5 μm polishing paper in order to remove the cladding and part of the core. After 20 complete strokes with a "Figure 8" pattern in order to completely expose the core, a 1 μm polishing paper was used for another 20 complete strokes with a "Figure 8" pattern. The realized sensing region was about 10 mm in length. The buffer of Microposit S1813 photoresist was realized by using a spin coating machine. The Microposit S1813 photoresist was deposited in one drop (about 0.1 mL) on the center of the substrate. The sample was then spun at 6000 rpm for 60 s. The final thickness of photoresist buffer was about 1.5 μm. Finally, a thin gold film was sputtered by using a sputtering machine (Bal-Tec SCD 500). The sputtering process was repeated twice with a current of 60 mA for 35 s (20 nm for

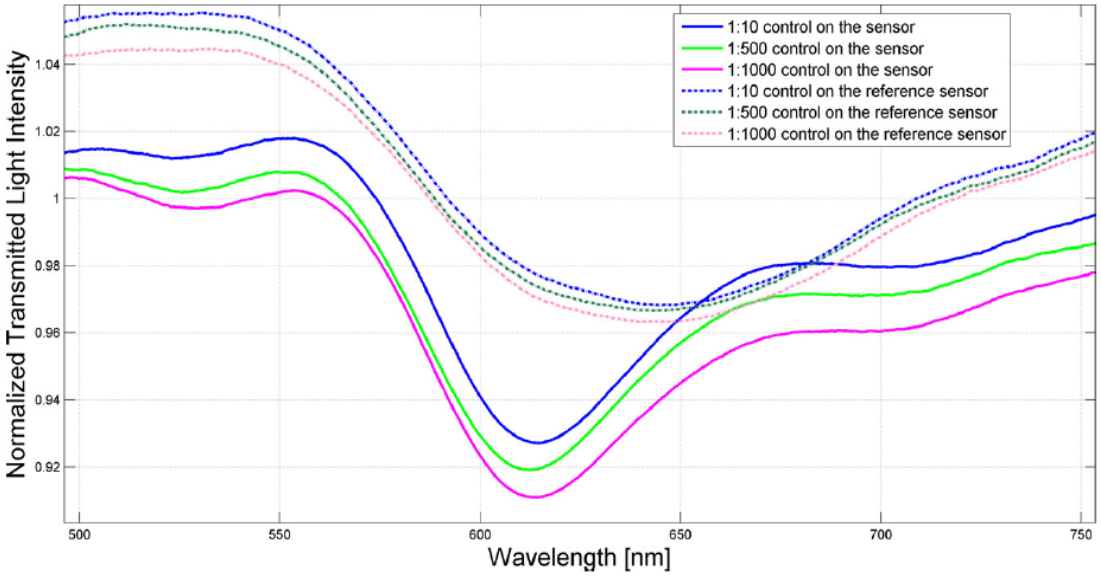

Fig. 4. SPR transmission spectra, normalized to the air spectrum, for different control analyte concentrations for the both sensors (with and without tTG).

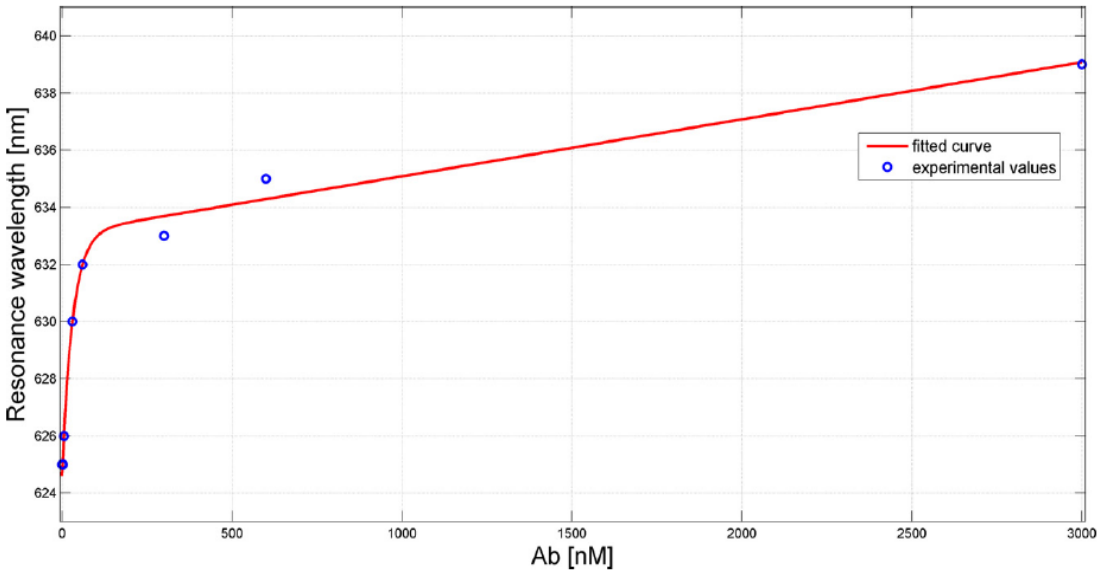

Fig. 5. Plasmon resonance wavelength, as a function of the analyte concentration (blue circles), along with the corresponding fitting curve (red solid line) for the sensor with tTG (in linear scale). (For interpretation of the references to color in this figure legend, the reader is referred to the web version of this article.)

plasmon wave (SPW), which propagates along the interface. When the p-polarized light is incident to a metal–dielectric interface in the way that the propagation constant (and energy) of resultant evanescent wave is equal to that of the SPW, a strong absorption of light takes place as a result of transfer of energy and the output signal demonstrates a sharp dip at a particular wavelength known as resonance wavelength. The so-called resonance condition is given by following expression [10,11]:

$$K_0 n_c \ \sin\vartheta = K_0 \left(\frac{\varepsilon_{mr} n_s^2}{\varepsilon_{mr} + n_s^2} \right)^{1/2} ; K_0 = \frac{2\pi}{\lambda} \quad (1)$$

The term on the left-hand side is the propagation constant (K_{inc}) of the evanescent wave generated as a result of attenuated total reflection (ATR) of the light incident at an angle θ through a light coupling device (such as prism or optical fiber) of refractive index n_c. The right-hand term is the SPW propagation constant (K_{SP}), with ε_{mr} as the real part of the metal dielectric constant (ε_m) and n_s as the refractive index of the sensing (dielectric) layer. This matching condition of propagation constants is heavily sensitive to even a slight change in the outer ambience, which makes this technique a powerful tool for sensing of different parameters.

In SPR sensors with spectral interrogation, the resonance wavelength (λ_{res}) is determined with reference to the refractive index of the sensing layer (n_s). If the refractive index of the sensing layer is

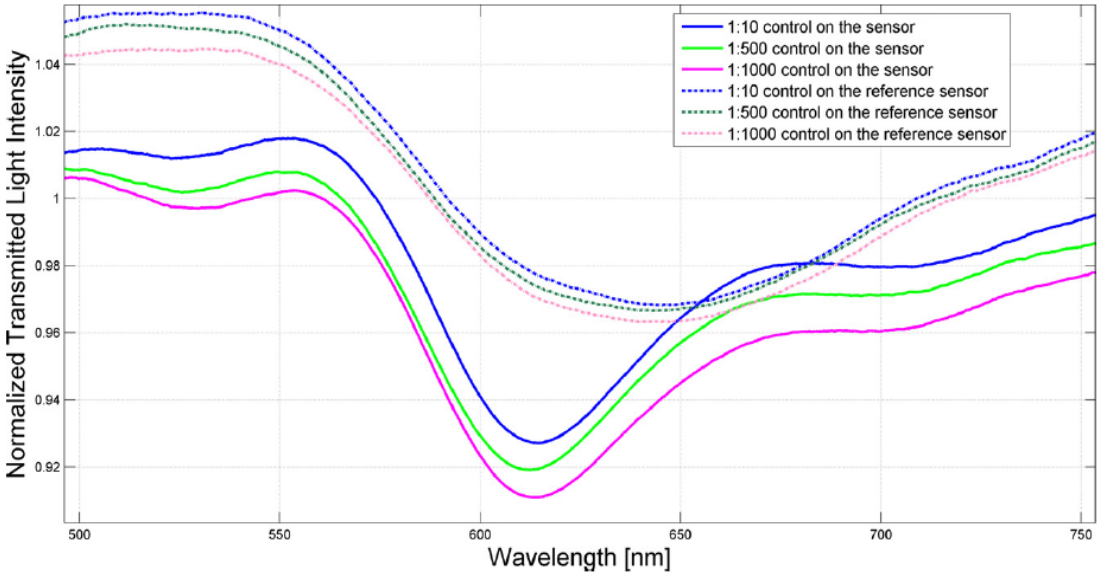

Fig. 4. SPR transmission spectra, normalized to the air spectrum, for different control analyte concentrations for the both sensors (with and without tTG).

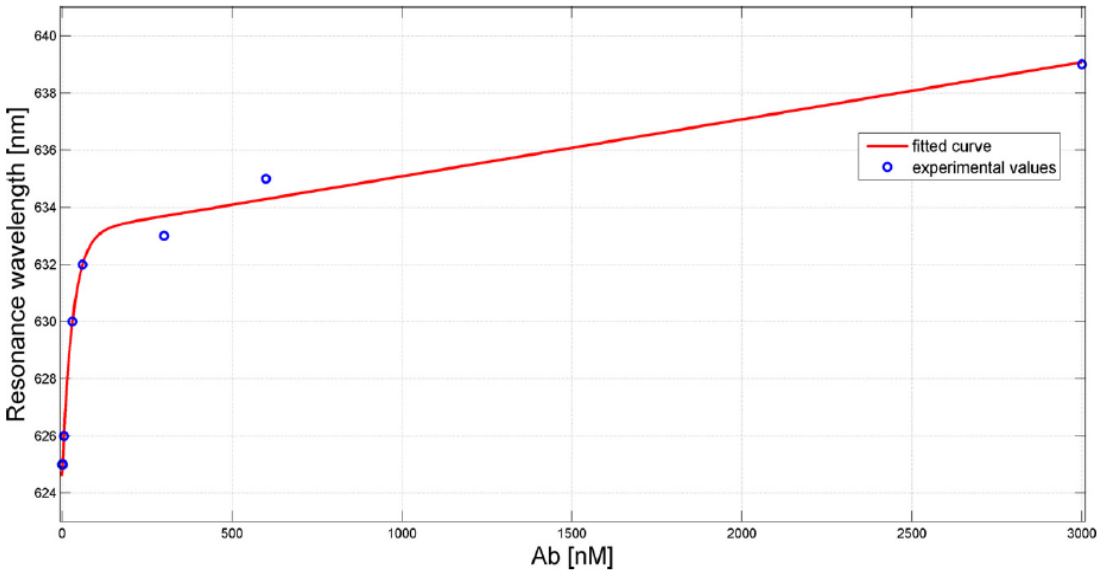

Fig. 5. Plasmon resonance wavelength, as a function of the analyte concentration (blue circles), along with the corresponding fitting curve (red solid line) for the sensor with tTG (in linear scale). (For interpretation of the references to color in this figure legend, the reader is referred to the web version of this article.)

plasmon wave (SPW), which propagates along the interface. When the p-polarized light is incident to a metal–dielectric interface in the way that the propagation constant (and energy) of resultant evanescent wave is equal to that of the SPW, a strong absorption of light takes place as a result of transfer of energy and the output signal demonstrates a sharp dip at a particular wavelength known as resonance wavelength. The so-called resonance condition is given by following expression [10,11]:

$$K_0 n_c \ \sin\vartheta = K_0 \left(\frac{\varepsilon_{mr} n_s^2}{\varepsilon_{mr} + n_s^2} \right)^{1/2} ; K_0 = \frac{2\pi}{\lambda} \quad (1)$$

The term on the left-hand side is the propagation constant (K_{inc}) of the evanescent wave generated as a result of attenuated total reflection (ATR) of the light incident at an angle θ through a light coupling device (such as prism or optical fiber) of refractive index n_c. The right-hand term is the SPW propagation constant (K_{SP}), with ε_{mr} as the real part of the metal dielectric constant (ε_m) and n_s as the refractive index of the sensing (dielectric) layer. This matching condition of propagation constants is heavily sensitive to even a slight change in the outer ambience, which makes this technique a powerful tool for sensing of different parameters.

In SPR sensors with spectral interrogation, the resonance wavelength (λ_{res}) is determined with reference to the refractive index of the sensing layer (n_s). If the refractive index of the sensing layer is

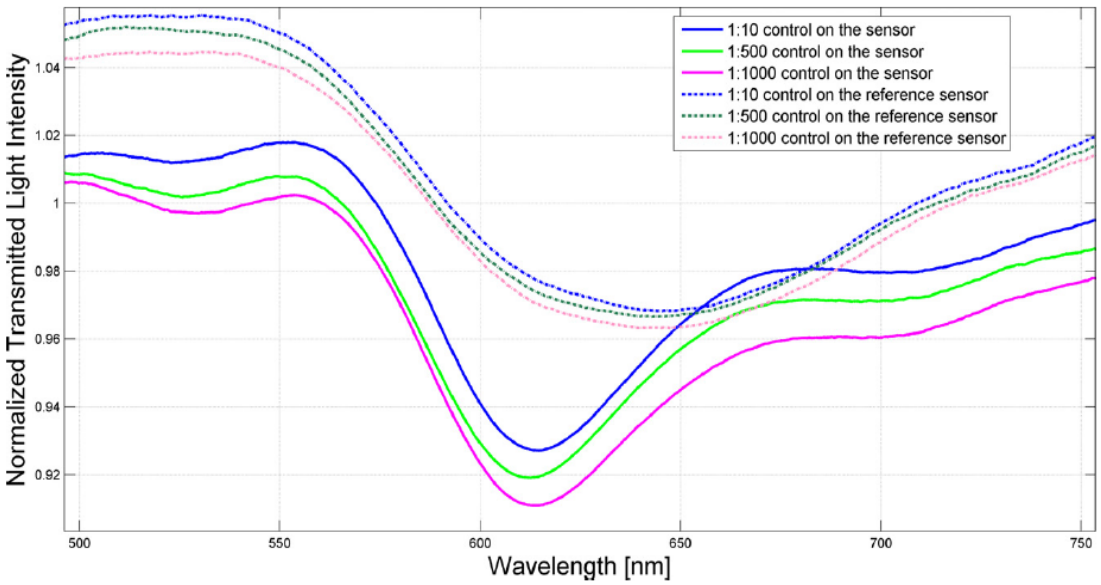

Fig. 4. SPR transmission spectra, normalized to the air spectrum, for different control analyte concentrations for the both sensors (with and without tTG).

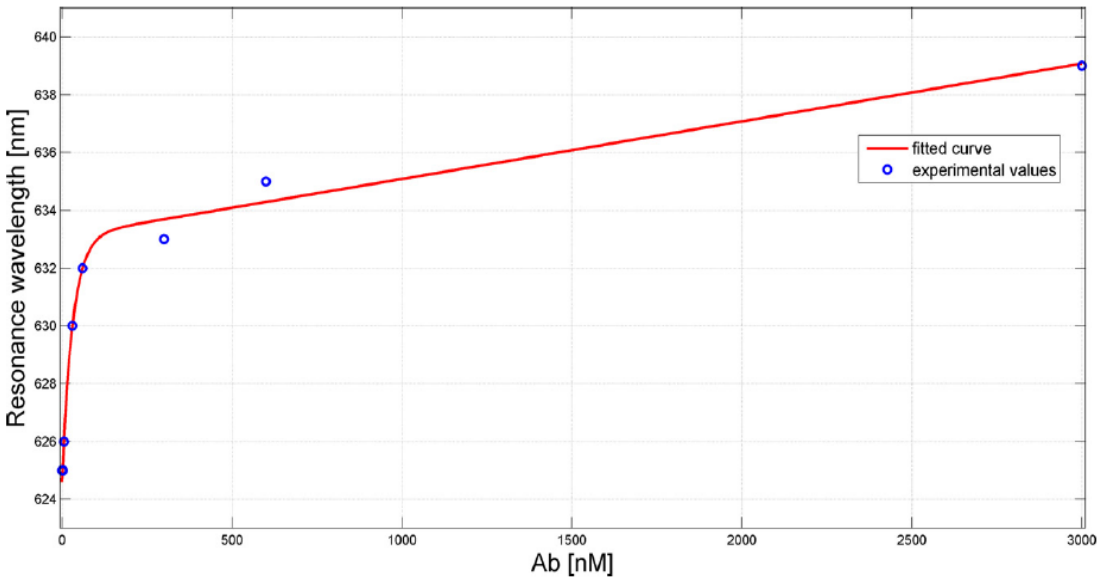

Fig. 5. Plasmon resonance wavelength, as a function of the analyte concentration (blue circles), along with the corresponding fitting curve (red solid line) for the sensor with tTG (in linear scale). (For interpretation of the references to color in this figure legend, the reader is referred to the web version of this article.)

plasmon wave (SPW), which propagates along the interface. When the p-polarized light is incident to a metal–dielectric interface in the way that the propagation constant (and energy) of resultant evanescent wave is equal to that of the SPW, a strong absorption of light takes place as a result of transfer of energy and the output signal demonstrates a sharp dip at a particular wavelength known as resonance wavelength. The so-called resonance condition is given by following expression [10,11]:

$$K_0 n_c \sin\vartheta = K_0 \left(\frac{\varepsilon_{mr} n_s^2}{\varepsilon_{mr} + n_s^2} \right)^{1/2}; K_0 = \frac{2\pi}{\lambda} \quad (1)$$

The term on the left-hand side is the propagation constant (K_{inc}) of the evanescent wave generated as a result of attenuated total reflection (ATR) of the light incident at an angle θ through a light coupling device (such as prism or optical fiber) of refractive index n_c. The right-hand term is the SPW propagation constant (K_{SP}), with ε_{mr} as the real part of the metal dielectric constant (ε_m) and n_s as the refractive index of the sensing (dielectric) layer. This matching condition of propagation constants is heavily sensitive to even a slight change in the outer ambience, which makes this technique a powerful tool for sensing of different parameters.

In SPR sensors with spectral interrogation, the resonance wavelength (λ_{res}) is determined with reference to the refractive index of the sensing layer (n_s). If the refractive index of the sensing layer is

increase in the refractive index at the metal surface). The refractive index increase gives rise to an increase in the propagation constant of SPW propagating along the metal surface which can be accurately measured by optical means. The magnitude of the change in the propagation constant of an SPW depends on the refractive index change and its distribution with respect to the profile of the SPW field. If the binding occurs within the whole depth of the SPW field, the binding-induced refractive index change, produces a change in the real part of the propagation constant, which is directly proportional to the refractive index change. The binding-induced change in the propagation constant of the SPW is proportional to the refractive index change and the depth of the area within which the change occur.

2.4. SPR measurements

The experimental setup was settled to measure the transmitted light spectrum and was characterized by a halogen lamp, illuminating the sensor system (with and without MRE), and a spectrum analyzer [9], as shown in Fig. 1. The employed halogen lamp exhibits a wavelength emission range from 360 nm to 1700 nm, while the spectrum analyzer detection range was from 200 nm to 850 nm. An Ocean Optics USB2000 + UV-VIS spectrometer was employed. The spectral resolution ($\delta\lambda_{DR}$) of the spectrometer was 1.5 nm (FWHM). The spectrometer is finally connected to a computer. The SPR curves along with data values were displayed online on the computer screen and saved with the help of advanced software provided by Ocean Optics for signal processing. Two different experimental controls were performed in order to be sure that the obtained results were actually due to the interaction between the anti tTG and the immobilized tTG on chip. First, the binding experiments were performed by using the sensor system without immobilized tTG. After, the sensor system was tested after tTg functionalization and with different sera in which antibodies against tTG were absent.

2.5. Binding measurements

Binding experiments of different dilutions of anti-transglutaminase (anti-tTG) serum were performed on the functionalized tTG-chip. The diluted serum contained IgG antibodies able to bind with high affinity the tTG. Every sample was prepared with diluted serum in a solution of Tris/HCl 2 mM pH 7.4. The range of anti-tTG concentration was from 0 to 3000 nM and, before each measurement, the sample was incubated on the chip surface for 5 min. After the measurements, an extensive washing step with Tris/HCl 2 mM pH 7.4 was done. The sensor system without immobilized tTG was used as reference sensor.

3. Results and discussion

The presented experimental results were obtained by measuring SPR transmission spectra, normalized to the spectrum achieved with air as the surrounding medium, for different analyte concentrations. The observed absorption band is the result of the convolution of different resonance peaks. Each peak is obtained for a specific resonance condition, defined by a given angle-wavelength couple [10,12,13].

In Fig. 2 are presented the experimentally obtained SPR transmission spectra, normalized to the spectrum achieved with air as the surrounding medium, for the reference sensor (without tTG), for six different analyte concentration values between 0.0 nM and 3000 nM. It is evident that when the tTG is not present, no significant shifts of PRW occurs as a function of the analyte concentrations.

In Fig. 3 are displayed the SPR transmission spectra, normalized to the spectrum achieved with air as the surrounding medium, for the sensor (with tTG). It is possible to notice that a shift of PRW occurs, as a function of analyte concentrations for the sensor with tTG. The comparative analysis of the results indicates that the plasmon resonance wavelength shifts are exclusively due to the binding process.

In Fig. 4 are presented the SPR transmission spectra, normalized to the spectrum achieved with air as the surrounding medium, for the sensor in the absence and in the presence of tTG at different concentrations of a compound that cannot interact with tTG. As expected, there is no evidence of any PRW shift.

Fig. 5 shows the PRW variations versus different analyte concentrations obtained with the presence of tTG. In the same figure is also presented the fitting to the experimental data.

Fig. 6(a) shows the resonance wavelength versus the analyte concentration in a semi-log scale with the linear fitting to the log experimental data. The Pearson's correlation coefficient is presented with the relative equation. Fig. 6(b) presents the sensitivity curve of the sensor in semi-log scale. In this case the sensitivity is defined as:

$$S = \frac{\partial \lambda_{\text{resonance wavelength}}}{\partial Ab} \ [\text{nm/nM}] \quad (3)$$

In other words, the sensitivity (S) can be defined by calculating the shift in resonance wavelength per unit change in analyte concentration (nm/nM).

Fig. 6(b) shows as the sensor response is non-linear. The sensitivity of the realized optical sensor depends on the sensing region length, on the thickness of the photoresist buffer and on the thickness of the gold film [14,15].

In conclusion, our work presents a new low cost sensor based on the utilization of SPR with a POF. The sensing method of the sensor is based on the variation of the excitation of surface plasmons at the interface between the medium and a thin gold layer deposited on a photoresist buffer deposited on the plastic fiber core. On the gold layer surface a Guinea pig tTG protein was immobilized and tested versus different concentrations of specific anti-tTG antibodies. The obtained results show that the POF-sensor is able to sense the transglutaminase/anti-transglutaminase complex in the range of concentrations between 30 nM and 3000 nM. In celiac patients the specific antibodies concentration against tTG are in the range 0.4–3 mM, about 1.0–10.0% of all IgA present in the serum of normal adults (4.4 and 31.2 mM). The protein concentrations detected in our experiments is in the nanomolar range, indicating that our biosensor is a good candidate for the diagnosis and follow-up of CD [7]. The proposed sensing methodology could be easily expanded to the determination of different compounds.

Acknowledgments

This project was realized within the CNR Commessa ""Progettazione e Sviluppo di Biochip per la Sicurezza Alimentare e Salute Umana". The project was partially funded by the CNR project "Conoscenze integrate per sostenibilità e innovazione del Made in Italy agroalimentare (CISIA)" and Project PON01_01525 "MONICA".

References

[1] J. Homola, Present and future of surface plasmon resonance biosensors, Analytical and Bioanalytical Chemistry 377 (2003) 528–539.
[2] R.C. Jorgenson, S.S. Yee, A fiber-optic chemical sensor based on surface plasmon resonance, Sensors and Actuators B 12 (1993) 213–220.
[3] A. Trouillet, C. Ronot-Trioli, C. Veillas, H. Gagnaire, Chemical sensing by surface plasmon resonance in a multimode optical fibre, Pure and Applied Optics 5 (1996) 227–237.

[4] V.M. Muñoz-Berti, A.C. López-Pérez, B. Alén, J.L. Costa-Krämerm, A. García-Martín, M. Lomer, J.M. López-Higuera, Low cost plastic optical fiber sensor based on surface plasmon resonance, Proceedings of SPIE 7653 (2010) 765327.
[5] N. Cennamo, D. Massarotti, L. Conte, L. Zeni, SPR in plastic optical fibers: a simple geometry for low-cost biosensors, in: Proceedings of 4th EOS Topical Meeting on Optical Microsystems, Capri, Italy, 26–28 September, 2011.
[6] R.J. Bartlett, R. Philip-Chandy, P. Eldridge, D.F. Merchand, R. Morgan, P.J. Scully, Plastic optical fibre sensors and devices, Transactions of the Institute of Measurement and Control 22 (2000) 431–457.
[7] S. D'Auria, E. Apicella, M. Staiano, S. Di Giovanni, G. Ruggiero, M. Rossi, P. Sarkar, R. Luchowski, I. Gryczynski, Z. Gryczynski, Engineering resonance energy transfer for advanced immunoassays: the case of celiac disease, Analytical Biochemistry 425 (1) (2012) 13–17.
[8] M. Staiano, E.G. Matveeva, M. Rossi, R. Crescenzo, Z. Gryczynski, I. Gryczynski, L. Iozzino, I. Akopova, S. D'Auria, Nanostructured silver-based surfaces: new emergent methodologies for an easy detection of analytes, ACS Applied and Material Interfaces 1 (12) (2009) 2909–2916.
[9] N. Cennamo, D. Massarotti, L. Conte, L. Zeni, Low cost sensors based on SPR in a plastic optical fiber for biosensor implementation, Sensors 11 (2011) 11752–11760.
[10] M. Kanso, S. Cuenot, G. Louarn, Sensitivity of optical fiber sensor based on surface plasmon resonance: modeling and experiments, Plasmonics 3 (2008) 49–57.
[11] Y.S. Dwivedi, A.K. Sharma, B.D. Gupta, Influence of design parameters on the performance of a SPR based fiber optic sensor, Plasmonics 3 (2008) 79–86.
[12] J.E. Sipe, The ATR spectra of multipole surface plasmons, Surface Science 84 (1979) 75–105.
[13] D. Roy, Surface plasmon resonance spectroscopy of dielectric coated gold and silver films on supporting metal layers: reflectivity formulas in the Kretschmann formalism, Applied Spectroscopy 55 (2001) 1046–1052.
[14] M. Iga, A. Sek, K. Watanabe, Gold thickness dependence of SPR-based hetero-core structured optical fiber sensor, Sensors and Actuators B: Chemistry 106 (2005) 363–368.
[15] K. Anuj, R.J. Sharma, B.D. Gupta, Fiber-optic sensors based on surface plasmon resonance: a comprehensive review, IEEE Sensors Journal 7 (2007) 1118–1129.

Biographies

Nunzio Cennamo is a post-doc at the Department of Information Engineering at Second University of Naples, Italy. His main interest deals with the design of advanced optical sensors.

Antonio Varriale is a biochemist with a post-doc position at the Institute of Protein Biochemistry, CNR, Naples, Italy. The main interests of Dr. Varriale are the realization of innovative protein-based sensors.

Anna Pennacchio is a PhD student in Dr. D'Auria's lab. Her PhD work is focused on the design of new optical biosensors for food safety.

Maria Staiano is a permanent scientist at the Institute of Protein Biochemistry, CNR, Naples, Italy. Her interests are on the identification, expression and manipulation of biomolecules to use as specific probe in bio/sensing approaches.

Davide Massarotti is a PhD student at University of Naples Federico II, Naples, Italy. His main interests are focused on the characterization of new materials.

Luigi Zeni is full professor of electronics at the Second University of Naples and president of the Research Consortium on Advanced Remote Sensing Systems – CO.RI.S.T.A., Naples, Italy. His research interests include the design and fabrication of optical fiber sensors and optoelectronic devices.

Sabato D'Auria is a senior scientist with a tenured position at the National Research Council of Italy. He is the head of the Laboratory for Molecular Sensing at the Institute of Protein Biochemistry, Naples, Italy. The main interest of Dr. D'Auria's lab are the design of advanced optical protein-based sensors for a wide range of compounds.

Journal of Photochemistry and Photobiology B: Biology 118 (2013) 66–73

Contents lists available at SciVerse ScienceDirect

Journal of Photochemistry and Photobiology B: Biology

journal homepage: www.elsevier.com/locate/jphotobiol

Amino acid transport in thermophiles: Characterization of an arginine-binding protein from *Thermotoga maritima*. 3. Conformational dynamics and stability

A. Ausili [a,*], A. Pennacchio [a], M. Staiano [a], J.D. Dattelbaum [b], D. Fessas [c], A. Schiraldi [c], S. D'Auria [a,*]

[a] Laboratory for Molecular Sensing, IBP-CNR, Naples 80131, Italy
[b] Department of Chemistry, University of Richmond, Richmond, VA 23173, USA
[c] Università di Milano, DeFENS, Milan, Italy

ARTICLE INFO

Article history:
Received 17 October 2012
Received in revised form 7 November 2012
Accepted 8 November 2012
Available online 29 November 2012

Keywords:
Fluorescence
Phosphorescence
Arginine
Extremophiles
Unfolding
Thermodynamics

ABSTRACT

Arginine-binding protein from *Thermotoga maritima* (TmArgBP) is a 27.7 kDa protein possessing the typical two domain structure of the periplasmic binding protein family. The protein is characterized by high specificity and affinity for binding a single molecule of L-arginine.

In this work, the effect of temperature and/or guanidine hydrochloride on structure and stability of the protein in the absence and in the presence of L-arginine has been investigated by differential scanning calorimetry, far-UV circular dichroism and intrinsic tryptophan phosphorescence and fluorescence. The results revealed that TmArgBP undergoes an irreversible one-step thermal unfolding process in a cooperative mode. The TmArgBP melting temperature was recorded at 115 °C. The presence of L-arginine did not change the protein secondary structure content as well as the intrinsic phosphorescence and fluorescence protein properties, even if it increases the structural stability of the protein.

The obtained results are discussed in combination with a detailed inspection of the three-dimensional structure of the protein.

1. Introduction

Periplasmic binding proteins (PBPs) constitute a widely distributed protein superfamily involved in the passage of ligands through bacterial cell membranes [1]. In this function, PBPs are associated with ATP-binding cassette (ABC) transport systems, which are multi-protein complexes constituted of two transmembrane domains and two ATP-binding domains that cooperate for nutrient uptake [2,3]. Although PBPs are able to bind many different ligands with diverse degrees of affinity, they show a highly conserved structure. PBPs are single chain polypeptides that appear to be composed of two well defined domains linked by a rotating hinge that can make the protein change its conformation from open to close form and vice versa depending on the absence or presence of ligand [4,5]. Due to the variety of binding specificities, PBPs from *Escherichia coli* have been utilized as design platforms for fluorescent and electrochemical protein biosensors capable of targeting many naturally-occurring ligands, including sugars, anions, and amino acids [6–8]. Arginine-binding protein (ArgBP) is a monomeric protein member of the PBP superfamily and is involved in arginine recruitment and transport; it binds L-arginine with a very high affinity [9]. Here, we have investigated an arginine-binding protein from *Thermotoga maritima* (TmArgBP) a hyper-thermophilic eubacterium originally isolated from various geothermal heated marine sediments with an optimum growth temperature of 80 °C [10]. TmArgBP is an ultra-stable protein with an estimated transition temperature of 116 °C, a monomeric molecular mass of 27.7 kDa and it presents the two domain structure typical of PBPs, each domain consisting of a β-sheet core surrounded by helices [11]. Unlike other arginine-binding proteins, TmArgBP seems to exist not only as monomer but also as dimer and trimer [12], but like all PBPs, the arginine-dependent conformational change (K_d = 20 μM) stabilizes the protein [11,12]. For its characteristics of sensitivity, selectivity and high stability, TmArgBP could be a good potential candidate for the development of an arginine-binding protein-based fluorescent biosensor for real-time and continuous detection of the level of blood arginine that is an important marker of hyper-argininemia, an autosomal recessive disorder of the urea cycle where a deficiency of the enzyme arginase causes a build-up of arginine and ammonia in the blood [13]. Reagentless fluorescent biosensors have the advantage of avoiding the production of secondary components and the modification of the sensor itself [14], for this reason several proteins with these characteristics, in particular from PBP superfamily, have been engineered to make them suitable biosensors, modifying their specificity [15] or conjugating with fluorescent probes [16,17]. In this work, we have investigated the thermodynamic

* Corresponding authors. Address: Institute of Protein Biochemistry, CNR, Via Pietro Castellino, 111, 80131 Napoli, Italy. Tel.: +39 0816132312; fax: +39 0816132273 (A. Ausili), tel.: +39 0816132250; fax: +39 0816132273 (S. D'Auria).
E-mail addresses: a.ausili@ibp.cnr.it (A. Ausili), s.dauria@ibp.cnr.it (S. D'Auria).

1011-1344/$ - see front matter © 2012 Elsevier B.V. All rights reserved.
http://dx.doi.org/10.1016/j.jphotobiol.2012.11.004

and structural characteristics of TmArgBP in the presence and in the absence of L-arginine by means of differential scanning calorimetry, circular dichroism and phosphorescence and fluorescence spectroscopy.

2. Materials and methods

2.1. Materials

Arginine-binding protein from *T. maritima* was cloned, expressed and purified according to previously reported procedures [12]. L-arginine was purchased from Sigma. All other reagents and solvents were commercial samples of the highest purity.

2.2. DSC experiments

Calorimetric measurements were carried out in 5 mM phosphate buffer, pH 7.5, 0.8 mg/ml protein solutions, with a nano DSC (CSC, TA Instruments distributor, USA) apparatus at 0.5 °C/min scan rate in the 10–130 °C range. This instrument uses capillary cells with 0.3 ml sensitive volume. The systems considered were: wild type protein (TmArgBP) alone and TmArgBP in the presence of L-arginine in excess conditions (L-arginine/protein ratio (r); $r = 477$). For each system three measurements where performed. A second heating run was also performed (after cooling with the same scan rate) for each system. No signal was observed in the second heating run in both cases indicated that the protein does not refold after thermal denaturation (at least in the time span of the measurements).

Data were analyzed by means of the software THESEUS [18]. The excess molar (monomer) heat capacity $\langle \Delta C_p \rangle$ or $C_P^E(T)$, i.e., the difference between the apparent molar heat capacity $Cp(T)$ of the sample and the molar heat capacity of the "native state", $Cp_{,N}(T)$, was recorded across the scanned temperature range. The methods to treat the raw data (baselines scaling, etc.) are reported elsewhere [19,20]. Suffice here to say that in all cases the signal was rather disturbed in the 25–50 °C range and the apparent denaturation enthalpy $\Delta_d H$ was affected by a rather large error (20–30%) in spite of a very good reproducibility both of the temperature of the denaturation peaks maximum, T_{max}, (that is above 100 °C) and the signal profile. The average values of the apparent denaturation enthalpy $\Delta_d H$ were 680 and 645 kJ mol^{-1} (monomer) for the TmArgBP and TmArgBP with L-arginine systems, respectively.

A possible explanation is that, in our conditions, partial precipitation occurred during the heating run and the effective concentration of the protein in the sensitive volume of the capillary cell became randomly different from the nominal one. Also, the heat capacity drop, $\Delta_d Cp$, across the signal was affected by a rather large error and was therefore not taken into account in the present work. Fortunately the uncertainty in the apparent denaturation enthalpy $\Delta_d H$ did not prevent the thermodynamic analysis (see below) and did not require further experimental efforts to avoid this phenomenon. The theoretical models used to fit the experimental data were tested through the non-linear Levenberg–Marquardt method [21].

2.3. Thermodynamic model

Even in the presence of an irreversible process that prevents the refolding after denaturation, the thermal denaturation of proteins can sometimes be described with a suitable thermodynamic model [27].

Details on the fitting equations of the thermodynamic model used to obtain the parameters presented in Table 1 are reported elsewhere [19]. This model can be formally summarized as a process of dissociation of an oligo- homo-meric protein with concomitant denaturation of the monomers:

$$N_n \overset{K}{\leftrightarrow} nU \tag{1}$$

and the normalized experimental profile can be simulated by the equation:

$$\frac{d\theta}{dT} = \frac{\Delta H^{vH}}{RT^2} \frac{\theta(1-\theta)}{n - \theta(1-\theta)} \tag{2}$$

where θ is the degree of advancement of the total process and can be calculated from the experimental signal (T_i being a pre-denaturation temperature):

$$\theta(T) = \frac{\int_{T_i}^{T} C_p^E(T)}{\Delta_d H} \tag{3}$$

The relevant van't Hoff enthalpy, ΔH^{vH}, can be calculated independently from the experimental data by using the equation:

$$\Delta H^{vH} = (\sqrt{n} + 1)^2 R T_{max}^2 C_p^E(T_{max}) / \Delta_d H \tag{4}$$

where $C_p^E(T_{max})$ is the excess heat capacity at T_{max}. The van't Hoff enthalpy value calculated with Eq. (4) is expressed per mole of protein considered as an n-monomer oligomer. This means that the calculated value has to be divided by n to obtain the enthalpy per mole of monomer.

The uncertainty of the calculated ΔH^{vH} was less than 10% in all cases. It is obvious that such a value does not depend on protein concentration errors (see Eq. (4)) since these are included in the common multiplication factor of $C_p^E(T_{max})$ and $\Delta_d H$, so that the relevant ratio is not affected.

Consequently the best fit of the model can be performed either for the normalized signal profile or directly for the experimental data using

$$C_p^E(T) = \Delta_d H \frac{d\theta}{dT} \tag{5}$$

In all cases, the only compatible value of n used to obtain a satisfactory fit was $n = 2$.

Table 1
Thermodynamic parameters of the denaturation of TmArgBP at pH 7.0, with and without the presence of L-arginine. Each value is the average of three measurements. The error of temperature T_{max} does not exceed 0.3 °C. The uncertainty of ΔH^{vH} enthalpy is less than 10%.

System	T_{max} (°C)	ΔH^{vH} (kJ mol^{-1})
Wild type	114.9	720
Wild type + L-arginine	118.8	910

We observe that the protein is stabilized in the presence of L-arginine with a slight entropic contribution (increasing the T_{max}) and a substantial enthalpic contribution (increasing the ΔH^{vH}) which suggests a specific binding that may promote conformational changes in the overall protein structure.

2.4. CD measurements

Far-UV (from 260 nm to 190 nm) CD spectra were obtained on a Jasco 810 spectrophotometer under constant nitrogen stream at 20 and 95 °C. An external bath circulator (Julabo F25) was used to maintain the desired temperature controlled by a thermocouple placed directly on the cell holder. Spectra were collected in a 0.1 cm path length quartz cell with a step size of 1 nm, a bandwidth of 1 nm and an averaging time of 4 s. The protein concentration was 0.1 mg/ml (≈3.6 μM) in 5 mM phosphate buffer, pH 7.5 in the absence and in the presence of 0.6 mM L-arginine, and in the presence of different concentrations of guanidine hydrochloride (GdmCl). For all spectra, an average of five scans was obtained.

CD spectra of the buffers were recorded and subtracted from the protein spectra. Heating from 20 °C to 95 °C was performed with a scan rate of 30 °C/h and the values of ellipticity at 222 nm were recorded every 0.5 °C. Concentration of GdmCl was determined by refractive index with a Abbe refractometer [22].

2.5. Intrinsic phosphorescence and fluorescence of TmArgBP

Typically, before all the experiments, TmArgBP samples were dialyzed overnight against 5 mM phosphate buffer, pH 7.5 with six buffer exchanges and the final protein concentration was of around 10 μM. For low-temperature studies, the samples contained 60% (v/v) glycerol. Experiments were performed in the absence and in the presence of L-arginine and in the absence and in the presence of 4 M and 8 M of urea. Protein samples were placed into a $5 \times 5\ mm^2$ quartz cuvette, deoxygenated by cycles of vacuum followed by inlet of a stream of pure N_2, as previously described [23]. Fluorescence and phosphorescence spectra and decays were all measured with pulsed excitation ($\lambda_{ex} = 292$ nm) on a homemade apparatus [23]. Pulsed excitation was provided by a frequency-doubled Nd/Yag-pumped dye laser (Quanta System, Milan, Italy) with pulse duration of 5 ns and a typical energy per pulse of 0.5–1 mJ. Emission spectra were collected at 90° from the excitation and dispersed by 0.3 m focal length triplet grating imaging spectrograph (SpectraPro-2300i, Acton Research Corporation, Acton, MA) with a band-pass of 0.2 nm for low T spectra and of 1.0 nm for room T spectra. The emission was monitored by a back-illuminated 1340 × 400 pixels CCD camera (Princeton Instruments Spec-10:400B (XTE), Roper Scientific Inc., Trenton, NJ) cooled to −60 °C. In low temperature glasses, the phosphorescence spectrum was recorded after a 2 s delay from the exciting pulse. Background of free Trp spectra was obtained by opening the mechanical shutter controlling the emission to the spectrograph after a delay of 2 s. In fluid solutions, spectra were recorded by integrating multiple excitation pulses at a repetition frequency up to 10 Hz. To block overlapping prompt fluorescence and short-lived background from the detector, laser excitation was synchronized to a fast mechanical chopper opening the emission slit 50 μs after the laser pulse. In general, less than 20 pulses were sufficient to obtain satisfactory *S*/*N* ratios.

Phosphorescence decays were monitored by collecting the emission at 90° from vertical excitation through a filter combination with a transmission window of 405–445 nm (WG405, Lot-Oriel, Milano Italy, plus interference filter DT-Blau, Balzer, Milano, Italy). The photomultiplier (EMI 9235QA, Middlesex, UK) was protected against fatigue from the strong excitation/fluorescence pulse by the mechanical chopper synchronized to the laser trigger, which closed the emission slit during the excitation pulse. The time resolution of this apparatus depends on the chopper speed and, for the experiments reported here, was maintained constant to 50 μs, the same as for spectral acquisitions. The photocurrent was amplified by a current-to-voltage converter (SR570, Stanford Research Systems, Stanford, CA) and digitized by a 16 bits high speed (1.25 MHz) multifunction data acquisition board (NI 6250 PCI, National Instrument Italy, Milano, Italy) supported by LabVIEW software capable of averaging multiple sweeps. Typically, less than 20 sweeps were sufficient for a good signal-to-noise ratio even for the shortest decays. Prompt fluorescence was simultaneously collected through a 310–375 band-pass filter combination (WG305 nm plus Schott UG11) and detected by a UV-enhanced photodiode (OSD100-7, Centronics, Newbury Park, CA). An analogue circuit was used to integrate the photocurrent and its output was digitized and averaged by a multifunctional board (PCI-20428, Intelligent Instrumentation, Tucson, Texas) utilizing LabVIEW software. The prompt fluorescence intensity was used to account for possible variations in the laser output between measurements as well as to obtain fluorescence normalized phosphorescence intensities. All phosphorescence decays were analyzed in terms of a sum of exponential components by a nonlinear least-squares fitting algorithm (DAS6, fluorescence decay analysis software, Horiba Jobin Yvon, Milano, Italy). Each spectral and lifetime determination was repeated at least three times. Acrylamide quenching experiments were also performed and carried out as described before [24].

3. Results and discussion

3.1. Differential scanning calorimetry

Fig. 1A reports the thermal denaturation trace of the TmArgBP and some tentative fitting approaches. The traces show an asymmetric endothermic peak with a maximum at high temperature (about 115 °C), in line with the expectation for such hyperthermophilic proteins. Because of the asymmetry, the simplest thermodynamic interpretation, namely, one step equilibrium denaturation had to be ruled out. A tentative complex interpretation, i.e. the insertion of an irreversible step or the possibility of a multi-domain unfolding, was also excluded since it did not give satisfactory fits in any case. A satisfactory result was instead obtained with a very simple equilibrium model (see experimental procedures) that implies one-step dissociation of a homo-dimeric protein coupled with a one-step denaturation of the monomers.

$$N_2 \leftrightarrow 2U$$

This model allows us to single out the van't Hoff denaturation enthalpy of each monomer, ΔH^{vH}, which is the relevant thermodynamic parameter used to characterize the enthalpic contribution to the protein stability. This satisfactory fitting is in line with previous findings on the dimeric status of this protein even under strong denaturing conditions [12]. On the other hand, although the presence of structural domains is detectable and reported in the literature, our findings suggest that only one energetic domain is present in each monomer and that the presence of L-arginine increases the overall stability of the protein.

Fig. 1B shows the thermal denaturation traces (grey lines) and the fitting curves (black lines) drawn according to the dimer dissociation model for wild type protein with and without the presence of L-arginine. The overall denaturation mechanism in the presence of L-arginine remains the same as in the wild type and the dissociation model fits well in both cases. The maximum of the DSC signal, T_{max}, and the calculated values of ΔH^{vH} (monomer) are reported in Table 1.

3.2. Circular dichroism

In Fig. 2, far-UV CD spectra of TmArgBP at 20 °C in the absence and in the presence of L-arginine are reported. As it was previously demonstrated [11], the binding of L-arginine to TmArgBP induces small changes in the secondary structure content of the protein. The recorded CD data are in good agreement with this, being only detected a small effect on spectrum profile of the protein upon ligand binding.

In order to evaluate the content of secondary structure of the protein, we analyzed the far-UV CD spectra using the k2d algorithm [25]. The analysis revealed that the protein structure content consisted approximately of 36% α-helices and 14% β-sheets for TmArgBP, which is consistent with the three-dimensional model of the protein [11]. The binding of L-arginine to TmArgBP results in a small variation of the α and β protein structures content that is estimated to become 32% and 17%, respectively.

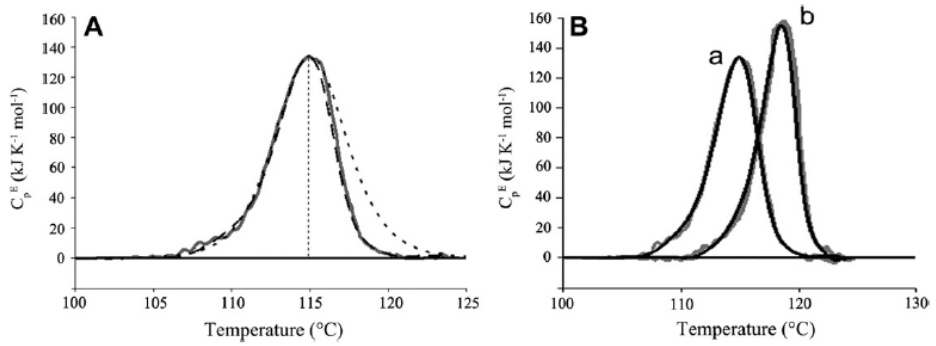

Fig. 1. (A) Experimental (continuous line) and theoretical DSC thermal denaturation curves of TmArgBP. The theoretical curves were calculated according to the single step denaturation (dotted line) and the dissociation models (dashed line). (B) Experimental (grey) and theoretical (black) DSC thermal denaturation curves. In the figure the wild type protein in the absence and in the presence of L-arginine (a and b, respectively) are reported. The theoretical curves were calculated by the dissociation model. Conditions: 5 mM phosphate buffer, pH 7; protein concentration 1.0 mg/ml; L-arginine/protein ratio (r); $r = 477$ for the TmArgBP + L-arginine system. 0.5 °C/min scan rate.

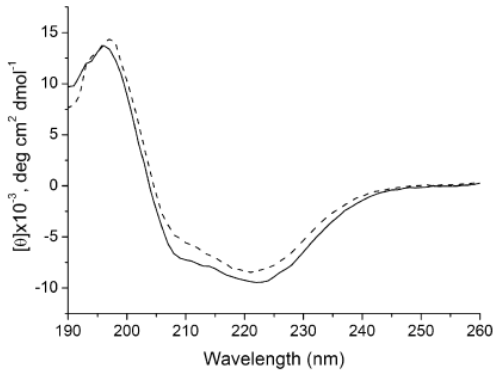

Fig. 2. Far-UV CD spectra of TmArgBP in the absence and in the presence of L-arginine (solid and dashed line, respectively) in 5 mM phosphate buffer, pH 7.5 at 20 °C. The protein solutions were at 0.1 mg/ml and L-arginine concentration was 0.6 mM. Spectra were recorded in the 260–190 nm spectral range in a 1 mm path length cell.

The stability of TmArgBP structure in the absence and in the presence of increasing amounts of GdmCl was investigated by CD experiments (Fig. 3). At 20 °C high concentrations of GdmCl are needed to induce relevant changes in TmArgBP secondary structure content. A complete denaturation of the protein can be detected at the highest GdmCl concentration reached in our experiments (7.8 M). In the presence of 2.6 M GdmCl and at 95 °C the CD spectrum of TmArgBP shows a totally random structure profile (Fig. 3). The binding of L-arginine to TmArgBP leads to an increase of the stability of the protein as revealed by the absence of a complete protein denaturation pattern at 20 °C, even in the presence of 7.8 M GdmCl. The complete thermal unfolding of the protein was recorded at 95 °C in the presence of 3.9 M GdmCl.

Thermal unfolding curves of TmArgBP at different GdmCl concentrations were obtained by monitoring the ellipticity at 222 nm as a function of temperature (Fig. 4). In agreement with the data reported in Fig. 3, at 95 °C it is observed that the complete protein unfolding process is reached in the presence of 2.6 M GdmCl. The binding of L-arginine increases the protein stability.

In all cases, a cooperative thermal unfolding process is observed with a transition temperature that decreases with increasing GdmCl concentrations up to 7.8 M. At specific concentrations of GdmCl, increasing the temperature from 20 °C to 95 °C results in unfolding of the protein structure through an apparent two-state mechanism both in the absence and in the presence of L-arginine. The different degrees of protein thermo-stability were also compared by the estimation of the melting temperature (T_m) in the presence of 3.9 M GdmCl. This concentration value of GdmCl allows for a visualization of the denaturation curve from the folded to the unfolded state of the protein samples. The values of T_m at this concentration value of GdmCl are 73.2 and 79.2 °C for ArgBP and ArgBP with L-arginine, respectively.

3.3. Emission characteristics of Trp^{226}

From low temperature emission spectra analysis in glycerol/buffer glasses, it appears that the phosphorescence spectrum is well structured (Fig. 5A), which is indicative of homogeneity in the Trp environment. Although the $\lambda_{0,0}$ peak is at 407.2 nm, which is the same wavelength as free Trp in this solvent, the bandwidth (the width at half height) is relatively narrow (4.42 nm c.f. to 9.5 nm for solvent exposed Trp) implying that the indole ring is largely buried within the protein fold [26]. The spectrum of Trp^{226} is blue shifted for an internal residue, which are often located near moderately polar sites. These values are also possible if the ground state energy, $E(S_0)$, is lowered by attractive interactions with nearby charges.

As shown in Fig. 5A, the phosphorescence spectrum remains relatively well resolved in 5 mM phosphate buffer, pH 7.5 at 20 °C. Moreover, it undergoes to a limited red-shift upon thermal relaxation of the surrounding structure ($\lambda_{0,0}$ shifts from 407.2 to 409.9 nm c.f. to 414–416 nm for solvent exposed or flexible sites). This is consistent with a relatively ordered and rigid site, again confirming little if any exposure of the indole ring to the solvent. The fluorescence spectrum of the protein is peaked at 338 nm having relaxed from $F_{max} = 226$ nm in rigid glasses (Fig. 5B). The red-shift on thermal relaxation is significant but much less than expected for solvent exposed or flexible sites. Since a very small spectral shift would be expected upon structural relaxation for non-polar sites, we infer that the Trp environment of the protein is polar and rather rigid.

The phosphorescence decays in buffer are homogeneous, consistent with uniformity in the Trp environment/dynamical structure in the millisecond time scale. The lifetime is 8.4 ms at 0 °C and 3.4 ms at 20 °C. This τ is long with respect to a Trp exposed to the solvent but it is still short for an internal protein rigid site. The lifetime is indicative of a superficially buried Trp residue where the indole ring is not in direct contact with the aqueous

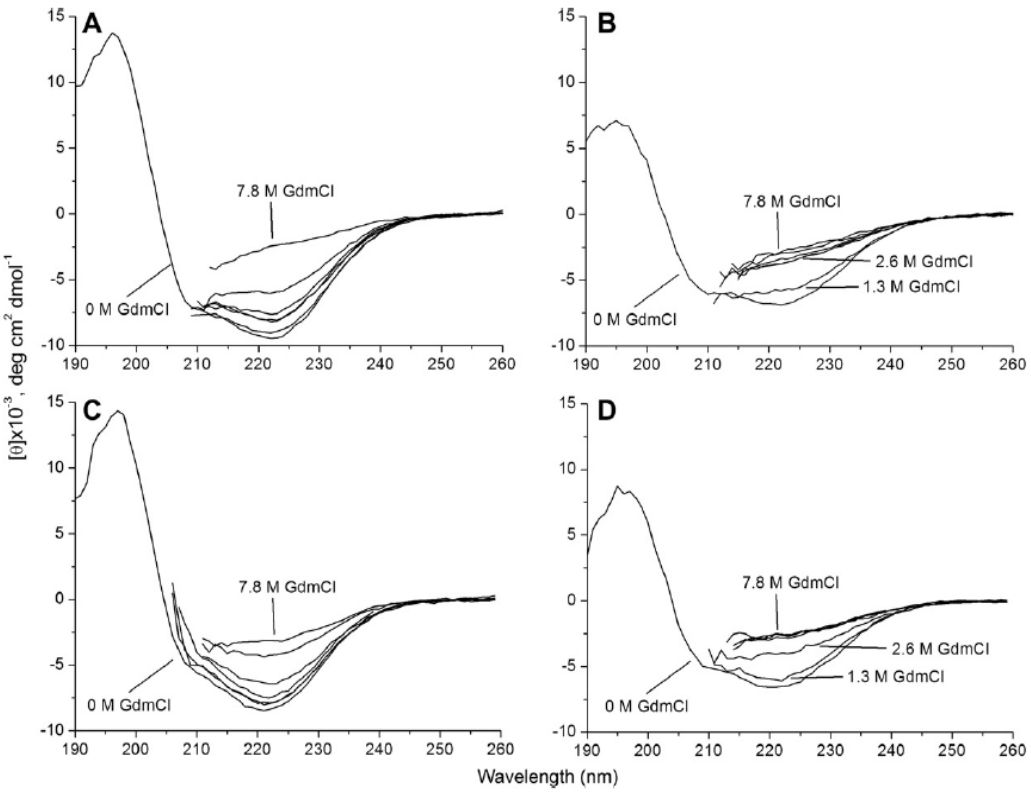

Fig. 3. Changes of far-UV CD spectra of TmArgBP in the absence and in the presence of L-arginine induced by increasing amount of GdmCl at 20 °C (panel A and C, respectively) and 95 °C (panel B and D, respectively). The protein solutions were at 0.1 mg/ml and L-arginine concentration was 0.6 mM while the GdmCl concentration was increased from 0 to 7.8 M with 1.3 M concentration increments. Spectra in the presence of GdmCl were recorded from 260 to 210 nm, cell path length was 1 mm.

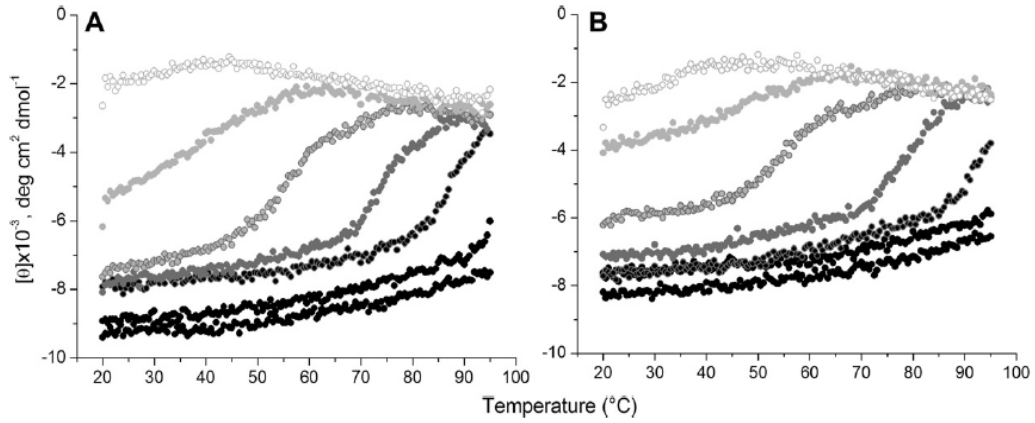

Fig. 4. Temperature dependence of ellipticity at 222 nm at pH 7.5 of TmArgBP (A), and TmArgBP with L-arginine (B), in the presence of different concentrations of GdmCl: grey scale of symbols is proportional to GdmCl concentration, from 0 M (black circles) to 7.8 M (white circles) with 1.3 M increments.

phase, but it is very near to it. This indicated that it can be effectively quenched by any quencher impurity in the solvent and/or by the His tail of the protein. It may be possible that the true intrinsic lifetime, which reflects the site flexibility [27], may be longer than the measured value.

We measured the effect of pH in the range between 5 and 10 on TmArgBP τ. At acid pH the TmArgBP τ decreases by 2–3-fold but there is little further variation above pH 7.5. Since His residues are stronger quenchers in the protonated state, it is possible that the τ reduction at acid pH is due to quenching by the protein His tag. However, the independence of τ on the protein concentration (reduced from 10 to 3 μM) suggests that the process is not intermolecular.

Quenching analysis of the protein Trp^{226} phosphorescence by acrylamide was performed. The gradient of the Stern–Volmer lifetime plot yields quenching rate constants of (1.02 and

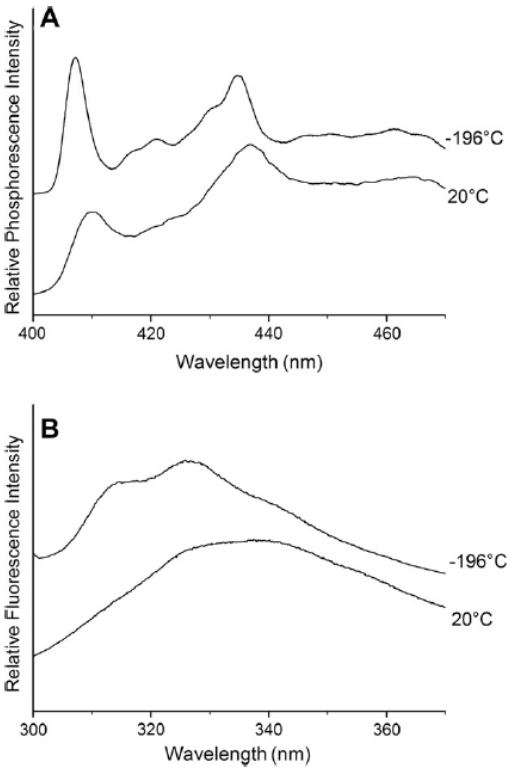

Fig. 5. Trp phosphorescence (panel A) and fluorescence (panel B) spectra of TmArgBP in a glycerol/buffer glass at −196 °C and in buffer at 20 °C. The protein concentration was 10 μM. Spectral intensities are offset for clarity.

1.77) × 10^8 $M^{-1}s^{-1}$, at 0 and 20 °C, respectively. This value is large indicating that Trp^{226} is readily accessible to acrylamide quenching (c.f. kq = 1.5 × 10^9 for NATA and 10^4–10^5 for the Trp of RNaseT1 and parvalbumin, which are buried 2–3 Å from the aqueous interface [28]). Hence, if Trp^{226} is not directly exposed to the solvent then it must be very near to it (<0.5 Å) in order for acrylamide quenching from the solvent be so efficient. In order to estimate the effect of the protein subunit dissociation in the Trp microenvironment, τ value in 4.0 M and 8.0 M urea was measured. It was found that there is a modest reduction of the protein lifetime. However, as the lifetime reduction is small and is observed also in 4 M urea, which is insufficient to dissociate the oligomer, it is important to consider that this lifetime shorting may be due to the presence of impurities present in urea solution.

Since no changes were observed in the protein fluorescence spectrum we can conclude that the region of Trp^{226} is not involved in the association of the subunits and also that monomer formation has no significant impact on the protein structure near the indolic residue.

None of the various spectroscopic features examined is detectably affected by L-arginine binding to the protein. This is a highly surprising result especially since the binding process involves a large structural rearrangement as the rotation-closing of the two domains. As evident in Fig. 6, no changes are present in phosphorescence (panel A) and fluorescence spectra (panel B) and in phosphorescence decay (panel C) in the absence and in the presence of L-arginine.

In our best knowledge, this is the first protein that does not report changes in phosphorescence emission upon ligand binding. This suggests that not only the binding site is far from Trp^{226} but

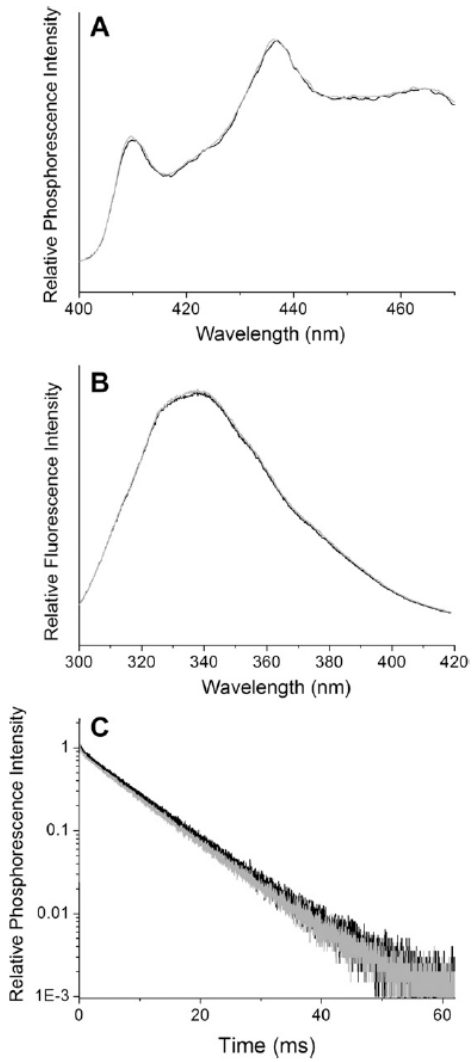

Fig. 6. Effect of L-arginine on Trp phosphorescence (panel A), fluorescence (panel B) and phosphorescence decay (panel C) at 20 °C. Black and grey curves represent TmArgBP in the absence and in the presence of L-arginine, respectively.

also that its local structure/dynamics is totally disconnected from the binding site region.

3.4. Analysis of Trp^{226} microenvironment by using the TmArgBP predicted structure

From the analysis of the interactions involving the Trp^{226} microenvironment and based on the predicted structure of TmArgBP [11], it is possible to notice the presence of stabilizing interactions between the carboxyl group of Asp^{39} facing the positive end of the Trp^{226} indole dipole (N1) (atomic length = 3.0 Å) and between the positive charge of Lys^{225} facing the negative end of the Trp^{226} dipole (C4–C5) (atomic length = 4.2 Å). In the closed form, it seems that the microenvironment of Trp^{226} does not undergo evident changes (Fig. 7) and the interaction distances remain roughly unvaried which is consistent with our hypothesis that the structural changes due to the adoption of the closed conformation does

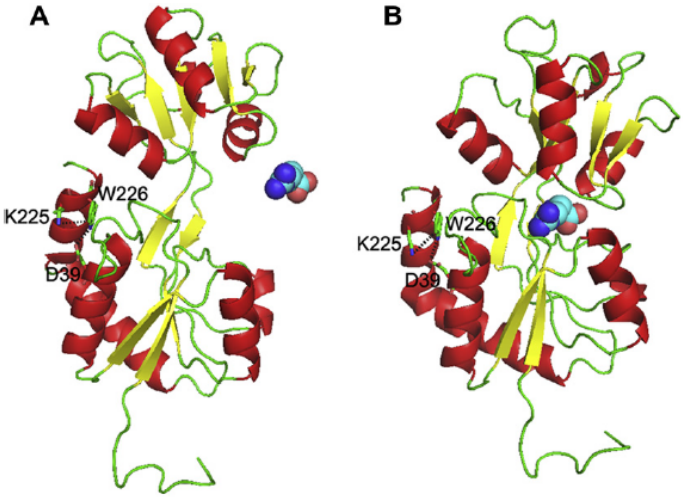

Fig. 7. 3D cartoon models of open (A), and closed (B) TmArgBP forms. Trp^{226} and amino acids which interact with Trp^{226} are displayed in sticks and labeled. L-arginine is displayed in spheres and the black dashed lines represent the amino acid distances. The PDB models were previously generated by Scire et al. [11] and displayed by PyMOL (version 1.1 eval) [32].

not involve Trp^{226} and its microenvironment. However, the different conformations of the open and closed forms could be used to detect the presence of L-arginine. Using the protein three-dimensional model, strategic amino acid residues could be mutated in order to make TmArgBP optically sensitive to the presence of L-arginine detectable by the presence of a new fluorescent intrinsic residue or by the introduction of an appropriate fluorescent probe that allows for the transduction of the ligand-binding event into a quantifiable optical signal variation.

In conclusion, TmArgBP was previously cloned, purified and partially characterized [11,12,29]. Some of its peculiar features investigated in this work such as the high specificity for the binding L-arginine and the extreme stability to high temperature could make this protein a perfect scaffold for the design of a new optical fluorescent biosensor for the detection of L-arginine [16,30].

In fact, a novel method for a fast real-time and continuous detection an of L-arginine in plasma, serum and urine would be of high interest to prevent the consequences of hyper-argininemia on health, especially in neonatal age [31].

4. Abbreviations

DSC	differential scanning calorimetry
TmArgBP	arginine-binding protein from *Thermotoga maritima*
GdmCl	guanidine hydrochloride
CD	circular dichroism

Acknowledgments

This work was in the frame of the CNR Commessa AGP05. The authors wish to thank Dr. Giovanni Strambini and Dr. Margherita Gonnelli for the phosphorescence measurements.

Appendix A. Supplementary material

Supplementary data associated with this article can be found, in the online version, at http://dx.doi.org/10.1016/j.jphotobiol.2012.11.004.

References

[1] G.F. Ames, Bacterial periplasmic transport systems: structure, mechanism, and evolution, Annu. Rev. Biochem. 55 (1986) 397–425.
[2] A.S. Ethayathulla, Y. Bessho, A. Shinkai, B. Padmanabhan, T.P. Singh, P. Kaur, S. Yokoyama, Purification, crystallization and preliminary X-ray diffraction analysis of the putative ABC transporter ATP-binding protein from *Thermotoga maritima*, Acta Crystallogr. Sect. F Struct. Biol. Cryst. Commun. 64 (2008) 498–500.
[3] C.F. Higgins, ABC transporters: from microorganisms to man, Annu. Rev. Cell Biol. 8 (1992) 67–113.
[4] R. Tam, M.H. Saier Jr., Structural, functional, and evolutionary relationships among extracellular solute-binding receptors of bacteria, Microbiol. Rev. 57 (1993) 320–346.
[5] A.L. Davidson, E. Dassa, C. Orelle, J. Chen, Structure, function, and evolution of bacterial ATP-binding cassette systems, Microbiol. Mol. Biol. Rev. 72 (2008) 317–364 (table of contents).
[6] M.J. Cuneo, A. Changela, A.E. Miklos, L.S. Beese, J.K. Krueger, H.W. Hellinga, Structural analysis of a periplasmic binding protein in the tripartite ATP-independent transporter family reveals a tetrameric assembly that may have a role in ligand transport, J. Biol. Chem. 283 (2008) 32812–32820.
[7] J.C. Pickup, F. Hussain, N.D. Evans, O.J. Rolinski, D.J. Birch, Fluorescence-based glucose sensors, Biosens. Bioelectron. 20 (2005) 2555–2565.
[8] D.E. Benson, D.W. Conrad, R.M. de Lorimier, S.A. Trammell, H.W. Hellinga, Design of bioelectronic interfaces by exploiting hinge-bending motions in proteins, Science 293 (2001) 1641–1644.
[9] U. Wissenbach, S. Six, J. Bongaerts, D. Ternes, S. Steinwachs, G. Unden, A third periplasmic transport system for L-arginine in *Escherichia coli*: molecular characterization of the artPIQMJ genes, arginine binding and transport, Mol. Microbiol. 17 (1995) 675–686.
[10] R. Huber, T.A. Langworthy, H. König, M. Thomm, C.R. Woese, U.B. Sleytr, K.O. Stetter, *Thermotoga maritima* sp. nov. represents a new genus of unique extremely thermophilic eubacteria growing up to 90 °C, Arch. Microbiol. 144 (1986) 324–333.
[11] A. Scire, A. Marabotti, M. Staiano, L. Iozzino, M.S. Luchansky, B.S. Der, J.D. Dattelbaum, F. Tanfani, S. D'Auria, Amino acid transport in thermophiles: characterization of an arginine-binding protein in *Thermotoga maritima*. 2. Molecular organization and structural stability, Mol. Biosyst. 6 (2010) 687–698.
[12] M.S. Luchansky, B.S. Der, S. D'Auria, G. Pocsfalvi, L. Iozzino, D. Marasco, J.D. Dattelbaum, Amino acid transport in thermophiles: characterization of an arginine-binding protein in *Thermotoga maritima*, Mol. Biosyst. 6 (2010) 142–151.
[13] S.W. Brusilov, A.L. Horwich, Urea cycle enzymes, in: C.R. Scriver, A.L. Beaudet, W.S. Sly, D. Valle (Eds.), The Metabolic Basis of Inherited Disease, McGraw-Hill, New York, 1989, pp. 629–663.
[14] H.W. Hellinga, J.S. Marvin, Protein engineering and the development of generic biosensors, Trends Biotechnol. 16 (1998) 183–189.
[15] O.V. Stepanenko, A.V. Fonin, K.S. Morozova, V.V. Verkhusha, I.M. Kuznetsova, K.K. Turoverov, M. Staiano, S. D'Auria, New insight in protein-ligand interactions. 2. Stability and properties of two mutant forms of the D-galactose/D-glucose-binding protein from *E. coli*, J. Phys. Chem. B 115 (2011) 9022–9032.

[16] Y. Tian, M.J. Cuneo, A. Changela, B. Hocker, L.S. Beese, H.W. Hellinga, Structure-based design of robust glucose biosensors using a *Thermotoga maritima* periplasmic glucose-binding protein, Protein Sci. 16 (2007) 2240–2250.
[17] V. Scognamiglio, M. Staiano, M. Rossi, S. D'Auria, Protein-based biosensors for diabetic patients, J. Fluoresc. 14 (2004) 491–498.
[18] G. Barone, P. Del Vecchio, D. Fessas, C. Giancola, G. Graziano, Theseus: a new software package for the handling and analysis of thermal denaturation data of biological macromolecules, J. Therm. Anal. 38 (1992) 2779–2790.
[19] S. D'Auria, R. Barone, M. Rossi, R. Nucci, G. Barone, D. Fessas, E. Bertoli, F. Tanfani, Effects of temperature and SDS on the structure of beta-glycosidase from the thermophilic archaeon *Sulfolobus solfataricus*, Biochem. J. 323 (Pt 3) (1997) 833–840.
[20] D. Fessas, S. Iametti, A. Schiraldi, F. Bonomi, Thermal unfolding of monomeric and dimeric beta-lactoglobulins, Eur. J. Biochem. 268 (2001) 5439–5448.
[21] W.H. Press, B.P. Flannery, S.A. Teukolsky, W.T. Vetterling, in: C.U. Press (Ed.), Numerical recipes: The art of scientific computing, Cambridge, UK, 1989, pp. 521–538.
[22] Y. Nozaki, The preparation of guanidine hydrochloride, Methods Enzymol. 26 PtC (1972) 43–50.
[23] G.B. Strambini, B.A. Kerwin, B.D. Mason, M. Gonnelli, The triplet-state lifetime of indole derivatives in aqueous solution, Photochem. Photobiol. 80 (2004) 462–470.
[24] P. Cioni, G.B. Strambini, Acrylamide quenching of protein phosphorescence as a monitor of structural fluctuations in the globular fold, J. Am. Chem. Soc. 120 (1998) 11749–11757.
[25] M.A. Andrade, P. Chacon, J.J. Merelo, F. Moran, Evaluation of secondary structure of proteins from UV circular dichroism spectra using an unsupervised learning neural network, Protein Eng. 6 (1993) 383–390.
[26] M.V. Hershberger, A.H. Maki, W.C. Galley, Phosphorescence and optically detected magnetic resonance studies of a class of anomalous tryptophan residues in globular proteins, Biochemistry 19 (1980) 2204–2209.
[27] M. Gonnelli, G.B. Strambini, Phosphorescence lifetime of tryptophan in proteins, Biochemistry 34 (1995) 13847–13857.
[28] G.B. Strambini, M. Gonnelli, Protein phosphorescence quenching: distinction between quencher penetration and external quenching mechanisms, J. Phys. Chem. B 114 (2010) 9691–9697.
[29] A. Ruggiero, J.D. Dattelbaum, A. Pennacchio, L. Iozzino, M. Staiano, M.S. Luchansky, B.S. Der, R. Berisio, S. D'Auria, L. Vitagliano, Crystallization and preliminary X-ray crystallographic analysis of ligand-free and arginine-bound forms of *Thermotoga maritima* arginine-binding protein, Acta Crystallogr. Sect. F Struct. Biol. Cryst. Commun. 67 (2011) 1462–1465.
[30] M. Strianese, M. Staiano, G. Ruggiero, T. Labella, C. Pellecchia, S. D'Auria, Fluorescence-based biosensors, Methods Mol. Biol. 875 (2012) 193–216.
[31] S. Jain-Ghai, S.C. Nagamani, S. Blaser, K. Siriwardena, A. Feigenbaum, Arginase I deficiency: severe infantile presentation with hyperammonemia: more common than reported?, Mol Genet. Metab. 104 (2011) 107–111.
[32] W. DeLano, The PyMOL Molecular Graphics System, in, DeLano Scientific LLC., Palo Alto, California, USA, 2008, pp. <http://www.pymol.org>.

Biochimie 99 (2014) 208–214

Contents lists available at ScienceDirect

Biochimie

journal homepage: www.elsevier.com/locate/biochi

Research paper

Tryptophan-scanning mutagenesis of the ligand binding pocket in *Thermotoga maritima* arginine-binding protein

Lindsay J. Deacon [a], Hilbert Billones [a], Anne A. Galyean [b], Teraya Donaldson [a], Anna Pennacchio [c], Luisa Iozzino [a,c], Sabato D'Auria [c], Jonathan D. Dattelbaum [a,*]

[a] Department of Chemistry, University of Richmond, Richmond, VA 23173, USA
[b] Department of Environmental Sciences and Engineering, University of North Carolina, Chapel Hill, NC 27599, USA
[c] Laboratory for Molecular Sensing, IBP-CNR, Via Pietro Castellino 111, 80131 Napoli, Italy

ARTICLE INFO

Article history:
Received 1 April 2013
Accepted 11 December 2013
Available online 25 December 2013

Keywords:
Periplasmic binding protein
Fluorescence
Tryptophan-scanning mutagenesis
Anisotropy decay
Asymmetric flow field flow fractionation

ABSTRACT

The *Thermotoga maritima* arginine binding protein (TmArgBP) is a member of the periplasmic binding protein superfamily. As a highly thermostable protein, TmArgBP has been investigated for the potential to serve as a protein scaffold for the development of fluorescent protein biosensors. To establish a relationship between structural dynamics and ligand binding capabilities, we constructed single tryptophan mutants to probe the arginine binding pocket. Trp residues placed around the binding pocket reveal a strong dependence on fluorescence emission of the protein with arginine for all but one of the mutants. Using these data, we calculated dissociation constants of 1.9–3.3 μM for arginine. Stern–Volmer quenching analysis demonstrated that the protein undergoes a large conformational change upon ligand binding, which is a common feature of this protein superfamily. While still active at room temperature, time-resolved intensity and anisotropy decay data suggest that the protein exists as a highly rigid structure under these conditions. Interestingly, TmArgBP exists as a dimer at room temperature in both the presence and absence of arginine, as determined by asymmetric flow field flow fractionation (AF4) and supported by native gel-electrophoresis and time-resolved anisotropy. Our data on dynamics and stability will contribute to our understanding of hyperthermophilic proteins and their potential biotechnological applications.

1. Introduction

The hyperthermophilic bacterium *Thermotoga maritima* encodes an arginine binding protein (TmArgBP) as part of a putative amino acid uptake system. This protein is a member of the periplasmic binding protein (PBP) superfamily and displays the stability characteristic of most *T. maritima* proteins. As part of the PBP family, TmArgBP maintains the common structural architectural features of a single polypeptide chain composed of upper and lower domains connected by a hinge region. Interaction between the protein and its binding partner allows a large hinge-bending conformational transition to occur. A number of fluorescence-based strategies exist to detect this large conformational change in response to ligand binding. Consequently, members of the PBP superfamily are widely studied as potential fluorescent protein biosensors for the analytical detection of small molecule targets. Mesophilic PBPs that bind glucose [1–5], ribose [6–8], glutamine [9–11], maltose [12–16], and phosphate [17–19], to name a few, have been exploited in various fluorescence-based assays to detect their respective ligands for both in vivo and in vitro applications [20,21]. While this group of proteins is generally stable, particularly in the presence of ligand, the addition of multiple mutations to optimize the dynamic range for ligand sensitivity often has deleterious effects on protein stability. The ability to tune the range of concentrations over which a protein can detect ligand is a long-standing goal of this community.

To overcome this challenge, many groups are turning to the thermostable PBP homologs found in hyperthermophilic bacteria. These proteins may provide both the desired level of sensitivity as well as an increase in stability making multiple-scale mutagenesis an easier task. A recently discovered representative of this group is the TmArgBP which binds arginine (K_D = ~20 μM) and displays stability in the presence of high levels of chemical denaturants, as

Abbreviations: TmArgBP, *Thermotoga maritima* arginine binding protein; PBP, periplasmic binding protein; SLIM, site-directed ligase-independent mutagenesis; TCSPC, time correlated single photon counting; AF4, asymmetric flow field flow fractionation; QELS, quasi-elastic light scattering.

* Corresponding author. Tel.: +1 804 484 1587.
E-mail address: jdattelb@richmond.edu (J.D. Dattelbaum).

0300-9084/$ – see front matter © 2013 Elsevier Masson SAS. All rights reserved.
http://dx.doi.org/10.1016/j.biochi.2013.12.011

well as high temperatures [22,23]. TmArgBP is a potential candidate for the development of a protein-based fluorescent biosensor for continuous detection of serum arginine, which is an important marker of hyperargininemia. This autosomal recessive disorder of the urea cycle results from a deficiency in the enzyme arginase causing a build-up of arginine and ammonia in the blood [24]. In this study, we investigate the specific nature of arginine binding within the binding pocket of TmArgBP. Initial X-ray crystallographic data for this protein [25], as well as the production of several well-defined homology models [22,23] was used to construct a series of single tryptophan mutants within the binding pocket which serve as intrinsic fluorescent reporters. Because this amino acid displays strong spectral sensitivity to environmental factors, such as polarity and rotational motion, this probe will relay information about ligand binding and the resulting conformational alterations in TmArgBP in order to provide an initial analysis for the development of an arginine biosensor.

2. Materials and methods

2.1. Cloning and site-directed mutagenesis

The gene for the wild-type TmArgBP minus the signal sequence was cloned into the *NdeI-BamHI* restriction sites of pET21a as previously described [22]. A C-terminal 6xHis tag was added in-frame to provide for streamlined purification using metal affinity chromatography. Single Trp mutants of TmArgBP were created using site-directed ligase-independent (SLIM) mutagenesis protocols as previously described [26]. All mutants were confirmed by sequencing at the Nucleic Acids Research Facility at Virginia Commonwealth University.

2.2. Protein preparation

Protein was expressed from freshly transformed $CaCl_2$ competent *Escherichia coli* Rosetta cells (Novagen). Single colonies were incubated overnight at 37 °C with shaking in Terrific Broth containing ampicillin (100 μg/mL) and chloramphenicol (30 μg/mL). Fresh media was inoculated 1:100 from the overnight cultures and grown at 37 °C for approximately 3 h to an $OD_{600} \approx 0.6$. Cells were induced with IPTG (0.2 mM) for an additional 3 h, and then collected by centrifugation (3500 rpm, 10 min), re-suspended in 30 mL lysis buffer (50 mM phosphate, pH 8.0, 200 mM NaCl, 10 mM imidazole), and frozen at least overnight at −20 °C. Cells were thawed at room temperature, lysed by sonication and the TmArgBP was purified using Ni-NTA column chromatography. The protein concentration was determined by UV absorbance at 280 nm using 14,400 M^{-1} cm^{-1} as a predicted extinction coefficient [27]. It is essential to remove any arginine bound to the protein following purification. Extensive dialysis of the isolated protein was performed against 5 mM phosphate buffer for 5 days with twice daily buffer changes. Purification of proteins of the correct molecular weight was confirmed using SDS-PAGE and MALDI-TOF mass spectrometry (not shown).

2.3. Steady state Trp fluorescence

Tryptophan fluorescence emission spectra (uncorrected) were obtained with a Varian Cary Eclipse spectrofluorometer using excitation at 280 nm and 295 nm. Binding of TmArgBP single Trp mutants (1 μM) to increasing concentrations of arginine was performed in 5 mM phosphate buffer, pH 7.0 at room temperature. Data were fit to the Langmuir single binding isotherm using the nonlinear curve fitting functions in the Origin 7.0 software package as previously described [20]. Quenching of tryptophan emission at 325 nm was carried out using purified TmArgBP (3 μM) containing increasing concentrations of NaI (0–0.4 M) in phosphate buffer with NaCl added to achieve a consistent ionic strength of 0.5 M. To prevent iodine formation, 1 mM $Na_2S_2O_3$ was added. The data were analyzed using the Stern–Volmer equation: $F/F_0 = 1 + K_{sv}[Q]$, where K_{sv} is the Stern–Volmer quenching constant, Q is the concentration of quencher, and F and F_0 are the Trp emission intensities in the presence and absence of quencher, respectively. All measurements were performed at room temperature unless otherwise stated.

2.4. Time-resolved Trp fluorescence

Fluorescence lifetime and anisotropy decay data were obtained with an ISS Chronos time-resolved fluorometer equipped with Glan–Thompson polarizers and a micro-channel plate detector. Pulsed LED excitation at 280 nm was used to excite the single Trp mutant proteins. For determination of fluorescence lifetimes, excitation and emission polarizers were set to magic angle conditions (0° and 54.7°, respectively). Utilizing the software package provided by ISS, data were analyzed using a multi-exponential decay model $I(t) = \sum \alpha_i e^{-t/\tau_i}$, where α_i represent the pre-exponential factors of each lifetime component, τ_i. These values are used to determine the fractional intensity values, $f_i = \alpha_i\tau_i / \sum \alpha_i\tau_I$, which were used to calculate the intensity weighted average ($\overline{\tau}$) lifetime using $\overline{\tau} = \sum f_i\tau_i$. For determination of anisotropy decays parameters, data were fit to the exponential decay model $r(t) = r_o e^{-t/\theta}$, where r_o is the time anisotropy that would be observed in the absence of diffusion and θ is the associated rotational correlation time.

2.5. Asymmetric flow field flow fractionation

Asymmetric flow field flow fractionation (AF4) was performed using a Wyatt Technologies Eclipse DualTec separation controlled instrument with OpenLab CDS Chem Station edition software. Injections were made with an Agilent 1260 Infinity series isopump and autosampler. Phosphate buffered saline (PBS) at pH 7.4 (Sigma) was used for all experiments and was degassed with a Gastorr TG-14 at 100 hPa directly from solvent bottles and filtered in series by a polytetrafluoroethylene frit (RESTEK) and a 0.1 μm Durapore membrane filter (Millipore). Separation was performed using a Wyatt Technologies HF5 cartridge (Superon) containing a 400 μM polyethersulfone hollow fiber with a 10 kDa cutoff, an injector flow of 0.2 mL/min, a detector flow of 0.35 mL/min, a focus flow of 0.5 mL/min, and a cross flow of 0.5 mL/min. Quasi-elastic light scattering (QELS) measurements were made with a Wyatt Technologies Dawn Heleos-II at detector 16 (140°) coupled with an Optilab T-rEX refractive index (RI) detector. TmArgBP samples (0.2 mg/mL) were run in amber glass vials with PTFE/silicone septa (Chemglass Life Sciences). For the ligand bound experiments, identical settings were utilized with the addition of 100 μM arginine to sample and buffer. Data were collected and analyzed with Astra Software version 6.1.1.17.

3. Results and discussion

3.1. Effect of arginine on TmArgBP Trp steady state fluorescence

A single Trp residue (W224) in the wild-type protein is located near the C-terminal end of the protein and does not appear to interact with the arginine binding site. In a previous study, we showed that the wild-type Trp residue does not display any changes to fluorescence emission maximum upon arginine binding. To begin this study, a W224Y mutant was prepared to remove the

wild-type Trp residue. This new gene was used as a starting background for preparing all single Trp mutant constructs.

An initial TmArgBP structure has been proposed using the strong homology among PBP family members, particularly the *E. coli* glutamine binding protein (Fig. 1) [23]. Experimental support for the structure of TmArgBP in the arginine free and bound states by X-ray crystallographic data analysis is on-going [25]. Amino acids within the binding pocket (G75, M76, and T127) were selected based on their proximity to the bound arginine without disrupting any potential contacts between protein and ligand. Additionally, based on strong homology to other PBPs, two sites in the hinge region (Q97 and V98) were also selected to report on the well-documented twist-bending motion common to this family of proteins in response to ligand binding. All proteins were expressed and purified as described in the Materials and Methods section, and the proper folding of each mutant was confirmed by far-UV CD spectroscopy (see Supplemental data).

Representative fluorescence emission spectra in the absence and in the presence of increasing concentrations of arginine (0–20 μM) are shown in Fig. 2. The three single Trp residues within the binding pocket (G75, M76, and T127) show an increase in emission intensity upon the addition of arginine (Table 1). G75W displays the largest increase in arginine-dependent emission (64%) along with an approximately 23 nm red-shift. This is an unusual outcome since typically for Trp emission a red-shift in the emission spectra is indicative of a more polar microenvironment and results in a lower emission yield. It would seem that there are large electronic effects as well for this mutant position. In contrast, Trp residues found in the hinge region show a small decrease in fluorescence intensity (Q97W) or display no change in emission properties (V98W).

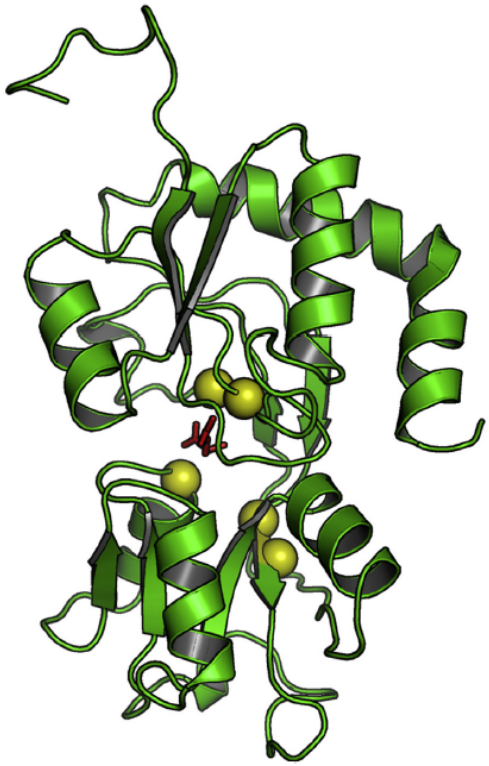

Fig. 1. Homology model of TmArgBP [23] in the presence and absence of arginine drawn using PyMOL [41]. Spheres indicate positions of the single Trp residues.

The fluorescence emission intensity values obtained from the titration data presented in Fig. 2 can be fit to a single binding isotherm to determine an apparent K_d for each mutant as previously described [20]. Based on the analysis of the data for these mutants (Fig. 2, inset), TmArgBP binds with high affinity to arginine (Table 1). A K_d in the 1–3 μM range is a value that is consistent with most PBP family members. Estimations of the dissociation constant (K_d) for arginine interactions with wild-type TmArgBP were previously determined to be approximately 20 μM [22]. This difference in binding constant is not surprising since the previous data using surface plasmon resonance employed a peptide containing an N-terminal arginine residue which may have altered the binding thermodynamics and decreased the apparent affinity for arginine.

3.2. Fluorescence Trp lifetime data

The fluorescence lifetime of each single Trp TmArgBP mutant in the presence and absence of arginine was determined using time-correlated single photon counting (Table 2). As described in the Material and Methods section, the data were collected and analyzed using the software package included with the ISS Chronos spectrofluorometer. While some mutants exhibited multi-exponential decay, most of the single Trp-containing proteins were well represented by a single fluorescence lifetime component. Additionally, the intensity average lifetime values ($\bar{\tau}$) show very little change in the presence of arginine. A notable exception to this trend is for G75W, which displayed a two-fold increase in the average lifetime upon the addition of arginine. This reinforces the unusual microenvironment surrounding this Trp residue resulting in a red-shift with a concomitant increase in steady state Trp emission intensity above (Fig. 2).

The use of multi-exponential decay analysis of Trp lifetime assumes that the protein is in a single conformation [28], and even single Trp residues found in most proteins can have extremely complex decay profiles [29]. The presence of relatively simple exponential decay properties of the TmArgBP mutants may be due to the rigid nature of thermophilic proteins at room temperature, which is well below the optimal range for *T. maritima*. The Trp lifetimes measured for the mutant TmArgBPs are high when compared to single Trp proteins from mesophilic organisms [30]. However, our values are consistent with previously reported data on the *Thermococcus litoralis* trehalose/maltose binding protein, which also found single Trp lifetimes ranging from 6.5 ns to 9.41 ns at 25 °C [31]. Their analysis of a similar hyperthermophilic binding protein used frequency-domain intensity decay measurements thus likely ruling out any artifacts that may have been due to our single photon counting ISS instrument. The relatively rigid nature imposed on this thermophilic protein when functioning at room temperature may produce a single conformation for arginine-free and arginine-bound TmArgBP structures.

3.3. Stern–Volmer quenching

The fluorescence emission and lifetime data support our model that arginine binds to TmArgBP Trp mutants. To confirm that TmArgBP undergoes the characteristic hinge-bending motion common to PBP family members, we used iodide quenching of Trp emission to calculate the Stern–Volmer quenching constants (K_{SV}) as well as the bimolecular quenching constant k_q (Table 1). The values of k_q observed in this study are well below the maximum value that may be calculated for a surface exposed Trp residue of approximately $4 \times 10^9\ M^{-1}\ s^{-1}$ being quenched by iodide in solution [32]. The data for two of the mutant proteins are shown in

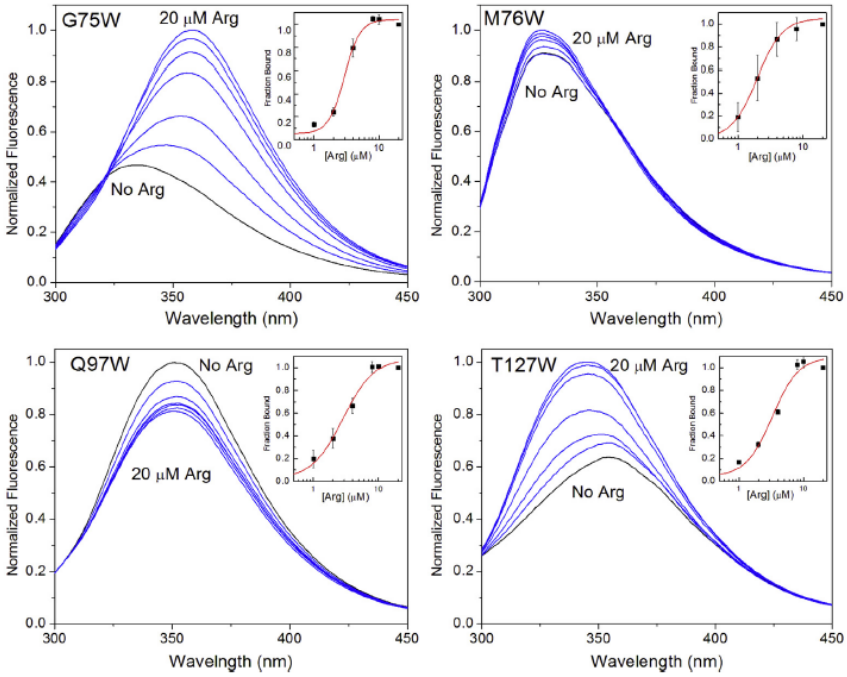

Fig. 2. Representative fluorescence spectral data for single Trp mutants of TmArgBP upon the addition of increasing concentrations of arginine. Insets show the binding data average of 3 trials.

Fig. 3. Q97W is found in the hinge region and displays an almost 3-fold increase in K_{SV} upon the addition of arginine. Additionally, the value for k_q can be seen to increase by a similar amount. This indicates that there is significantly more access to the hinge region following addition of arginine, which is consistent with a hinge-bending motion by TmArgBP. In contrast, T127W is located near the entrance to the arginine binding pocket in our model (Fig. 4). In this case the value of K_{SV} undergoes a sharp decrease in the presence of arginine indicating almost complete occlusion of Trp127 following ligand binding. When fluorescence lifetime effects are taken into account, the k_q remains over 10 fold lower in the presence of arginine compared to the ligand-free state (Table 2). Taken together these data provide further support that position 127 is near the arginine binding pocket and is almost completely shielded from water following a large, arginine-dependent conformational change.

Table 1
Steady state fluorescence data for TmArgBP single Trp mutants.

TmArgBP mutant	%ΔF[a]	Em max no Arg (nm)	$K_{a\ (\mu M)}$	K_{SV} − arg (M)	K_{SV} + arg (M)	k_q[b] ($\times 10^8$ M^{-1} s^{-1})
WT[c]	NC	320	23 ± 4	0.48	0.69	
G75W	+64	333[d]	2.9 ± 0.2	0.32	0.33	0.78/0.37
M76W	+12	325	1.9 ± 0.3	0.49	0.22	1.2/0.49
Q97W	−23	351	2.8 ± 0.4	0.60	1.68	0.83/2.7
V98W	NC	345	–	1.49	1.72	2.4/2.7
T127W	+38	354[e]	3.3 ± 0.6	0.91	0.05	1.3/0.052

[a] Fluorescence change calculated from $(I_{bound} - I_{free})/I_{bound} \times 100\%$.
[b] Values for bimolecular quenching constants ($K_{sv}/\bar{\tau}$) are listed for the absence/presence of arginine.
[c] Data from Ref. [22].
[d] Emission max shifts to 355 nm with Arg.
[e] Emission max shifts to 344 nm with Arg.

3.4. TmArgBP forms a multimer at room temperature

Time-resolved fluorescence anisotropy decays provide information on the hydrodynamic nature of a protein [30]. For an intrinsic fluorophore like Trp, information can usually be obtained in three areas: 1) the rotational motion of the entire protein, 2) the dynamic movement of the loop where the probe is located, and 3) information about the rotational fluctuations around the covalent bond attaching the probe to the protein. In this study, we wanted to see if the local movement of Trp residues inserted near the TmArgBP binding site could provide functional information about arginine binding.

We measured the anisotropy decay of each single Trp mutant in the presence and absence of arginine (Table 3). While many anisotropy decay profiles require three exponents to accurately fit the data, here we achieved optimal fits to a single rotational correlation time for all mutants. Rotational correlation times were calculated to range from 16.9 to 30.5 ns for each mutant. This value

Table 2
Time resolved intensity decay data for TmArgBP single Trp mutants.

TmArgBP mutant	τ_1 (ns)	τ_2 (ns)	f_1	f_2	$\bar{\tau}$ (ns)	χ^2_R
G75W	1.51	4.46	0.13	0.87	4.08	1.07
G75W + arg	8.90		1.0		8.90	0.99
M76W	4.20		1.0		4.20	0.88
M76W + arg	4.48		1.0		4.48	1.09
Q97W	2.00	7.55	0.06	0.94	7.22	0.98
Q97W + arg	0.66	6.53	0.07	0.93	6.12	1.20
V98W	6.10		1.0		6.10	1.11
V98W + arg	6.30		1.0		6.30	1.10
T127W	7.11		1.0		7.11	1.07
T127W + arg	9.48		1.0		9.48	1.00

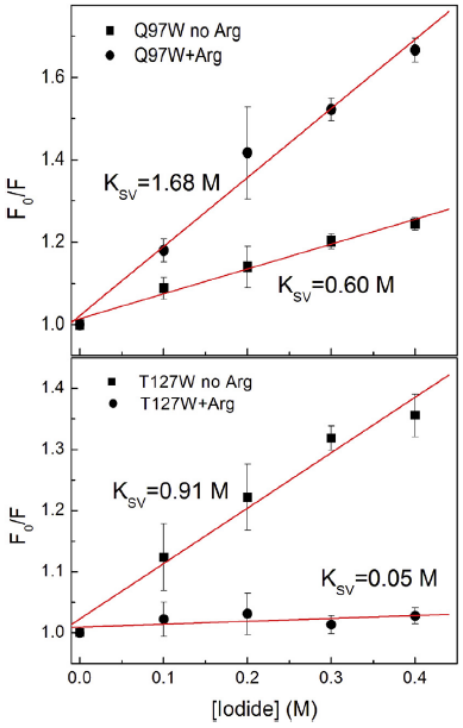

Fig. 3. Stern–Volmer quenching plots of Q97W (top) and T127W (bottom) single Trp mutants of TmArgBP. The data represent an average of three independent iodide quenching experiments.

does not seem to vary much with the addition of arginine or with the different probe locations around the binding pocket or hinge region. For a 27.7 kDa protein acting like an anhydrous sphere in solution, a theoretical rotational correlation time of 10.5 ns can be calculated according to $\theta = nM/RT$, where n is the viscosity, M is the protein molecular weight, R is the ideal gas constant, and T is temperature [30]. The observed correlation time of approximately

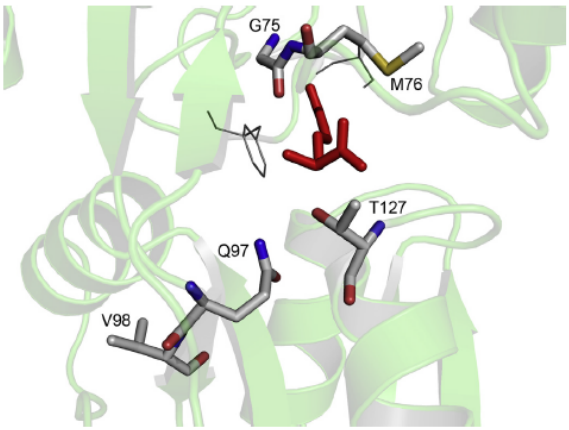

Fig. 4. TmArgBP binding pocket. Amino acids mutated to Trp in this study are shown as sticks and arginine is shown in red.

Table 3
Time resolved anisotropy decay data for TmArgBP single Trp mutants.

TmArgBP mutant	θ (ns)	r_0	χ^2_R
G75W	21.4	0.14	1.12
G75W + arg	16.9	0.12	1.06
M76W	28.9	0.16	2.58
M76W + arg	26.3	0.16	1.14
Q97W	30.5	0.11	1.29
Q97W + arg	22.3	0.12	1.68
V98W	23.2	0.12	1.20
V98W + arg	21.2	0.12	1.20
T127W	20.2	0.11	1.33
T127W + arg	26.9	0.12	1.18

20 ns is two-fold higher than the calculated value, which suggests that the protein exists as a dimer in the presence and absence of arginine. The observed rotational correlation time most likely represents the dynamic motion of the entire homodimeric protein. We do not detect additional shorter rotational correlation time components, which would have represented local probe or segmental movements within the protein. In contrast, previous anisotropy decay data collected for the *E. coli* glutamine binding protein, which has significant homology to TmArgBP, showed both long (16.1 ns) and short (1.0 ns) rotational correlation times at 25 °C [33]. Placement of the Trp residues around the binding pocket does not affect our ability to detect these shorter time scale motions that would normally be expected for a typical mesophilic protein.

Because most of the PBPs examined to date exist as a monomer in solution, we wanted to further examine and confirm the ability of this protein to dimerize. Upon purification of the TmArgBPs, SDS-PAGE and MALDI-TOF data (not shown) confirmed the presence of a single protein of approximately 27.8 kDa for all mutants. We performed native gel electrophoresis on the single Trp TmArgBP mutants in the presence and absence of arginine (see Supplemental data). Four of the mutants displayed a strong protein band at approximately 55 kDa indicative of the formation of a homodimer. In all cases, the presence of the dimer was not dependent on the concentration of the protein.

To conclusively determine if TmArgBP exists as a dimer, we performed asymmetric flow field flow fractionation (AF4) with quasi-elastic light scattering (QELS) (Fig. 5). QELS determined the molar mass of TmArgBP both with and without arginine as a function of time as the protein elutes from the AF4 channel. QELS, through measurement of time-dependent fluctuations of scattered light, establishes the weight-averaged molar mass of material eluting in each fractionated slice from the AF4. These measured values are used together with concentration measurements from the online RI detector to calculate the molar mass moments. This method clearly demonstrated the presence of two dominant species corresponding to the dimer and tetramer forms of TmArgBP. There was no significant difference in the molar mass measurements or distribution with the addition of arginine (not shown). While most mesophilic PBPs exist as monomers, there is increasing evidence in the literature suggesting that hyperthermophilic PBPs from *T. maritima* prefer to multimerize under the experimental conditions used here and by others [6,34]. Taken together with our quenching experimental results, these data are consistent with TmArgBP consisting of 2 identical subunits existing as a rigid macromolecule at room temperature, which may be a consequence of high thermophilic stability for this protein.

4. Conclusion

The PBP superfamily has great potential in the development of sensitive and specific biological assay systems [35,36]. In particular,

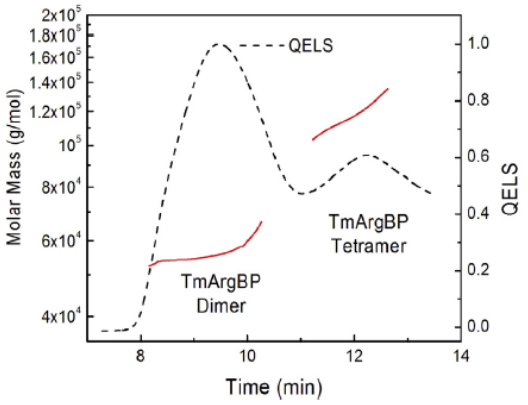

Fig. 5. Asymmetric flow field flow fraction (AF4) of TmArgBP. The dashed line indicates the quasi-elastic light scattering (QELS) signal, while the solid lines indicate the weight-averaged molar mass associated with each peak.

there is a great need for receptor proteins that are chemically well-characterized and are expressed in high yield. There is a large amount of interest in protein scaffolds that meet this criteria to serve as antibody mimics, for example ankyrin repeat proteins [37], lipocalins [38], knottins [39], and defensins [40] to name a few. In this report, we increased our knowledge about arginine binding to a recently identified, thermophilic arginine binding protein [22]. Using a variety of fluorescence spectroscopic techniques, we demonstrated that the protein binds arginine at room temperature and undergoes the large conformational changes consistent with other PBP family members. Several amino acid positions around the binding pocket or in the hinge region were utilized in a fluorescence detection system for arginine binding. The time-resolved analysis of single Trp mutants of TmArgBP demonstrated that the protein is a rigid structure in either the open or closed conformation. Interestingly, we demonstrated that this protein exists primarily as a dimer at room temperature. More data will be needed to determine if the observed dimerization is an artifact of performing the measurements at room temperature and to identify the origin of the specific dimerization domain. While these experiments provide spectroscopic information about arginine binding, future experiments will investigate the locations identified in this study for the covalent attachment of external probes that fluoresce in the visible region, which is better suited for biosensor development. Within the binding pocket (Fig. 4) Ser16 and Phe19 are potential sites for mutagenesis as well; however, based on their proximity to arginine they likely form direct interactions and may alter the binding specificity of TmArgBP. Additionally, because normal plasma concentrations of arginine range from 72 μM to 115 μM, the high binding affinity of this protein will need to be altered via mutagenesis of the binding pocket, or the test samples will be quantitatively diluted about 100 fold. While TmArgBP may be utilized as a potential biosensor for arginine, the protein also exhibits a large increase in stability, which may be advantageous to the useful application of TmArgBP as a protein scaffold for additional biotechnology applications.

Acknowledgments

The authors would like to thank the University of Richmond School of Arts and Sciences for funding of research materials and student summer stipends to support this work.

Appendix A. Supplementary data

Supplementary data related to this article can be found at http://dx.doi.org/10.1016/j.biochi.2013.12.011.

References

[1] J. Siegrist, T. Kazarian, C.M. Ensor, J. Smita, M. Madou, P. Wang, S. Daunert, Continuous glucose sensor using novel genetically engineered binding polypeptides towards in vivo applications, Sens. Actuators B 149 (2010) 51–58.
[2] S. D'Auria, F. Alfieri, M. Staiano, P. Mosè, M. Rossi, A. Scire, F. Tanfani, E. Bertoli, Z. Gryczynyski, J.R. Lakowicz, Structural and thermal stability characterization of *Escherichia coli* D-galactose/D-glucose-binding protein, Biotechnol. Prog. 20 (2004) 330–337.
[3] B.S. Der, J.D. Dattelbaum, Construction of a reagentless glucose biosensor using molecular exciton luminescence, Anal. Biochem. 375 (2008) 132–140.
[4] X. Ge, L. Tolosa, G. Rao, Dual-labeled glucose binding protein for ratiometric measurements of glucose, Anal. Chem. 76 (2004) 1403–1410.
[5] F. Khan, I. Gunudi, J.C. Pickup, Fluorescence-based sensing of glucose using engineered glucose/galactose-binding protein: a comparison of fluorescence resonance energy transfer and environmentally sensitive dye labeling strategies, Biochem. Biophys. Res. Commun. 365 (2008) 102–106.
[6] M.J. Cuneo, L.S. Beese, H.W. Hellinga, Ligand-induced conformational changes in a thermophilic ribose-binding protein, BMC Struct. Biol. 8 (2008) 50.
[7] I. Lager, M. Fehr, W.B. Frommer, S. Lalonde, Development of a fluorescent nanosensor for ribose, FEBS Lett. 533 (2003) 85–89.
[8] N.C. Vercillo, K.J. Herald, J.F. Fox, B.S. Der, J.D. Dattelbaum, Analysis of ligand binding to a ribose biosensor using site-directed mutagenesis and fluorescence spectroscopy, Protein Sci. 16 (2007) 362–368.
[9] S. D'Auria, A. Scire, A. Varriale, V. Scognamiglio, M. Staiano, A. Ausili, A. Marabotti, M. Rossi, F. Tanfani, Binding of glutamine to glutamine-binding protein from *Escherichia coli* induces changes in protein structure and increases protein stability, Proteins Struct. Funct. Bioinf. 58 (2005) 80–87.
[10] J.D. Dattelbaum, J.R. Lakowicz, Optical determination of glutamine using a genetically engineered protein, Anal. Biochem. 291 (2001) 89–95.
[11] L. Tolosa, X. Ge, G. Rao, Reagentless optical sensing of glutamine using a dual-emitting glutamine-binding protein, Anal. Biochem. 314 (2003) 199–205.
[12] A.M. Dattelbaum, G.A. Baker, J.F. Fox, S. Iyer, J.D. Dattelbaum, PEGylation of a maltose biosensor promotes enhanced signal response when immobilized in a silica sol–gel, Bioconjugate Chem. 20 (2009) 2381–2384.
[13] J.D. Dattelbaum, L.L. Looger, D.E. Benson, K.M. Sali, R.B. Thompson, H.W. Hellinga, Analysis of allosteric signal transduction mechanisms in an engineered fluorescent maltose biosensor, Protein Sci. 14 (2005) 284–291.
[14] M. Fehr, W.B. Frommer, S. Lalonde, Visualization of maltose uptake in living yeast cells by fluorescent nanosensors, Proc. Natl. Acad. Sci. U. S. A. 99 (2002) 9846–9851.
[15] G. Gilardi, L.Q. Zhou, L. Hibbert, A.E. Cass, Engineering the maltose binding protein for reagentless fluorescence sensing, Anal. Chem. 66 (1994) 3840–3847.
[16] J.S. Marvin, E.E. Corcoran, N.A. Hattangadi, J.V. Zhang, S.A. Gere, H.W. Hellinga, The rational design of allosteric interactions in a monomeric protein and its applications to the construction of biosensors, Proc. Natl. Acad. Sci. 94 (1997) 4366–4371.
[17] M. Brune, J.L. Hunter, J.E.T. Corrie, M.R. Webb, Direct, real-time measurement of rapid inorganic phosphate release using a novel fluorescent probe and its application to actomyosin subfragment ATPase, Biochemistry 33 (1994) 8262–8271.
[18] M.P. Okoh, J.L. Hunter, J.E. Corrie, M.R. Webb, A biosensor for inorganic phosphate using a rhodamine-labeled phosphate binding protein, Biochemistry 45 (2006) 14764–14771.
[19] L.L. Salins, S.K. Deo, S. Daunert, Phosphate binding protein as the biorecognition element in a biosensor for phosphate, Sens. Actuators B Chem. 97 (2004) 81–89.
[20] J.D. Dattelbaum, Genetically engineered proteins as recognition receptors, in: M. Zourob (Ed.), Recognition Receptors in Biosensors, Springer, New York, 2009.
[21] R.M. deLorimier, J.J. Smith, M.A. Dwyer, L.L. Looger, K.M. Sali, C.D. Paavola, S.S. Rizk, S. Sadigov, D.W. Conrad, L. Loew, H.W. Hellinga, Construction of a fluorescent biosensor family, Protein Sci. 11 (2002) 2655–2675.
[22] M.S. Luchansky, B.S. Der, S. D'Auria, G. Pocsfalvi, L. Iozzino, D. Marasco, J.D. Dattelbaum, Amino acid transport in thermophiles: characterization of an arginine-binding protein in *Thermotoga maritima*, Mol. BioSyst. 6 (2010) 132–141.
[23] A. Scire, A. Marabotti, M. Staiano, L. Iozzino, M.S. Luchansky, B.S. Der, J.D. Dattelbaum, F. Tanfani, S. D'Auria, Amino acid transport in thermophiles: characterization of an arginine-binding protein in *Thermotoga maritima*. 2. molecular organization and structural stability, Mol. BioSyst. 6 (2010) 687–698.
[24] S.W. Brusilow, A.L. Horwich, Urea cycle enzymes, in: C.R. Scriver, A.L. Beaudet, W.S. Sly, D. Valle (Eds.), The Metabolic Basis of Inherited Disease, McGraw-Hill, New York, 1989, pp. 629–663.
[25] A. Ruggiero, J.D. Dattelbaum, A. Pennacchio, L. Iozzino, M. Staiano, M.S. Luchansky, B.S. Der, R. Berisio, S. D'Auria, L. Vitagliano, Crystallization and preliminary X-ray crystallographic analysis of ligand-free and arginine-bound forms of *Thermotoga maritima* arginine-binding protein, Acta Crystallogr. F67 (2011) 1462–1465.

[26] J. Chiu, D. Tillett, I.W. Dawes, P.E. March, Site-directed, ligase-independent mutagenesis (SLIM) for highly efficient mutagenesis of plasmids greater than 8kb, J. Microbiol. Methods 73 (2008) 195–198.
[27] E. Gasteiger, C. Hoogland, A. Gattiker, S. Duvaud, M.R. Wilkins, R.D. Appel, A. Bairoch, Protein identification and analysis tools on the ExPASy server, in: J.M. Walker (Ed.), The Proteomics Protocols Handbook, Humana Press, 2005, pp. 571–607.
[28] J.M. Beechem, L. Brand, Time-resolved fluorescence of proteins, Annu. Rev. Biochem. 54 (1985) 43–71.
[29] J.A. Ross, D.M. Jameson, Time-resolved methods in biophysics 8. Frequency domain fluorometry: applications to intrinsic protein fluorescence, Photochem. Photobiol. Sci. 7 (2008) 1301–1312.
[30] J.R. Lakowicz, Principles of Fluorescence Spectroscopy, Springer, New York, 2006, p. 698.
[31] P. Herman, M. Staiano, A. Marabotti, A. Varriale, A. Scirè, F. Tanfani, J. Vecer, M. Rossi, S. D'Auria, D-Trehalsoe/D-maltose-binding protein from the hyperthermophilic archaeon *Thermococcus litoralis*: the binding of trehalose and maltose results in different protein conformational states, Proteins Struct. Funct. Bioinf. 63 (2006).
[32] M. Eftink, Fluorescence quenching, in: J.R. Lakowicz (Ed.), Topics in Fluorescence Spectroscopy, Plenum Press, New York, 1991.
[33] P. Herman, J. Vecer, V. Scognamiglio, M. Staiano, M. Rossi, S. D'Auria, A recombinant glutamine-binding protein from *Escherichia coli*: effect of ligand-binding on protein conformational dynamics, Biotechnol. Prog. 20 (2004) 1847–1854.
[34] M.J. Cuneo, A. Changela, A.E. Miklos, L.S. Beese, J.K. Krueger, H.W. Hellinga, Structural analysis of a periplasmic binding protein in the tripartite ATP-independent transporter family reveals a tetrameric assembly that may have a role in ligand transport, J. Biol. Chem. 283 (2008) 32812–32820.
[35] M.A. Dwyer, H.W. Hellinga, Periplasmic binding proteins: a versatile superfamily for protein engineering, Curr. Opin. Struct. Biol. 14 (2004) 495–504.
[36] E.A. Moschou, L.G. Bachas, S. Daunert, S.K. Deo, Binding proteins: unraveling their analytical potential, Anal. Chem. 78 (2006) 6693–6700.
[37] P. Parizek, L. Kummer, P. Rube, A. Prinz, F.W. Herberg, A. Pluckthun, Designed ankyrin repeat proteins (DARPins) as novel isoform-specific intracellular inhibitors of c-Jun n-terminal kinases, Chemical Biology 7 (2010) 1356–1366.
[38] J. Liu, B. Ninq, M. Liu, Y. Sun, Z. Sun, Y. Zhange, X. Fan, Z. Zhou, Z. Gao, Construction of ribosome display library based on lipocalin scaffold and screening anticalins with specificity for estradiol, Analyst 137 (2012) 2470–2479.
[39] J.A. Getz, J.J. Rice, P.S. Daugherty, Protease-resistant peptide ligands from a knottin scaffold library, Chem. Biol. 6 (2011) 837–844.
[40] N. Antcheva, F. Morgera, L. Creatti, L. Vaccari, U. Pag, S. Pacor, Y. Shai, H.-G. Sahl, A. Tossi, Artificial β-defensin based on a minimal defensin template, Biochem. J. 421 (2009) 435–447.
[41] W.L. DeLano, The PyMOL Molecular Graphics System, Delano Scientific, San Carlos, CA, 2002.

Acta Crystallographica Section F
Structural Biology and Crystallization Communications
ISSN 1744-3091

Alessia Ruggiero,[a]* Jonathan D. Dattelbaum,[b] Anna Pennacchio,[c] Luisa Iozzino,[c] Maria Staiano,[c] Matthew S. Luchansky,[b] Bryan S. Der,[b] Rita Berisio,[a] Sabato D'Auria[c] and Luigi Vitagliano[a]*

[a]Institute of Biostructures and Bioimaging, CNR, Via Mezzocannone 16, I-80134 Naples, Italy, [b]Department of Chemistry, University of Richmond, Richmond, VA 23173, USA, and [c]Laboratory for Molecular Sensing, IBP–CNR, Naples, Italy

Correspondence e-mail: alessia.ruggiero@unina.it, luigi.vitagliano@unina.it

Received 22 July 2011
Accepted 13 September 2011

Crystallization and preliminary X-ray crystallographic analysis of ligand-free and arginine-bound forms of *Thermotoga maritima* arginine-binding protein

The arginine-binding protein from *Thermotoga maritima* (TmArgBP) is an arginine-binding component of the ATP-binding cassette (ABC) transport system in this hyperthermophilic bacterium. This protein is endowed with an extraordinary stability towards thermal and chemical denaturation. Its structural characterization may provide useful insights for the clarification of structure–stability relationships and for the design of new biosensors. Crystallization trials were set up for both arginine-bound and ligand-free forms of TmArgBP and crystals suitable for crystallographic investigations were obtained for both forms. Ordered crystals of the arginine adduct of TmArgBP could only be obtained by using the detergent LDAO as an additive to the crystallization medium. These crystals were hexagonal, with unit-cell parameters a = 78.2, c = 434.7 Å, and diffracted to 2.7 Å resolution. The crystals of the ligand-free form were orthorhombic, with unit-cell parameters a = 51.8, b = 91.9, c = 117.9 Å, and diffracted to 2.25 Å resolution.

1. Introduction

In many living organisms, the passage of small ligands through the cell membrane is mediated by complex macromolecular assemblies named ATP-binding cassettes (ABCs; Higgins, 1992; Oldham *et al.*, 2008). ABC transport systems constitute a large superfamily of proteins which couple the hydrolysis of ATP to the passage of metabolites through the cell membrane (Ethayathulla *et al.*, 2008). The expressed ABC transporters consist of two transmembrane domains and two ATP-binding domains for the transportation of a specific ligand across the membrane. In Gram-negative bacteria, each transporter relies on a soluble periplasmic binding protein (PBP) that is capable of interacting with a specific ligand essential for metabolic and nutrient gathering (Davidson *et al.*, 2008; Nanavati *et al.*, 2005). The PBPs associated with ABC transport systems are of remarkable interest for the development of protein-based biosensors (de Lorimier *et al.*, 2002; Marvin *et al.*, 1997). Indeed, owing to the variety of their binding specificities, they are currently utilized as designated platforms for fluorescent protein biosensors for many naturally occurring ligands (sugars, anions, amino acids *etc.*; Tolosa *et al.*, 1999). Moreover, re-engineering the binding site of these proteins as a designed scaffold may significantly expand the number of small-molecule analytes for which sensors may be generated. In this framework, it is evident that proteins isolated from thermophilic organisms possess added intrinsic value in the design of new biosensing technologies that require enhanced stability.

Recently, we characterized a PBP that is involved in the amino-acid transport system of *Thermotoga maritima* (Luchansky *et al.*, 2010; Scirè *et al.*, 2010). Integrated biochemical and biophysical characterization of this protein (hereafter referred to as TmArgBP) has shown that it is an arginine-binding protein that is endowed with remarkable structural stability even under strongly denaturating conditions. Indeed, the native protein could not be denatured when

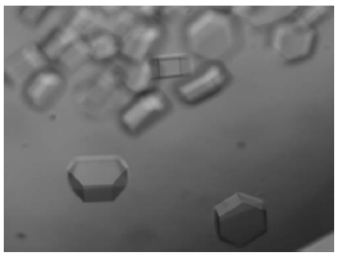

Table 1
Data-collection parameters and data-processing statistics.

Values in parentheses are for the highest resolution shell.

	HoloTmArgBP	ApoTmArgBP
Radiation source	Beamline X12, EMBL/DESY	In-house rotating anode
Wavelength (Å)	1.000	1.5418
Crystal-to-detector distance (mm)	260	55
Oscillation angle per frame (°)	0.10	0.50
Crystal symmetry and presumed space group	Hexagonal, *P*622	Orthorhombic, $P2_12_12_1$
Unit-cell parameters (Å)	$a = 78.2$, $b = 78.2$, $c = 434.7$	$a = 51.8$, $b = 91.9$, $c = 117.9$
Resolution (Å)	50.0–2.70 (2.80–2.70)	50.0–2.25 (2.33–2.25)
Mean multiplicity	3.2	4.7
Completeness (%)	94.0 (79.7)	89.7 (85.5)
Total reflections	68279	115134
Unique reflections	21612	24691
R_{merge}†	0.124 (0.356)	0.126 (0.242)
Mean $I/\sigma(I)$	11.6 (2.7)	14.0 (5.2)

† $R_{merge} = \sum_{hkl}\sum_i |I_i(hkl) - \langle I(hkl)\rangle| / \sum_{hkl}\sum_i I_i(hkl)$, where $I_i(hkl)$ is the intensity of the *i*th measurement of reflection *hkl* and $\langle I(hkl)\rangle$ is the mean value of the intensity of reflection *hkl*.

heated to 373 K. Moreover, it is quite stable (T_m of 351 K) even when treated with 6.0 *M* guanidinium hydrochloride. On this basis, it has been suggested that this ultrastable protein has the potential to be exploited for the generation of durable and highly specific sensors for arginine. The structural characterization of TmArgBP at the atomic level will therefore be extremely useful for potential biotechnological applications of this protein and for elucidation of the determinants of its exceptional stability. Moreover, structural studies will also provide useful insights into the interfaces involved in the mixture of oligomeric states (homodimers and homotrimers) detected for TmArgBP. Here, we report the crystallization and preliminary crystallographic investigations of TmArgBP.

2. Experimental methods

2.1. Cloning, expression and purification

In previous characterizations of TmArgBP, a construct presenting an extension of 22 residues at the C-terminus, including a 6×His-tag motif, was used. To increase the crystallizability of the protein, a new construct was prepared by the insertion of a stop codon that removes this C-terminal extension. This construct, which was also deprived of the signal sequence for perisplasmic export of the protein, corresponds to the region 20–246 (227 residues) of the protein sequence (UniProt code Q9WZ62). This sequence region was cloned into the *Nde*I–*Bam*HI site of a pET21a vector. The resulting positive plasmid was used to transform Rosetta(DE3)pLysS competent cells. Expression of the protein was carried out using the transformed cells, which were grown overnight at 310 K in LB containing 50 µg ml^{-1} kanamycin and 30 µg ml^{-1} chloramphenicol. When an OD_{600} of 0.6 was reached, the cells were induced for 3 h with 0.5 m*M* IPTG.

The absence of the 6×His affinity tag from the present TmArgBP construct required some modifications of the protein-purification protocol. The cells were resuspended in 20 m*M* Tris–HCl buffer pH 8.0 containing a protease-inhibitor cocktail (Roche Diagnostic) and sonicated. The cell debris was removed by centrifugation at 18 000 rev min^{-1} for 40 min. The protein supernatant was initially purified by thermoprecipitation (343 K water bath for 30 min). The heat-denatured proteins were removed by centrifugation. The soluble protein extract was loaded onto a 5 ml Resource Q column (Pharmacia) equilibrated with Tris buffer pH 8.0. After washing with ten volumes of buffer, a linear gradient of NaCl (0–500 m*M*) was applied to elute the protein. The fractions containing TmArgBP were pooled and dialyzed against a buffer consisting of 20 m*M* Tris–HCl pH 8.0, 150 m*M* NaCl at 277 K. After dialysis, the protein was concentrated for further purification by size-exclusion chromatography on Superdex 200 (GE Healthcare; 50 m*M* Tris–HCl, 150 m*M* NaCl pH 8.0). The homogeneity of the protein was evaluated by SDS–PAGE analysis. The molecular mass of the purified protein (25 270 Da) was checked by mass spectrometry and no proteolysis of the protein was detected.

2.2. Crystallization experiments

Crystallization trials were performed at 293 K using the hanging-drop vapour-diffusion method. A preliminary screening for crystallization conditions was carried out using commercially available sparse-matrix kits (Crystal Screen, Crystal Screen 2 and Index from Hampton Research; Jancarik & Kim, 1991). Optimization of the crystallization conditions was performed by fine-tuning the protein and precipitant concentrations and by the use of crystallization additives (Additive Screen from Hampton Research; McPherson *et al.*, 2011).

2.3. Data collection and processing

Preliminary diffraction data for both the apo and holo forms of TmArgBP were collected in-house at 100 K using a Rigaku MicroMax-007 HF generator producing Cu $K\alpha$ radiation and equipped with a Saturn944 CCD detector. This equipment was also used for

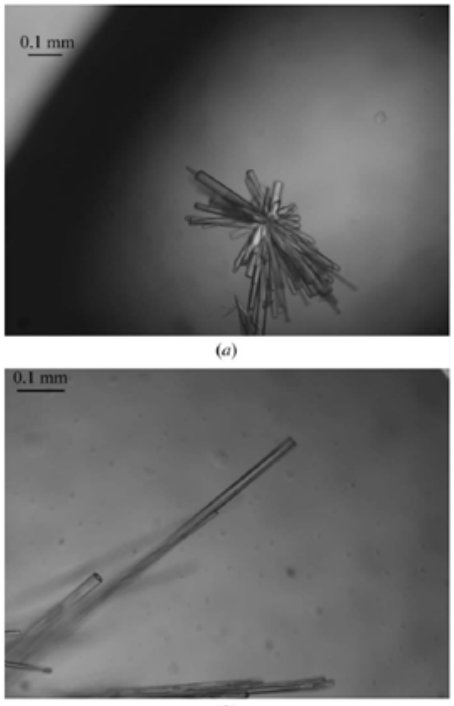

Figure 1
(*a*) Crystals of HoloTmArgBP grown in 17%(*w*/*v*) PEG 10 000, 0.1 *M* bis-tris pH 5.5, 0.1 *M* ammonium acetate. The crystals shown in (*b*) were grown under the same conditions with the addition of LDAO detergent [0.5%(*v*/*v*)].

the collection of the diffraction data from the apo form. Data were collected at 100 K from crystals cryoprotected by adding a solution of 14%(*v*/*v*) ethylene glycol to the precipitating solution. Diffraction data for the holo form of TmArgBP were collected on the X12 synchrotron beamline at the DORIS storage ring, DESY (Hamburg, Germany) using a MAR225 CCD detector at 100 K from crystals cryoprotected by adding 14%(*v*/*v*) ethylene glycol to the precipitating solution. The diffraction data were collected using a small rotation angle of 0.1° and a crystal-to-detector distance of 260 mm owing to the long *c* axis.

All data sets were scaled and merged using the *HKL*-2000 program package (Otwinowski & Minor, 1997). Statistics of data collection are reported in Table 1.

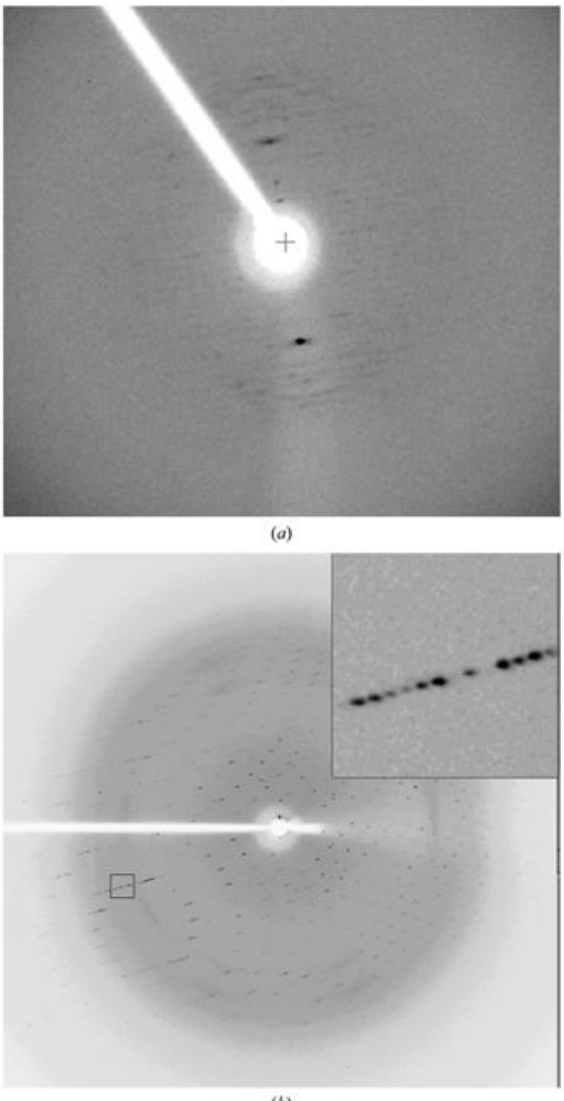

(*a*)

(*b*)

Figure 2
Diffraction patterns of HoloTmArgBP crystals obtained in the absence (*a*) or in the presence (*b*) of the additive LDAO.

3. Results and discussion

Previous characterizations of TmArgBP have clearly indicated that the protein purifies as a complex with arginine. Analysis of the thermal stability of the TmArgBP sample obtained using the purification procedure adopted here demonstrates that it also corresponds to the arginine-bound complex (HoloTmArgBP). The protein does not unfold in aqueous solutions when heated to 373 K. Thermal denaturation was observed at 351 K when 6.0 *M* guanidinium hydrochloride was added to the solution, in line with previous analyses carried out on the arginine-bound complex.

An initial screening of commercially available solutions provided promising crystallization conditions for HoloTmArgBP in the presence of PEG 10 000 as a precipitant. The size and morphology of the HoloTmArgBP crystals were improved by fine-tuning the concentrations of the protein and the precipitating agent. Crystals that were suitable for diffraction experiments were obtained using vapour-diffusion techniques and a protein concentration of 20–25 mg ml^{-1}. The composition of the reservoir solution was 17%(*w*/*v*) PEG 10 000, 0.1 *M* ammonium acetate, 0.1 *M* bis-tris buffer pH 5.5. Despite their good morphology (Fig. 1*a*), these crystals were highly disordered, as shown by their fibre-like diffraction pattern (Fig. 2*a*). In order to improve the quality of these crystals, a number of additives were added to the crystallization drops. Long rod-shaped crystals (0.05 × 0.1 × 0.6 mm) were obtained using 0.5%(*w*/*v*) *n*-dodecyl-*N*,*N*-dimethylamine-*N*-oxide (LDAO) as an additive (Fig. 1*b*). These crystals reached their optimal size in 1 d. Analysis of the diffraction pattern exhibited by these new crystals clearly indicated that the additive greatly improved the crystal quality (Fig. 2*b*). Indexing of the

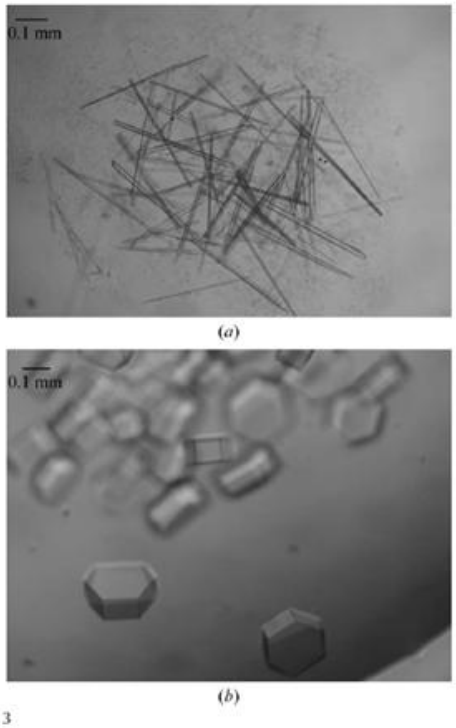

(*a*)

(*b*)

Figure 3
Crystals of ApoTmArgBP grown in the presence of (*a*) 20%(*w*/*v*) PEG 3350, 0.1 *M* HEPES pH 7.5, 0.15 *M* ammonium acetate and (*b*) 20%(*w*/*v*) PEG MME 2000, 0.1 *M* Tris–HCl pH 8.5, 0.2 *M* trimethylamine *N*-oxide dihydrate.

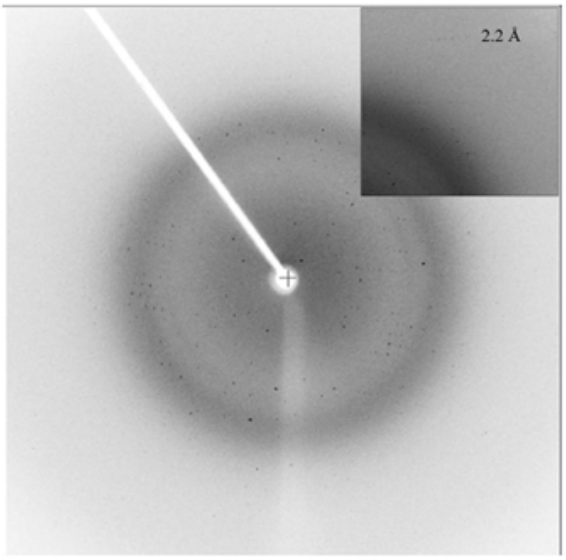

Figure 4
Diffraction pattern of ApoTmArgBP crystals grown in 20%(*w*/*v*) PEG 3350, 0.1 *M* HEPES pH 7.5, 0.15 *M* ammonium acetate.

diffraction pattern demonstrated that these crystals present a very long unit-cell axis (~435 Å; Fig. 2*b* and Table 1). To avoid overlaps of diffraction spots, a long crystal-to-detector distance (260 mm) was used for data collection. Moreover, although the long axis of the crystal was almost parallel to the spindle axis, we prudently used a small oscillation range (0.1°). The crystals presented a primitive hexagonal symmetry. Statistics of data processing and scaling are reported in Table 1, assuming space group *P*622. Matthews coefficient calculations (Matthews, 1968) suggest the presence of either three (V_M = 2.5 Å^3 Da^{-1}, 51% solvent content) or four (V_M = 1.9 Å^3 Da^{-1}, 35% solvent content) molecules per asymmetric unit.

The apo form of the protein (ApoTmArgBP) was prepared using the procedure reported by Luchansky *et al.* (2010). Briefly, the protein was incubated with 6.0 *M* guanidinium hydrochloride under dialysis for 3 d. The denaturant was removed by dialysis (Luchansky *et al.*, 2010) against a solution consisting of 20 m*M* Tris–HCl, 150 m*M* NaCl pH 8.0. The melting temperature (336 K) of this protein sample in 6.0 *M* guanidinium hydrochloride was virtually identical to that exhibited by the apo form in previous studies (Luchansky *et al.*, 2010). Crystallization screenings performed using commercial kits led to the identification of several promising crystallization conditions. Crystals suitable for X-ray diffraction testing were obtained using either 20%(*w*/*v*) PEG 3350, 0.1 *M* HEPES pH 7.5, 0.15 *M* ammonium acetate or 20%(*w*/*v*) PEG MME 2000, 0.1 *M* Tris–HCl pH 8.5, 0.2 *M* trimethylamine *N*-oxide dihydrate (Figs. 3*a* and 3*b*) as precipitating solutions. In both cases the protein concentration was in the range 15–20 mg ml^{-1}. The crystals obtained from the solution containing PEG MME 2000 displayed a poor diffraction pattern (lower than 6 Å resolution) despite their good morphology (Fig. 3*b*). In contrast, the crystals obtained using PEG 3350 as precipitant proved to be suitable for crystallographic data collection (Fig. 4). These crystals reached their optimal size within one week. The crystals were orthorhombic, with unit-cell parameters *a* = 51.8, *b* = 91.9, *c* = 117.9 Å, and diffracted to 2.25 Å resolution (Table 1). Matthews coefficient calculations suggested the presence of two molecules (V_M = 2.8 Å^3 Da^{-1}, 56% solvent content) per asymmetric unit (Matthews, 1968).

Attempts to solve the structures of both the apo and holo forms of the protein are in progress. In particular, models of ArgBP isolated from *Salmonella typhimurium* (Stamp *et al.*, 2011) and *Geobacillus stearothermophilus* (Vahedi-Faridi *et al.*, 2008), which share ~37% sequence identity with TmArgBP, are being used in the trials. As molecular-replacement trials may be complicated by the large unit cell of the holo form and by the intrinsic flexibility of amino-acid-binding proteins in their ligand-free state, selenomethionine derivatives of TmArgBP are being prepared.

This work was funded by the MIUR (FIRB Contract No. RBRN07BMCT). We acknowledge the staff of beamline X12 at EMBL/DESY (Hamburg, Germany) for providing the synchrotron-radiation facilities and for valuable assistance during data collection. We also thank Ms Flavia Squeglia for her help during sample preparation.

References

Davidson, A. L., Dassa, E., Orelle, C. & Chen, J. (2008). *Microbiol. Mol. Biol. Rev.* **72**, 317–364.
Ethayathulla, A. S., Bessho, Y., Shinkai, A., Padmanabhan, B., Singh, T. P., Kaur, P. & Yokoyama, S. (2008). *Acta Cryst.* F**64**, 498–500.
Higgins, C. F. (1992). *Annu. Rev. Cell Biol.* **8**, 67–113.
Jancarik, J. & Kim, S.-H. (1991). *J. Appl. Cryst.* **24**, 409–411.
Lorimier, R. M. de, Smith, J. J., Dwyer, M. A., Looger, L. L., Sali, K. M., Paavola, C. D., Rizk, S. S., Sadigov, S., Conrad, D. W., Loew, L. & Hellinga, H. W. (2002). *Protein Sci.* **11**, 2655–2675.
Luchansky, M. S., Der, B. S., D'Auria, S., Pocsfalvi, G., Iozzino, L., Marasco, D. & Dattelbaum, J. D. (2010). *Mol. Biosyst.* **6**, 142–151.
Marvin, J. S., Corcoran, E. E., Hattangadi, N. A., Zhang, J. V., Gere, S. A. & Hellinga, H. W. (1997). *Proc. Natl Acad. Sci. USA*, **94**, 4366–4371.
Matthews, B. W. (1968). *J. Mol. Biol.* **33**, 491–497.
McPherson, A., Nguyen, C., Cudney, R. & Larson, S. B. (2011). *Cryst. Growth Des.* **11**, 1469–1474.
Nanavati, D. M., Nguyen, T. N. & Noll, K. M. (2005). *J. Bacteriol.* **187**, 2002–2009.
Oldham, M. L., Davidson, A. L. & Chen, J. (2008). *Curr. Opin. Struct. Biol.* **18**, 726–733.
Otwinowski, Z. & Minor, W. (1997). *Methods Enzymol.* **276**, 307–326.
Scirè, A., Marabotti, A., Staiano, M., Iozzino, L., Luchansky, M. S., Der, B. S., Dattelbaum, J. D., Tanfani, F. & D'Auria, S. (2010). *Mol. Biosyst.* **6**, 687–698.
Stamp, A. L., Owen, P., El Omari, K., Lockyer, M., Lamb, H. K., Charles, I. G., Hawkins, A. R. & Stammers, D. K. (2011). *Proteins*, **79**, 2352–2357.
Tolosa, L., Gryczynski, I., Eichhorn, L. R., Dattelbaum, J. D., Castellano, F. N., Rao, G. & Lakowicz, J. R. (1999). *Anal. Biochem.* **267**, 114–120.
Vahedi-Faridi, A., Eckey, V., Scheffel, F., Alings, C., Landmesser, H., Schneider, E. & Saenger, W. (2008). *J. Mol. Biol.* **375**, 448–459.

Analytical Methods

Dynamic Article Links

Cite this: *Anal. Methods*, 2012, **4**, 4187

www.rsc.org/methods

PAPER

A new competitive fluorescence immunoassay for detection of *Listeria monocytogenes*

Stéphane Beauchamp,[a] Sabato D'Auria,*[b] Anna Pennacchio[b] and Monique Lacroix[a]

Received 5th September 2012, Accepted 13th October 2012
DOI: 10.1039/c2ay25997d

A new competitive immunoassay has been designed using a specific monoclonal antibody labeled with a fluorophore. A specific and highly conserved peptide of 11 amino acids from the protein p60 of *L. monocytogenes* has been synthesised and used for the production of a monoclonal anti-p60. This antibody was used in the conception of a detection test able to detect 1 CFU of *L. monocytogenes* after only 18 hours of incubation with a minimum of manipulation. The test is based on a competition principle between the recombinant p60 protein and the p60 from *L. monocytogenes* present in the sample. A column containing a sepharose matrix was used to immobilize the recombinant p60 protein and the labeled monoclonal antibody, which is captured by the p60 from the sample when added to the column. An increase of the fluorescence signal of the eluate means a positive result. No cross-reactivity was observed with non-pathogenic *Listeria* species and each serotype of *L. monocytogenes* can be detected whereas some other immunological methods show cross-reactivity and false negative.

Introduction

Listeria monocytogenes is an important foodborne pathogen involved in several outbreaks around the world resulting in considerable economic and human losses. Its widespread presence in the environment and its persistence in food plants lead to a labored control of this microorganism. *L. monocytogenes* is a Gram-positive, rod-shaped facultative anaerobic bacterium. This microbe can grow in a wide range of temperatures (1 °C to 45 °C) between pH 4.6 and 9.5 and at a water activity as low as 0.92.[1] It finds favorable growth conditions on floors, drains and equipment within food industry premises, notably in the cold and wet atmosphere of refrigerated rooms where only psychrotrophic bacteria can survive.[2] In a review published in 2004, few studies are mentioned in which persistence of *L. monocytogenes* is demonstrated.[3] Refrigerated and ready-to-eat foods constitute thereby a potential risk for contamination.[4,5] To counter cross-contamination, the control of the environment by detecting the bacteria on the working surfaces and instruments could be an important tool. Several well-known outbreaks and food recalls due to *L. monocytogenes*[6–9] combined with the high case-fatality rate of 20–30% (ref. 10) have increased the need for more rapid, sensitive, and specific methods for detection of this bacterium not only in food, but also in the working environment.

L. monocytogenes is a widespread microorganism that can be readily isolated from a number of sources, such as soil, water, meat, and vegetables.[11,12] Thus, the bacterium can easily be introduced in the human food chain and it becomes difficult to avoid contamination. Many reliable and accurate culture methods and media have been already developed for the detection of *L. monocytogenes.*[13,14] However, these methods remain laborious, time-consuming and involve complicated procedures.[15–19] Some standard methods for the detection of *L. monocytogenes* can require up to 7 days to yield results, as they rely on the ability of microorganisms to multiply to visible colonies.[13] Existing DNA detection based methods are also expensive.

To overcome the difficulty of recovering *L. monocytogenes* in the presence of non-pathogenic *Listeria* species and increase the sensitivity of the detection, several PCR-based methods have been developed. These PCR methods[14,18–20] provide sensitive, specific, and reproducible detection of pathogenic bacteria. Despite showing valuable advantages, the fact remains that the limitations of applying PCR techniques cannot be disregarded. Among them, there is the presence of inhibitory substances,[21,22] complexity of matrices, sample preparation and DNA extraction procedures.[14,23] Moreover, from an industrial point of view, routine detection of microbes using PCR can be expensive as it requires specialized equipment and qualified workers to carry out the tests. On the other hand, methods based on antigen–antibody bindings constitute a good alternative for detection of foodborne pathogens. The field of immunology-based methods provides very powerful analytical tools for a wide range of targets

[a]*Research Laboratories in Sciences Applied to Food, Canadian Irradiation Center, Institute of Nutraceutical and Functional Foods (INAF), INRS-Institut Armand-Frappier, 531 Boulevard des Prairies, Laval, Québec H7V 1B7, Canada*
[b]*Laboratory for Molecular Sensing, IBP-CNR, Via Pietro Castellino 111, 80131 Naples, Italy. E-mail: s.dauria@ibp.cnr.it; Fax: +39-0816132277; Tel: +39-0816132250*

including bacterial cells, spores, viruses and toxins.[24] Only for *L. monocytogenes*, few immunology-based methods already exist.[25–34] Various antibody types and formats are available for immune-detection. These include conventional and heavy chain antibodies, as well as polyclonal, monoclonal or recombinant antibodies. While polyclonal antibodies are limited both in terms of their specificity and abundance, monoclonal antibodies are often more useful for specific detection because they provide an indefinite supply of single antibodies directed against a single and unique epitope. The progress of hybridoma techniques and the emergence of the recombinant antibody phage display technology have led to more sensitive, specific, reproducible and reliable immunological detection with many commercial immunoassays adapted for a variety of microbes and their products.[35]

The protein p60 of *L. monocytogenes*, which is encoded by the *iap* (invasion-associated protein) gene, is considered an important virulence factor, although the exact role of the protein is not completely known.[36,37] Mutants of *L. monocytogenes*, which impair synthesis of p60, show a rough-colony morphology (R mutants) and are strikingly attenuated in virulence in mice. These mutants have also lost the capability of invading 3T6 mouse fibroblasts and form particularly long cell chains. Treatment of these mutants with partially purified p60 from wild-type *L. monocytogenes* restores their invasiveness and cell morphology.

The p60 protein could be a potential target for immunological detection because of its high abundance in the culture supernatant and high immunogenicity.[31,38] Nevertheless, it has been shown that an antiserum raised against the whole p60 is not appropriate for specific detection of *L. monocytogenes*, since cross-reactivity occurred with p60-related proteins in the culture supernatant of all *Listeria* species.[39] For this reason, the production of antibodies using p60 protein should be directed against an epitope, which is specific to *L. monocytogenes*. Many attempts have been made to produce *Listeria*-specific antibodies, but in most cases the potential was limited by the cross-reactivity with non-pathogen *Listeria* species or by the non-recognition of certain *L. monocytogenes* strains, which is not suitable for specific immunodetection.[40] In a previous work, a short hydrophilic peptide of eleven amino acids (QQQTAPKAPTE) namely PepD has been identified within the p60 protein to be a highly conserved region specific to all *L. monocytogenes* strains.[39] The polyclonal antibodies raised against this peptide showed a highly specific recognition for the p60 protein of all stains of *L. monocytogenes* tested and no cross-reactivity with non-pathogen *Listeria* spp. The results of this experiment allow us to consider this small peptide a good target for the development of an immune-detection test. However, due to the possible low titers of the polyclonal antibodies, a large amount of the precipitated protein was necessary to perform the analysis. Moreover, from a standpoint of a manufacturer producing a detection test using these antibodies, the repeated production of enough polyclonal antibodies may be demanding. Considering all of these limitations, the production of a monoclonal antibody using the same peptide of eleven amino acids specific to the p60 of *L. monocytogenes* was chosen. The aim of this study was to develop a competitive fluorescence immunoassay for the detection of *L. monocytogenes* using a p60 monoclonal antibody of *L. monocytogenes*.

Material and methods

Synthetic peptide, monoclonal antibody and recombinant P60 production

The peptide synthesis and the production of the anti-P60 monoclonal antibody were carried out by the company GenScript USA Inc., NJ, USA. First, the antigenic peptide PepD (QQQTAPKAPTE) derived from p60 of *L. monocytogenes* (accession number AEO02672 in the NCBI protein database) was synthesized by stepwise solid-phase peptide synthesis (SPPS) with an additional N-terminal cysteine residue for coupling.[38] Synthetic peptide was purified by reverse-phase HPLC and coupled *via* the SH group of the N-terminal cysteine residue to the keyhole limpet hemocyanin (KLH) carrier protein in order to stimulate the immune response. Five Balb/c mice were inoculated by intraperitoneal injection with 25–100 μg of the conjugated peptide emulsified in the TiterMax adjuvant for primary immunization and boosted 3 times with 12.5–50 μg of the conjugated peptide, also emulsified in the TiterMax adjuvant on days 14, 35 and 63. Cell fusion, subcloning of positive parental clones and expansion of positive subclones were screened using ELISA. Monoclonal antibodies from the hybridoma culture supernatant were purified using the protein A/G affinity column. ELISA and Western blot were performed to determine the purity, the concentration and the reactivity of the final antibody. Recombinant P60 protein has also been produced by Genscript. The pUC57 DNA plasmid was transformed into competent *E. coli BL21 (DE3)*. The recombinant P60 protein was purified using the nickel column *via* polyhistidine-tag. Final protein concentration was found to be 0.531 mg ml^{-1} as determined by the Bradford protein assay with BSA as a standard. A purity of about 80% was estimated using Coomassie blue-stained sodium dodecyl sulphate-polyacrylamide gel electrophoresis (SDS-PAGE).

Bacterial strains and growth conditions

Several strains of *Listeria* were used in this experiment: *L. monocytogenes* 2812, *L. monocytogenes* 1043 and *L. monocytogenes* 2569 (serotypes 1/2a), *L. monocytogenes* 2558, *L. monocytogenes* 2739 and *L. monocytogenes* 2371 (serotypes 1/2b), *L. innocua* LSPQ 3285 (purchased from Laboratoire de Santé Publique du Québec, Ste-Anne-de-Bellevue, Québec, Canada). 1 ml of the fresh culture of all the strains were subcultured in 9 ml of Tryptic Soy Broth (TSB, Difco Laboratory, Detroit, MI) at 37 °C under stirring. Culture supernatants were collected after centrifugation at 5500 rpm for 10 minutes followed by filtration using a 0.25 μm syringe filter (Sarstedt, Montreal, Quebec) in order to obtain cell-free supernatants.

ELISA experiments

Protein samples were prepared as follows: recombinant p60 protein was diluted with a coating buffer (9 mM N_2CO_3, 0.02 M $NaHCO_3$, 1 mM NaN_3, pH 9.6) to obtain a concentration of 1.0 μg ml^{-1}. For bacterial samples, 50 μl of cell-free supernatants from overnight cultures was diluted with 50 μl of the coating buffer. The coating of the recombinant protein and supernatants was performed in microplates (LockWell, Maxisorp from Nunc)

overnight at 4 °C (100 µl per well). After coating, the plates were washed three times (10 min per washing) with a washing buffer (PBS (137 mM NaCl, 2.7 mM KCl, 10 mM Na_2HPO_4, 2 mM KH_2PO_4, pH 7.4) containing 0.05% Tween 20) and blocked with 5% skimmed milk in PBS for 1 hour at 37 °C. The plates were sequentially incubated with the monoclonal IgG anti-p60 (18 µg ml^{-1}) and then with a horseradish peroxidase (HRP) labelled secondary antibody (Biolynx Inc., Brockville, Ontario), diluted as directed by the supplier. Both antibodies were diluted with a diluting buffer (washing buffer containing 1% skimmed milk). For colorimetric reaction, 100 µl of the enzyme substrate 3,3′,5,5′-tetramethylbenzidine (TMB) (Biolynx Inc., Brockville, Ontario) was added and the plates were incubated for 10 minutes at room temperature. Absorbance at 450 nm was measured using a microplate reader after the addition of 50 µl of 2 M H_2SO_4. For all ELISA experiments, two negative controls were performed using a sample of BSA and fresh TSB culture media (data not shown). A second ELISA was done to validate the competition principle of the test. An amount of 0.1 µg of recombinant p60 protein diluted in 100 µl of the coating buffer was primarily coated in each well overnight at 4 °C. After coating, the plates were washed three times (10 min per washing) with the washing buffer and blocked with 5% skimmed milk in PBS for 1 hour at 37 °C. Monoclonal IgG anti-p60 (18 µg ml^{-1}) was then added in each well and incubated for 1 hour at 37 °C. After another washing step, samples of 100 µl of each cell-free supernatant from the different *Listeria* strains were incubated in wells for 15 minutes at room temperature. The assay was then finalized as described above with the secondary antibody and the TMB substrate.

Western blot experiment

Cell-free supernatants from overnight cultures (4 ml) were concentrated by a factor of 66 after filtration through a 30 kDa Amicon Ultra centrifugal filter unit (Millipore, Ontario, Canada), diluted 1 : 1 with the Laemmli sample buffer (Bio-Rad Laboratories, Ontario, Canada) and heated at 100 °C for 5 minutes. Protein separation was achieved by SDS-PAGE in 10% polyacrylamide gels. Transfer onto nitrocellulose membranes was performed overnight at 4 °C. Membranes were blocked for 1 hour at room temperature under stirring in blocking buffer (PBS containing 5% skimmed milk). After three washings with PBS 0.05% Tween 20 (10 min per washing under stirring), the membranes were incubated with monoclonal IgG anti-p60 (0.4 µg ml^{-1}) for 1 hour at room temperature, washed three times as described above and then incubated with a horseradish peroxidase (HRP) labelled secondary antibody (Biolynx Inc.), diluted as directed by the supplier, for 1 hour at room temperature. The membranes were washed three times and then developed with the western blotting detection reagent Amersham ECL before being exposed to a photographic film (GE Healthcare Life Sciences, Québec, Canada). Recombinant P60 protein was used as a positive control.

Labeling of monoclonal IgG

A 0.5 ml sample of monoclonal anti-p60 IgG in 50 mM sodium borate buffer, pH 8.5 (2.0 mg ml^{-1}) was labelled using a Dylight 550 Antibody labeling kit (Thermo Fisher Scientific Inc., IL, USA). The labeling was achieved according to the supplier instructions. The degree of labelling (DOL), as calculated from the absorbance values at $\lambda = 280$ and 557 nm by applying a correction factor label absorption at $\lambda = 280$ nm, was found to be 2.88.

Affinity column preparation

The affinity column was obtained by conjugating the recombinant p60 protein with activated CH-Sepharose 4B (Sigma, Deisenhofen, Germany) as follows. One gram of dry resin powder was suspended in 200 ml of cold 1 mM HCl. The swollen resin was filtered in a polystyrene column (4 ml) (Bio-Rad Laboratories, Mississauga, Ont.) and washed with cold 1 mM HCl. A 3 ml sample of the p60 protein (0.531 mg ml^{-1}) was dialysed in 1 litre of 0.1 M sodium bicarbonate, pH 8.0, containing 0.5 M NaCl overnight at 4 °C using a dialysis membrane of 3500 Da. Dialysed protein was mixed with the resin at 4 °C overnight under slow inversion. After the coating, excess active groups were blocked with 0.1 M Tris–HCl buffer, pH 8.0 for 1 hour. To remove the unbound protein, the resin was washed successively with cold 0.1 M sodium bicarbonate (30 ml), 0.05 M Tris–HCl, 0.5 M NaCl, pH 8.0 (30 ml), 0.05 M sodium acetate, 0.5 M NaCl, pH 4.0 (30 ml), PBS, pH 7.4 (30 ml) and stored in PBS containing 0.05% sodium azide at 4 °C. The stored column was then washed 5 times with PBS. A 0.5 ml sample of labeled monoclonal IgG and 1.5 ml of PBS were added to the resin and incubated overnight at 4 °C under inversion to fix the IgG on the recombinant p60 protein. The resin was washed with PBS until the fluorescence signal returned to the minimum level ($\lambda = 550$ nm excitation, $\lambda = 576$ nm emission).

Detection of *L. monocytogenes*

1 ml of the fresh culture of each bacterial strain was sub-cultured in 10 ml of TSB for 18 hours at 37 °C and successively diluted by serial dilutions with sterile physiological water (0.85% NaCl). 0.1 ml of each dilution was plated on trypticase soy agar (TSA, Difco Laboratory, Detroit, MI) in order to achieve a bacterial count. The right volume was calculated to obtain a theoretical amount of 1 CFU that has been inoculated in 10 ml of TSB for another 18 hours at 37 °C. The cell-free supernatant from this last 18 hours culture (2 ml) was incubated with the resin for 10 minutes at room temperature under inversion. At the end of the incubation, 2 ml of the flow-through containing the free p60–IgG–fluorophore complexes was harvested from the column. The fluorescence emission signal of this flow-through was measured at $\lambda_{em} = 576$ nm with an excitation wavelength of $\lambda_{ex} = 550$ nm and compared with the fluorescence signal of the background which corresponds to the residual fluorescence signal after the last wash of the column before the incubation with the bacterial sample. The column was then washed several times with PBS until the fluorescence signal returned to a minimum and constant level before being reused for another assay.

Results and discussion

Western blot analysing with monoclonal IgG anti-p60

The anti-p60 produced was tested to determine whether it was suitable for the specific detection of the *L. monocytogenes* p60

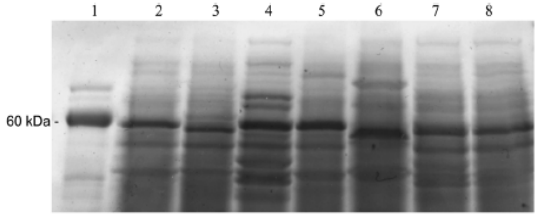

Fig. 1 Protein separation of concentrated cell-free supernatants from overnight cultures of various *Listeria* species by 10% SDS-PAGE electrophoresis. Lanes: 1, recombinant p60 protein; 2, *L. monocytogenes* HPB 2569; 3, *L. monocytogenes* HPB 2558; 4, *L. monocytogenes* HPB 1043; 5, *L. monocytogenes* HPB 2812; 6, *L. monocytogenes* HPB 2739; 7, *L. monocytogenes* HPB 2371; 8, *L. innocua*.

protein. For this purpose, a Western blot analysis with the supernatant proteins of various *Listeria* strains was performed. The six strains of *L. monocytogenes* used for the experiment belong to two of the three serotypes responsible for up to 96% of the cases of human listeriosis.[41] *L. innocua* was used as non-pathogenic *Listeria* species. The protein pattern of the culture supernatants obtained by SDS-PAGE is shown in Fig. 1. A 60 kDa protein band is clearly visible for each of the strains which correspond to the protein p60 or the p60-related protein of *L. innocua*.[38] The important background on the gel and the large amount of protein bands are due to the fact that supernatants concentrated by a factor of 66 were used to reach a sufficient concentration of the p60 protein that allowing its visualization on the gel. As shown in Fig. 2, the monoclonal anti-p60 reacted specifically with the p60 protein of *L. monocytogenes* whereas no cross reactivity with the p60-related protein of *L. innocua* could be observed. These results are consistent with those obtained by Bubert *et al.* (1992). It can be assumed, based on the results, that the monoclonal antibody used in this study, raised against the same PepD, is highly specific and can recognise all of the 13 serotypes of *L. monocytogenes* evaluated in this study.

Detection of the native p60 protein in supernatants by ELISA

While the Western blot analysis allows verifying the recognition of denatured proteins by antibodies, an ELISA test performed with fresh supernatants allows verifying the recognition of native proteins. The possibility that the epitope is inaccessible when the

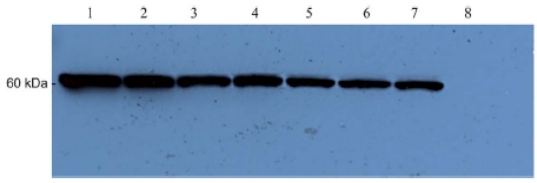

Fig. 2 Western blot analysis of concentrated cell-free supernatants from overnight cultures of various *Listeria* species using a monoclonal anti-p60 antibody. Lanes: 1, recombinant p60 protein; 2, *L. monocytogenes* HPB 2569; 3, *L. monocytogenes* HPB 2558; 4, *L. monocytogenes* HPB 1043; 5, *L. monocytogenes* HPB 2812; 6, *L. monocytogenes* HPB 2739; 7, *L. monocytogenes* HPB 2371; 8, *L. innocua*.

Table 1 Reactivity of the monoclonal anti-p60 with supernatants from different *Listeria* strains by direct ELISA

Organism	Optical density
Listeria innocua	0.088
Listeria monocytogenes	
HPB 2812	1.022
HPB 1043	0.961
HPB 2569	1.123
HPB 2558	0.962
HPB 2739	1.113
HPB 2371	0.865

protein is in its native form cannot be excluded. Therefore, it is important to perform both of these tests in order to confirm the detection of the epitope in the native and denatured form. Direct ELISA tests were performed with fresh cell-free culture supernatants of the different strains of *Listeria*. Since ELISA is more sensitive than the Western blot, it was achieved with non-concentrated supernatants. Results are shown in Table 1 and it can be seen that the monoclonal anti-p60 recognized all the *L. monocytogenes* strains tested while it presented no cross-reaction with the supernatant of non-pathogenic *L. innocua*. The recombinant p60 protein was used as a positive control, and fresh TSB broth alone, used as a negative control, did not show any reaction (data not shown).

Validation of the principle of the test by ELISA

The detection test is based on a principle of competition between the recombinant p60 protein, to which the labeled monoclonal anti-p60 is fixed in the column, and the p60 protein secreted by bacterial strains. The determinant factor that underpins the success of the test is the ability of these fixed antibodies of being naturally displaced by competition on the free p60 protein from the bacterial culture sample after its injection into the column. The amount of antibodies transferred depends on the concentration of the free p60 protein. The new antibody-free p60 protein complexes can be harvested at the end of the column and the fluorescence rate is measured. In order to verify whether the antibodies can be transferred, a competition ELISA has been designed to recreate what happens in the column. However, it is not a classical competition ELISA since both of the antigens were not added at the same time. First, 0.1 µg of the recombinant p60 protein was coated in each well on which a certain amount of antibodies was then fixed. A volume of the supernatant from the *Listeria* culture was added to each well and incubated for 15 minutes at room temperature to allow the antibodies to get transferred on the free p60 protein from supernatants. These new antibody-free p60 protein complexes were washed and the lost in the initial amount of antibodies is revealed by a diminution of the optical density after the reaction with a secondary antibody. The results of this competition ELISA show that supernatants obtained from *L. monocytogenes* cultures can dislodge antibodies from their initial position while the supernatant from *L. innocua* cannot (Table 2). It means that the antibodies recognise only the p60 protein in the supernatant of the *L. monocytogenes* strains and that this protein can capture a certain amount of antibodies already fixed on the recombinant p60 protein. The same

Table 2 Non-classical competition ELISA[a] designed to visualise the displacement of the monoclonal anti-p60 from the immobilized recombinant p60 protein to the free p60 protein from supernatants

Supernatant added	Optical density
None	1.239
Recombinant p60 (0.1 μg)	0.623
L. innocua	1.241
L. innocua diluted	1.229
L. monocytogenes	
HPB 2812	0.661
HPB 2812 diluted	0.996
HPB 1043	0.593
HPB 1043 diluted	0.983
HPB 2569	0.701
HPB 2569 diluted	1.086
HPB 2558	0.638
HPB 2558 diluted	1.018
HPB 2739	0.777
HPB 2739 diluted	1.070
HPB 2371	0.663
HPB 2371 diluted	1.069

[a] First, 0.1 μg of the recombinant p60 protein was coated in each well on which a certain amount of antibodies was then fixed. A volume of supernatant from the *Listeria* culture was added to each well and incubated for 15 minutes at room temperature to allow the antibodies to get transferred on the free p60 protein from supernatants. The lost in the initial amount of antibodies is revealed by a diminution of the optical density after the reaction with the secondary antibody.

experiment was also performed with supernatants diluted to half to see if the diminution of the optical density would be less important. This is indeed what has been observed and all these results confirm that the competition principle can be applied in the column for the detection test.

Detection of *L. monocytogenes*

The preparation of the column was carried out by fixing the labeled monoclonal anti-p60 to the recombinant p60 protein, which is immobilized on a Sepharose 4B matrix. The detection of the bacteria is possible due to the displacement of the labeled monoclonal anti-p60 by the p60 protein secreted by *L. monocytogenes*. Displaced fluorescent antibodies are measured by fluorescence emission of the eluate and represent a measure of the amount of free p60 protein in the supernatant and thus, if the initial sample was contaminated by *L. monocytogenes*. Before testing any sample, the column was washed several times with a neutral buffer until the fluorescence signal of the eluate was minimal and constant. This signal was considered as the background. A volume (2 ml) of cell-free supernatants from an 18 hour culture inoculated with a theoretical amount of 1 CFU was added to the column and incubated for 10 minutes at room temperature. A 2 ml eluate fraction was collected and the fluorescence emission was measured and compared with the background signal. A significant increase in the fluorescence signal means that *L. monocytogenes* was present in the initial sample. The increase of fluorescence signal for each bacterial strain is shown in Fig. 3. For each strain of *L. monocytogenes* tested, a significant increase in fluorescence emission was observed compared to the background whereas the signal for *L. innocua* remained constant.

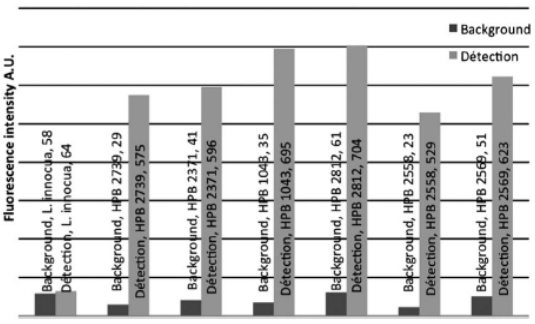

Fig. 3 Fluorescence immunoassay for detection of *L. monocytogenes*. Fluorescence emission was recorded at $\lambda_{em} = 576$ nm and is a representative of the labeled antibody eluted from the column after incubation with cell-free supernatants from overnight cultures of various *Listeria* species. Background signals represent the minimal and constant fluorescence emission after several washes. Excitation wavelength was at $\lambda_{ex} = 550$ nm.

Conclusions

In conclusion, a monoclonal antibody has been produced using a small 11 amino acid peptide of which the sequence is highly conserved in the protein p60 of *L. monocytogenes*. Our results showed that this antibody is very specific to the p60 protein of *L. monocytogenes* and presents no cross-reactivity with the p60-related protein of non-pathogenic *Listeria* species. This antibody was successfully used in the conception of a competitive fluorescent immunoassay for the detection of *L. monocytogenes*. The method consisted of the fixation of the labeled monoclonal anti-p60 on a recombinant p60 protein, which is immobilized on a Sepharose 4B matrix. The addition of a cell-free supernatant from a bacterial culture containing the secreted p60 protein induces the displacement of the antibody, which results in an increase in the fluorescence signal of the eluate at the emission wavelength of the fluorophore. The assay allowed the detection of the 6 strains of *L. monocytogenes* tested after only 18 hours of incubation with a theoretical initial inoculum of 1 CFU. No false positive with *L. innocua* was observed and thus, this assay represents a promising way to develop a sensitive, specific and rapid detection test not only for *L. monocytogenes*, but also for many other pathogens. Other experiments are in progress for the optimisation of the test and also for the establishment of a standardized procedure applicable in the industry.

Acknowledgements

This research was supported by the Ministry of Economic Development, Innovation and Export Trade, International Program (MDEIE). S. Beauchamp was also supported by a fellowship from Nature Research and Technology: International Training Program. The project was also partially funded by the CNR project "Conoscenze integrate per sostenibilità e innovazione del Made in Italy agroalimentare (CISIA)" to A.P. and S.D.

References

1 M. Gandhi and M. L. Chikindas, *Int. J. Food Microbiol.*, 2007, **113**, 1–15.

2 B. Carpentier and O. Cerf, *Int. J. Food Microbiol.*, 2011, **145**, 1–8.
3 T. Møretrø and S. Langsrud, *Biofilms*, 2004, **1**, 107–121.
4 S. D. Ha, S. Y. Park, J. W. Choi, J. Yeon and M. J. Lee, *et al.*, *J. Microbiol. Biotechnol.*, 2005, **15**, 1323–1329.
5 C. W. Donnelly, *Nutr. Rev.*, 2009, **59**, 183–194.
6 P. D. MacDonald, R. E. Whitwam, J. D. Boggs, J. W. Reardon and R. R. Saah, *et al.*, *Clin. Infect. Dis.*, 2001, **33**, 1236.
7 S. J. Olsen, M. C. Evans, S. Hunter, V. Reddy and L. Kornstein, *et al.*, *Clin. Infect. Dis.*, 2001, **33**, 1237.
8 K. C. Klontz, S. Wong, D. Street and S. I. Delgado, *J. Food Prot.*, 2000, **63**, 1113–1116.
9 E. C. D. Todd and S. Notermans, *Food Control*, 2011, **22**, 1484–1490.
10 B. Swaminathan and P. Gerner-Smidt, *Microbes Infect.*, 2007, **9**, 1236–1243.
11 M. Magnani, G. Amagliani, G. Brandi, E. Omiccioli and A. Casiere, *et al.*, *Food Microbiol.*, 2004, **21**, 597–603.
12 D. H. Chung, W. B. Shim, J. G. Choi, J. Y. Kim and Z. Y. Yang, *et al.*, *J. Microbiol. Biotechnol.*, 2007, **17**, 1152–1161.
13 V. Velusamy, K. Arshak, O. Korostynska, K. Oliwa and C. Adley, *Biotechnol. Adv.*, 2010, **28**, 232–254.
14 M. Zunabovic, K. J. Domig and W. Kneifel, *LWT–Food Sci. Technol.*, 2011, **44**, 351–362.
15 D. Y. Hao, L. R. Beuchat and R. E. Brackett, *Appl. Environ. Microbiol.*, 1987, **53**, 955–957.
16 D. McClain and W. H. Lee, *J. - Assoc. Off. Anal. Chem.*, 1988, **71**, 660–664.
17 S. B. Barbuddhe, V. S. Parihar, M. L. Danielsson-Thm and W. Tham, *Food Control*, 2008, **19**, 566–569.
18 M. Drake, J. Isonhood and L. A. Jaykus, *Food Microbiol.*, 2006, **23**, 584–590.
19 K. Balakrishna, H. S. Murali and H. V. Batra, *J. Food Saf.*, 2010, **30**, 263–275.
20 Z. G. Li, W. Chen, Y. W. Yang and W. Deng, *J. Food, Agric. Environ.*, 2010, **8**, 96–99.
21 M. C. Simon, D. I. Gray and N. Cook, *Appl. Environ. Microbiol.*, 1996, **62**, 822–824.
22 P. G. Lantz, B. Hahn-Hägerdal and P. Rådström, *Trends Food Sci. Technol.*, 1994, **5**, 384–389.
23 A. Agersborg, R. Dahl and I. Martinez, *Int. J. Food Microbiol.*, 1997, **35**, 275–280.
24 S. S. Iqbal, M. W. Mayo, J. G. Bruno, B. V. Bronk and C. A. Batt, *et al.*, *Biosens. Bioelectron.*, 2000, **15**, 549–578.
25 C. S. Chen and R. A. Durst, *Talanta*, 2006, **69**, 232–238.
26 R. L. Churchill, H. Lee and J. C. Hall, *J. Microbiol. Methods*, 2006, **64**, 141–170.
27 V. Gangar, M. S. Curiale, A. D'Onorio, A. Schultz and R. L. Johnson, *et al.*, *J. AOAC Int.*, 2000, **83**, 903–918.
28 K. Hibi, A. Abe, E. Ohashi, K. Mitsubayashi and H. Ushio, *et al.*, *Anal. Chim. Acta*, 2006, **573–574**, 158–163.
29 J. A. Hudson, R. J. Lake, M. G. Savill, P. Scholes and R. E. McCormick, *J. Appl. Microbiol.*, 2001, **90**, 614–621.
30 Y. S. Jung, J. F. Frank and R. E. Brackett, *J. Food Prot.*, 2003, **66**, 1283–1287.
31 K. Y. Yu, Y. Noh, M. Chung, H. J. Park and N. Lee, *et al.*, *Clin. Diagn. Lab. Immunol.*, 2004, **11**, 446–451.
32 M. Magliulo, P. Simoni, M. Guardigli, E. Michelini and M. Luciani, *et al.*, *J. Agric. Food Chem.*, 2007, **55**, 4933–4939.
33 A. M. Sewell, D. W. Warburton, A. Boville, E. F. Daley and K. Mullen, *Int. J. Food Microbiol.*, 2003, **81**, 123–129.
34 W. B. Shim, J. G. Choi, J. Y. Kim, Z. Y. Yang and K. H. Lee, *et al.*, *J. Microbiol. Biotechnol.*, 2007, **17**, 1152–1161.
35 P. Leonard, S. Hearty, J. Brennan, L. Dunne and J. Quinn, *et al.*, *Enzyme Microb. Technol.*, 2003, **32**, 3–13.
36 A. Bubert, M. Kuhn, W. Goebel and S. Kohler, *J. Bacteriol.*, 1992, **174**, 8166–8171.
37 M. Kuhn and W. Goebel, *Infect. Immun.*, 1989, **57**, 55–61.
38 A. Bubert, P. Schubert, S. Kohler, R. Frank and W. Goebel, *Appl. Environ. Microbiol.*, 1994, **60**, 3120–3127.
39 A. Bubert, S. Kohler and W. Goebel, *Appl. Environ. Microbiol.*, 1992, **58**, 2625–2632.
40 S. Hearty, P. Leonard, J. Quinn and R. O'Kennedy, *J. Microbiol. Methods*, 2006, **66**, 294–312.
41 R. B. Tompkin, *J. Food Prot.*, 2002, **65**, 709–725.

MICROBIAL DIVERSITY 2011

ENVIRONMENTAL STRESS AND ADAPTATION

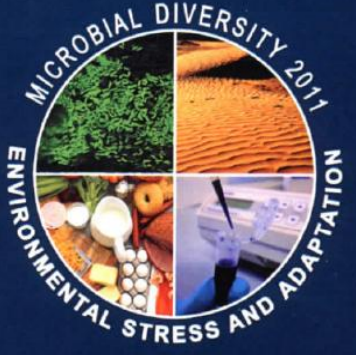

MD 2011

EDITED BY

S. CASELLA, D. DAFFONCHIO, M. GOBBETTI, E. PARENTE

A NEW OPTICAL METHOD TO SENSE COMPOUNDS OF HIGH SOCIAL INTEREST

STRIANESE Maria (1), STAIANO Maria (2), DI GIOVANNI Stefano (2), PENNACCHIO Anna (2), DELL'ANGELO Valentina (2), RUGGIERO Giuseppe (2), LABELLA Tullio (2), PELLECCHIA Claudio (1), and D'AURIA Sabato (2)*

(1) University of Salerno, Salerno, Italy. (2) Laboratory for Molecular Sensing, IBP-CNR, Napoli, Italy. * s.dauria@ibp.cnr.it

Introduction

The field of optical sensors has been a growing research area over the last three decades. A wide range of books and review articles has been published by experts in the field who have highlighted the advantages of optical sensing over other transduction methods. Fluorescence is by far the method most often applied and comes in a variety of schemes. Research and development in this field are wide-ranging and multidisciplinary, spanning biochemistry, inorganic chemistry, physical chemistry, medicine, electrochemistry, electronics and software engineering. (Borisov et al., 2008; McDonagh et al., 2008)

Performance parameters like sensitivity, stability, reusability, selectivity, robustness are the most relevant ones when implementing a sensing device. Advantages like simplicity, rapidity, cheapness in setting up the system and broad applicability make the developed devices realistic alternatives to the often time-consuming and expensive conventional assays.

In the present communication a new methodology for practical sensing applications by means of optical spectroscopy is described. Its overall characteristics make it an attractive candidate in the construction of industrially produced devices. (Strianese et al., 2011)

The method builds on the possibility of modulating the excitation intensity of a fluorescent probe used as a transducer and a sensor molecule whose absorption is strongly affected by the binding of an analyte of interest used as a filter.

The two simple conditions that have to be fulfilled for the method to work are: a) the absorption spectrum of the sensor placed inside the cuvette and acting as the recognition element for the analyte of interest should strongly change upon the binding of the analyte; b) the fluorescence dye transducer should exhibit an excitation band which overlaps with one or more absorption bands of the sensor. The absorption band of the sensor affected by the binding of the specific analyte should overlap with the excitation band of the transducer. More precisely, the proposed method uses a commercial cuvette filled with the sensor and whose external surface, downstream of the sensor on the light path, is uniformly covered with the fluorescence transducer. The photo-detector reads the fluorescence intensity emission of the transducer. The reading is proportional to the amount of excitation light which in turns depends on the amount of the analyte bound to the sensor.

In this work we describe the results obtained with three different pairs of sensor-transducers: i) pyridoxal 5'-phosphate-dependent D-serine dehydratase (Dsd) paired with fluorescein for the

detection of D-serine; ii) Myoglobin (Mb) paired with fluorescein for detection of oxygen; iii) Cytochrome c peroxidase (CcP) paired with fluorescein for detection of NO. These systems were selected because they all involve the monitoring of particularly interesting analytes, spanning several fields of interest. In particular, a method to sense D-serine levels is extremely important in the medical field to assess the physiological role and clinical relevance of D-serine. D-serine is a D-amino acid that plays an important role in the regulation of NMDA (N-methyl-D-aspartate) signalling in the central nervous system (CNS) and modulates brain functions.(Mothet et al., 2000) Moreover, release of endogenous D-serine may contribute to neuronal damage in the cerebral cortex and hippocampus by excitotoxicity in the neurological diseases. As for Oxygen, it plays a universal role in biological systems and is one of the most important substances for substaining aerobic life, thus, there is a continuous need in fields like chemical or clinical analysis or environmental monitoring to improve the available oxygen sensing techniques. (Amao, 2003) NO plays a crucial role in a variety of physiological and pathophysiological functions within the body and also is one of the hazardous exhaust gases generated by motor vehicles. (Born et al., 2006; Dooly et al., 2007) With such diverse interests in NO, there is a pressing need for methods to detect NO in both aqueous and gaseous media.(Boon et al., 2006)

Materials and Methods

Sensor preparation

In a typical experiment the sensor was prepared as follows. A commercially available nitrocellulose strip (*Schleicher & Schuell BioScience*) was uniformly covered with a milliQ water solution of the dye-label fluorescein. After drying, the strip was carefully fixed to one of the external windows of a 10 x 10 mm^2 airtight quartz fluorescence cuvette (Hellma Benelux bv, Rijswijk, Netherlands). To fix the nitro-cellulose strip a black tape was used. The dye-labeled cuvette was then filled with either CcP, Mb or Dsd (2-10 μM) in 100mM potassium phosphate buffer (pH 6.8) or 10mM Tris/HCl buffer (pH =9.0) and the measurement was started. A quenching of the initial fluorescence intensity was normally observed when adding the protein into the cuvette. The intensity of the quenching was dependent on the concentration of the protein in the cuvette and on the amount of fluorophore.

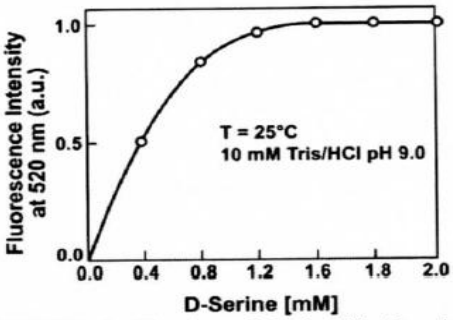

FIGURE 1. Titration of Dsd with D-serine monitored by the dye emission (520 nm). The fluorescence intensity of Dsd normalized on the fluorescence intensity in the absence of D-serine is plotted versus the total D-serine concentration. The solid line represents the best fit to the data. Protein concentration: 2.0 μM in 10mM Tris/HCl buffer (pH =9.0).

Results and discussion

D-serine detection. Dsd from *S. cerevisiae* is a pyridoxal 5'- phosphate (PLP)-dependent enzyme which catalyzes the dehydration of D-serine to produce pyruvate and ammonia. Spectroscopic features of Dsd make it ideally suited for implementing an optical biosensor for D-serine detection. Specifically, while the absorption spectrum of Dsd exhibits three characteristic bands centered at 280 nm, 310 nm and at 430 nm, D-serine addition quenches the 430 nm

band. Upon interacting with D-serine, Dsd, and more specifically PLP, undergoes to structural alterations which result in the quenching of the 430 nm band. This change of the absorption spectrum strongly modulates the fluorescence intensity of the dye label (fluorescein) acting as fluorescence transducer and used for functionalizing the cuvette. A fast increase in label emission (50%) was clearly observed upon adding D-serine to an end concentration of 2 mM (i.e., in considerable excess over the Dsd concentration), data not shown. This finding is in accordance with the quenching of the 430 nm absorption band observed in the absorption spectrum of Dsd when adding the substrate D-serine. To calibrate our system, D-serine titrations of Dsd were performed while monitoring the fluorescence intensity of fluorescein. Figure 1 shows a typical fluorescence titration of Dsd with increasing amounts of D-serine.

Oxygen detection. Myoglobin is a 18-kDa protein which is commonly acknowledged as an oxygen storage protein. It reacts with molecular oxygen by a simple association reaction, most likely due to its monomeric form. Aiming at implementing an oxygen sensing device by exploiting the potential of our methodology, we considered myoglobin perfectly suited for proof-of-principle experiments. Since O_2 has a strong preference for binding Mb in the Fe^{2+} state, in all our experiments we first reduced Mb to the Fe^{2+} form. The absorption spectrum of Mb in the metMb(Fe^{3+}) features a characteristic Soret band at 409 nm and two less intense bands centered respectively at 503 nm and 636 nm. When adding a 3 mM sodium dithionite excess over the Mb concentration, thus turning the metMb(Fe^{3+}) into the oxygen-free(Fe^{2+}), a clear shift of

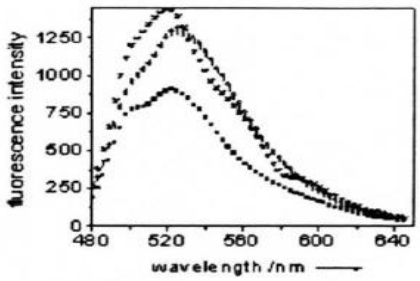

FIGURE 2. Room temperature emission spectrum of Mb paired with fluorescein (exc 450 nm) (○ trace), upon reduction to O_2-free(Fe^{2+})Mb (■ trace), upon addition (* trace) and removal (trace) of O_2. Protein concentration: 10 μM in 100 mM potassium phosphate buffer (pH =6.8).

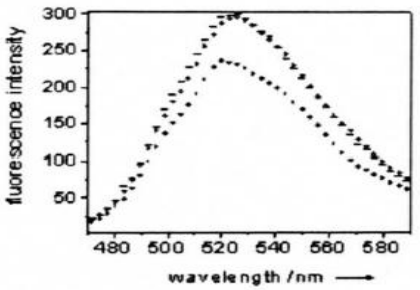

FIGURE 3. Room temperature emission spectrum of CcP paired with fluorescein (exc 450 nm) (— trace), upon addition (● trace) and removal (○ trace) of NO. Protein concentration: 5 μM in 100 mM potassium phosphate buffer (pH =6.8). In this particular experiment the molar ratio NO to CcP was about 40 to 1.

the Soret band to 434 nm and the appearance of a band centered around 560nm occur. These bands are diagnostics of the oxygen-free(Fe^{2+})Mb form. Upon oxygen binding the Soret band shifts again (to 417 nm) whereas the 560 nm band is quenched and two new absorption bands centered at 545 and 580 nm appear. This

change of the absorption spectrum strongly modulates the fluorescence intensity of the dye-transducer (fluorescein) used for functionalizing the cuvette. Figure 2 shows a typical fluorescence trace of a solution containing 10 μM of Mb when excited at 450 nm. Upon Mb reduction to the oxygen-free (Fe^{2+}) state, a 35% quenching of the dye-fluorescence is observed as a result of the fact that more light is absorbed by the Mb (see fig. 2). As soon as oxygen binds Mb the fluorescence of the label increases (40%), (see fig. 2). In the oxygen-bound state the fluorescein fluorescence is essentially uninhibited since the Soret band of Mb is quenched if compared to metMb(Fe^{3+}) and shifts its maximum intensity to 417 nm. When adding $K_3Fe(CN)_6$ (0.1 mM) the oxygen-bound Mb(Fe^{2+}) turns to the initial metMb(Fe^{3+}) and the initial fluorescence intensity of fluorescein is restored (see fig. 2). It follows that the dye fluorescence is a sensitive reporter of the oxygen bound to the iron center. The cycle could be repeated many times. This finding showed that the O_2 binding process is reversible, which is crucial for practical sensing applications.

NO detection. CcP is a soluble 34-kDa heme protein, located in the inter-membrane space of yeast mitochondria. Resting state CcP (Fe^{III}) contains a non-covalently bound heme with a five-coordinate, high spin iron (S= 5/2). The sixth coordination position is vacant, allowing ligands like NO to bind. We have recently shown that fluorescently labeled CcP can be successfully used as a "turn-on" FRET-based biosensor for NO detection. (Strianese *et al.*, 2010). Drawing upon these findings, in the current work we explore the use of CcP as sensor to place inside the fluorescein-labeled cuvette and acting as the NO recognition element. In the present case no direct labeling of the CcP was performed. The fluorescence intensity of the dye-label is modulated by the different amounts of light absorbed by the CcP in the NO-free and NO-bound states. The absorption spectrum of CcP shows a characteristic Soret band at 408 nm and two less intense bands centered respectively at 510 nm and 645 nm, upon NO binding to CcP, the Soret band shifts from 409nm to 420nm and its intensity increases. By functionalizing the cuvette with the fluorescein dye, this change in absorption upon NO binding can be translated into a change of fluorescence intensity of the label. The fluorescence intensity of the fluorescein was monitored during a change from an NO-free environment to an NO-saturated environment. Figure 3 shows a typical fluorescence trace of a solution containing 5 μM of CcP when excited at 450 nm. When adding NO to the system (in considerable excess over the CcP concentration) a 20% decrease of the dye-label fluorescence was detected (fig 3). This finding is in accordance with the enhancement of the intensity of the Soret band of the CcP in the NO-bound form which leads the protein to absorb more photons. Subsequent bubbling of argon through the solution removed the NO again and made the fluorescence of the dye-label to go back to the initial level (fig 3). This showed that the NO binding process is reversible and our system works successfully when applied for monitoring NO.

Conclusions

Our proposal is new in that it is based on a new principle , viz., the possibility of tuning the fluorescence emission of a dye-label (used to functionalize one of the window of a commercial fluorescence cuvette) by the different amounts of light absorbed by the protein which acts as sensing material.

A notable advantage of the new methodology we are proposing herein is its broad applicability. In principle it is a sensitive way to follow any event of interest given that it affects the absorption spectrum

of the molecule acting as the recognition element.
Differently from already existing fluorescence-based sensing devices, it avoids delaying steps due to the purification of the molecule acting as the recognition element upon fluorescent labeling. (D'Auria et al., 2001; Staiano et al., 2005; Varriale et al., 2007)

Acknowledgments
This project was realized in the frame of the CNR Commessa "Diagnostica Avanzata ed Alimentazione".

References

Amao Y. (2003). Microchim. Acta 143: 1-12.
Boon E.M., Marletta M.A. (2006). J. Am. Chem. Soc. 128: 10022-10023.
Borisov S.M., Wolfbeis O.S. (2008). Chem. Rev.
D'Auria S., Lakowicz J.R. (2001). Curr. Opin. Biotechnol. 12: 99-104.
Dooly G., Fitzpatrick C., Lewis E. (2007). Energy 33: 657-666.
McDonagh C., Burke C.S., Maccraith B.D. (2008). Chem. Rev.
Mothet J.P., Parent A.T., Wolosker H., Brady R.O., Jr., Linden D.J., Ferris C.D., Rogawski M.A., Snyder S.H. (2000). Proc. Natl. Acad. Sci U. S. A 97: 4926-4931.
Staiano M., Bazzicalupo P., Rossi M., D'Auria S. (2005). Mol. Biosyst. 1: 354-362.
Strianese M., De M.F., Pavone V., Lombardi A., Canters G.W., Pellecchia C. (2010). J. Inorg. biochem. 104: 619-624.
Strianese M., Varriale A., Staiano M., Pellecchia C., D'Auria S. (2011). Nanoscale 3: 298-302.
Varriale A., Staiano M., Rossi M., D'Auria S. (2007). Anal. Chem 79: 5760-5762.

BIOSENSOR: ADVANCED METHODOLOGY FOR DETECTION OF OCHRATOXIN A IN FOOD OF ANIMAL ORIGIN

Russo R[1], Varriale A[2], Pennacchio A[2], Iozzino L[1], Anastasio A[1], Florio S[1], D'Auria S[2], Severino L[1]

[1]Faculty of Veterinary Medicine, University of Naples, Naples, Italy; [2]Institute of Protein Biochemistry - CNR, Naples, Italy.

Ochratoxin A (OTA) is a mycotoxins produced by fungi belonging to *Asperigillus* and *Penicillium* families commonly found as food contaminant in both USA and UE mainly in cereal grains, coffee, cocoa, and spices (1). OTA could contaminate food of animal origin as well, such as pork meat and derived products (2). OTA is of great toxicological concern for the toxic effects in humans and animals which include nephrotoxicity, carcinogenicity, genotoxicity and immunotoxicity (3). Maximum permissible levels in different matrices have also been established for OTA by UE legislation (Reg. CE 1881/2006). As these are quite low, analytical detection methods have to be both sensitive and specific. Therefore, regarding food safety, it is useful to have a sensible and rapid analytical methodologies to be used as screening methods for the detection of levels of OTA in a large number of food samples. Conventional analytical detection methods involve chromatographic analysis, such as HPLC, GC and, more recently, LC-MS and LC-MS (4-5). However, although these techniques are reproducible and very sensitive, extensive protocols of sample clean up are required prior to the analysis; moreover, such analysis are expensive, time consuming and required specialized equipment. An immunochemical analytical method, based on highly specific antigen-antibody interactions, would be desirable, offering several advantages compared to conventional techniques such as low costs per sample, high selectivity, and high throughput. The aim of the current study was to realized an innovative fluorescence assay for the detection of traces of OTA in food samples. Briefly, glutamine binding protein from *E. coli* was conjugated with OTA and then labelled with fluorescein-5-isothiocyanate (FITC). Antibodies anti-BSA-OTA were produced by inoculating rabbits with the antigen. The measurement was carried out by fluorescence correlation spectrometry (FCS). Detection limit was 0.0078 ng of OTA suggesting the application of such experimental strategy for analysis in which high sensitivity detection is required.

In conclusion, the development of highly specific screening methods could be useful to reveal the presence of residues of contaminants in various foods analyzing a large number of samples in a short time so enabling the rapid commercialization of food products and sending to the confirmatory analysis only the positive samples.

Keywords: ochratoxin A; biosensor; food safety.

References

1. Sangare-Tigori et al., *Food Addit Contam.* 2006 23(10):1000-1007.
2. Jørgensen K, *Food Addit Contam.* 2005; 22:26-30.
3. Pfohl-Leszkowicz A and Manderville RA, *Mol. Nutr. Food Res.* 2007, 51(1):61-99.
4. Kralj Cigić I and Prosen H, *Int. J. Mol. Sci.* 2009, 10, 62-115.

Varriale A et al., *Prot Pept Lett.* 2009, 16:1425-1428.